

ALTERED DNA REPAIR, ANTIOXIDANT AND
CELLULAR PROLIFERATION STATUS AS
DETERMINANTS OF SUSCEPTIBILITY TO
METHYLMERCURY TOXICITY *IN VITRO*

by

Stephanie Lee Ondovcik

A thesis submitted in conformity with the requirements
for the degree of Doctor of Philosophy

Graduate Department of Pharmaceutical Sciences
University of Toronto

© Copyright by Stephanie Lee Ondovcik 2013

Altered DNA Repair, Antioxidant and Cellular Proliferation Status as Determinants of Susceptibility to Methylmercury Toxicity *in Vitro*

Stephanie Lee Ondovcik

Doctor of Philosophy

Graduate Department of Pharmaceutical Sciences
University of Toronto

2013

ABSTRACT

Methylmercury (**MeHg**) is a pervasive environmental contaminant with potent neurotoxic, teratogenic and likely carcinogenic activity, for which the underlying molecular mechanisms remain largely unclear. Base excision repair (**BER**) is important in mitigating the pathogenic effects of oxidative stress, which has also been implicated in the mechanism of MeHg toxicity, however the importance of BER in MeHg toxicity is currently unknown. Accordingly, we addressed this question using: (1) spontaneously- and Simian virus 40 (**SV40**) large T antigen-immortalized oxoguanine glycosylase 1-*null* (**Ogg1**^{-/-}) murine embryonic fibroblasts (**MEFs**); and, (2) human Ogg1 (**hOgg1**)- or formamidopyrimidine glycosylase (**Fpg**)-expressing human embryonic kidney (**HEK**) cells; reciprocal *in vitro* cellular models with deficient and enhanced ability to repair oxidatively damaged DNA respectively. When spontaneously-immortalized wild-type and *Ogg1*^{-/-} MEFs were exposed to environmentally relevant, low micromolar concentrations of MeHg, both underwent cell cycle arrest but *Ogg1*^{-/-} cells exhibited a greater sensitivity to MeHg than wild-type controls with reduced clonogenic survival and increased apoptosis, DNA damage and DNA damage response activation. Antioxidative catalase alleviated the MeHg-initiated DNA damage in both wild-type and *Ogg1*^{-/-} cells, but failed to block MeHg-mediated apoptosis at micromolar concentrations. As in spontaneously immortalized MEFs, MeHg induced cell cycle arrest in SV40 large T antigen-immortalized MEFs, with increased

sensitivity to MeHg persisting in the *Ogg1*^{-/-} MEFs. Importantly, cells seeded at a higher density exhibited compromised proliferation, which protected against MeHg-mediated cell cycle arrest and DNA damage. In the reciprocal model of enhanced DNA repair, hOgg1- and Fpg-expressing cells appeared paradoxically more sensitive than wild-type controls to acute MeHg exposure for all cellular and biochemical parameters, potentially due to the accumulation of toxic intermediary abasic sites. Accordingly, our results provide the first evidence that Ogg1 status represents a critical determinant of risk for MeHg toxicity independent of cellular immortalization method, with variations in cellular proliferation and interindividual variability in antioxidative and DNA repair capacities constituting important determinants of risk for environmentally-initiated oxidatively damaged DNA and its pathological consequences.

ACKNOWLEDGMENTS

I would first like to thank my supervisor, Dr. Peter Wells, for taking a chance on a grad student with little laboratory experience and allowing me to pursue my PhD under your supervision. Thank you for providing this learning experience, and for your constant support and encouragement to grow both personally and professionally over the years.

I would also like to thank my advisory committee members: Dr. Jeffrey Henderson, Dr. Jason Matthews and Dr. Peter McPherson, for your invaluable help, suggestions and insight that assisted in shaping my thesis project.

I would especially like to thank Dr. Peter McPherson and his laboratory for making me an honorary member, allowing me to carry out much of the latter stages of my research within their lab. I will be forever grateful for all of the time you invested in my project, and the guidance, encouragement and insight you provided. Without you, the project would not be what it is. To the McPherson lab members: Laura Tamblyn, you are perhaps the most knowledgeable person I have ever met, and taught me so much in the short time we worked together I cannot even begin to thank you enough; and Meghan Larin, one of the best lab mates you could ask for, thank you for your generous help, ideas and company in the lab.

To the past and present members of the Wells lab: Dr. Julia P. Abramov, Dr. Crystal Lee, Margaret Loniewska, Dr. Gordon McCallum, Lutfiya Miller, Dr. Thomas Preston, Dr. Annmarie Ramkissoon, Kyla Schwarz-Lam, Nicole Sweeting, Aaron Shapiro and Michelle Siu, thank you all for the countless shenanigans and memories over the years, both in and out of the lab, you guys made this experience unforgettable!

Last, but certainly not least, I'd like to thank my family: Mom, Dad and Mal, and John and Hercules, for your continual love, support, encouragement and welcome distraction from life at the lab. Without you guys none of this would be possible, love you!

TABLE OF CONTENTS

CHAPTER 1: INTRODUCTION.....	1
1.1 RATIONALE AND RESEARCH OBJECTIVES.....	2
1.2 REACTIVE OXYGEN SPECIES.....	6
1.2.1 Overview of reactive oxygen species.....	6
1.2.2 Sources of reactive oxygen species.....	8
1.2.2.1 Endogenous sources of ROS.....	8
1.2.2.2 Exogenous sources of ROS.....	8
1.2.3 Antioxidative defense mechanisms.....	11
1.2.3.1 Enzymatic detoxification of ROS.....	11
1.2.3.2 Non-enzymatic detoxification of ROS.....	11
1.2.4 Effects of ROS.....	14
1.2.4.1 Physiological effects of ROS.....	14
1.2.4.2 Pathological effects of ROS.....	14
1.3 METHYLMERCURY OVERVIEW.....	16
1.3.1 Comparison of the chemical forms of mercury.....	16
1.3.1.1 Physical and chemical properties.....	16
1.3.1.2 Overview of the toxicology of relevant mercury species.....	19
1.3.2 Human exposure to MeHg.....	23
1.3.2.1 Environmental sources of MeHg.....	23
1.3.2.2 Documented exposure levels.....	24
1.3.2.3 Clinical manifestation of MeHg neurotoxicity in the adult.....	27
1.3.2.4 Clinical manifestation of MeHg neurotoxicity in the embryo/fetus.....	27
1.3.3 Molecular mechanisms and cellular targets involved in MeHg-mediated toxicity.....	28
1.3.3.1 Induction of glutamate excitotoxicity.....	35
1.3.3.2 Disruption of intracellular calcium homeostasis.....	35
1.3.3.3 Induction of oxidative stress.....	35

1.3.3.4	Inhibition of nucleic acid biosynthesis	39
1.3.3.5	DNA damage	39
1.3.3.6	Protein binding	39
1.3.3.7	Microtubule disruption	40
1.4	DNA DAMAGE	41
1.4.1	Introduction to DNA damage.....	41
1.4.2	Oxidatively damaged DNA and the 8-oxo-2'-deoxyguanosine lesion	43
1.4.3	DNA double-strand breaks and γ H2AX.....	47
1.5	DNA REPAIR	50
1.5.1	Major pathways for the repair of DNA damage	50
1.5.2	Base excision repair.....	54
1.5.2.1	Oxoguanine glycosylase 1	54
1.5.2.2	Formamidopyrimidine glycosylase	55
1.5.2.3	The base excision repair pathway.....	56
1.5.2.4	Other proteins involved in 8-oxodG repair	60
1.5.2.5	The importance of BER in disease	62
1.6	THE CELL CYCLE	64
1.6.1	Overview of the eukaryotic cell cycle	64
1.6.2	Overview of eukaryotic cell cycle regulation	67
CHAPTER 2: STUDIES.....		70
2.1	STUDY 1: OXOGUANINE GLYCOSYLASE 1 (OGG1) PROTECTS CELLS FROM DNA DOUBLE-STRAND BREAK DAMAGE FOLLOWING METHYLMERCURY (MeHg) EXPOSURE.....	71
2.1.1	Abstract	72
2.1.2	Introduction	73
2.1.3	Materials and Methods	75

2.1.4	Results	77
2.1.5	Discussion	92
2.1.6	Acknowledgements.....	98
2.2	STUDY 2: SENSITIVITY TO METHYLMERCURY TOXICITY IS ENHANCED IN OXOGUANINE GLYCOSYLASE 1 KNOCKOUT MURINE EMBRYONIC FIBROBLASTS AND IS DEPENDENT ON CELLULAR PROLIFERATION CAPACITY	99
2.2.1	Abstract	100
2.2.2	Introduction	101
2.2.3	Materials and Methods	104
2.2.4	Results	106
2.2.5	Discussion	120
2.2.6	Acknowledgements.....	125
2.3	STUDY 3: EXPRESSION OF HUMAN OXOGUANINE GLYCOSYLASE 1 (hOgg1) OR FORMAMIDOPYRIMIDINE GLYCOSYLASE (Fpg) IN HUMAN EMBRYONIC KIDNEY (HEK) 293 CELLS EXACERBATES METHYLMERCURY (MeHg) TOXICITY <i>IN VITRO</i>	126
2.3.1	Abstract	127
2.3.2	Introduction	128
2.3.3	Materials and Methods	131
2.3.4	Results	134
2.3.5	Discussion	155
CHAPTER 3: SUMMARY, CONCLUSIONS AND FUTURE STUDIES.....		160
3.1	SUMMARY AND CONCLUSIONS	161
3.2	FUTURE STUDIES.....	165

CHAPTER 4: REFERENCES	168
CHAPTER 5: APPENDICES	183
I. SUPPLEMENTAL FIGURES FOR STUDY 1.....	184
Figure S-1. Polyethylene glycol (PEG)-conjugated catalase attenuates hydrogen peroxide (H₂O₂)-initiated apoptosis in spontaneously-immortalized wild-type and OGG1-null (<i>Ogg1</i>^{-/-}) cells, despite its inability to similarly mitigate MeHg-initiated apoptosis.....	185
Figure S-2. Extended exposure to a submicromolar concentration of MeHg does not illicit increased apoptosis in spontaneously-immortalized wild-type and <i>Ogg1</i>^{-/-} cells	187
II. SUPPLEMENTAL FIGURE FOR STUDY 2.....	189
Figure S-1. MeHg-initiated H2AX phosphorylation at serine 139 (γH2AX) is exacerbated in Simian virus 40 (SV40) large T antigen-immortalized wild-type and <i>Ogg1</i>^{-/-} cells when serum starvation is used as a means of stalling cellular proliferation.....	190
III. MODULATORY EFFECT OF THE FREE RADICAL SPIN TRAP, α-PHENYL-N-TERT-BUTYLNITRONE (PBN), ON MeHg-INITIATED DECREASED CELLULAR VIABILITY AND REACTIVE OXYGEN SPECIES FORMATION	192
Figure 1. An experimental summary of the modulatory effect of the free radical spin trap, PBN, on cellular viability and reactive oxygen species (ROS) production in spontaneously-immortalized wild-type and <i>Ogg1</i>^{-/-} MEFs.....	193
IV. THE MODULATORY EFFECT OF PEG-CATALASE ON MeHg-INITIATED DECREASED CELLULAR VIABILITY AND ROS FORMATION	195
Figure 1. Antioxidative PEG-catalase does not attenuate MeHg-initiated decreased cellular viability in spontaneously-immortalized wild-type and <i>Ogg1</i>^{-/-} MEFs.....	196

Figure 2. Antioxidative PEG-catalase attenuates both basal and MeHg-initiated ROS formation in spontaneously-immortalized wild-type and *Ogg1*^{-/-} MEFs 198

V. HUMAN OXOGUANINE GLYCOSYLASE 1-EXPRESSING TRANSGENIC MICE.....200

Table 1. Overview of the *in vivo* characterization profile completed on 15 and 17 Line human *Ogg1*-expressing transgenic mice 201

V.i Rederivation of hOgg1-expressing transgenic mice to specific and opportunistic pathogen free status by embryo transfer 204

Figure 1. Representative genotyping gel confirming continued hOgg1 transgene expression following rederivation..... 205

LIST OF TABLES

SECTION 1: INTRODUCTION

TABLE 1.	ANTIOXIDANT MICRONUTRIENTS.....	13
TABLE 2.	PHYSICAL AND CHEMICAL PROPERTIES OF VARIOUS MERCURY COMPOUNDS.....	17
TABLE 3.	VOLATILITY OF VARIOUS MERCURY SPECIES AS EVIDENCED BY THEIR EXPERIMENTALLY DETERMINED HENRY'S LAW CONSTANTS (<i>H</i>).....	18
TABLE 4.	THE TOXICOLOGY OF RELEVANT MERCURY SPECIES.....	20
TABLE 5.	EXPERIMENTAL EVIDENCE SUPPORTING SOME OF THE MAJOR PROPOSED MOLECULAR MECHANISMS AND TARGETS INVOLVED IN MeHg-MEDIATED NEUROTOXICITY.....	30
TABLE 6.	CYTOTOXICITY AND MUTAGENICITY OF SOME ENDOGENOUSLY GENERATED DNA LESIONS.....	42
TABLE 7.	OVERVIEW OF THE SIX MAJOR DNA REPAIR PATHWAYS.....	51
TABLE 8.	PROTEINS INVOLVED IN BASE EXCISION REPAIR.....	58

LIST OF FIGURES

SECTION 1: INTRODUCTION

FIGURE 1.	SCHEMATIC OUTLINING THE THESIS OBJECTIVES.....	5
FIGURE 2.	THE O ₂ REDUCTION PATHWAY AND THE FAMILY OF REACTIVE OXYGEN SPECIES.....	7
FIGURE 3.	SOURCES OF ROS AND THE GENERAL MECHANISMS BY WHICH OXIDATIVE STRESS CAN ALTER CELLULAR FUNCTION.....	9
FIGURE 4.	BIOCHEMICAL PATHWAYS FOR THE FORMATION, DETOXIFICATION AND CELLULAR EFFECTS OF XENOBIOTIC FREE RADICAL INTERMEDIATES AND ROS.....	10
FIGURE 5.	MeHg LEVELS IN SOME COMMONLY CONSUMED FISH AND SEAFOOD SPECIES.....	26
FIGURE 6.	THE INTERPLAY BETWEEN MeHg-INDUCED OXIDATIVE STRESS, Ca ²⁺ AND GLUTAMATE (GLU) DYSHOMEOSTASIS IN THE MECHANISM OF MeHg-MEDIATED NEUROTOXICITY.....	37
FIGURE 7.	EFFECTS OF MeHg ON THE GSH ANTIOXIDANT SYSTEM.....	38
FIGURE 8.	STRUCTURES OF THE MAJOR PRODUCTS OF OXIDATIVE DAMAGE TO DNA BASES.....	45
FIGURE 9.	8-OXODG FORMATION AND FATE.....	46
FIGURE 10.	INDUCTION OF γ H2AX AND THE DNA DAMAGE RESPONSE.....	49
FIGURE 11.	SHORT- AND LONG-PATCH BER IN MAMMALIAN CELLS.....	59
FIGURE 12.	8-OXODG REPAIR BY OGG1 AND THE RELATED PROTEINS MUTYH (MYH) AND MTH1.....	61
FIGURE 13.	THE FATE OF A SINGLE PARENTAL CHROMOSOME THROUGHOUT THE EUKARYOTIC CELL CYCLE.....	66
FIGURE 14.	CURRENT MODEL FOR REGULATION OF THE EUKARYOTIC CELL CYCLE.....	69

SECTION 2: STUDIES

Study 1.

FIGURE 1.	OXOGUANINE GLYCOSYLASE 1-NULL (<i>Ogg1</i> ^{-/-}) CELLS ARE MORE SENSITIVE TO METHYLMERCURY (MeHg).....	78
-----------	--------------------------------------------------------------------------------------------------------------------	----

FIGURE 2.	SUSCEPTIBILITY OF <i>Ogg1</i> ^{-/-} CELLS TO MeHg-INITIATED PROLIFERATION ARREST	81
FIGURE 3.	SUSCEPTIBILITY OF <i>Ogg1</i> ^{-/-} CELLS TO UNDERGO MeHg-INITIATED APOPTOSIS AND THE INABILITY OF POLYETHYLENE GLYCOL (PEG)-CATALASE TO AMELIORATE MeHg-INITIATED APOPTOSIS	84
FIGURE 4.	INCREASED NUMBER OF <i>Ogg1</i> ^{-/-} CELLS WITH ELEVATED MeHg-INITIATED γ H2AX AND REDUCTION OF DNA DAMAGE BY PEG-CATALASE PRETREATMENT	87
FIGURE 5.	INCREASED NUMBER OF <i>Ogg1</i> ^{-/-} CELLS WITH ELEVATED MeHg-INITIATED ATM PHOSPHORYLATION AT SERINE 1981	90

Study 2.

FIGURE 1.	SIMIAN VIRUS 40 (SV40) LARGE T ANTIGEN-IMMORTALIZED OXOGUANINE GLYCOSYLASE 1-NULL (<i>Ogg1</i> ^{-/-}) CELLS DEMONSTRATE REDUCED CLONOGENIC SURVIVAL FOLLOWING EXPOSURE TO METHYLMERCURY (MeHg)	107
FIGURE 2.	SV40 LARGE T ANTIGEN-IMMORTALIZED WILD-TYPE CELLS SEEDING AT EXPONENTIALLY GROWING AND CONFLUENT DENSITIES	110
FIGURE 3.	INCREASED CELL SEEDING DENSITY LEADS TO IMPAIRED PROLIFERATION AND ATTENUATES THE SUSCEPTIBILITY OF WILD-TYPE AND <i>Ogg1</i> ^{-/-} CELLS TO MeHg-INITIATED CELL CYCLE ARREST	112
FIGURE 4.	MeHg-INITIATED H2AX PHOSPHORYLATION AT SERINE 139 (γ H2AX) ACCUMULATION IN SV40 LARGE T ANTIGEN-IMMORTALIZED WILD-TYPE AND <i>Ogg1</i> ^{-/-} CELLS PERSISTS AND IS DEPENDENT ON CELLULAR PROLIFERATION CAPACITY	115
FIGURE 5.	MeHg-INITIATED MICRONUCLEUS FORMATION IN WILD-TYPE AND <i>Ogg1</i> ^{-/-} CELLS IS ALSO DEPENDENT ON CELLULAR PROLIFERATION CAPACITY AND FUNCTIONALLY CONFIRMS γ H2AX RESULTS	118

Study 3.

FIGURE 1.	ANTI-FLAG-MEDIATED WESTERN BLOTTING CONFIRMS STABLE NUCLEAR (N) AND MITOCHONDRIAL (Mt) EXPRESSION OF HUMAN OXOGUANINE GLYCOSYLASE 1 (hOgg1)-FLAG AND FORMAMIDOPYRIMIDINE GLYCOSYLASE (Fpg)-FLAG PROTEINS	135
FIGURE 2.	hOgg1- AND Fpg-EXPRESSING HEK 293 CELLS DEMONSTRATE REDUCED CLONOGENIC SURVIVAL FOLLOWING ACUTE EXPOSURE TO METHYLMERCURY (MeHg)	138

FIGURE 3.	hOgg1- AND Fpg-EXPRESSING HEK 293 CELLS DEMONSTRATE REDUCED CELL GROWTH BOTH BASALLY, AND FOLLOWING ACUTE MeHg EXPOSURE.....	141
FIGURE 4.	MeHg-INITIATED CYTOTOXICITY MEASURED AS LACTATE DEHYDROGENASE (LDH) RELEASE IS EXACERBATED IN hOgg1- AND Fpg-EXPRESSING HEK 293 CELLS.....	144
FIGURE 5.	MeHg ENHANCES REACTIVE OXYGEN SPECIES (ROS) FORMATION IN WILD-TYPE CELLS WITH A SUSTAINED ELEVATION PERSISTING AT 24 H.....	147
FIGURE 6.	hOgg1- AND Fpg-EXPRESSING HEK 293 CELLS HAVE CONSTITUTIVELY LOWER LEVELS OF 8-OXO-2'-DEOXYGUANOSINE (8-OXODG), BUT APPEAR TO ACCUMULATE 8-OXODG TO A GREATER DEGREE UPON ACUTE MeHg EXPOSURE COMPARED TO WILD-TYPE CELLS.....	150
FIGURE 7.	APURINIC/APYRIMIDINIC (AP) SITE FORMATION IS EXACERBATED IN hOgg1- AND Fpg-EXPRESSING HEK 293 CELLS UPON ACUTE EXPOSURE TO MeHg COMPARED TO WILD-TYPE CELLS.....	153

LIST OF ABBREVIATIONS

1meA	1-methyladenine
3meA	3-methyladenine
3meC	3-methylcytosine
6meG	O6-methylguanine
8-OHdG	8-hydroxy-2'-deoxyguanosine (enol tautomer) (without sugar: 8-hydroxyguanine; 8-OHG)
8-oxodG	8-oxo-2'-deoxyguanosine (keto tautomer; full name: 7,8-dihydro-8-oxo-2'-deoxyguanosine) (without sugar: 8-oxoguanine/7,8-dihydro-8-oxoguanine; 8-oxoG)
ALA-D	delta-aminolevulinate dehydratase
AP	apurinic/apyrimidinic
APC	anaphase-promoting complex
APE1	apurinic/apyrimidinic endonuclease 1
APV	D-2-amino-5-phosphonovaleric acid
ATM	ataxia telangiectasia mutated
ATR	ataxia telangiectasia and Rad3-related protein
BAPTA	1,2-bis(2-aminophenoxy)ethane-N,N,N',N'-tetraacetic acid tetrakis(acetoxymethyl)ester
bcl-2	B-cell lymphoma 2
BCNU	1,3-N,N'-bis(2-chloroethyl)-N-nitrosourea
BER	base excision repair
BrdU	bromodeoxyuridine
Ca ²⁺	calcium
CAT	catalase
CBP	CREB1-binding protein
CCBR	Centre for Cellular and Biomolecular Research

Cdk	cyclin-dependent kinase
CdkC	cyclin-dependent kinase complex
CFIA	Canadian Food Inspection Agency
$\text{CH}_3\text{CH}_2\text{Hg}^+$	ethylmercury
$\text{CH}_3\text{CH}_3\text{Hg}$	dimethylmercury
CM-H ₂ DCFDA	5-(and-6)-chloromethyl-2',7'-dichlorodihydrofluorescein diacetate acetyl ester
CNP	2',3'-cyclic nucleotide phosphohydrolase
CNS	central nervous system
DAPI	4'-6-diamidino-2-phenylindole
DCF	dichlorodihydrofluorescein
DCM	Division of Comparative Medicine
DEM	diethyl maleate
dG	deoxyguanosine
DMSO	dimethyl sulfoxide
DNA-PK	DNA-dependent protein kinase
DR	direct reversal
dRP	deoxyribose phosphate
DSB	double-strand break
DTT	dithiothreitol
EAA	excitatory amino acid
EPA	United States Environmental Protection Agency
FACS	fluorescence-activated cell sorting
Fapy	formamidopyrimidine
FapyA	4,6-diamino-5-formamidopyrimidine
FapyG	2,6-diamino-4-hydroxy-5-formamidopyrimidine

FBS	fetal bovine serum
FEN1	flap endonuclease 1
FITC	fluorescein isothiocyanate
<i>Fpg</i> ; Fpg	formamidopyrimidine glycosylase (gene; protein)
G6PD	glucose-6-phosphate dehydrogenase
GAD	glutamic acid decarboxylase
GD	gestational day
GGR	global genome repair
γ H2AX	variant H2A histone H2AX phosphorylated at serine 139
GLU	glutamate
GPx	glutathione peroxidase
GR	glutathione reductase
GSH	reduced glutathione
GSSG	oxidized glutathione, glutathione disulfide
H ₂ O ₂	hydrogen peroxide
HCG	human chorionic gonadotropin
HEK	human embryonic kidney cells
Hg ⁰	elemental or metallic mercury
Hg ¹⁺	mercurous mercury
Hg ²⁺	mercuric mercury
HhH-GPD	helix-hairpin-helix element with a glycine/proline-rich loop and a conserved aspartic acid motif
<i>hOgg1</i> ; hOGG1/hOgg1	human oxoguanine glycosylase 1 (gene; protein)
HPLC-UV	high-performance liquid chromatography with detection by ultraviolet absorbance
HR	homologous recombination
IHC	immunohistochemistry

i.p.	intraperitoneal
KSOM	potassium simplex optimized medium
LAT1	L-type large neutral amino acid transporter 1
LDH	lactate dehydrogenase
LIG	DNA ligase
LPO	lipoxygenase
M	mitosis
MAPK	mitogen-activated protein kinase
MeHg; CH ₃ Hg ⁺	methylmercury
MEF	murine embryonic fibroblast
MLS	mitochondrial localization signal
MMR	mismatch repair
Mn-SOD	manganese superoxide dismutase
mRNA	messenger ribonucleic acid
Mt	mitochondrial
MTH1	MutT homolog 1
MTT	3-[4,5-dimethylthiazol-2-yl]-2,5-diphenyl tetrazolium bromide
MutYH; MYH	MutY homolog
N	nuclear
NAC	N-acetylcysteine
NADPH	nicotinamide adenine dinucleotide phosphate
NEIL	nei (endonuclease VIII)-like proteins
NER	nucleotide excision repair
NF-κB	nuclear factor kappa B
NHEJ	non-homologous end joining
NLS	nuclear localization signal

NMDA	N-methyl D-aspartate
NOX	nicotinamide adenine dinucleotide phosphate oxidase
O ₂	molecular oxygen
O ₂ ^{•-}	superoxide anion
<i>Ogg1</i> ; OGG1/Ogg1	oxoguanine glycosylase 1 (gene; protein)
<i>Ogg1</i> ^{-/-}	oxoguanine glycosylase 1- <i>null</i>
[•] OH	hydroxyl radical
P450	cytochromes P450 (current abbreviation: CYP)
pATM	ataxia telangiectasia mutated phosphorylated on serine 1981
PBN	α-phenyl-N-tert-butyl nitron
PCB	polychlorinated biphenyl
PCNA	proliferating cell nuclear antigen
PEG-catalase	polyethylene glycol-conjugated catalase
PHS	prostaglandin H synthase
PI	propidium iodide
PMSG	pregnant mares' serum gonadotropin
Polβ	DNA polymerase β
Rb	retinoblastoma protein
ROS	reactive oxygen species
SOD	superoxide dismutase
SOPF	specific and opportunistic pathogen free
SSB	single-strand break
SV40	Simian virus 40
T _{1/2}	Half-life
TBST	tris-buffered saline
TCP	Toronto Centre for Phenogenomics

TCR	transcription-coupled repair
Tg	thymine glycol
Tg/+	heterozygous transgenic human oxoguanine glycosylase 1-expressing mouse
U	uracil
XO	xanthine oxidase
XRCC	X-ray cross-complementing

LIST OF PUBLICATIONS AND PRESENTATIONS ARISING FROM THIS THESIS

Refereed Papers

- 1. McCallum GP, Siu M, Ondovcik SL, Sweeting JN and Wells PG** (2011) Methanol exposure does not lead to accumulation of oxidative DNA damage in bone marrow or spleen of mice, rabbits or primates. *Molecular Carcinogenesis* 50(3): 163-172.
- 2. Ondovcik SL, Tamblyn L, McPherson, JP and Wells PG** (2012) Oxoguanine glycosylase 1 (OGG1) protects cells from DNA double-strand break damage following methylmercury (MeHg) exposure. *Toxicological Sciences* 128(1): 272-283.
- 3. Ondovcik SL, Tamblyn L, McPherson, JP and Wells PG** (2012) Sensitivity to methylmercury toxicity is enhanced in oxoguanine glycosylase 1 knockout murine embryonic fibroblasts and is dependent on cellular proliferation capacity. (submitted)
- 4. Ondovcik SL, Preston TJ, McCallum, GP and Wells PG** (2012) Expression of human oxoguanine glycosylase 1 (hOgg1) or formamidopyrimidine glycosylase (Fpg) in human embryonic kidney (HEK) 293 cells exacerbates methylmercury (MeHg) toxicity *in vitro*. (submitted)

Invited Review

- 1. Wells PG, McCallum GP, Lam KCH, Henderson JT and Ondovcik SL** (2010) Oxidative DNA damage and repair in teratogenesis and neurodevelopmental deficits. *Birth Defects Research Part C: Embryo Today: Reviews* 90(2): 103-109.

Abstracts

- 1. Ondovcik SL, Preston TJ, McCallum GP and Wells PG** (2007) Effect of altered DNA repair status on methylmercury-initiated oxidative DNA damage and cytotoxicity. *Birth Defects Research Part A: Clinical and Molecular Teratology* 79(5): 416 (P21).
- 2. Ondovcik SL, Preston TJ, Ho SK, Henderson JT, Lam K and Wells PG** (2008) A novel transgenic mouse model expressing a human enzyme for repair of oxidative DNA damage. *Toxicological Sciences (Supplement: The Toxicologist)* 102(1): 46 (No. 226).

3. McCallum GP, Siu M, Ondovcik SL and Wells PG (2010) Methanol exposure does not lead to accumulation of oxidative DNA damage in mice, rabbits or primates. *Toxicological Sciences (Supplement: The Toxicologist)* 114(1): 150 (No. 708).

4. Ondovcik SL, McCallum GP and Wells PG (2010) Effect of deficient base excision repair (BER) status on methylmercury (MeHg)-initiated toxicity *in vitro*. *Toxicological Sciences (Supplement: The Toxicologist)* 114(1): 150 (No. 705).

5. Ondovcik SL, Tamblyn L, McPherson, JP and Wells PG (2012) Oxoguanine glycosylase 1 (OGG1) protects cells from DNA double-strand break damage following methylmercury (MeHg) exposure. *FASEB J* 26: (No. 1050.10).

6. Wells PG, Abramov JP, Lam KCH, Miller, L, McPherson JP, Ondovcik SL, Ramkissoon A, Shapiro AM, Siu M, Sweeting JN and Wiley MJ (2012) Embryonic and fetal biochemical determinants of reactive oxygen species-mediated chemical teratogenesis and neurodevelopmental deficits. *Proceedings of the 7th Meeting of the Canadian Oxidative Stress Consortium*, p. 43, Lakehead University, Thunder Bay, Ontario, May.

CHAPTER 1: INTRODUCTION

1.1 RATIONALE AND RESEARCH OBJECTIVES

Methylmercury (**MeHg**) is a potent neurotoxin, teratogen and probable carcinogen, most notorious for the large-scale outbreaks of human poisoning in Minamata Bay, Japan, and in Iraq. Today, exposure to MeHg occurs primarily via dietary consumption of fish and seafood, and remains a significant health concern given that a lowest observed adverse effect level has yet to be established for more subtle outcomes following low dose MeHg exposure scenarios akin to those in fish eating populations (Castoldi *et al.*, 2001). Moreover, despite considerable research, the precise underlying molecular mechanisms of MeHg's potent neurotoxic action remain to be elucidated. Although reactive oxygen species (**ROS**), their pathogenic consequences and MeHg's effects on the cell cycle have been at the forefront of many investigations, there have been no studies examining the effects of variable base excision repair (**BER**) capacity on MeHg toxicity. Given that with compromised DNA repair, ROS-mediated DNA damage can not only lead to mutations, but may also have other non-mutational effects resulting in gene expression changes, some of which may be critical for the development, organization, function and defense of the adult central nervous system and/or the embryo and fetus, it is plausible that this may constitute a major determinant of risk for MeHg toxicity (Wells *et al.*, 2010). A better understanding of the precise molecular mechanisms underlying MeHg toxicity will enable the identification of novel risk factors, and provide more a definitive basis for public health recommendations regarding environmental exposure to MeHg.

Accordingly, this research employs reciprocal *in vitro* cellular models with deficient [oxoguanine glycosylase 1-*null* (**Ogg1**^{-/-}) murine embryonic fibroblasts (**MEFs**)] and enhanced [human oxoguanine glycosylase 1 (**hOgg1**)- or formamidopyrimidine glycosylase (**Fpg**)-expressing human embryonic kidney (**HEK**) cells] ability to repair oxidatively damaged DNA. These models of altered BER capacity were used to delineate the contribution of ROS-mediated oxidatively damaged DNA and cellular proliferation capacity in the mechanism of MeHg toxicity, and to additionally probe the role of DNA repair status as a potential risk factor for MeHg-mediated toxicity.

My hypothesis was that ROS-mediated oxidatively damaged DNA contributes in part to the mechanism of MeHg toxicity *in vitro*, with toxicity additionally dependent upon cellular proliferative capacity and DNA repair status, whereby actively proliferating cells such as in the

developing embryo and fetus, and cells with compromised DNA repair capacity, would be more sensitive to MeHg-mediated toxicity and vice versa.

My objectives, also depicted schematically in **Figure 1**, were as follows:

1. To assess the contribution of ROS and deficient DNA repair status in the mechanism of MeHg toxicity in **spontaneously**-immortalized wild-type and *Ogg1*^{-/-} MEFs. My results offered the first report of an increased sensitivity of DNA repair-deficient cells to MeHg, which was blocked by the antioxidative enzyme catalase, and constituted the most direct evidence to date that ROS-mediated clastogenic DNA damage may contribute to the pathological consequences of MeHg exposure via a non-mutagenic mechanism, suggesting that interindividual variability in repair activity and antioxidant capacity may modulate the risk of toxicological consequences.
2. To first solidify our previous findings of an increased sensitivity of spontaneously-immortalized *Ogg1*^{-/-} MEFs to MeHg through generation of **Simian virus 40 (SV40) large T antigen**-immortalized wild-type and *Ogg1*^{-/-} MEFs; and secondly to employ these cells in determining whether MeHg toxicity is proliferation-dependent. My results using this new cell model provided the first corroborating and mechanistically most definitive evidence that Ogg1 status is a critical modulator of risk for MeHg toxicity, with susceptibility persisting in *Ogg1*^{-/-} MEFs independent of cellular immortalization method; an important observation given that different means of cellular transformation may yield distinct phenotypes (Kelekar and Cole, 1987; Boukamp *et al.*, 1988; Pecoraro *et al.*, 1989). This study also demonstrated for the first time that the increased susceptibility of *Ogg1*^{-/-} MEFs to MeHg-mediated DNA damage is additionally dependent on cellular proliferation, suggesting that variations in proliferative capacity and interindividual variability in repair activity may modulate the risk of toxicological consequences.
3. To further evaluate the contribution of ROS and oxidatively damaged DNA in the mechanism of MeHg toxicity in a reciprocal model of enhanced DNA repair employing HEK 293 cells expressing hOgg1 or Fpg. My results served as the first report of a seemingly paradoxical increased sensitivity of hOgg1- and Fpg-expressing cells to MeHg-mediated cytotoxicity, supporting a role for ROS-mediated oxidatively damaged

DNA in the mechanism of MeHg toxicity, and implicating interindividual variations in DNA repair activity as a significant determinant of risk.

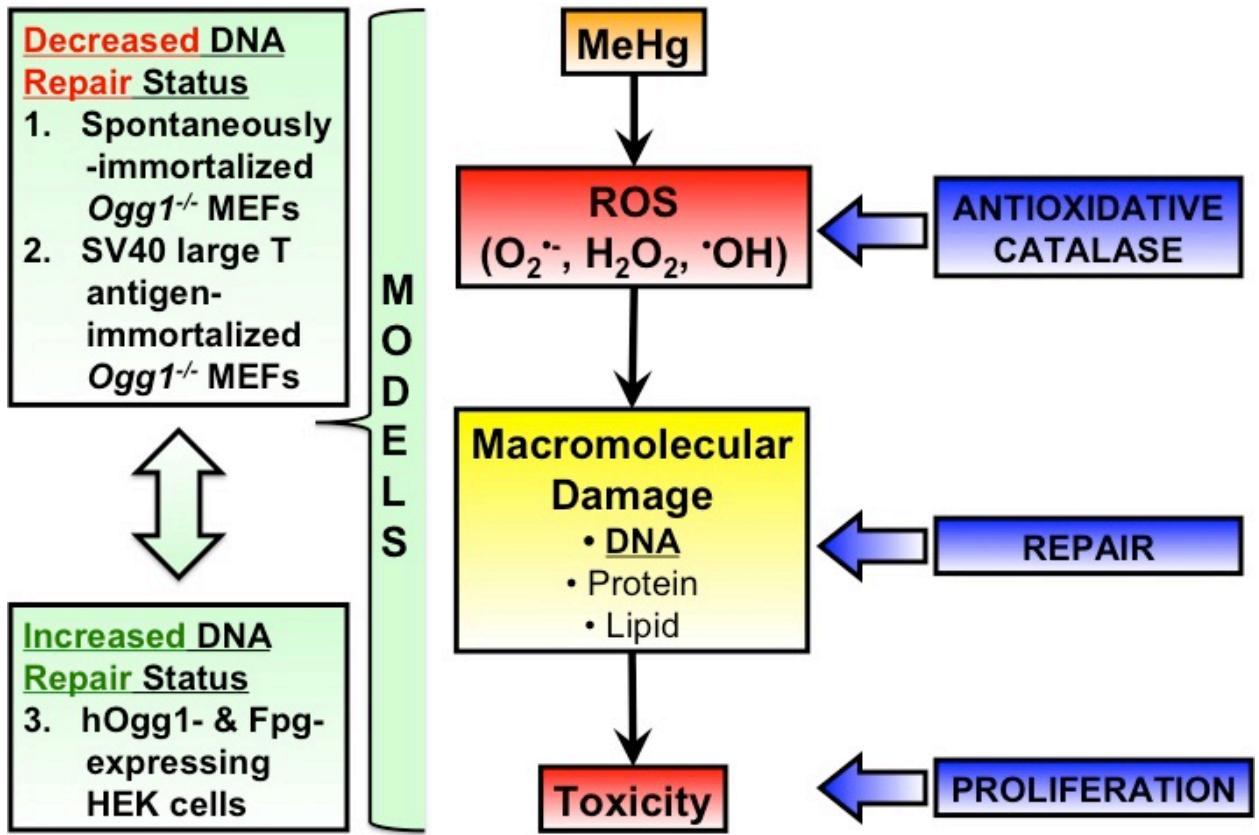


Figure 1. Schematic outlining the thesis objectives.

1.2 REACTIVE OXYGEN SPECIES

1.2.1 Overview of reactive oxygen species

Reactive oxygen species (**ROS**) collectively refer to oxygen radicals such as superoxide anion ($\text{O}_2^{\bullet-}$) and the hydroxyl radical ($\bullet\text{OH}$), as well as non-radical oxidants with radical-forming potential such as hydrogen peroxide (H_2O_2) (Buonocore *et al.*, 2010; Miller *et al.*, 1990). These are the three most common ROS and vary significantly in their reduction potentials, half-lives and physiological concentrations, lending to their varied effects within biological systems (**Fig. 2**). Of the three, H_2O_2 is the least reactive and found at the highest concentration *in vivo*, and thus is the principal player in ROS-mediated signal transduction (Giorgio *et al.*, 2007) (**Fig. 2**). $\text{O}_2^{\bullet-}$ is primarily formed by one electron reduction of molecular oxygen (O_2) during cellular respiration within the mitochondrial electron transport chain, but can also result from heme oxidation and the action of oxidative enzymes such as dihydrorotate dehydrogenase, aldehyde oxidase, xanthine oxidase (**XO**) and nicotinamide adenine dinucleotide phosphate (**NADPH**) oxidases (**NOXs**) (Buonocore *et al.*, 2010). Due to its inherent reactivity, $\text{O}_2^{\bullet-}$ is considered a primary ROS capable of interacting directly, or indirectly through enzyme- or metal-catalyzed processes, with other molecules to spawn more ROS, as in the case of H_2O_2 generation via superoxide dismutase (**SOD**)-mediated oxidation of $\text{O}_2^{\bullet-}$ (Buonocore *et al.*, 2010). $\bullet\text{OH}$ is the most reactive form of ROS and is produced largely under conditions of excess $\text{O}_2^{\bullet-}$ and H_2O_2 in the Haber-Weiss reaction, but can also be formed from ionizing radiation-mediated water decomposition, photolytic breakdown of alkylhydroperoxides and metal-catalyzed H_2O_2 decomposition via the Fenton reaction (Buonocore *et al.*, 2010). ROS are largely regarded as a double-edged sword whereby they are required at physiological levels for beneficial cellular processes including host defense, signal transduction and mitogenic response induction; however, when the production of ROS overpowers the cell's defense mechanisms, a state of oxidative stress ensues resulting in oxidative damage to cellular macromolecules and aberrant cell signaling (Buonocore *et al.*, 2010; Droge, 2002; Valko *et al.*, 2007).

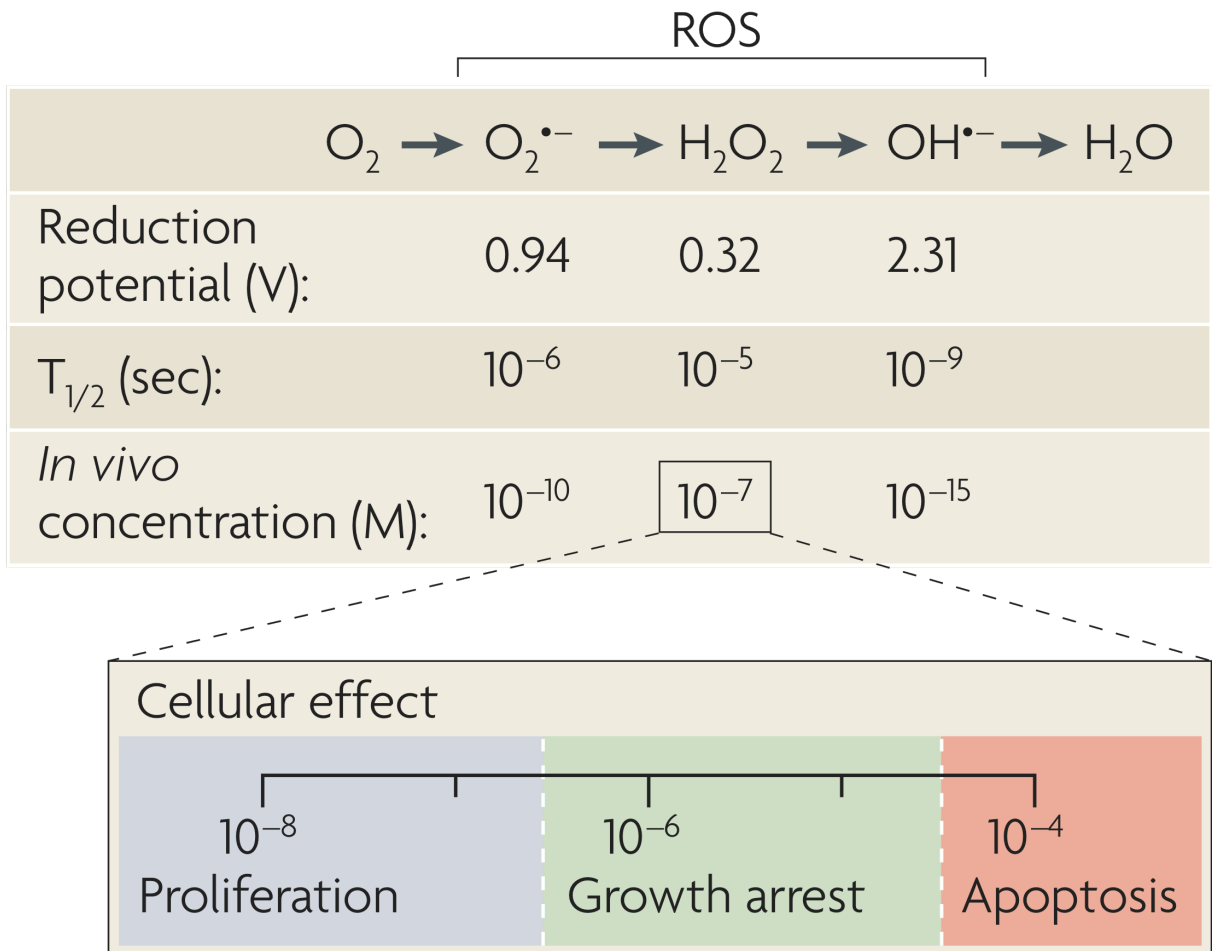


Figure 2. The O_2 reduction pathway and the family of reactive oxygen species.

From: Giorgio et al., 2007 with permission.

1.2.2 Sources of reactive oxygen species

ROS originate from a variety of endogenous sources within the cell, yet their formation can also be influenced and mediated by exogenous factors (**Fig. 3**).

1.2.2.1 Endogenous sources of ROS

Given that ROS have a vast array of physiological functions within biological systems, a number of endogenous sources for their production exist (**Fig. 3**). The primary site for endogenous ROS generation is during cellular respiration within the mitochondrial electron transport chain (Buonocore *et al.*, 2010). However, a number of other metabolic enzymes yield ROS via endogenous substrate metabolism including cytochromes P450 (**P450**), XO, nitric oxide synthase, the monooxygenase system and NOXs (Buonocore *et al.*, 2010). Additionally, peroxisomes, microsomes and activated inflammatory cells (neutrophils, eosinophils and macrophages) can also contribute to endogenous ROS production, as can the presence of free metals assisting in the catalysis of endogenous ROS and its amplification (Buonocore *et al.*, 2010). ROS production by endogenous sources can also be stimulated by an ischemic episode, such as a myocardial infarction, in an ischemic-reperfusion injury (Kahles and Brandes, 2012).

1.2.2.2 Exogenous sources of ROS

A variety of exogenous factors can influence and mediate ROS formation, particularly environmental agents such as radiation and xenobiotics (Buonocore *et al.*, 2010; Kahles and Brandes, 2012; Wells *et al.*, 2005) (**Fig. 3**). Ionizing radiation-mediated ROS result directly from the ionization and excitation of water forming water radiolysis products such as $\cdot\text{OH}$ and H_2O_2 ; however, radiation can also stimulate the formation of ROS by endogenous biological sources through the upregulation of mitochondrial electron transport chain function (Riley, 1994; Yamamori *et al.*, 2012). Xenobiotics can be bioactivated by enzymes such as P450s, prostaglandin H synthases (**PHSs**) and lipoxygenases (**LPOs**) to free radical intermediates that can subsequently react with molecular oxygen to form ROS, or alternatively may undergo NADPH P450 reductase-catalyzed bioactivation to a semiquinone intermediate capable of redox cycling and generating ROS in the process (Wells *et al.*, 2009) (**Fig. 4**).

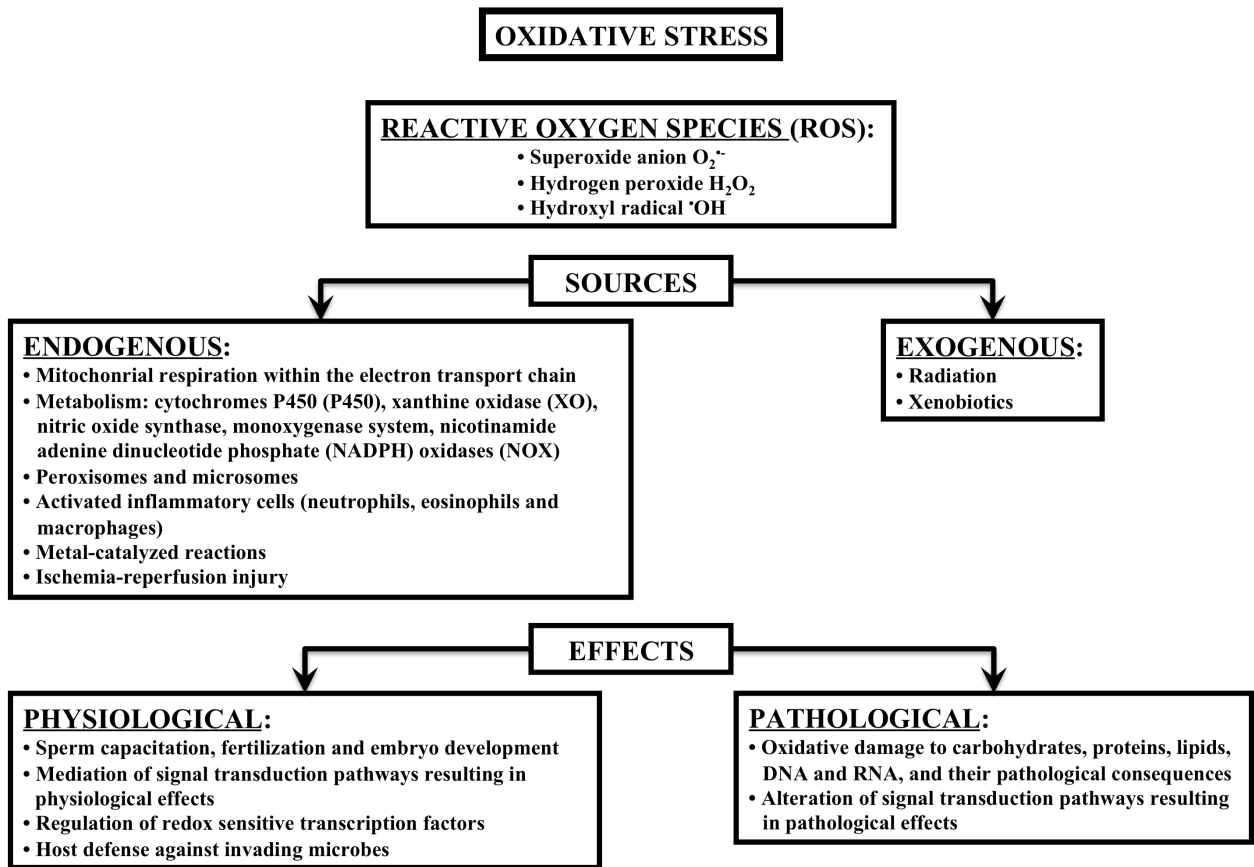


Figure 3. Sources of ROS and the general mechanisms by which oxidative stress can alter cellular function.

Modified from: Buonocore et al., 2010 and Wells et al., 2009 with permission.

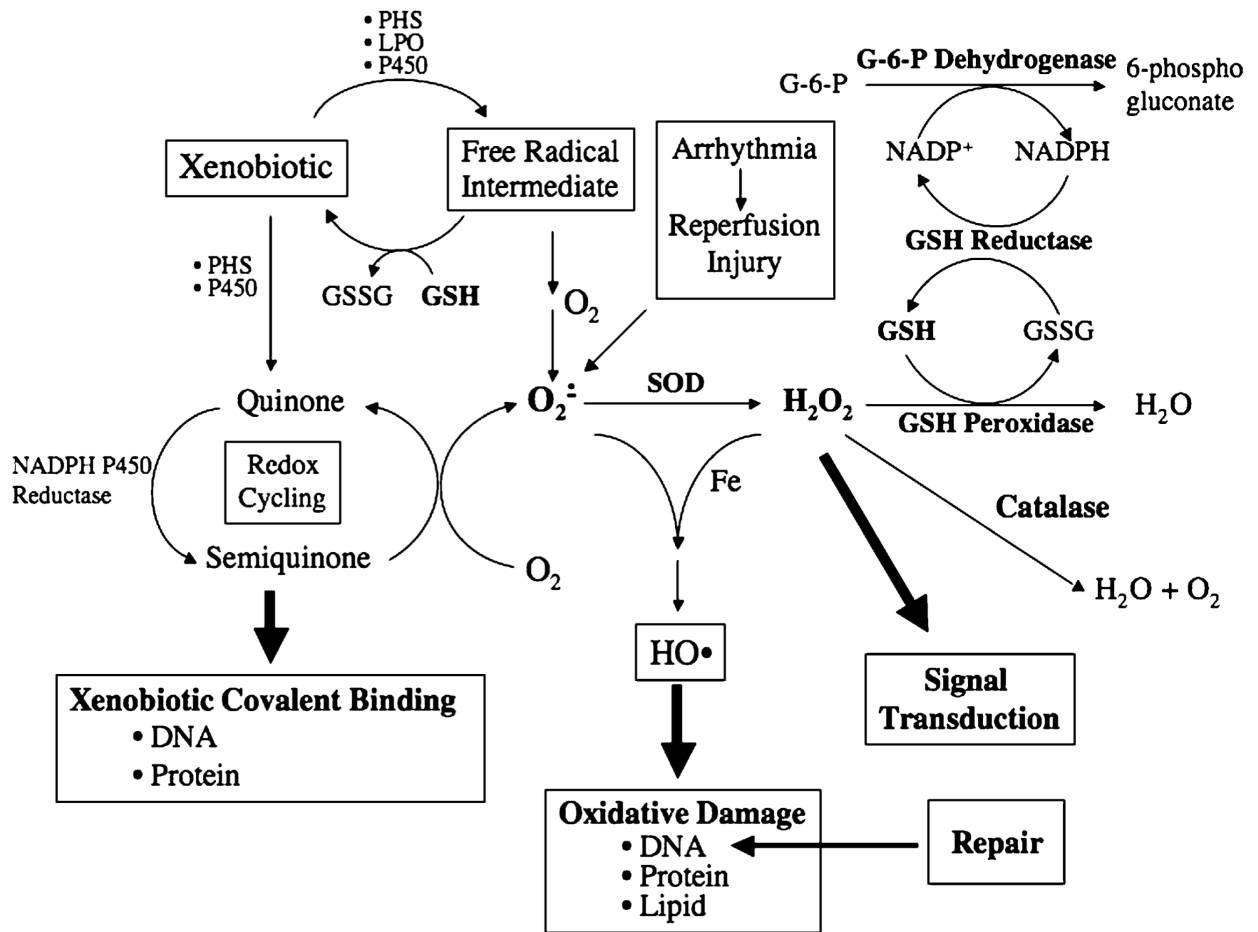


Figure 4. Biochemical pathways for the formation, detoxification and cellular effects of xenobiotic free radical intermediates and ROS.

Abbreviations: Fe, iron; GSH, glutathione; GSSG, glutathione disulfide; H_2O_2 , hydrogen peroxide; $\cdot OH$, hydroxyl radical; $NADP^+$, nicotinamide adenine dinucleotide phosphate; $O_2^{\cdot-}$, superoxide; SOD, superoxide dismutase; P450, cytochromes P450; PHS, prostaglandin H synthase; LPO, lipoxygenase; G-6-P, glucose-6-phosphate; G6PD, glucose-6-phosphate dehydrogenase.

From: Wells et al., 2009 with permission.

1.2.3 Antioxidative defense mechanisms

A number of enzymatic and non-enzymatic antioxidative defense mechanisms are in place to maintain a tight balance between the formation and detoxification of ROS, thereby limiting oxidative stress and its pathological consequences. Of important note is the limited antioxidative capacity of the developing embryo and fetus, with the activity of enzymes like SOD and catalase (**CAT**) amounting to only 5% of maternal activity, thus rendering the conceptus particularly susceptible to ROS-mediated insult (Wells *et al.*, 2005).

1.2.3.1 Enzymatic detoxification of ROS

Cells have evolved an interrelated network of enzymatic detoxification mechanisms to maintain ROS at physiological levels (**Fig. 4**). Levels of $O_2^{\cdot-}$ are kept in check through the action of SOD, which is responsible for catalyzing its dismutation into H_2O_2 and O_2 (Al-Gubory *et al.*, 2010; Chance *et al.*, 1979; Wells *et al.*, 2009). However, hyperactive SOD can lead to an increased production of H_2O_2 that can subsequently combine with $O_2^{\cdot-}$ to produce $\cdot OH$ via an iron-mediated Haber-Weiss reaction. Thus, regulation of H_2O_2 is critical in limiting the propagation of ROS and is achieved by the antioxidative action of **CAT** and glutathione peroxidase (**GPx**). **CAT** mediates the decomposition of H_2O_2 to water and O_2 , while **GPx** converts H_2O_2 to water using the reducing power of glutathione (**GSH**) (Al-Gubory *et al.*, 2010; Chance *et al.*, 1979; Wells *et al.*, 2009). A number of key enzymes are responsible for maintaining GSH homeostasis allowing its direct use as an antioxidant, and as a cofactor for **GPx**-mediated H_2O_2 detoxification. These include GSH reductase (**GR**) which uses the reducing power of NADPH to return oxidized GSH (**GSSG**) to its reduced state (GSH), and glucose-6-phosphate dehydrogenase (**G6PD**) which maintains adequate levels of NADPH for cellular redox reactions (Al-Gubory *et al.*, 2010; Chance *et al.*, 1979; Wells *et al.*, 2009). Together, the concerted efforts of these enzymes ensure the maintenance of homeostatic levels of ROS.

1.2.3.2 Non-enzymatic detoxification of ROS

In addition to the enzymatic detoxification of ROS, a number of non-enzymatic molecules possess antioxidative properties rendering them effective combatants against ROS.

Table 1 summarizes the scavenging effects of the micronutrients vitamin E (α -tocopherol), vitamin C (ascorbic acid) and carotenoids such as β -carotene and lycopene, as well as the trace elements zinc, selenium, copper, iron and manganese, which are indirect antioxidants by virtue of their necessity in the aforementioned antioxidative enzyme systems. More recently, dietary-derived polyphenols have garnered much attention for their antioxidant potential. These include the flavonoids catechins, resveratrol, quercetin, anthocyanins and hesperitin derivatives, as well as phenolic acids such as phytic, caffeic and chlorogenic acids (Al-Gubory *et al.*, 2010). Phytic acid, for example, forms an iron chelate thereby limiting iron-catalyzed oxidative reactions, particularly $\cdot\text{OH}$ formation, and also inhibits polyphenol oxidase, which is responsible for the browning of fruits and vegetables via oxidation of phenolic compounds to reactive quinone metabolites, thus rendering it a useful preservative (Al-Gubory *et al.*, 2010; Graf and Eaton, 1990). Similarly, other iron chelators such as desferoxamine have antioxidative properties given their ability to limit iron-mediated $\cdot\text{OH}$ generation (Wells *et al.*, 2005). GSH is possibly one of the most critical cellular antioxidants serving as a reducing agent in GPx-mediated reduction reactions, and also possessing the ability to directly react with free radical reactive intermediates, blocking their initiation of subsequent ROS formation (Pompella *et al.*, 2003; Wells *et al.*, 2009). Likewise, free radical spin trapping agents such as phenyl N-tert-butyl nitron (**PBN**) serve an antioxidative role by quenching free radicals and attenuating their propagation, and have been shown to mitigate ROS-mediated teratogenesis and oxidative damage *in vivo* (Pompella *et al.*, 2003; Wells *et al.*, 2009). Thus, both enzymatic and non-enzymatic antioxidant defense systems are critical in combating the pathogenic effects of ROS.

Table 1. Antioxidant micronutrients.

Nutrient	Activity
Vitamin C (ascorbic acid)	Important water-soluble cytosolic chain-breaking antioxidant; reacts directly with superoxide, singlet oxygen; regenerates tocopherol from tocopheroxy radical
Vitamin E (α -tocopherol)	Major membrane-bound, lipid-soluble chain-breaking antioxidant; reacts directly with superoxide, singlet oxygen
β -Carotene	Most potent singlet oxygen quencher, antioxidant properties particularly at low oxygen pressure, lipid soluble
Zinc	Constituent of cytosolic superoxide dismutase
Selenium	Constituent of glutathione peroxidase
Copper	Constituent of cytosolic superoxide dismutase and ceruloplasmin
Iron	Constituent of catalase
Manganese	Constituent of mitochondrial superoxide dismutase

From: Machlin et al., 1987 with permission.

1.2.4 Effects of ROS

The effects of ROS within biological systems are highly tissue-, cell-, time- and stimulus-specific. At physiological levels, ROS are vital for a number of essential cellular processes (**Fig. 3**). However, when the production of ROS exceeds the antioxidative capacity of the cell, a state of oxidative stress ensues leading to oxidative macromolecular damage, aberrant cell signaling and potentially altered cellular function and cell death (**Figs. 3 and 4**).

1.2.4.1 Physiological effects of ROS

Figure 3 provides a representative summary of the numerous physiologically relevant roles of ROS. These roles largely involve H₂O₂-mediated signaling via the selective oxidation of protein sulfhydryl groups that result in various molecular modifications such as the formation of protein-protein and GSH-protein mixed disulfides (Wells *et al.*, 2009). These are enzymatically reversible at physiological H₂O₂ concentrations, but may have pathological consequences under conditions of oxidative stress with excessive S-oxidation as discussed below (Wells *et al.*, 2009). ROS-mediated signal transduction facilitates the actions of various growth factors, cytokines, pro-apoptotic factors and calcium signaling (Auten and Davis, 2009). ROS can initiate apoptosis intrinsically by the mitochondrial pathway or extrinsically via membrane-associated death receptors, a process essential to normal embryonic development (Al-Gubory *et al.*, 2010). ROS also have important roles in sperm capacitation, fertilization and embryonic development due to their ability to regulate redox-sensitive transcription factors associated with the expression of genes necessary for these processes (Buonocore *et al.*, 2010). Lastly, ROS play a vital role in host defense due to the antimicrobial action of O₂^{•-} generated by NOX in neutrophils and macrophages (Al-Gubory *et al.*, 2010; Buonocore *et al.*, 2010; Nauseef, 2008).

1.2.4.2 Pathological effects of ROS

When the physiological balance is tipped in favor of ROS production, excessive ROS are available to oxidatively damage cellular macromolecules, including carbohydrates, proteins, lipids, DNA and RNA, the consequences of which can include altered cellular function or cell death (**Figs. 3 and 4**). Oxidative damage to proteins can result in loss of structural integrity

and/or enzymatic activity, and the inability to carry out their designated cellular function (Stadtman and Levine, 2000). Elevated levels of oxidized proteins, as measured by protein carbonyls, have been documented in a variety of diseases, notably ageing (Stadtman and Levine, 2000). Lipid membrane integrity can be compromised upon oxidative attack, and lipid peroxidation can also lead to apoptosis via sphingomyelinase activation, ceramide release and phosphorylation of pro-apoptotic mitogen-activated protein kinases (**MAPK**), or by direct action on mitochondria and their release of pro-apoptotic factors (Fruhworth and Hermetter, 2008). Of particular importance to this thesis are the pathogenic effects of oxidatively damaged DNA, which will be covered in greater detail in section 1.4. This damage can take the form of DNA lesions like 8-oxo-2'-deoxyguanosine (**8-oxodG**), DNA single- or double-strand breaks, DNA cross-links, and purine, pyrimidine or deoxyribose modifications, damage which has been implicated in mutagenesis, altered transcription and gene expression, aberrant cell signaling and genomic instability that may ultimately lead to the development of cancer, teratogenesis and/or neurodegeneration (Buonocore *et al.*, 2010; Khobta *et al.*, 2010; Kitsera *et al.*, 2011; Marnett, 2000; Pastoriza-Gallego *et al.*, 2007; Wells *et al.*, 2009).

As described above, physiological levels of H_2O_2 are essential for normal cell signaling cascades; however, a state of oxidative stress can lead to aberrant signal transduction (**Figs. 3 and 4**). This theory is supported by evidence from studies examining the mechanism of thalidomide teratogenesis, the hallmark of which is shortened limbs. Thalidomide, a known ROS-generator, was found to inhibit the redox-sensitive transcription factor nuclear factor kappa B (**NF- κ B**), which is critical in initiating the expression of genes involved in limb bud outgrowth (Hansen, 2006; Hansen *et al.*, 2002a; Hansen *et al.*, 2002b). Moreover, NF- κ B activity, and expression of associated genes, was restored when thalidomide was given in combination with the free radical spin trap PBN or the GSH precursor N-acetylcysteine (**NAC**) (Hansen, 2006; Hansen *et al.*, 2002a; Hansen *et al.*, 2002b). Similarly, the ability of antisense oligonucleotides against NF- κ B to block ROS-mediated elevations in NF- κ B activity and embryopathies caused by another ROS-initiating teratogen, the antiepileptic drug phenytoin, suggests an equally important pathological role for ROS-mediated signal transduction (Kennedy *et al.*, 2004; Wells *et al.*, 2009).

1.3 METHYLMERCURY OVERVIEW

1.3.1 Comparison of the chemical forms of mercury

Mercury is a complex transition metal that can take on many chemical forms and can also be converted between species both in the environment as well as *in vivo*. The most common and environmentally relevant forms of mercury from a toxicological standpoint are: inorganic forms such as elemental or metallic mercury (Hg^0), mercurous mercury (Hg^{1+}) and mercuric mercury (Hg^{2+}); and organic forms such as methylmercury (MeHg ; CH_3Hg^+), ethylmercury ($\text{CH}_3\text{CH}_2\text{Hg}^+$) and dimethylmercury ($\text{CH}_3\text{CH}_3\text{Hg}$). Their physical, chemical and toxicological properties and implications are further discussed and summarized below.

1.3.1.1 Physical and chemical properties

Although all are mercury-based compounds, the various chemical forms of mercury exhibit widely varying physical and chemical properties, most notably with regard to their solubility and density (**Table 2**). These in turn constitute important determinants for their fates both in the environment and *in vivo*. Another strikingly varied property of the different mercury species is their volatility as determined experimentally by their air to water partition coefficient (Henry's Law constant), and illustrated in **Table 3**. Particularly noteworthy is the 1.6×10^4 times greater volatility that dimethylmercury possesses compared to MeHg. This property accounts for its superior lipophilicity, potency, and the need for additional safety measures when working with dimethylmercury in the wake of the fatal exposure of a chemist in the United States to mere drops of the compound on her latex gloves (Nierenberg *et al.*, 1998).

Table 2. Physical and chemical properties of various mercury compounds.

Chemical Name	Elemental Mercury ^a	Mercuric Chloride	Mercurous Chloride ^b	Methylmercuric Chloride ^c	Dimethylmercury
Molecular formula	Hg ⁰	HgCl ₂	Hg ₂ Cl ₂	CH ₃ HgCl	C ₂ H ₆ Hg
Molecular structure		Cl-Hg-Cl	Cl-Hg-Hg-Cl	CH ₃ -Hg-Cl	CH ₃ -Hg-CH ₃
Molecular weight	200.59	271.52	472.09	251.1	230.66
Solubility	5.6 × 10 ⁻⁵ g/L at 25°C	69 g/L at 20°C	2.0 × 10 ⁻³ g/L at 25°C	0.100 g/L at 21°C	1 g/L at 21°C
Density	13.534 g/cm ³ at 25°C	5.4 g/cm ³ at 25°C	7.15 g/cm ³ at 19°C	4.06 g/cm ³ at 20°C	3.1874 g/cm ³ at 20°C
Oxidation state	+1, +2	+2	+1	+2	+2

^aAlso known as metallic mercury.

^bAlso known as calomel.

^cMethylmercuric chloride is used experimentally to investigate the effects of methylmercury.

Note: solubility reflects the solubility in water at the indicated temperature.

From: Committee on the Toxicological Effects of Methylmercury, Board on Environmental Studies and Toxicology, National Research Council, 2000 with permission.

Table 3. Volatility of various mercury species as evidenced by their experimentally determined Henry's Law constants (H).

<u>MERCURY SPECIES</u>	<u>TEMPERATURE (°C)</u>	<u>VOLATILITY (v/v)</u> <u>$[H = \{HgX(g)\} / \{HgX(aq)\}]$</u>
Hg ⁰	20	0.29
(CH ₃) ₂ Hg	25	0.31
CH ₃ HgCl	25	1.9 x 10 ⁻⁵
Hg(OH) ₂	25	3.2 x 10 ⁻⁶
HgCl ₂	25	2.9 x 10 ⁻⁸

1.6x10⁴
times **LESS**
volatile



Volatility (H) represents the air to water distribution constant as determined from the ratio of the concentration of Hg in the gaseous phase $\{HgX(g)\}$ to its concentration in the aqueous phase $\{HgX(aq)\}$.

Modified from: Lindqvist and Rodhe, 1985 with permission.

1.3.1.2 Overview of the toxicology of relevant mercury species

As would be expected based on their range of physical and chemical properties, the toxicological consequences following exposure to three of the most relevant forms of mercury, MeHg (CH_3Hg^+), elemental mercury (Hg^0) and mercuric mercury (Hg^{2+}), vary too. Their toxicological properties in terms of sources of exposure, biomonitoring, toxicokinetics, toxicodynamics, and potential mobilizing and antagonizing compounds are summarized in **Table 4**.

Table 4. The toxicology of relevant mercury species.

<u>Methylmercury</u> (CH₃Hg⁺)	<u>Elemental Mercury</u> (Hg⁰)	<u>Mercuric Mercury</u> (Hg²⁺)
<u>Sources of Exposure</u> - Fish, marine mammals, crustaceans, animals and poultry fed fish meal	- Dental amalgams, occupational exposure, Caribbean religious ceremonies, fossil fuels, incinerators	- Oxidation of elemental mercury or demethylation of MeHg; deliberate or accidental poisoning with HgCl ₂
<u>Biological Monitoring</u> - Hair, blood, cord blood	- Urine, blood	- Urine, blood
<u>Toxicokinetics</u>		
<i>Absorption</i> <u>Inhalation:</u> Vapors of MeHg absorbed <u>Oral:</u> Approximately 95% of MeHg in fish readily absorbed from GI tract <u>Dermal:</u> In guinea pigs, 3-5% of applied dose absorbed in 5 h	<u>Inhalation:</u> Approximately 80% of inhaled dose of Hg ⁰ readily absorbed <u>Oral:</u> GI absorption of metallic Hg is poor; any released vapor in GI tract converted to mercuric sulfide and excreted <u>Dermal:</u> Average rate of absorption of Hg ⁰ through human skin, 0.024 ng/cm ² for every 1 mg/m ³ in air	<u>Inhalation:</u> Aerosols of HgCl ₂ absorbed <u>Oral:</u> 7-15% of ingested dose of HgCl ₂ absorbed from the GI tract; absorption proportional to water solubility of mercuric salt; uptake by neonates greater than adults <u>Dermal:</u> In guinea pigs, 2-3% of applied dose of HgCl ₂ absorbed
<i>Distribution</i> - Distributed throughout body since lipophilic; approximately 1-10% of absorbed oral dose of MeHg distributed to blood; 90% of blood MeHg in RBCs - MeHg-cysteine complex ^a involved in transport of MeHg into cells - Half-life in blood, 50 d; 50% of dose found in liver; 10% in head - Readily crosses blood-brain and placental barriers	- Rapidly distributed throughout the body since it is lipophilic - Half-life in blood, 45 d (slow phase); half-life appears to increase with increasing dose - Readily crosses blood-brain and placental barriers	- Highest accumulation in kidney; fraction of dose retained in kidney dose dependent - Half-life in blood, 19.7-65.6 d; 1st phase, 24 d, 2nd phase, 15-30 d - Does not readily penetrate blood-brain or placental barriers - In neonate, mercuric Hg not concentrated in kidneys; therefore, more widely distributed to other tissues - In fetus and neonate, blood-brain barrier incompletely formed, so mercuric Hg brain concentrations higher than those in adults

<p><i>Biotransformation</i></p> <ul style="list-style-type: none"> - MeHg slowly demethylated to mercuric Hg (Hg^{2+}) - Tissue macrophages, intestinal flora, and fetal liver are sites of tissue demethylation - Mechanisms of demethylation unknown; free radicals demethylate MeHg <i>in vitro</i>; bacterial demethylation enzymes studied extensively, none has been characterized or identified in mammalian cells 	<ul style="list-style-type: none"> - Hg^0 in tissue and blood oxidized to Hg^{2+} by catalase and hydrogen peroxide (H_2O_2); H_2O_2 production the rate-limiting step 	<ul style="list-style-type: none"> - Hg^0 vapor exhaled by rodents following oral administration of mercuric Hg - Mercuric Hg not methylated in body tissues but GI microorganisms can form MeHg - Binds and induces metallothionein
<p><i>Excretion</i></p> <ul style="list-style-type: none"> - Daily excretion, 1% of body burden; major excretory route is bile and feces; 90% excreted in feces as Hg^{2+}; 10% excreted in urine as Hg^{2+} - Lactation increases clearance from blood; 16% of Hg in breast milk is MeHg 	<ul style="list-style-type: none"> - Excreted as Hg^0 in exhaled air, sweat, and saliva, and as mercuric Hg in feces and urine 	<ul style="list-style-type: none"> - Excreted in urine and feces; also excreted in saliva, bile, sweat, exhaled air and breast milk
<p><i>Half-Life Elimination</i></p> <ul style="list-style-type: none"> - (Whole body) 70-80 d; dependent on species, dose, sex and animal 	<ul style="list-style-type: none"> - 58 d 	<ul style="list-style-type: none"> - 1-2 mo
<p><u>Toxicodynamics</u></p>		
<p><i>Critical target organ</i></p>		
<ul style="list-style-type: none"> - Brain, adult and fetal 	<ul style="list-style-type: none"> - Brain and kidney 	<ul style="list-style-type: none"> - Kidney
<p><i>Causes of Toxicity</i></p> <ul style="list-style-type: none"> - Demethylation of MeHg to Hg^{2+} and the intrinsic toxicity of MeHg 	<ul style="list-style-type: none"> - Oxidation of Hg^0 to Hg^{2+} 	<ul style="list-style-type: none"> - Hg^{2+} binding to thiols (e.g. cysteine) in critical enzymes and structural proteins
<p><i>Latency period</i></p> <ul style="list-style-type: none"> - In Iraq, from weeks to month; in Japan, more than a year; differences suggested to be caused by selenium in fish; no toxic signs during latency period 		

<p><u>Mobilization</u> - DMPS, DMSA</p>	<p>- After oxidation to Hg²⁺: DMPS, DMSA</p>	<p>- DMPS, DMSA</p>
<p><u>Possible Antagonists</u> - Selenium, garlic, zinc</p>		
<p>^aMeHg-cysteine complex is structurally analogous to methionine. Abbreviations: HgCl₂, mercuric chloride; DMPS, 2,3-dimercapto-1-propane sulfonate; DMSA, meso 2,3-dimercaptosuccinic acid; GI, gastrointestinal tract; RBC, red blood cells.</p>		

Adapted from: Committee on the Toxicological Effects of Methylmercury, Board on Environmental Studies and Toxicology, National Research Council, 2000 with permission.

1.3.2 Human exposure to MeHg

MeHg is an organomercurial compound and persistent environmental contaminant with potent neurotoxic properties. Historically, MeHg is most notorious for two large-scale cases of human poisoning: via contaminated seafood in Minamata, Japan (Harada, 1995) and through tainted seed grain in Iraq (Amin-Zaki *et al.*, 1974). Yet quietly in our own backyard, reports of Minamata disease are surfacing in the indigenous communities of Grassy Narrows and White Dog in northern Ontario, the result of aquatic mercury contamination in the late 1960s (Harada *et al.*, 2005). However, MeHg toxicity primarily persists as a significant public health concern today due to society's attempt to foster a healthier lifestyle by reaping the benefits of increased fish and seafood consumption, which are coincidentally the primary sources of human exposure to MeHg given the cessation of its use in fungicides (Clarkson *et al.*, 2003). Moreover, it is prudent to note the difference in risk between an individual who may consume fish once or twice a week compared to a population whose diet is primarily composed of fish and seafood, such as Canadian Aboriginals, populations in the Seychelles and Faeroe Islands, as well as individuals in Iceland, Japan and Norway who have the highest per capita fish and seafood consumption in the world (Food and Agriculture Organization of the United Nations). The latter may be at greater risk for the harmful effects associated with chronic low-dose MeHg exposure, albeit the fact that this risk will also be a function of the anthropogenic mercury emissions in the area, the type of fish consumed, as well as other components found within the fish which may potentiate or antagonize the adverse effects of MeHg.

1.3.2.1 Environmental sources of MeHg

In the environment, elemental mercury (Hg^0) evaporates from the earth's soil and water and is emitted by volcanoes, coal-burning power stations and incinerators into the atmosphere where it is converted to soluble mercuric mercury (Hg^{2+}) via oxidation or photochemically in the presence of halogens, and returns to the earth in rainwater (Clarkson *et al.*, 2003). Microorganisms present in the soil and water may reconvert Hg^{2+} to Hg^0 allowing its return to the atmosphere and perpetuating its cycling. However, Hg^{2+} in aquatic sediments can be methylated by methanogenic bacteria to form MeHg that subsequently bioaccumulates up the aquatic food chain concentrating in top predatory species (Clarkson *et al.*, 2003). Their dietary

consumption constitutes the primary source of human exposure to MeHg, while a resurgence in activities such as coal burning and gold mining help contribute to the overall environmental mercury burden (Bhavsar *et al.*, 2010; Guedron *et al.*, 2011; Kinghorn *et al.*, 2007).

1.3.2.2 Documented exposure levels

In the infamous case of Minamata Bay, the National Institute for Minamata Disease estimates that more than 900 fatalities resulted from the consumption of MeHg-contaminated seafood which contained up to 40 ppm ($\approx 184 \mu\text{M}$) MeHg (Harada, 1995). Other documented cases of fatal human poisonings reported levels of MeHg in the blood and cerebellum of $75 \mu\text{M}$ and $15\text{-}25 \mu\text{M}$ respectively (Hilmy *et al.*, 1976).

In the United States, MeHg exposure continues to be a matter of public health concern as dietary and occupational exposure levels, which can range from $0.09\text{-}1.8 \mu\text{g/kg/day}$ (Barbosa *et al.*, 2001; Harada *et al.*, 2001; Tsuchiya *et al.*, 2008; Vahter *et al.*, 2000), can overlap those ($0.2\text{-}1.8 \mu\text{g/kg/day}$) associated with postnatal neurobehavioral deficits in humans after *in utero* MeHg exposure (Grandjean *et al.*, 1998; Grandjean *et al.*, 1997). Today, the US Environmental Protection Agency (EPA) employs a reference dose for MeHg of $0.1 \mu\text{g/kg/day}$, reflecting the estimated daily oral exposure in humans which is unlikely to pose an appreciable risk of adverse effects over a lifetime, and correlates with a blood mercury level of $5.8 \mu\text{g/L}$ ($\approx 0.027 \mu\text{M}$ MeHg), where 100% of the total mercury measured is assumed to be MeHg for the purpose of risk assessment. Furthermore, this reference dose equates to the weekly consumption of one 7-oz can of tuna for an adult (Clarkson *et al.*, 2003). In Canada, the allowable limit set by the Canadian Food Inspection Agency (CFIA) for mercury in fish and seafood is 0.5 ppm ($\approx 2.3 \mu\text{M}$ MeHg). According to Health Canada, widely consumed species of fish including swordfish, shark, pike and bass contain some of the highest concentrations of MeHg, some greater than 1 ppm ($\approx 4.6 \mu\text{M}$ MeHg) (Fig. 5). Additionally, a study of Canadian aboriginals whose diet is primarily comprised of fish found 25% of this population to have blood mercury levels greater than $0.09 \mu\text{M}$, and 2% with levels greater than $0.46 \mu\text{M}$, with the highest maternal blood and cord blood concentrations reported to be $0.4 \mu\text{M}$ and $1 \mu\text{M}$ respectively; concentrations, as will be elaborated upon in the subsequent sections, within the range associated with the clinical manifestation of MeHg toxicity in both the adult, and developing embryo and fetus (Wheatley and Paradis, 1995).

Thus, our working concentrations employed herein are well below the range associated with fatalities, and within the more relevant concentration range found in various fish and seafood species, as well as in at-risk populations. Importantly, we have observed effects at the cellular level at a concentration only 0.003 μM higher than the current blood mercury equivalent of the US EPA reference dose.

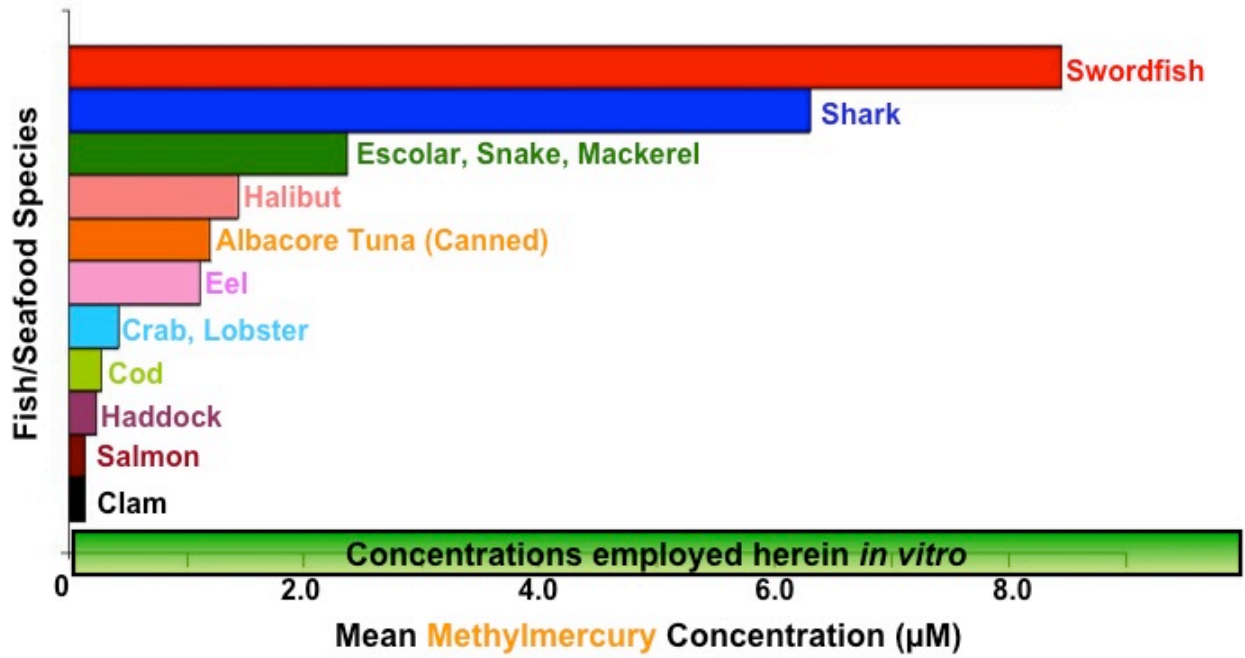


Figure 5. MeHg levels in some commonly consumed fish and seafood species.

Created from: Scientists of the Bureau of Chemical Safety, Food Directorate, Health Products and Food Branch, Health Canada, 2007.

1.3.2.3 Clinical manifestation of MeHg neurotoxicity in the adult

In the adult, clinical signs and symptoms of MeHg toxicity may be delayed weeks to months following exposure (Castoldi *et al.*, 2001; Clarkson *et al.*, 2003). Symptoms of adult neurotoxicity are dose- and time-dependent, usually manifesting at blood mercury levels greater than 200 µg/L (≈ 0.93 µM MeHg) (Clarkson *et al.*, 2003). Symptoms present as visual abnormalities and constriction of the visual field, impaired sensation in the extremities, perioral dysesthesia, ataxia, hearing loss, muscle weakness, tremors, mental deterioration, and in extreme cases, death (Castoldi *et al.*, 2001; Clarkson *et al.*, 2003). MeHg appears to target specific areas of the adult central nervous system (CNS) leading to the region-specific aforementioned clinical indications. These targets primarily include the visual cortex neurons, granule cells of the cerebellar granule layer and axon degeneration of the peripheral nerve sensory branch (Castoldi *et al.*, 2001; Clarkson *et al.*, 2003; Costa *et al.*, 2004).

1.3.2.4 Clinical manifestation of MeHg neurotoxicity in the embryo/fetus

The developing nervous system appears to be exquisitely sensitive to MeHg with *in utero* MeHg exposure associated with a range of structural and postnatal functional neurodevelopmental deficits in the absence of overt maternal toxicity (Castoldi *et al.*, 2001). Analysis of brains of infants prenatally exposed to MeHg show widespread damage with decreased brain volume, atrophy of the cerebrum and cerebellum, decreased numbers of neurons, disordered cytoarchitecture of the cerebral cortex and white matter astrocytosis (Choi, 1989). Clinically, this damage can manifest in cerebral palsy, severe mental retardation, blindness and deafness following “high dose” exposures (> 10 µM), and seizures, low birth weight and developmental delays in such areas as walking and speech following “low dose” exposures (≈ 0.4 - 0.5 µM) (Castoldi *et al.*, 2003; Choi, 1989; Davis *et al.*, 1994). While the effects of “high dose” cases of poisonings are irrefutable, much controversy surrounds the effects of “low dose” exposure such as those expected in fish-eating populations, given that a definitive lowest observed adverse effect level for MeHg-mediated postnatal neurodevelopmental deficits has not been established (Castoldi *et al.*, 2001). In an attempt to rectify these discrepancies, two populations, one in the Faeroe Islands and another in the Seychelles, whose diets are primarily fish-based, have been studied extensively. However, these studies produced conflicting results

whereby an association was found between MeHg levels in cord blood and postnatal neurodevelopmental deficits in the Faeroe Islands population, but not in the Seychelles children (Clarkson *et al.*, 2003; Costa *et al.*, 2004). These differences have been attributed to the consumption of highly MeHg-laden pilot whale and concomitant polychlorinated biphenyl (PCB) exposure in the Faeroe Islands thereby confounding the risk assessment, yet providing a realistic scenario of the complexities of assessing risk in any fish-eating population (Clarkson *et al.*, 2003; Costa *et al.*, 2004).

1.3.3 Molecular mechanisms and cellular targets involved in MeHg-mediated toxicity

MeHg toxicity is complex, likely involving the concerted efforts of a number of integral factors. MeHg has been documented to interfere with numerous cellular constituents and processes, making elucidation of the precise underlying molecular mechanisms of its potent neurotoxic action a challenge. Discussed below and summarized in **Table 5** are some of the known molecular mechanisms and targets of MeHg that may contribute in part to its toxicity. However, the probes employed experimentally to implicate a given mechanism in MeHg toxicity are limited in their specificity as they may have other effects, both known and unknown, at the concentrations used which may confound the interpretation of the results. The molecular mechanisms and targets of MeHg presented herein are by no means an exhaustive list, nor are they mutually exclusive, as alteration of one may affect multiple pathways. Of those discussed, the interrelated contributions of calcium (Ca^{2+}) dyshomeostasis, glutamate excitotoxicity and oxidative stress are the three mechanisms which have garnered much of the scientific community's attention, and are regarded as the three critical events contributing to MeHg-mediated neurotoxicity. Importantly, these three mechanisms appear overall to be induced at low, micromolar concentrations of MeHg, akin to those levels in fish eating populations, underscoring their potential mechanistic relevance in postnatal neurodevelopmental deficits following *in utero* MeHg exposure when compared to mechanisms such as direct protein binding, which is likely more active at higher concentrations of MeHg. This, however, does not preclude the involvement of additional molecular mechanisms and targets discussed below, which have also been implicated at similar concentrations of MeHg and may reflect downstream consequences of an initial insult as in the case of ROS-mediated DNA damage. Overall, experimental studies provide important mechanistic insight into MeHg toxicity, but are limited in

their translatability to the human scenario given that most are conducted in rodents or isolated cells using various routes and durations of exposure, and the concentration of MeHg achieved within the cell/animal is often not measured thus preventing its direct correlation to the mechanism investigated.

Table 5. Experimental evidence supporting some of the major proposed molecular mechanisms and targets involved in MeHg-mediated neurotoxicity.

<u>Induction of glutamate excitotoxicity</u>	
(Aschner <i>et al.</i> , 1993)	MeHg (10 μ M-1 mM) reduced uptake and increased efflux of the excitatory amino acids (EAAs) L-glutamate and D-aspartate in a concentration- and time-dependent manner in neonatal rat cortical primary astrocyte cultures; furosemide (5 mM), an inhibitor of the hypotonic-media-induced efflux of EAAs, reversed MeHg-mediated increases in glutamate and aspartate efflux.
(Park <i>et al.</i> , 1996)	MeHg (20 μ M)-mediated neurotoxicity in neonatal mouse cerebral neurons was blocked by the NMDA receptor antagonists MK-801 (25-100 μ M; non-competitive antagonist), D-2-amino-5-phosphonovaleric acid (APV) (10-100 μ M; competitive antagonist) and 7-chlorokynurenic acid (1-100 μ M; antagonist at the glycine site associated with the NMDA receptor).
(Rajanna <i>et al.</i> , 1997)	MeHg itself elicited concentration-dependent inhibition of NMDA-specific glutamate receptor binding in neonatal (0.25-4 μ M MeHg) and adult (10-200 μ M MeHg) rat cerebral cortex.
(Matyja <i>et al.</i> , 1993)	Neuronal lesions typical of excitotoxic stimulation appeared upon co-application of nontoxic concentrations of MeHg (1 μ M) and glutamate (100 μ M).
<u>Disruption of intracellular calcium homeostasis</u>	
(Sakamoto <i>et al.</i> , 1996)	Pretreatment of rats with the Ca ²⁺ channel blockers flunarizine, nifedipine, nicardipine, or verapamil (all 20 mg/kg/day) prevented MeHg (5 mg/kg/day x 14 days)-initiated decreases in body weight and/or symptoms of neurological disorders.

(Marty and Atchison, 1998)	Acute MeHg (0.5-1 μM)-mediated losses in cerebellar granule cell viability were prevented by pretreatment with the Ca^{2+} chelator 1,2-bis(2-aminophenoxy)ethane-N,N,N',N'-tetraacetic acid tetrakis(acetoxymethyl)ester (BAPTA) (10 μM) and the Ca^{2+} channel blockers omega-conotoxin MVIIC and nifedipine (both 1 μM).
<u>Induction of oxidative stress</u>	
(Sarafian <i>et al.</i> , 1994)	Hypothalamic neural cells expressing the anti-apoptotic proto-oncogene, B-cell lymphoma 2 (bcl-2), displayed attenuated ROS formation and protection against MeHg (5-10 μM)-mediated cell death.
(Park <i>et al.</i> , 1996)	MeHg (20 μM)-mediated neurotoxicity in neonatal mouse cerebral neurons was blocked by the ROS scavengers GSH (1-8 mM), catalase (1-40 $\mu\text{g/ml}$), selenium (40-80 μM) and cysteine (0.8 mg/ml).
(Naganuma <i>et al.</i> , 1998)	Constitutive overexpression of Mn-superoxide dismutase (Mn-SOD), a mitochondrial matrix enzyme responsible for $\text{O}_2^{\cdot-}$ decomposition, in HeLa cells decreased their sensitivity to MeHg (50-100 μM).
(Dare <i>et al.</i> , 2000)	Cerebellar granule cells were protected from MeHg (0.1-1.5 μM)-mediated apoptosis (morphological alterations, chromatin fragmentation, and calpain activation) by the antioxidants, 17-beta-estradiol and the delta-(8,9)-dehydro derivative of 17-alpha-estradiol J811 (both 10 μM).

(Kaur <i>et al.</i> , 2006)	Primary cerebellar neurons and astrocytes pretreated with diethyl maleate (DEM) (1.8-3.0 mM) to deplete intracellular GSH showed enhanced MeHg (5 μ M)-initiated ROS formation, while pretreatment with the GSH precursor N-acetylcysteine (NAC) (200-250 μ M) increased intracellular GSH, provided protection against MeHg (5 μ M)-induced oxidative stress and attenuated MeHg (5 μ M)-initiated cytotoxicity as measured by [3-(4,5-dimethylthiazol-2-yl)-2,5-diphenyltetrazolium bromide (MTT).
(Mori <i>et al.</i> , 2007)	Cerebellar mitochondria supplemented with 7-15 mM succinate + 1 μ M rotenone from MeHg (5 mg/kg/day x 5 days)-treated rats showed enhanced ROS generation, implicating involvement of complex II-III of the electron transport chain.
<u>Inhibition of nucleic acid biosynthesis</u>	
(Burke <i>et al.</i> , 2006)	MeHg (3 mg/kg) inhibited hippocampal DNA synthesis by 40% in newborn rats that correlated with long-term reductions in total cell number.
(Falluel-Morel <i>et al.</i> , 2007)	MeHg (5 mg/kg) inhibited perinatal rat hippocampal DNA synthesis by 44% that correlated with 21% reduction in hippocampal size, 16% reduction in granule cell layer cell numbers, 50% reduction in hilus cell numbers of the dentate gyrus, and hippocampal-dependent learning deficits in juvenile rats on a spatial navigation task.
(Das <i>et al.</i> , 2008)	MeHg (0.1-10 μ M) reduced RNA and DNA synthesis in human and free-ranging harbor seal T-lymphocytes.
<u>DNA damage</u>	
(Morimoto <i>et al.</i> , 1982)	MeHg (3 μ M) induced sister-chromatid exchanges in human whole-blood cultures.

(Belletti <i>et al.</i> , 2002)	MeHg (0.1-10 μ M) increased levels of the oxidative lesion 8-oxodG in C6 glioma cell cultures.
(Li <i>et al.</i> , 2006)	MeHg (0.5 μ M-0.5 mM) rapidly and strongly covalently binds to DNA forming a stable complex.
(Crespo-Lopez <i>et al.</i> , 2007)	Exposure of human glioblastoma (U373) and neuroblastoma (B103) cells to MeHg (0.1-1 μ M) resulted in an increased frequency of micronuclei and/or an increased micronucleation index.
<u>Protein binding</u>	
(Ballatori and Clarkson, 1982)	The mercury atom of MeHg (1 mg/kg) interacts directly with the thiol group of GSH forming a GS-HgCH ₃ complex that can be excreted.
(Kung <i>et al.</i> , 1987)	MeHg (100 μ M) decreased the activity of the brain cell-specific marker enzymes choline acetyltransferase, glutamic acid decarboxylase (GAD), 2',3'-cyclic nucleotide phosphohydrolase (CNP) and enolase; activities were restored upon addition of the sulfhydryl protecting reagents dithiothreitol (DTT) or sodium thioglycolate (both 2 mM).
(Rocha <i>et al.</i> , 1993)	MeHg (6.9-9.2 mg/kg/day x 5 days) treatment reduced brain and hepatic specific activity of the sulfhydryl-containing enzyme delta-aminolevulinate dehydratase (ALA-D) postnatally in rats.
<u>Microtubule disruption</u>	
(Abe <i>et al.</i> , 1975)	MeHg (5 mM) blocked axonal protein transport in the frog <i>in vivo</i> and depolymerized cerebral microtubules <i>in vitro</i> at concentrations of 50-100 μ M via binding to tubulin sulfhydryl groups.

(Miura <i>et al.</i> , 1984)	MeHg (25-50 μ M) disrupted the microtubule network and inhibited tubulin polymerization in mouse glioma cells.
(Wasteneys <i>et al.</i> , 1988)	MeHg (0.1-10 μ M) initiated concentration- and time-dependent microtubule disassembly in mitotic and interphase embryonal carcinoma cells, with increased sensitivity in spindle microtubules of mitotic cells.
(Castoldi <i>et al.</i> , 2000)	MeHg (0.5-1 μ M) induced fragmentation of neuronal networks and depolymerization of microtubules in rat primary cerebellar granule cells.

1.3.3.1 Induction of glutamate excitotoxicity

Extensive research in various models has looked at the contribution of glutamate excitotoxicity to MeHg-mediated neurotoxicity. The scientific community largely regards this mechanism as one of the principal contributors to the toxicological consequences following MeHg exposure, and experimental evidence supporting this hypothesis is outlined in **Table 5**. Glutamate is the primary excitatory neurotransmitter in the mammalian CNS involved in development, learning, memory and injury response, but can be toxic at high concentrations (Farina *et al.*, 2011; Featherstone, 2010). MeHg exposure inhibits astrocytic glutamate uptake and increases its release thereby enhancing synaptic glutamate concentrations, which result in hyperactivation of N-methyl D-aspartate (**NMDA**)-type glutamate receptors and neuronal toxicity mediated by Ca^{2+} and Na^{+} influx (Farina *et al.*, 2011). The aforementioned is depicted in **Figure 6** and further illustrates the critical interplay between glutamate excitotoxicity, Ca^{2+} dyshomeostasis and oxidative stress in mediating MeHg neurotoxicity.

1.3.3.2 Disruption of intracellular calcium homeostasis

The second of the triad of mechanisms thought largely to govern MeHg-mediated toxicity is the disruption of intracellular Ca^{2+} levels. Intracellular cation levels are tightly regulated and perturbations in their balance can have deleterious consequences. **Table 5** presents some experimental evidence supporting the involvement of Ca^{2+} dyshomeostasis in the mechanism of MeHg toxicity. As discussed above and illustrated in **Figure 6**, MeHg-mediated glutamate excitotoxicity leads to the influx of Ca^{2+} into postsynaptic neurons, which can activate cell death pathways or be taken up by mitochondria compromising their function and increasing the formation of reactive oxygen species (**ROS**), further substantiating the important interplay between glutamate excitotoxicity, Ca^{2+} imbalance and oxidative stress in MeHg-mediated toxicity (Farina *et al.*, 2011; Hidalgo and Donoso, 2008; Reynolds and Hastings, 1995).

1.3.3.3 Induction of oxidative stress

The last of the three major mechanisms thought to play a critical role in the mechanism of MeHg-mediated neurotoxicity, and a primary focus of this thesis, is the induction of oxidative

stress. MeHg has been shown to generate ROS both *in vitro* and *in vivo*, with a ROS-mediated component to its toxicity implicated by the modulatory effects of antioxidant pretreatment, altered antioxidative enzyme expression and glutathione depletion on a variety of toxic outcomes (**Table 5**). As noted above, a critical interplay exists between glutamate excitotoxicity, Ca^{2+} dyshomeostasis and oxidative stress. Glutamate excitotoxicity-mediated influxes of Ca^{2+} , and the direct action of MeHg, both lead to mitochondrial ROS generation, with perpetuation of the excitotoxic cycle achieved via ROS-mediated inhibition of astrocytic glutamate uptake (Allen *et al.*, 2001; Farina *et al.*, 2011; Mori *et al.*, 2007; Reynolds and Hastings, 1995) (**Fig. 6**).

Additionally, of the antioxidant systems responsible for combating ROS, MeHg appears to target the glutathione (**GSH**) system, a likely observation given that in all tissues, including the CNS, it is the most abundant intracellular low molecular weight thiol compound (Dringen, 2000). **Figure 7** illustrates the effects of MeHg on the GSH antioxidant system, which contributes to the formation of ROS such as hydrogen peroxide (H_2O_2) and superoxide anion ($\text{O}_2^{\cdot-}$), and a state of oxidative stress via its ability to disrupt the mitochondrial electron transport chain, bind GSH leading to its depletion and hinder glutathione reductase (**GR**) and glutathione peroxidase (**GPx**) activities (Farina *et al.*, 2003; Farina *et al.*, 2011; Franco *et al.*, 2007; Franco *et al.*, 2009; Mori *et al.*, 2007; Stringari *et al.*, 2008) (**Fig. 7**).

Oxidative stress is arguably the most prominent contributor to MeHg-mediated toxicity given its expansive effects. Beyond those effects described above, the ability of ROS to damage cellular macromolecules as well as alter signal transduction enable them to affect multiple pathways and contribute a role in nearly every facet of MeHg-mediated toxicity.

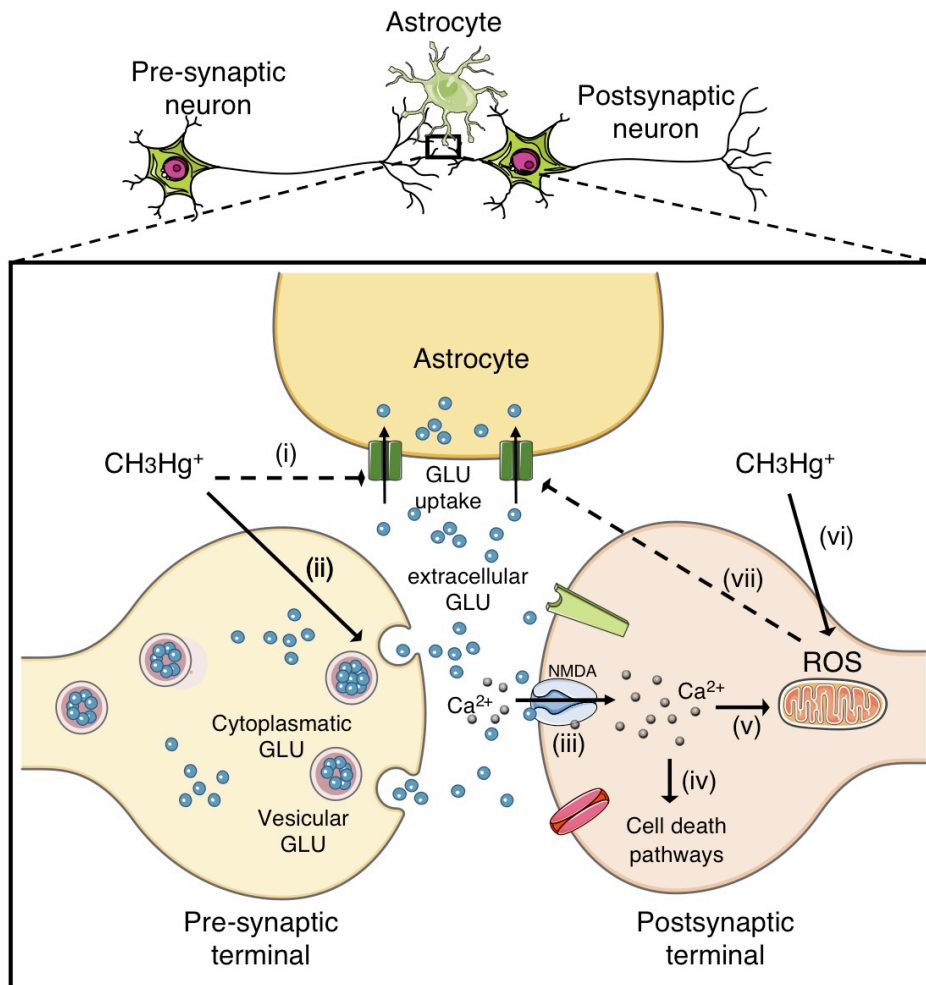


Figure 6. The interplay between MeHg-induced oxidative stress, Ca²⁺ and glutamate (GLU) dyshomeostasis in the mechanism of MeHg-mediated neurotoxicity.

MeHg (CH₃Hg⁺): (i) inhibits astrocytic GLU uptake and (ii) increases GLU release leading to elevated extracellular GLU levels and (iii) hyperactivation of NMDA-type GLU receptors. In turn, there is an increased influx of Ca²⁺ into postsynaptic neurons (iv) activating cell death pathways, or (v) being taken up by mitochondria inducing their dysfunction and increased production of ROS, which can also be stimulated by MeHg directly (vi). The excitotoxic cycle is perpetuated with (vii) increased ROS (mainly H₂O₂) directly decreasing astrocytic GLU uptake.

From: Farina et al., 2011 with permission.

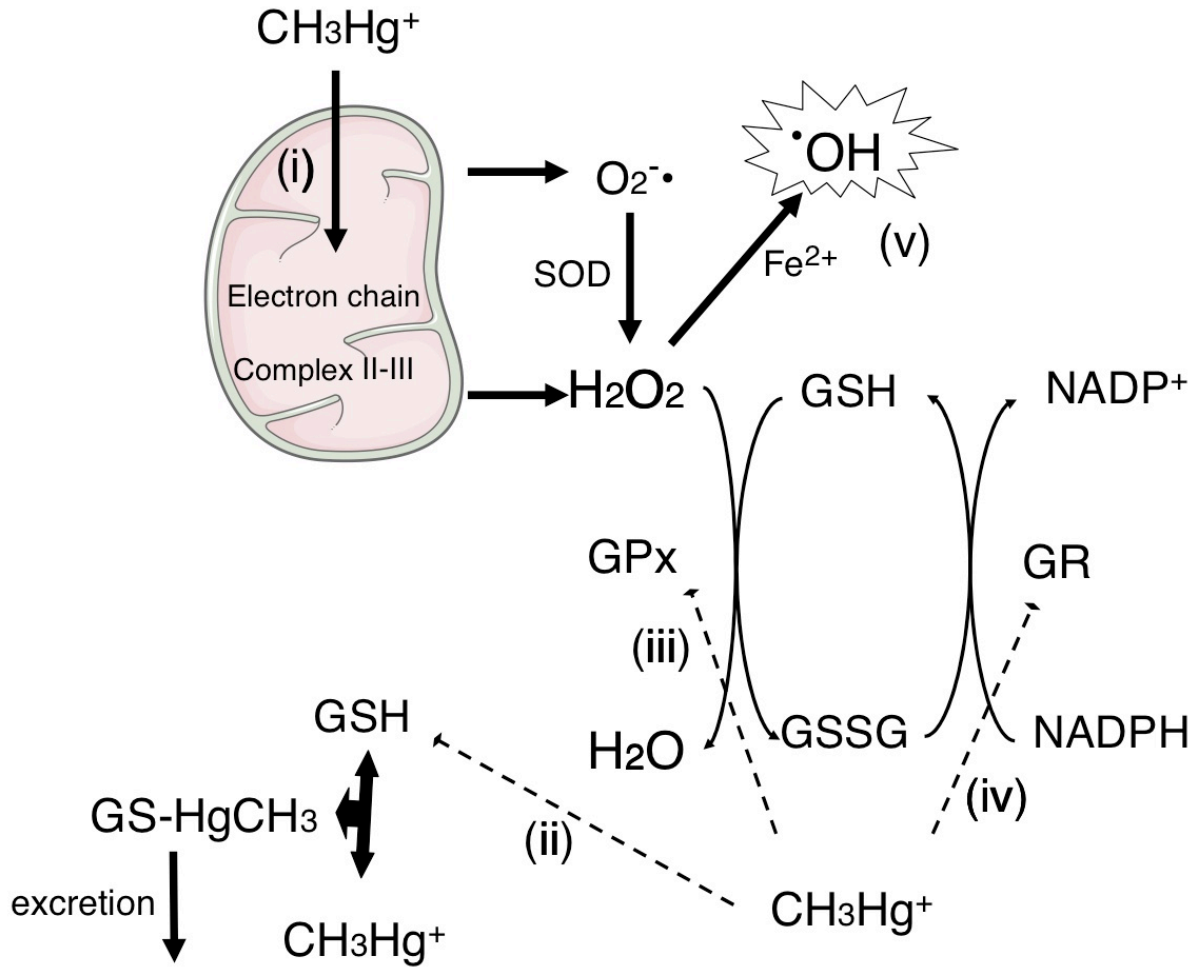


Figure 7. Effects of MeHg on the GSH antioxidant system.

MeHg (CH_3Hg^+): (i) disrupts the mitochondrial electron transport chain, leading to increased formation of ROS such as H_2O_2 and $\text{O}_2^{\bullet-}$; (ii) reacts with GSH, leading to its depletion due to the formation of a MeHg-GSH (GS-HgCH_3) complex which is excreted from the body; (iii) and (iv) hinders the physiological increase in glutathione reductase (GR) and glutathione peroxidase (GPx) activities in the rodent CNS during the early postnatal period, and also decreases GPx activity in adult animals. Together these events result in increased ROS generation and a state of oxidative stress (v).

From: Farina et al., 2011 with permission.

1.3.3.4 Inhibition of nucleic acid biosynthesis

As outlined in **Table 5**, inhibition of nucleic acid biosynthesis can have detrimental implications as a potential contributor in the mechanism of MeHg toxicity given that these components constitute the cellular blueprint. The precise mechanisms by which MeHg accomplishes this inhibition remain unknown, but could be the consequence of covalent binding to sulfhydryl groups on key proteins, and/or ROS-mediated changes in signal transduction and gene expression. This inhibition in turn halts progression through the cell cycle, and suggests that actively proliferating cells, such as in the developing embryo and fetus, may constitute a prime target for MeHg.

1.3.3.5 DNA damage

MeHg is highly electrophilic in nature, and as such, has a high affinity for cellular nucleophiles such as DNA. There is an increasing body of evidence that implicates the genotoxic properties of MeHg as a contributing factor in its mechanism of toxicity. However, given the vast array of DNA lesions observed in response to MeHg, the involvement of its genotoxicity in the mechanism of toxicity is likely complex. **Table 5** describes some of the experimental evidence supporting MeHg's ability to interact with DNA directly or indirectly to induce damage ranging from micronuclei and sister-chromatid exchanges to ROS-mediated oxidative lesions like 8-oxo-2'-deoxyguanosine (**8-oxodG**). DNA damage can have deleterious implications both during development and beyond, as unrepaired DNA damage can not only lead to mutations, but may also have other non-mutational effects resulting in gene expression changes, some of which may be critical for the development, organization, function and defense of the adult CNS and/or the embryo and fetus (Khobta *et al.*, 2010; Kitsera *et al.*, 2011; Pastoriza-Gallego *et al.*, 2007; Wells *et al.*, 2010).

1.3.3.6 Protein binding

As mentioned, MeHg is highly electrophilic and thus will readily covalently bind to nucleophilic macromolecules, particularly thiol-containing proteins. As **Table 5** outlines, this interaction can lead to the inhibition of enzymes critical for cellular function, or reduce the

bioavailability of non-enzymatic proteins and peptides such as GSH. This covalent interaction can compromise normal cellular function, cell-cell interactions and host defense responses among others, with the spectrum of toxicological consequences varying depending on the particular protein to which MeHg binds. Thus, the high affinity of MeHg for protein sulfhydryl groups and the extensive cellular implications of their interaction, render protein binding a potentially important contributor in the mechanism of MeHg toxicity.

1.3.3.7 Microtubule disruption

The microtubule component of the cytoskeleton has been investigated extensively as a macromolecular target of MeHg contributing to its mechanism of toxicity. **Table 5** outlines selected microtubular effects that have been observed in a variety of models, and which are likely mediated through MeHg-sulfhydryl group interactions. These effects are likely key players in MeHg-mediated developmental neurotoxicity as functional microtubules are required for proper nervous system development. In their absence, cell proliferation, neuronal migration, extension and stabilization of neurites, and axonal transport of key factors are compromised, most or all of which are consistent with the neuropathological findings in children exposed *in utero* to MeHg (Castoldi *et al.*, 2001).

1.4 DNA DAMAGE

1.4.1 Introduction to DNA damage

The DNA of all living organisms is continually inundated with insult from both exogenous sources including radiation and xenobiotics, as well as from endogenous sources such as the by-products of cellular metabolism (Akbari and Krokan, 2008). The damage induced can range from single base damage to DNA strand breaks, yielding both mutagenic and cytotoxic consequences due to perturbation of transcription and replication (Akbari and Krokan, 2008) (**Table 6**). The severity of toxicity observed as a result of DNA damage is dictated by the type and amount of damage, whether the damage has occurred in a promoter region, intron, exon, or the actively transcribed strand of a gene, as well as the type of cell and its stage within the cell cycle (Akbari and Krokan, 2008). Discussed in more detail below are two types of DNA damage central to this thesis: the oxidative base lesion 8-oxo-2'-deoxyguanosine (**8-oxodG**) and DNA double-strand breaks (**DSB**).

Table 6. Cytotoxicity and mutagenicity of some endogenously generated DNA lesions.

Type of DNA lesion	Cytotoxicity-mutagenicity	Type of mutation
Apurinic/aprimidinic (AP) site	Frequent, stalls DNA replication and transcription	AP site → T, frameshifts, deletions
Cytosine deamination (uracil)	Relatively frequent, low toxicity, highly mutagenic, rapid repair, mutated RNA transcripts	CG → TA
5-Methylcytosine deamination (thymine)	Relatively frequent, highly mutagenic, slow repair	5-MeCG → TA
Adenine deamination (hypoxanthine)	Relatively infrequent, low toxicity, highly mutagenic,	AT → GC
Guanine deamination (xanthine)	Relatively infrequent, unknown toxicity, mutagenic	GC → AT
Guanine deamination (oxanine)	Forms cytotoxic protein-DNA crosslinks that stall replication, mutagenic	GC → AT, GC → TA (from crosslinks)
8-OxoG	Bypassed in replication, highly mutagenic	GC → TA
Thymine glycol	Blocks DNA replication and transcription, weakly mutagenic	TA → CG
FapyG	Stalls DNA replication, mutagenic	GC → TA
5-Hydroxycytosine	May stall replication	CG → TA, CG → GC
5-Hydroxyuracil	Possibly toxic via mutated RNA transcripts	CG → TA, CG → GC, CG → AT
5,6-Dihydrouracil	Not established	CG → TA, CG → AT
Etheno-adducts	Block DNA replication, mutagenic	AT → GC, AT → CG
O ⁶ -Methylguanine	Highly cytotoxic in cells with functional MMR	GC → AT
3-Methyladenine	Stalls DNA replication, increased depurination	Very weakly mutagenic via AP-site generation
1-Methyladenine	Stalls DNA replication	Very weakly mutagenic
3-Methylcytosine	Stalls DNA replication	
Single-strand break	Stalls RNA polymerase, Causes DSB during replication	

From: Akbari et al., 2008 with permission.

1.4.2 Oxidatively damaged DNA and the 8-oxo-2'-deoxyguanosine lesion

Oxidative base lesions constitute one of the most common forms of DNA damage with reactive oxygen species (**ROS**) originating from a myriad of sources, including radiation, xenobiotics, enzymes, oxygen metabolism, apoptosis and inflammatory and immune responses, and thus are readily available to react with DNA (Akbari and Krokan, 2008; Sedelnikova *et al.*, 2010). Oxidative DNA damage is most often mediated by the highly reactive hydroxyl radical (**$\cdot\text{OH}$**) which either adds to the double bonds of heterocyclic DNA bases, or abstracts a hydrogen atom from the methyl group of thymine and each of the carbon-hydrogen bonds of 2'-deoxyribose (Dizdaroglu, 2003). These interactions manifest as modified bases and sugars, DNA-protein cross-links, strand breaks, abasic sites, tandem lesions and clustered damaged sites, with some of the more than 60 lesions already identified illustrated in **Figure 8** (Dizdaroglu, 2003; Klungland and Bjelland, 2007).

Because of their low oxidation potential, guanine bases are the most readily oxidized (Klungland and Bjelland, 2007). Oxidation of guanine at the eight-carbon position leads to the formation of 8-oxoguanine, or its 8-hydroxyguanine tautomer, one of the most frequently occurring lesions with high mutagenic potential (Klungland and Bjelland, 2007; Klungland *et al.*, 1999; Lindahl, 1993) (**Fig. 9**). If not repaired via the base excision repair (**BER**) machinery, successive rounds of replication result in G:C to T:A transversion mutations that have been implicated in the carcinogenic process, and may also affect the expression and activity of proteins required for normal development and function (David *et al.*, 2007; Klungland and Bjelland, 2007; Klungland *et al.*, 1999; Wells *et al.*, 2010).

In addition to the well appreciated mutagenic consequences of the 8-oxo-2'-deoxyguanosine (**8-oxodG**) lesion, recent interest has been taken in its non-mutational pathogenesis involving altered transcription and gene expression; these having significant implications for structural and functional teratogenesis, as well as neurodegeneration. This hypothesis is supported by the observation that introduction of 8-oxodG lesions into the DNA template results in stalling of RNA polymerase (Viswanathan and Doetsch, 1998); however, this ability is dependent upon the promoter strength and sequence context surrounding the lesion (Pastoriza-Gallego *et al.*, 2007). Other mechanisms by which 8-oxodG may alter transcription,

and thus gene expression, include gene silencing by decreased histone acetylation in promoter regions (Khobta *et al.*, 2010), inhibition of DNA methyltransferase activity, decreasing DNA methylation to increase gene expression (Klaunig and Kamendulis, 2004) and transcriptional blockage by BER intermediates (Kitsera *et al.*, 2011). Additionally, 8-oxodG can regulate the binding efficiency of transcription factors such as nuclear factor kappa B (**NF- κ B**) to specific promoter elements thereby influencing the expression of genes under their control (Hailer-Morrison *et al.*, 2003). Lastly, *in vivo* evidence of 8-oxodG accumulation in susceptible genomic sites rather than being randomly distributed throughout the genome indicates the potential for gene-specific damage leading to pathway-specific effects, and may have important implications for understanding developmental and neurodegenerative pathologies given the possibility of organ- and cell-specific variations in DNA repair capacity (Toyokuni, 2008).

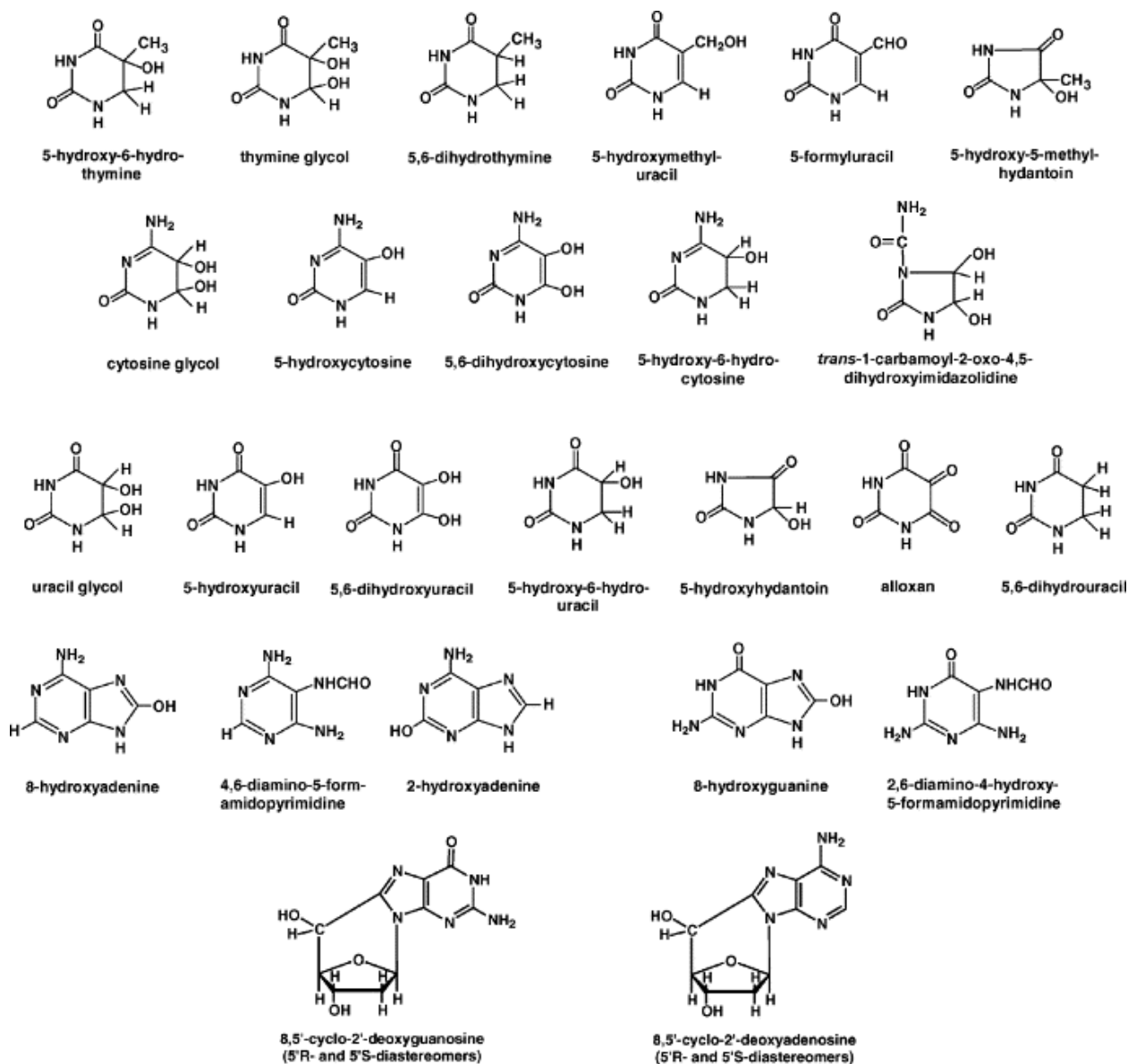


Figure 8. Structures of the major products of oxidative damage to DNA bases.

From: Dizdaroglu, 2003 with permission.

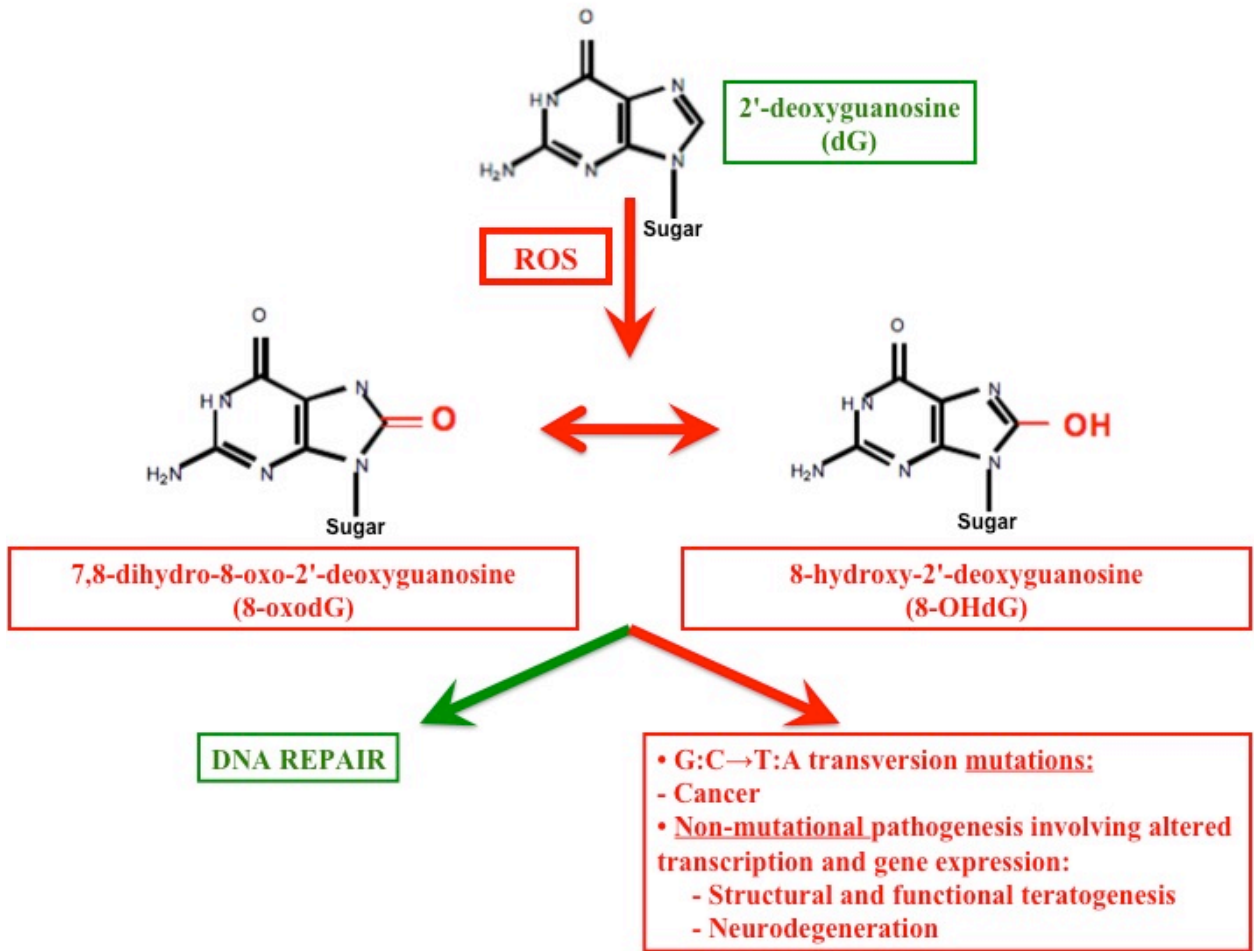


Figure 9. 8-oxodG formation and fate.

Modified from: Wells et al., 2009 with permission.

1.4.3 DNA double-strand breaks and γ H2AX

DNA double-strand breaks (**DSBs**) are one of the most lethal types of unrepaired DNA damaged forming as a result of two or more breaks occurring on opposite strands of DNA within 10-20 base pairs of each other (Nordstrand *et al.*, 2007). DNA DSBs can be induced by a variety of means including exposure to ionizing radiation, oxidative stress-induced DNA damage and its interference with replication and transcription, adjacent DNA single-strand breaks (**SSBs**), topoisomerase cleavage of SSBs and BER interference during DSB repair (Nordstrand *et al.*, 2007; Sedelnikova *et al.*, 2010). DSBs are also formed as an intermediate product in cellular recombination processes including meiotic recombination, antigen receptor gene arrangement, VDJ recombination and mating-type switching in yeast (Nordstrand *et al.*, 2007; Sedelnikova *et al.*, 2010)

Following DSB formation, the variant H2A histone H2AX becomes phosphorylated at serine 139 in the chromatin flanking the break site by members of the phosphatidylinositol-3 kinase family (Bonner *et al.*, 2008; Rogakou *et al.*, 1998) including ataxia telangiectasia mutated (**ATM**), ataxia telangiectasia and Rad3-related protein (**ATR**), and DNA-dependent protein kinase (**DNA-PK**) (Fernandez-Capetillo *et al.*, 2004; Stiff *et al.*, 2004; Stiff *et al.*, 2006) to form the gold standard DSB marker, **γ H2AX (Fig. 10)**. Of these three kinases, ATM is considered to play a prominent role in H2AX phosphorylation and activation following DSB damage (Falck *et al.*, 2005; Redon *et al.*, 2002; Stiff *et al.*, 2004; Stiff *et al.*, 2006), as the extent of ATM activation correlates strongly with the number of DSBs formed compared to other lesions generated (Ismail *et al.*, 2005). Autophosphorylation of ATM at serine 1981 results in ATM dimer dissociation and initiates cellular ATM kinase activity (Bakkenist and Kastan, 2003) and the transduction of signals allowing for the subsequent recruitment of DNA repair machinery (**Fig. 10**).

Although γ H2AX is classically viewed as the gold standard for DNA DSB measurement, it is becoming more widely accepted as a general marker of DNA damage and genomic instability given the interrelated nature of the way DSBs arise indirectly from other DNA lesions, and the evolving cross-talk between DNA repair pathways. Its broadened scope is also evident through its use in a variety of avenues in addition to basic DNA repair research including drug

development, translational studies, radiation research, environmental studies, tumorigenesis and in clinical trials and patient care (Dickey *et al.*, 2009). Elevated levels of γ H2AX have been documented in various human cancer cell systems from cervical cancer cells to neuroblastoma cells, as well as in colonocytes from patients with the chronic inflammatory disease ulcerative colitis (Dickey *et al.*, 2009). Interestingly, emerging research points to an age-related accumulation phenomenon with γ H2AX, as observed with 8-oxodG, revealing an exciting correlation between the two markers of DNA damage with important novel implications for understanding the pathogenesis of neurodegenerative disorders (Park *et al.*, 2012).

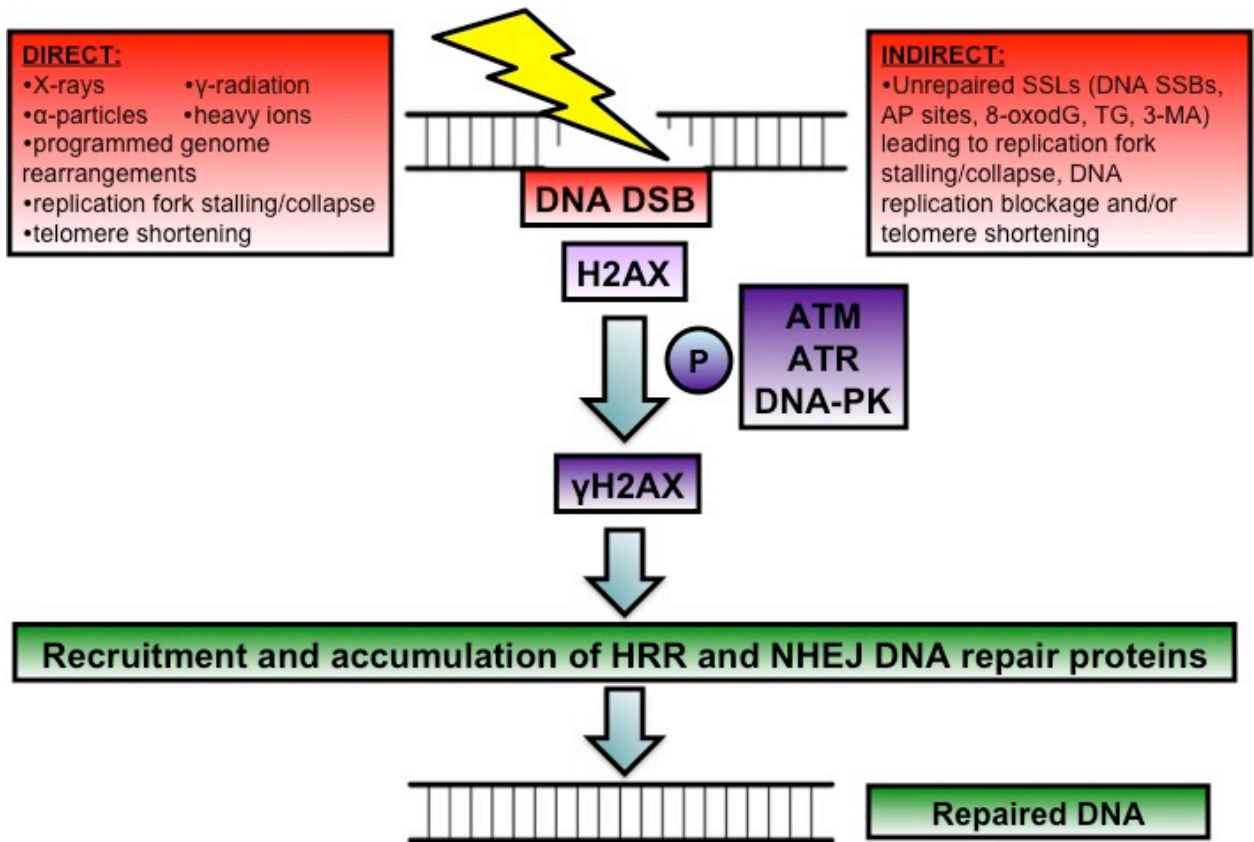


Figure 10. Induction of γ H2AX and the DNA damage response.

Abbreviations: 3-MA, 3-methyladenine; 8-oxodG, 8-oxo-2'-deoxyguanosine; AP, apurinic/aprimidinic; ATM, ataxia telangiectasia mutated; ATR, ataxia telangiectasia and Rad3-related protein; DSB, DNA double-strand break; DNA-PK, DNA-dependent protein kinase; SSB, DNA single-strand break; γ H2AX, variant H2A histone H2AX phosphorylated at serine 139; H2AX, variant H2A histone H2AX; HRR, homologous recombination repair; NHEJ, non-homologous end joining; P, phosphate; SSL, single-strand lesion; TG, thymine glycol.

1.5 DNA REPAIR

1.5.1 Major pathways for the repair of DNA damage

DNA damage is unavoidable, occurring spontaneously and as a result of exogenous environmental insult. As such, we have evolved, and are well equipped with, a number of DNA repair pathways tasked with combating this damage and mitigating its pathogenic effects. A summary of the six major DNA repair pathways is provided in **Table 7**.

Table 7. Overview of the six major DNA repair pathways.

<u>DNA Repair Pathway</u>	<u>Subpathways</u>	<u>Substrates</u>	<u>Description</u>
Direct reversal (DR)	None known	Alkylated bases: 1-methyladenine (1meA), 3-methylcytosine (3meC), O6-methylguanine (6meG)	Depending on the site of alkylation, DR repair is carried out by either a suicidal methyltransferase that transfers the methyl group from the DNA to a cysteine residue on itself, or a member of the AlkB family of dioxygenases which oxidatively demethylate the damaged base. This efficient repair pathway is advantageous in that it doesn't require sequence information carried on a complementary strand or sister chromatid for repair, nor does it create any cytotoxic or mutagenic intermediates.
Base excision repair (BER)	Short-patch and long-patch BER	Largest number of substrates: DNA single-strand breaks (SSB), uracil (U), 8-oxo-2'-deoxyguanosine (8-oxodG), 3-methyladenine (3meA), formamidopyrimidine (Fapy), thymine glycol (Tg)	BER is initiated by a lesion-specific DNA glycosylase that recognizes and excises the damaged base prior to strand incision, gap-filling with one (short-patch) or several (long-patch) nucleotides, and ligation in order to reinstate the proper DNA sequence. Clinically, BER defects are associated with increased cancer incidence and implicated in neurodegenerative disorders such as Alzheimer's disease.

Mismatch repair (MMR)	Multiple in eukaryotes	<p>Mismatches in DNA acquired during replication: base-base, small deletion and addition mismatches; structural distortions due to uncomplimentary base pairs or small unpaired loops</p>	<p>The multiple MMR pathways in eukaryotes are not well delineated and the proteins have roles in other DNA maintenance processes as well. Characteristic of MMR is the excision of the mismatch being coupled to the synthesis of a long track of DNA. Clinically, defects in MMR have been linked to hereditary non-polyposis colon cancer.</p>
Nucleotide excision repair (NER)	Global genome repair (GGR) and transcription-coupled repair (TCR)	<p>Helix-distorting lesions & bulky adducts that interfere with base pairing and obstruct transcription and replication: acetyl aminofluorene, cyclobutane pyrimidine dimers, pyrimidine-(6-4)-pyrimidone photoproducts, cisplatin</p>	<p>NER is a complex repair process involving the concerted effort of more than 30 different proteins that remove the lesion via incision on both sides, and using the complementary DNA strand as a template, synthesize a nascent strand to replace the excised portion. Defects in NER are associated clinically with the conditions xeroderma pigmentosum, Cockayne's syndrome and trichothiodystrophy that are characterized by a high cancer incidence, neurodegeneration and premature aging.</p>

Homologous recombination (HR)	None known	DNA double-strand breaks (DSBs): blunt-ends, hairpins, 5' and 3' overhangs	HR is an error-free repair process requiring the sequence information on the replicated sister chromatid for repair. The precise mechanism of HR remains to be elucidated but initially involves Rad51 and its paralogs as well as helicases and endonucleases. Werner, Rothmund-Thomson and Bloom syndromes are examples of the clinical manifestation of HR defects.
Non-homologous end joining (NHEJ)	None known	DSBs: blunt-ends, hairpins, 5' and 3' overhangs	NHEJ is an error-prone repair process given its capability to rejoin broken DNA strands despite the sequence, and involves the action of a DNA-dependent protein kinase tetramer along with Artemis, X-ray cross-complementing 4 (XRCC4) and DNA ligase IV. Deficiencies in NHEJ similarly manifest clinically in Werner and Bloom syndromes.

Created from: Nordstrand et al., 2007 and references therein.

1.5.2 Base excision repair

The base excision repair (**BER**) pathway is one highly conserved form of DNA repair responsible for maintaining both genomic stability and integrity. It does so by removing aberrant bases from the genome, and is largely regarded as the workhorse pathway of the cell handling the largest number, and most common forms of DNA damage (Wilson and Bohr, 2007). The BER pathway is primarily responsible for the repair of spontaneous hydrolytic, non-enzymatic alkylation, and oxidative DNA damage, including DNA single-strand breaks (**SSB**), uracil (**U**), 3-methyladenine (**3meA**), formamidopyrimidines (**Fapy**), thymine glycol (**TG**) and importantly, 8-oxo-2'-deoxyguanosine (**8-oxodG**) (Wilson and Bohr, 2007).

1.5.2.1 Oxoguanine glycosylase 1

Oxoguanine glycosylase 1 (**Ogg1**) is a bifunctional DNA glycosylase/apurinic/apyrimidinic (**AP**) lyase responsible for initiating BER in mammalian cells via recognition and excision of aberrant bases, primarily 2,6-diamino-4-hydroxy-5-formamidopyrimidine (**FapyG**) and 8-oxodG, as discussed below (Klungland *et al.*, 1999). In humans, the *Ogg1* gene is located on chromosome 3p25 and encodes two isoforms, α and β , that result from differential splicing of a single messenger RNA (**mRNA**) (Boiteux and Radicella, 2000). The more abundant α isoform is transcribed from exons 1-7 yielding a 345 amino acid (39 kDa) protein product that is primarily localized to the nucleus, while the 424 amino acid (47 kDa) β isoform is transcribed from exons 1-6 and 8 and localizes to the mitochondria (Boiteux and Radicella, 2000; Hashiguchi *et al.*, 2004). The first 316 amino acids are identical between the two isoforms (Boiteux and Radicella, 2000; Hashiguchi *et al.*, 2004). However, the C-termini vary considerably with amino acids 335-342 encoding a nuclear localization signal (**NLS**) in the α isoform that dominates the common mitochondrial localization signal (**MLS**) encoded by amino acids 9-26, thus accounting for its nuclear localization (Boiteux and Radicella, 2000; Hashiguchi *et al.*, 2004). Extensive studies on the α isoform identified the conserved helix-hairpin-helix element followed by a glycine/proline-rich loop and a conserved aspartic acid motif (**HhH-GPD**) as essential for DNA glycosylase and binding activity, with lysine 249 and aspartate 268 constituting critical residues in the active site (Boiteux and Radicella, 2000; Hashiguchi *et al.*, 2004). Subsequent studies also identified the valine 317 residue in the C-

terminal α O helix as a necessity for 8-oxodG binding and incision activity (Hashiguchi *et al.*, 2004).

The human *Ogg1* gene is constitutively expressed, with a CpG island rich promoter region lacking TATA and CAAT boxes, resembling that of a typical housekeeping gene (Boiteux and Radicella, 2000). *Ogg1* mRNA has been detected in both adult and fetal tissues suggesting that *Ogg1* is expressed throughout development (Boiteux and Radicella, 2000). One group estimated the interindividual variation in *Ogg1* mRNA levels to be 5- to 10-fold (Vogel *et al.*, 2002), while another group found a 2.8-fold interindividual variation in Ogg1 activity in healthy subjects, with no significant differences between males and females, although older males (> 55 years) showed significantly lower activity versus young males, a trend absent in females (Paz-Elizur *et al.*, 2007). Accordingly, variability in Ogg1 activity may constitute an important determinant of risk for pathologies mediated by DNA lesions repaired via BER.

The murine *Ogg1* gene has been localized to chromosome 6E and displays approximately 84% sequence homology with the human α isoform, possessing the same number and size of exons, although there has yet to be a report of a similar β isoform in rodents (Boiteux and Radicella, 2000). Thus, rodent models serve as an effective surrogate for human studies in delineating the contribution of Ogg1 in the pathogenesis of various diseases.

1.5.2.2 Formamidopyrimidine glycosylase

Formamidopyrimidine glycosylase (**Fpg**), or MutM, is the bacterial homolog to Ogg1. It is a bifunctional DNA glycosylase/AP lyase responsible for initiating BER in bacteria, and deficiencies in Fpg also lead to the accumulation of G:C to T:A transversion mutations (Frosina, 2006). The Fpg protein is a 269 amino acid (30.2 kDa) globular monomer comprised of two domains connected by a hinge polypeptide (Frosina, 2006; Gilboa *et al.*, 2002). The N-terminal domain is made up of eight β -strands that form a β -sandwich with two α -helices parallel to its edges, while the C-terminal domain contains four α -helices, two forming the helix-two turn-helix motif, and two β -strands that form a β -hairpin zinc finger DNA binding domain (Frosina, 2006; Gilboa *et al.*, 2002). Studies employing site-directed mutagenesis have uncovered a number of amino acid residues critical for Fpg's function. Histidine 89 and lysine 217 are required for recognition of the oxidatively damaged base, while DNA binding requires lysine 56, histidine 70,

asparagine 168 and arginine 258 for the formation of hydrogen bonds with the DNA backbone (Frosina, 2006).

Although expressed at comparable levels and functionally similar to Ogg1, Fpg is catalytically more efficient, excising 8-oxodG and FapyG 80-fold faster as evidenced by the higher k_{cat}/K_m values; a phenomenon attributed to higher substrate affinity and quicker intermediate hydrolysis, whereby Fpg releases product more readily from its catalytic incision site than does Ogg1 (Asagoshi *et al.*, 2000; Frosina, 2006). Fpg also differs from Ogg1 in that it possesses the ability to recognize 4,6-diamino-5-formamidopyrimidine (**FapyA**) as a substrate in addition to 8-oxodG and FapyG (Frosina, 2006). Notwithstanding some notable differences, both Fpg and Ogg1 are essential for limiting oxidative base damage and thus maintaining genomic integrity in their respective species.

1.5.2.3 The base excision repair pathway

Advances in molecular and biochemical techniques have allowed for the identification of a number of proteins involved in the BER pathway, and delineation of their substrates and functions (**Table 8**). BER is comprised of two subpathways: the major short-patch pathway, and the minor long-patch pathway. A general schematic detailing the steps in each pathway are outlined in **Figure 11**. However, the specific functions carried out by each protein in the pathway may vary slightly and are dictated by the particular lesion under repair and the initiating glycosylase.

Specific to the repair of 8-oxodG, short-patch BER (**Fig. 11**) is initiated by the lesion specific bifunctional DNA glycosylase/AP lyase Ogg1 in mammalian cells, and its functional homolog in bacteria, Fpg (Klungland *et al.*, 1999; Wilson and Bohr, 2007). In mammalian cells, 8-oxodG recognition and excision can also be carried out by the nei (endonuclease VIII)-like proteins 1 and 2 (**NEIL1** and **NEIL2**), albeit with lower activity, and NEIL2 playing a particular role in 8-oxodG removal from DNA bubble structures which form within regions of unpaired bases flanked by duplex DNA (Akbari and Krokan, 2008). Ogg1 acts to recognize and excise the damaged base by first hydrolyzing the N-glycosylic bond to create an AP site, and second, because of its bifunctional nature, also incising the DNA backbone 3' to the AP site via a β -elimination reaction (Wilson and Bohr, 2007). This results in the formation of a SSB with a 3'-

deoxyribose phosphate (**dRP**) that requires processing by AP endonuclease 1 (**APE1**) to a 3'-hydroxyl group and 5'-dRP before subsequent steps in the pathway can be carried out (Akbari and Krokan, 2008; Hazra *et al.*, 2007; Wilson and Bohr, 2007). DNA polymerase β (**Pol β**) then removes the 5'-dRP created by APE1 and replaces the excised nucleotide filling the gap, while DNA ligase III α (**LIG3 α**) in concert with X-ray cross-complementing 1 (**XRCC1**) seal the nick, completing the repair process yielding repaired DNA and restoring genomic integrity (Akbari and Krokan, 2008; Wilson and Bohr, 2007).

In instances when the terminal sugar-phosphate residue is more complex in structure as a result of AP site oxidation or reduction, and therefore resistant to Pol β cleavage, Pol δ/ϵ adds a few nucleotides to the 3' end to create a flap containing the 5' sugar phosphate, thereby activating the long-patch BER subpathway (Hung *et al.*, 2005b) (**Fig. 11**). In this reaction, the flap is removed by flap endonuclease 1 (**FEN1**), in concert with proliferating cell nuclear antigen (**PCNA**) stimulation and scaffolding, and LIG1 seals the nick to similarly complete the process yielding repaired DNA (Hung *et al.*, 2005b).

Table 8. Proteins involved in base excision repair.

Protein	Cellular localization	Known substrates/function
UNG1	M	Substrates overlap with UNG2 ssU, U:A, U:G, alloxan, isodialuric acid, 5-OHU
UNG2	N	
SMUG1	N	ssU, U:G, U:A, isodialuric acid, 5-OHU, alloxan, 5-OHmU:G, εC:G, 5-fU
TDG	N	T:G, U:G, εdC:G
MBD4	N	T:G, U:G, (in CpG context)
MYH	N and M	A:8-oxoG, 2-OH-A:G
hOGG1	N and M	8-oxoG:C, fapyG, (AP-lyase)
NTH1	N and M	Tg, DHU, 5-OHU, 5-OHC, fapyG, (AP-lyase)
NEIL1	N, M ^a	Substrates overlap with NTH1, fapyG, 8-oxoG, (β,δ elimination)
NEIL2	N	Substrates overlap with NEIL1, AP-sites, (β,δ elimination)
MPG	N	3-meA, 7-meG, 3-meG, HX, εA, εG
APE1	N and M	AP sites, PG
APE2	N and M	Weak 5'-endonuclease at AP-sites, 3'-5' exonuclease on mismatches
POLβ	N	DNA polymerase, dRPase (β-elimination)
POLδ	N	DNA polymerase
POLγ	M	DNA polymerase, dRPase (β-elimination)
LIG I	N	DNA ligation
LIG III	N and M	DNA ligation
FEN1	N	Incision of ssDNA flaps and RNA-DNA flaps, 5'-3' exonuclease
PCNA	N	Sliding clamp for replication and repair proteins
XRCC1	N	Protein scaffold
PNK	N	3'-P and 5'-OH end processing
PARP1	N	poly(ADP-ribosyl)ation of proteins
RPA	N	Binds ssDNA during replication and repair
WRN	N	3'-5' helicase, 3'-5' exonuclease, DNA dependent ATPase

Abbreviations: N, nuclear; M, mitochondrial; U, uracil; 5-OHmU, 5-hydroxymethyluracil; 5-OHC, 5-hydroxycytosine; 5-OHU, 5-hydroxyuracil; DHU, 5,6-dihydrouracil; Tg, thymine glycol; 8-oxoG, 7,8-dihydro-8-oxoguanine; fapyG, 2,6-diamino-4-hydroxy-5-formamidopyrimidine; O⁶-meG, O⁶-methylguanine; PG, 3'-phosphoglycolate; ε, etheno adduct; HX, hypoxanthine; 5-fU, 5-formyluracil. ^a Reported but needs further examination.

Modified from: Akbari et al., 2008 with permission.

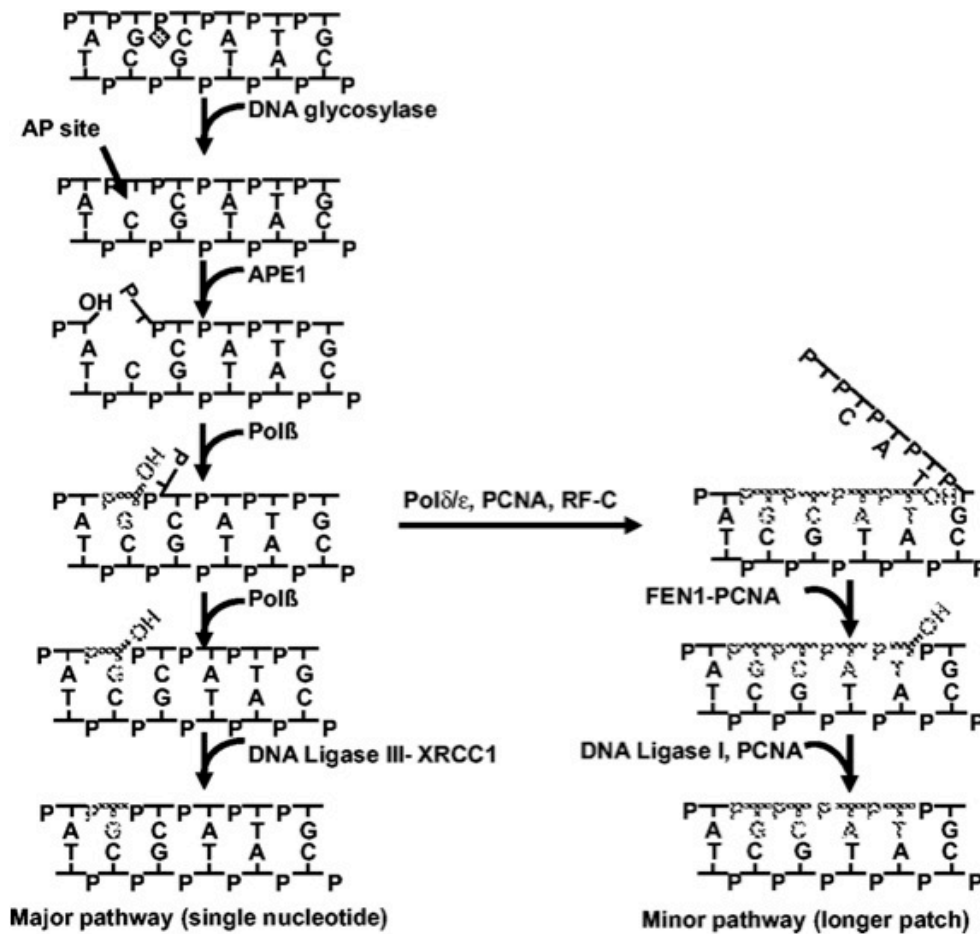


Figure 11. Short- and long-patch BER in mammalian cells.

The damaged base (G♦) is recognized and excised by a DNA glycosylase generating an apurinic/apyrimidinic (AP) site. AP endonuclease (APE1) cleaves the DNA backbone and recruits DNA polymerase β (Pol β) to fill the nucleotide gap. In short-patch BER, Pol β excises the 5'-deoxyribose phosphate (dRP), while X-ray cross-complementing 1 (XRCC1) complexed with DNA ligase III (LIG3) complete the repair process. In long-patch BER, the terminal sugar-phosphate is resistant to Pol β cleavage, thus Pol δ/ϵ adds several nucleotides to the 3' end generating a flap containing the 5' sugar phosphate. Flap endonuclease 1 (FEN1) subsequently removes this flap, in concert with reaction stimulation and scaffolding by proliferating cell nuclear antigen (PCNA), and the repair process is completed by the action of DNA ligase I (LIG1).

From: Hung et al., 2005b with permission.

1.5.2.4 Other proteins involved in 8-oxodG repair

Due to the high frequency of occurrence and mutagenic potential of 8-oxodG, organisms have evolved additional defense mechanisms to mitigate its deleterious consequences. Besides the additional DNA glycosylases capable of recognizing and excising 8-oxodG such as NEIL1 and NEIL2, the human counterparts to bacterial MutY and MutT, MutY homolog (**MYH** or **MutYH**) and MutT homolog 1 (**MTH1**) respectively, play an integral auxiliary role in 8-oxodG repair. Together with BER-initiating Ogg1, MYH and MTH1 comprise the 8-oxodG repair pathway commonly referred to as the “GO repair pathway” (David *et al.*, 2007) (**Fig. 12**). If 8-oxodG is not repaired via Ogg1-initiated BER, it will base pair with adenine following a single round of replication. Here, MYH acts to excise the adenine that has been misincorporated opposite 8-oxodG, thereby preventing G:C to T:A transversion mutations upon successive rounds of replication (David *et al.*, 2007). This creates an AP site that is subsequently repaired via a replication polymerase that reinstates an 8-oxodG:C base pair allowing Ogg1 a second chance at repair (David *et al.*, 2007). A complementary prophylactic role is carried out by MTH1, which prevents the incorporation of 8-oxodG into nascent DNA by polymerases via hydrolysis of free 8-oxodGTP to 8-oxodGMP, thus effectively removing it from the dNTP pool (David *et al.*, 2007; Michaels and Miller, 1992). Together, the concerted efforts of these players keep the mutagenic effects of 8-oxodG at bay.

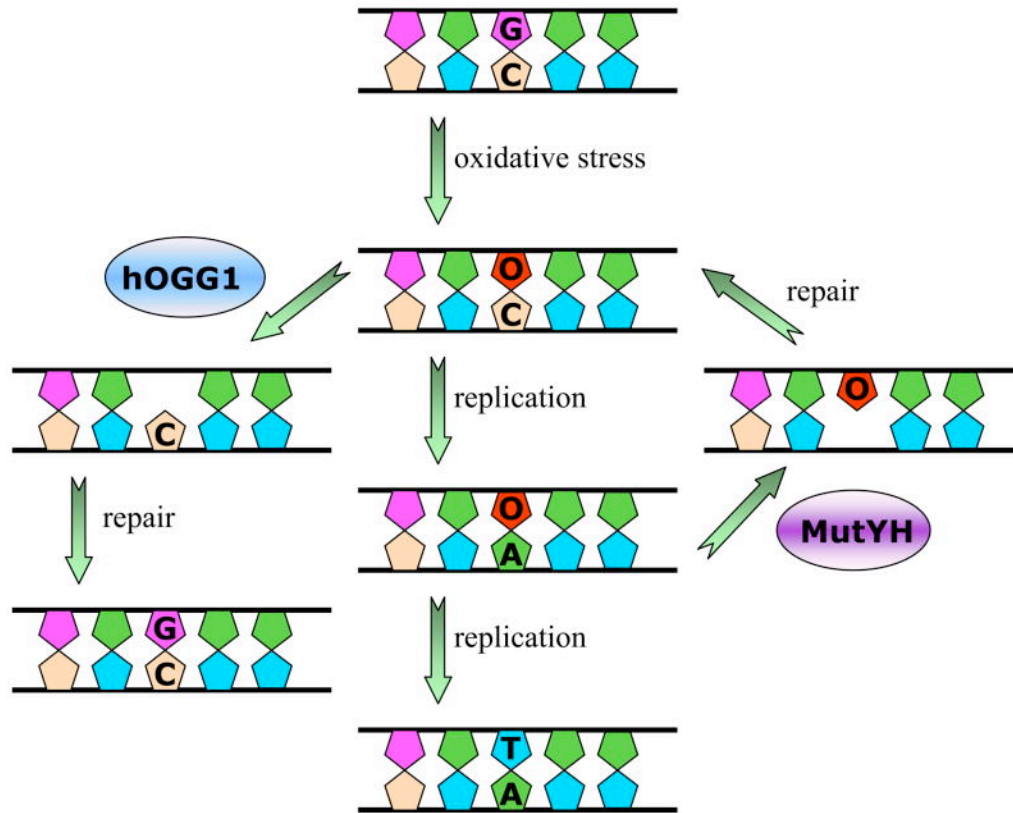


Figure 12. 8-oxodG repair by Ogg1 and the related proteins MutYH (MYH) and MTH1.

Unrepaired 8-oxodG (O) can result in G:C to T:A transversion mutations after sequential rounds of replication (center panel). Ogg1 initiates BER removing 8-oxodG, while MutYH (MYH) removes adenine (A) misincorporated opposite 8-oxodG during replication allowing another chance for its repair. MTH1 (not shown) prevents the incorporation of 8-oxodG into nascent DNA by hydrolyzing free 8-oxodGTP removing it from the dNTP pool.

From: David et al., 2007 with permission.

1.5.2.5 The importance of BER in disease

The importance of DNA repair in disease has been underscored by observations both *in vitro* and *in vivo*, in animals and humans, where deficiencies have proven deleterious. Deficiencies in the BER pathway, and specifically Ogg1, have been implicated in aging and age-related diseases such as cancer and neurodegeneration, as well as in embryonic and fetal toxicity from endogenous and xenobiotic-enhanced oxidative stress (Wells *et al.*, 2010; Wilson and Bohr, 2007).

In vitro, siRNA-mediated depletion of Ogg1 in human fibroblasts, H1299 and HeLa cells increases their sensitivity to oxidative stress-inducing hydrogen peroxide and menadione (de Souza-Pinto *et al.*, 2009; Youn *et al.*, 2007), while Ogg1-null (**Ogg1**^{-/-}) fibroblasts also void of MYH, responsible for excising adenine misincorporated opposite 8-oxodG during replication, similarly exhibit increased sensitivity to hydrogen peroxide (Xie *et al.*, 2008). *In vivo*, Ogg1^{-/-} mice, although they show no overt pathology, accumulate hepatic 8-oxodG corresponding to a 2-3-fold increased spontaneous mutation frequency (Klungland *et al.*, 1999; Minowa *et al.*, 2000), display increased postnatal neurodevelopmental deficits and enhanced brain 8-oxodG levels following *in utero* exposure to the ROS-initiating drug methamphetamine (Wong *et al.*, 2008), and with the combined absence of MYH, have an increased incidence of lung and small intestine cancer (Russo *et al.*, 2004). In humans, a serine to cysteine polymorphism at amino acid residue 326 of the Ogg1 protein compromises repair activity and has been associated with an increased cancer incidence (Goode *et al.*, 2002; Hung *et al.*, 2005a).

Given the severe consequences of compromised BER, especially under conditions of oxidative stress, one would logically postulate that upregulation of BER would be advantageous. However, whether enhancement of BER capacity through overexpression of Ogg1 or Fpg is protective remains unclear with conflicting reports in the literature. Overexpression of human Ogg1 (**hOgg1**) in the mitochondria of human hepatoma cells exacerbated cisplatin-mediated cytotoxicity (Zhang *et al.*, 2007), while the overexpression of *N*-methylpurine DNA glycosylase in human breast cancer cells similarly sensitized them to the alkylating agent methyl methanesulfonate (Rinne *et al.*, 2004). In contrast, expression of hOgg1 or Fpg in human lung epithelial cells protected against 1,3-N,N'-bis(2-chloroethyl)-N-nitrosourea (**BCNU**)-mediated

DNA damage and cytotoxicity (He *et al.*, 2002), as did their expression in human embryonic kidney (**HEK**) 293 cells for menadione-, cisplatin- and oxaliplatin-mediated toxicity (Preston *et al.*, 2009). The contradictory outcomes reported may be largely attributed to the key principle that biological systems thrive when in balance. As such, upregulation of DNA glycosylases results in enhanced glycosylase/AP lyase activity, which generates toxic DNA repair intermediates such as AP sites and DNA SSBs. If the amount of these lesions cannot be adequately managed due to the lack of compensatory upregulation of downstream components of the BER pathway, then toxicity ensues as a result of the perturbation of the normal balance that exists within the BER pathway.

Accordingly, restoring pre-existing deficiencies in BER, or upregulation of the machinery as a whole, may prove therapeutically useful as an intervention against oxidative stress-mediated toxicity. Glycosylase overexpression itself, however, may in some cases be better suited as a means of sensitizing cells for cancer and like therapies.

1.6 THE CELL CYCLE

1.6.1 Overview of the eukaryotic cell cycle

The eukaryotic cell cycle is divided into four major phases, G1, S, G2 and mitosis (**M**), which sequentially control the replication of cells (**Fig. 13**). In human cells that are rapidly dividing, the entire cell cycle can be traversed in approximately 24 h, with roughly 9 h spent in G1, 10 h in S phase, 4.5 h in G2 and mitosis lasting a mere 30 min (Lodish *et al.*, 2000). Rapidly growing yeast cells on the other hand can complete their entire cell cycle in about 90 min (Lodish *et al.*, 2000).

Newly divided cycling cells from diploid organisms containing $2n$ chromosomes will enter the cell cycle in the G1 phase, an initial growth phase during which cells carry out normal growth and metabolic processes (Lodish *et al.*, 2000). Following G1, cells enter S phase wherein DNA is synthesized for chromosome replication, and upon completion, cells contain $4n$ chromosomes (Lodish *et al.*, 2000). During the next phase, G2, cells continue to grow in preparation for cell division and the replicated DNA is double checked for errors and corrected if need be. After navigating through G2, cells are ready to undergo mitosis, a process composed of the individual stages of prophase, metaphase, anaphase, telophase and cytokinesis. Prophase is marked by chromosome condensation, followed by alignment and attachment of sister chromatids to the mitotic spindle at the center of the cell during metaphase (Lodish *et al.*, 2000). The sister chromatids are segregated to opposite spindle poles during anaphase, the nuclear envelope reforms around the segregated chromosomes as they decondense during telophase, and the division of the cytoplasm during cytokinesis completes the process yielding two daughter cells (Lodish *et al.*, 2000).

It is also possible for postmitotic cells to exit the cell cycle at G1, entering the G0 phase where they may reside anywhere from days to an entire lifetime as in the case of nerve cells and cells of the eye lens (Lodish *et al.*, 2000). Alternatively, G0 cells, or any cell that has fully differentiated, may reenter the cell cycle in S phase in a regulated process allowing for tight control of cell proliferation (Lodish *et al.*, 2000).

Accordingly, the highly integrated, multistep cell cycle provides numerous targeted opportunities for attack by endogenous, and exogenous environmentally-initiated insults. Importantly, the necessity of accurate DNA replication for normal growth underscores the importance of high fidelity DNA repair systems for maintaining genomic integrity both basally, and under conditions of genomic stress.

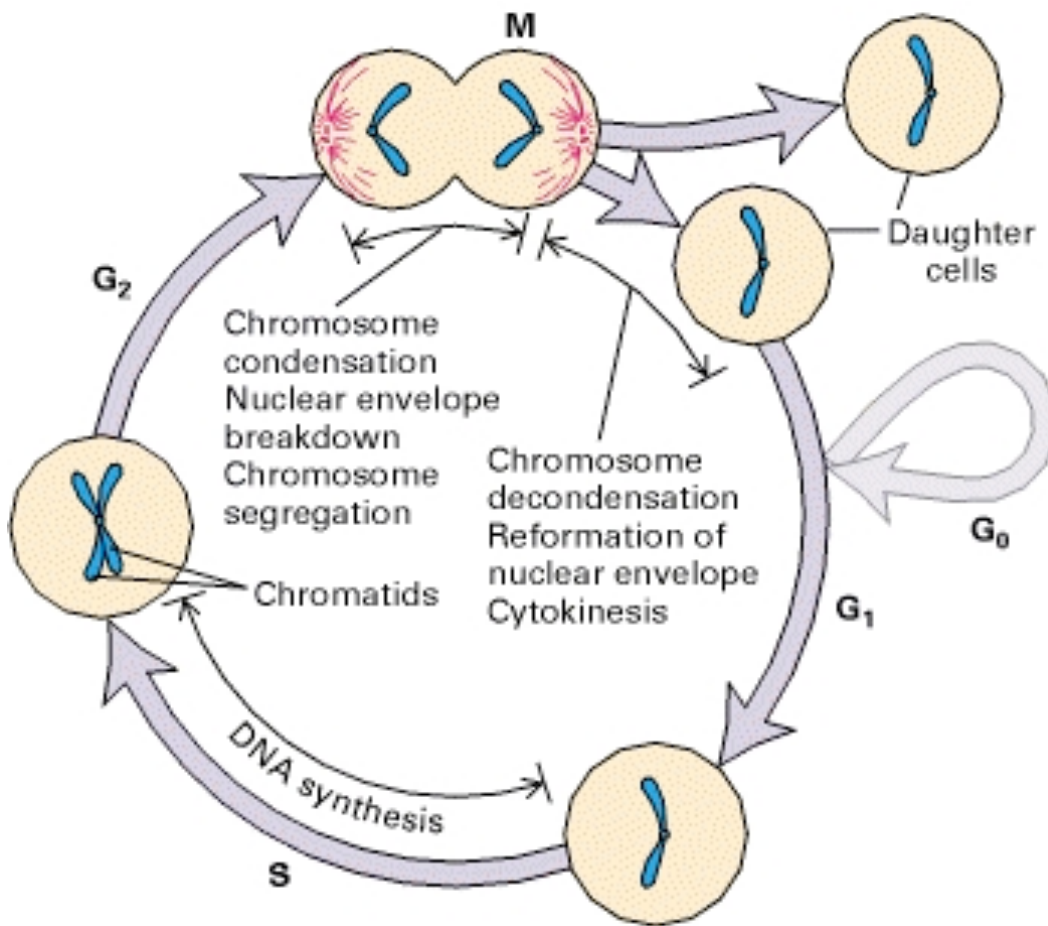


Figure 13. The fate of a single parental chromosome throughout the eukaryotic cell cycle.

Following mitosis (**M**), daughter cells in diploid organisms contain $2n$ chromosomes. In proliferating cells, G₁ is the period between the creation of daughter cells following mitosis, and S phase, marked by the initiation of DNA synthesis. At the end of S phase, cells from diploid organisms enter G₂ containing $4n$ chromosomes, twice the number as G₁ cells. The end of G₂ is marked by the onset of mitosis, during which numerous events culminate in cell division. The G₁, S, and G₂ phases are collectively referred to as interphase, the period between one mitosis and the next. Nonproliferating cells in vertebrates leave the cell cycle in G₁, entering the G₀ state.

From: Lodish et al., 2000 with permission.

1.6.2 Overview of eukaryotic cell cycle regulation

In general, transition through the eukaryotic cell cycle is controlled by protein phosphorylation via protein kinases, and protein degradation (**Fig. 14**). Specifically, G1, S phase and mitotic cyclin-dependent kinase complexes (**CdkCs**) composed of a regulatory cyclin subunit and a catalytic cyclin-dependent kinase (**Cdk**) subunit control cell cycle passage (Lodish *et al.*, 2000). This control is achieved by Cdk subunits associating with different cyclins, whose concentrations vary with each phase of the cell cycle, thus determining which proteins are phosphorylated by the CdkC (Lodish *et al.*, 2000). In higher organisms, regulation of G1 CdkC synthesis via mitogens and their activity additionally contribute to cell cycle control (Lodish *et al.*, 2000).

G1 CdkCs are expressed when cells are stimulated to replicate, and lead to the activation of transcription factors for the expression of DNA synthesis enzymes and S phase CdkCs, whose activity is initially inhibited (Lodish *et al.*, 2000). In late G1, G1 CdkCs activate S phase CdkCs by initiating S phase inhibitor degradation (Lodish *et al.*, 2000). Active S phase CdkCs permit entry into S phase and phosphorylate regulatory sites on proteins of DNA pre-replication complexes initiating DNA replication (Lodish *et al.*, 2000). These regulatory sites are dephosphorylated by phosphatases in early G1 of the subsequent cell cycle allowing for reassembly of the complexes at replication origins prior to the next S phase (Lodish *et al.*, 2000). Once DNA replication is complete, mitotic CdkCs synthesized during S phase and G2 are activated and initiate chromosome condensation, nuclear envelope breakdown, mitotic spindle apparatus assembly, and alignment of condensed chromosomes at the metaphase plate (Lodish *et al.*, 2000). Mitotic CdkCs also activate the anaphase-promoting complex (**APC**) which subsequently initiates ubiquitin-mediated degradation of anaphase inhibitors allowing anaphase to proceed, and also induces the degradation of mitotic cyclins, decreasing mitotic Cdk activity thereby allowing the completion of mitosis via telophase and cytokinesis (Lodish *et al.*, 2000). APCs are inactivated by G1 CdkCs in late G1 such that mitotic cyclins can accumulate during S phase and G2 of the subsequent cell cycle (Lodish *et al.*, 2000).

Interference with the control of the cell cycle by endogenous or exogenous factors can be as detrimental as interference with the cell cycle machinery itself. Control of the cell cycle is

also a complex integrated process, that if perturbed can have deleterious impacts on normal growth and development, but also poses an attractive avenue for therapeutic intervention in pathologies characterized by aberrant cell growth such as cancer.

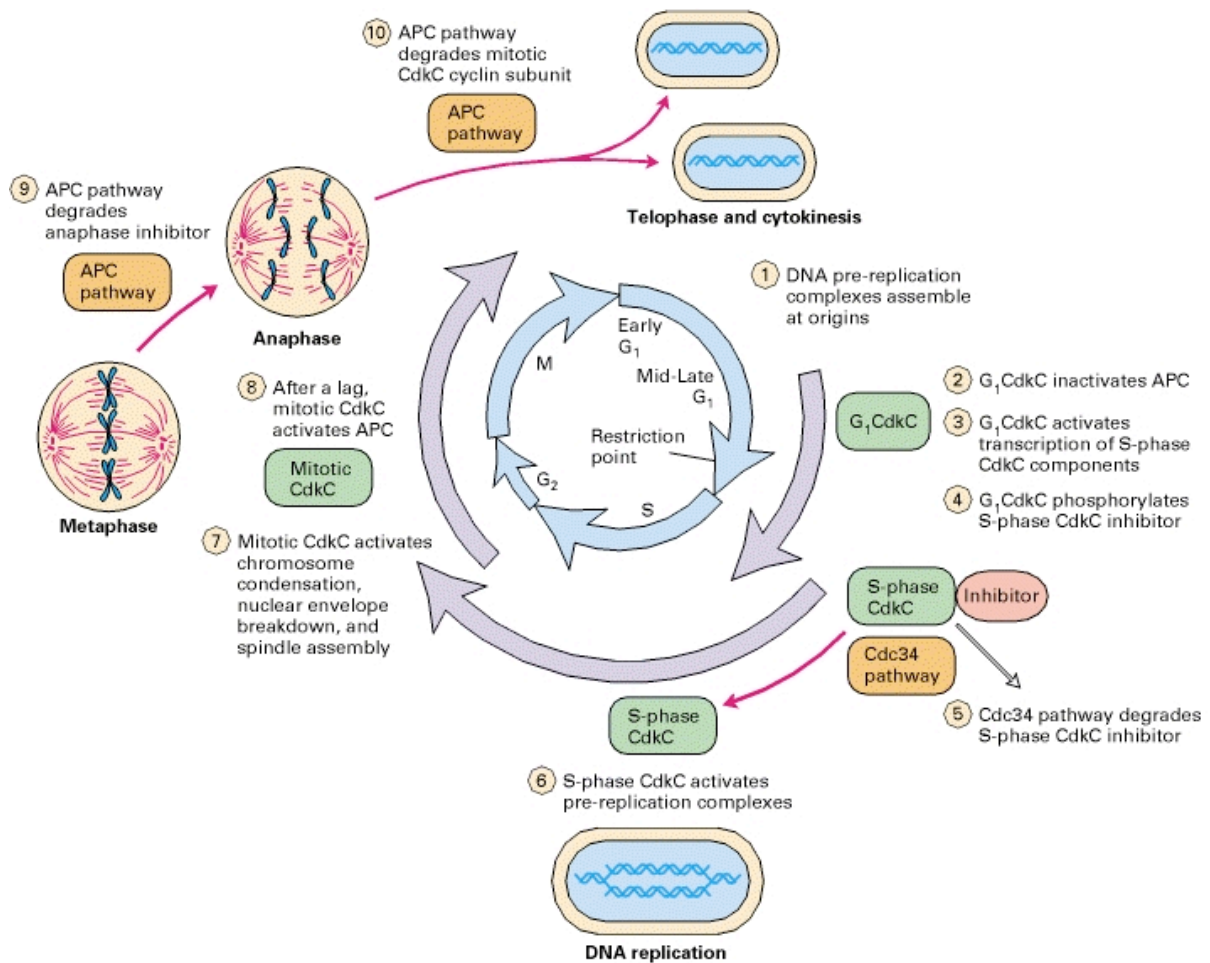


Figure 14. Current model for regulation of the eukaryotic cell cycle.

Passage through the cycle is controlled by G₁, S phase, and mitotic cyclin-dependent kinase complexes (**CdkCs**) (highlighted in green) that are composed of a regulatory cyclin subunit and a catalytic cyclin-dependent kinase subunit. Protein complexes (orange) in the Cdc34 pathway and anaphase-promoting complex (**APC**) pathway polyubiquitinate specific substrates including the S phase inhibitor, anaphase inhibitor, and mitotic cyclins, marking these substrates for degradation by proteasomes. Since protein degradation is irreversible, these pathways thus drive the cycle in one direction. Proteolysis of anaphase inhibitors inactivates the protein complexes that connect sister chromatids at metaphase (not shown), thereby initiating anaphase.

From: Lodish et al., 2000 with permission.

CHAPTER 2: STUDIES

2.1 STUDY 1: OXOGUANINE GLYCOSYLASE 1 (OGG1) PROTECTS CELLS FROM DNA DOUBLE-STRAND BREAK DAMAGE FOLLOWING METHYLMERCURY (MeHg) EXPOSURE^{a,b}

Running title: OGG1 and DNA damage following MeHg exposure

Stephanie L. Ondovcik^{*}, Laura Tamblyn[†], John Peter McPherson[†] and Peter G. Wells^{*,†,1}

Departments of ^{*}Pharmaceutical Sciences and [†]Pharmacology & Toxicology
University of Toronto
Toronto, Ontario, Canada

¹ Corresponding author:
Peter G. Wells, Pharm.D.
Faculty of Pharmacy, University of Toronto
144 College St., Toronto, Ontario, Canada M5S 3M2
Email: pg.wells@utoronto.ca
Phone 416-978-3221

a. A preliminary report of this research was presented at the 2012 annual meeting of the American Society for Pharmacology and Experimental Therapeutics at Experimental Biology [*FASEB J.*, 26 (No. 1050.10), 2012]. This work was supported by operating grants from the Canadian Institutes of Health Research (CIHR) [PGW], and the Cancer Research Society Inc. [JPM]. JPM is the recipient of a Province of Ontario Early Researcher Award, and SLO is the recipient of a CIHR Frederick Banting and Charles Best Canada Graduate Scholarship.

b. Full report of this research has been published:

Ondovcik SL, Tamblyn L, McPherson JP and Wells PG (2012) Oxoguanine Glycosylase 1 (OGG1) Protects Cells from DNA Double-Strand Break Damage Following Methylmercury (MeHg) Exposure. *Toxicological Sciences* 128(1): 272-283.

Tamblyn, L.- Assisted in the harvesting of cells for the Annexin V apoptosis assay and in the acquisition and analysis of the FACS data.

McPherson, J.P.- Acted in a co-supervisory capacity.

2.1.1 Abstract

Methylmercury (**MeHg**) is a potent neurotoxin, teratogen, and probable carcinogen, but the underlying mechanisms of its actions remain unclear. Although MeHg causes several types of DNA damage, the toxicological consequences of this macromolecular damage are unknown. MeHg enhances oxidative stress, which can cause various oxidative DNA lesions that are primarily repaired by oxoguanine glycosylase 1 (**OGG1**). Herein, we compared the response of wild-type and OGG1-*null* (**Ogg1**^{-/-}) murine embryonic fibroblasts to environmentally relevant, low micromolar concentrations of MeHg by measuring clonogenic efficiency, cell cycle arrest, DNA double-strand breaks (**DSBs**), and activation of the DNA damage response pathway. *Ogg1*^{-/-} cells exhibited greater sensitivity to MeHg than wild-type controls, as measured by the clonogenic assay, and showed a greater propensity for MeHg-initiated apoptosis. Both wild-type and *Ogg1*^{-/-} cells underwent cell cycle arrest when exposed to micromolar concentrations of MeHg; however, the extent of DSBs was exacerbated in *Ogg1*^{-/-} cells compared with that in wild-type controls. Pretreatment with the antioxidative enzyme catalase reduced levels of DSBs in both wild-type and *Ogg1*^{-/-} cells but failed to block MeHg-initiated apoptosis at micromolar concentrations. Our findings implicate reactive oxygen species-mediated DNA damage in the mechanism of MeHg toxicity; and demonstrate for the first time that impaired DNA repair capacity enhances cellular sensitivity to MeHg. Accordingly, the genotoxic properties of MeHg may contribute to its neurotoxic and teratogenic effects, and an individual's response to oxidative stress and DNA damage may constitute an important determinant of risk.

2.1.2 Introduction

Methylmercury (**MeHg**) is a persistent environmental contaminant with potent neurotoxic properties. Historically, MeHg is notorious for two large-scale cases of poisoning: via contaminated seafood in Minamata, Japan (Harada, 1995) and through tainted seed grain in Iraq (Amin-Zaki *et al.*, 1974). Today, exposure to MeHg is still of concern through society's attempt to foster a healthier lifestyle by increasing their dietary intake of fish and other seafood, as well as via increasing exposure from activities such as coal burning and gold mining (Bhavsar *et al.*, 2010; Guedron *et al.*, 2011; Kinghorn *et al.*, 2007). MeHg primarily targets the central nervous system, with the fetal brain displaying exquisite sensitivity. *In utero* exposure to MeHg can manifest in cerebral palsy, blindness, deafness, seizures, low birth weight and developmental delays in such areas as walking and speech (Castoldi *et al.*, 2003; Choi, 1989; Davis *et al.*, 1994). Analysis of brains of infants prenatally exposed to MeHg exhibit decreased brain volume, atrophy of the cerebrum and cerebellum, decreased number of neurons, abnormal cytoarchitecture and astrocytosis (Choi, 1989). Although the precise molecular mechanisms by which MeHg exerts its toxicity have yet to be elucidated, one plausible explanation for its effects involves the production of reactive oxygen species (**ROS**), and their subsequent damage to cellular macromolecules and interference with signal transduction pathways. MeHg has been shown to generate ROS both *in vitro* and *in vivo*, with antioxidants able to counteract a variety of toxic outcomes (Ali *et al.*, 1992; Burke *et al.*, 2006; Ganther, 1978; Garg and Chang, 2006; Gatti *et al.*, 2004; Jie *et al.*, 2007; Shanker *et al.*, 2005). Moreover, it has been demonstrated that MeHg has genotoxic potential with the ability to damage DNA, including chromosomal aberrations and oxidative lesions such as 7,8-dihydro-8-oxoguanine (**8-oxoG**) (Belletti *et al.*, 2002; Chen *et al.*, 2005; Choi, 1989; Crespo-Lopez *et al.*, 2007; Ehrenstein *et al.*, 2002; Liu *et al.*, 2002; Silva-Pereira *et al.*, 2005). A variety of molecular mechanisms have been proposed to explain the genotoxicity of MeHg and other mercuric compounds, including generation of DNA damage from oxidative stress (Crespo-Lopez *et al.*, 2007). Together, these suggest a potential role for oxidatively damaged DNA and subsequent pathologic consequences as a contributing factor in the mechanism of MeHg toxicity.

Oxidatively damaged DNA is primarily repaired by the base excision repair (**BER**) pathway, which in mammals is initiated by the bifunctional DNA

glycosylase/apurinic/aprimidinic lyase oxoguanine glycosylase 1 (**OGG1**) (Klungland and Bjelland, 2007). Deficiencies in the BER pathway, and specifically OGG1, have been implicated in aging and age-related diseases such as cancer and neurodegeneration (Wilson and Bohr, 2007), as well as in embryonic and fetal toxicity from endogenous and xenobiotic-enhanced oxidative stress (Wells *et al.*, 2010; Wong *et al.*, 2008) .

Although MeHg is known to damage DNA, there have been no studies examining the effects of variable DNA repair capacity on MeHg toxicity. Herein, we provide the first report of increased sensitivity of DNA repair-deficient cells to environmentally relevant, low micromolar concentrations of MeHg, which is blocked by the antioxidative enzyme catalase. This constitutes the most direct evidence to date that clastogenic DNA damage may contribute to the pathological consequences of MeHg exposure via a non-mutagenic mechanism, and that this DNA damage is ROS-mediated. Our findings demonstrate a critical role for OGG1 in the maintenance of genomic integrity following MeHg-initiated DNA damage, and suggest that interindividual variability in repair activity and antioxidant capacity may modulate the risk of toxicological consequences.

2.1.3 Materials and Methods

Cell culture. Wild-type and OGG1-*null* (**Ogg1**^{-/-}) murine embryonic fibroblasts were obtained from Dr. Bernd Epe, University of Mainz, Germany. Cells were maintained in Dulbecco's Minimum Essential Media containing 4.5 g/L D-glucose, pyridoxine HCl, and L-glutamine (Invitrogen Canada Inc., Burlington, Ontario). Media was supplemented with 1% penicillin/streptomycin solution and 10% heat-inactivated fetal bovine serum (both Sigma-Aldrich Canada Ltd., Oakville, Ontario).

Clonogenic assay. 5×10^2 cells were seeded into 60 mm dishes and either left untreated or exposed to various concentrations of methylmercury (II) chloride (MeHg, Sigma-Aldrich Canada Ltd.) for 24 hours. Surviving cells were allowed to grow into visible colonies, and were fixed and stained with methylene blue in methanol. Survival curves were produced from the mean value plus or minus the standard deviation of four to six determinations, and are presented as a percentage of control (MeHg-free) cells.

Cell cycle analysis by bromodeoxyuridine (BrdU) and propidium iodide (PI) double staining via flow cytometry. Cells seeded at 4×10^5 /100 mm dish were exposed to either 2 or 5 μ M MeHg for 0, 6, or 24 h. Cells were pulsed with 10 μ g/ml BrdU (Sigma-Aldrich Canada Ltd.) for 1 h before being collected at each time point. Staining and analysis of BrdU and PI (BD Biosciences, Mississauga, Ontario) were performed as previously described (Tamblyn *et al.*, 2009).

Analysis of apoptosis via Annexin V-FITC and PI double staining by flow cytometry. Cells were seeded at 4×10^5 /100 mm dish and left untreated, treated with 2 μ M MeHg for 6 h, or pretreated for 30 min with 500 U/ml polyethylene glycol (PEG)-conjugated catalase (PEG-catalase) (Sigma-Aldrich Canada Ltd.) prior to exposure to 2 μ M MeHg or 500 μ M hydrogen peroxide (H₂O₂) (Sigma-Aldrich Canada Ltd.). Cells were then harvested and evaluated for apoptosis by flow cytometry following staining with Annexin V-FITC and 50 μ g/ml PI.

Measurement of H2AX phosphorylated on serine 139 (γ H2AX)/Ataxia Telangiectasia Mutated phosphorylated on serine 1981 (pATM) and PI double staining by flow cytometry. Cells seeded at 4×10^5 /100 mm dish were exposed to either 2 or 5 μ M MeHg for 0, 3, 6, or 12 h, or

alternatively pretreated with 500 U/ml PEG-catalase for 30 min before 6 h exposure to 2 μ M MeHg, and collected by trypsinization at each time point. Cells were fixed with ice-cold 70% ethanol overnight at -20°C, washed with PBS and permeabilized with PBS containing 0.4% Triton X-100. Cells were stained for γ H2AX or pATM by incubating with an anti- γ H2AX (Millipore Canada Ltd., Etobicoke, Ontario) or anti-phospho-ATM(Ser1981) (10H11.E12, Cell Signaling, New England Biolabs Canada Ltd., Pickering, Ontario) primary antibody in PBS containing 0.2% Triton X-100 and 1% donkey serum for 3 h, followed by a 30 min incubation with a FITC-conjugated anti-mouse secondary antibody (Jackson, Cedarlane Laboratories, Hornby, Ontario). Cells were then washed with PBS, stained with 50 μ g/ml PI for 30 min, and analyzed by flow cytometry as previously described (Tamblyn *et al.*, 2009).

Statistical Analysis. Data comparing two groups were analyzed via an unpaired t-test, while multiple comparisons were analyzed using a one-way ANOVA followed by a Bonferroni or Dunnett post-test as appropriate, with the level of significance set to $p < 0.05$ in all cases (GraphPad Prism 5.0d, GraphPad Software Inc., La Jolla, CA).

2.1.4 Results

To investigate whether OGG1 status has an impact on the cytotoxicity of MeHg, we first compared the clonogenic survival of wild-type and OGG1-*null* (**Ogg1**^{-/-}) murine embryonic fibroblasts to varying concentrations of MeHg. Exposure to low micromolar concentrations (0.03-0.2 μM) of MeHg resulted in a greater concentration-dependent decrease in clonogenic survival in *Ogg1*^{-/-} cells compared to isogenic wild-type controls (**Fig. 1**).

Figure 1.

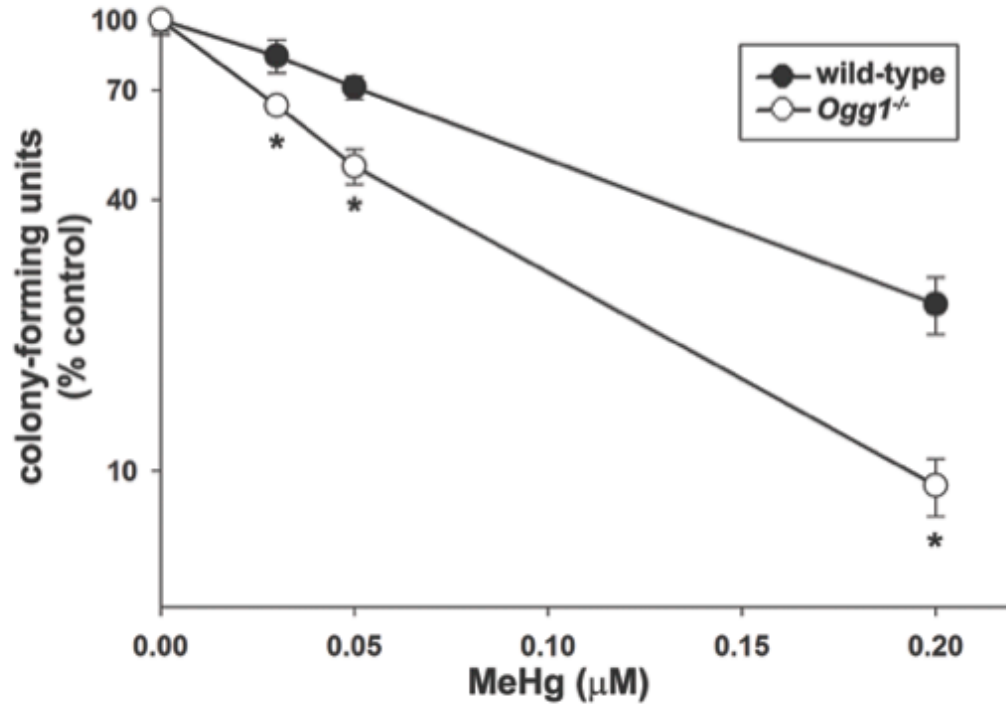


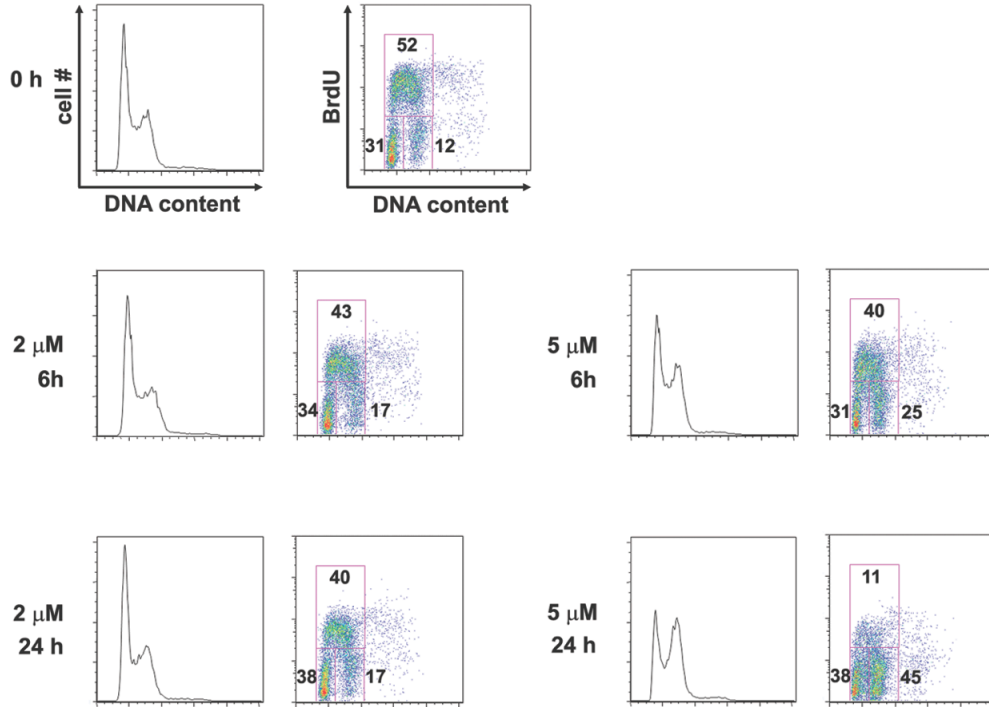
Figure 1. Oxoguanine glycosylase 1-null (*Ogg1*^{-/-}) cells are more sensitive to methylmercury (MeHg).

Sensitivity of wild-type and *Ogg1*^{-/-} murine embryonic fibroblasts was measured by clonogenic assay following exposure to MeHg. Each data point represents the mean \pm S.D. of 4-6 independent experiments. * Differences ($p < 0.001$) in sensitivity between wild-type and *Ogg1*^{-/-} cells at the specified concentrations.

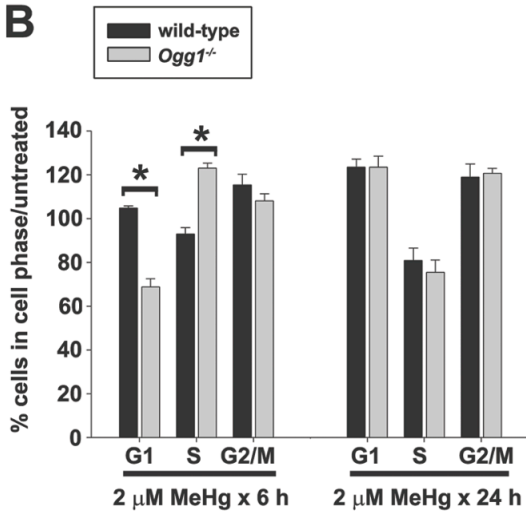
To assess whether the compromised survival of *Ogg1*^{-/-} cells following MeHg exposure might be due to altered capacity for cell cycle arrest, we examined the cell cycle status of wild-type and *Ogg1*^{-/-} cells following exposure to either 2 or 5 μM MeHg for 0, 6, or 24 h. Concentration- and incubation time-dependent effects of MeHg were observed. Following 6 h of incubation with 2 μM MeHg, wild-type cells showed very little deviation in the percentage of cells in G1, S and G2/M phases compared to untreated cells (**Fig. 2A, left panel and Fig. 2B**). In contrast, *Ogg1*^{-/-} cells showed a marked decline in the fraction of G1 cells and a marked accumulation of cells in S phase (**Fig. 2B**). Following 24 h of incubation, both wild-type and *Ogg1*^{-/-} cells exhibited equivalent increases in G1 and G2/M fractions, consistent with the onset of cell cycle arrest (**Fig. 2A, right panel and Fig. 2C**). Induction of cell cycle arrest in wild-type and *Ogg1*^{-/-} cells appeared equivalent when cells were exposed to a higher 5 μM concentration of MeHg for 6 or 24 h (**Fig. 2A, right panel and Fig. 2C**). Under these conditions, both wild-type and *Ogg1*^{-/-} cells showed a clear propensity for undergoing G2/M arrest.

Figure 2.

A



B



C

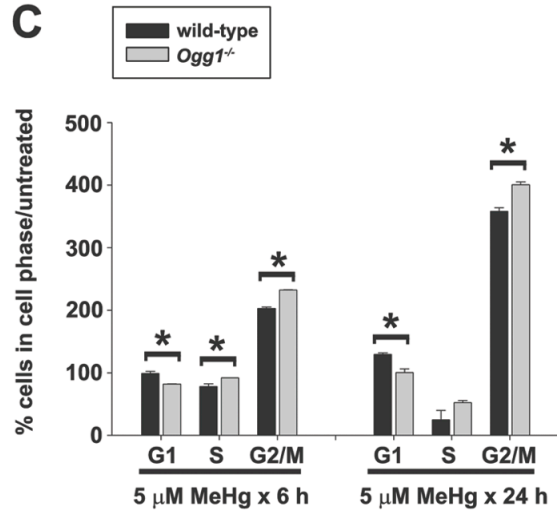


Figure 2. Susceptibility of *Ogg1*^{-/-} cells to MeHg-initiated proliferation arrest.

Wild-type and *Ogg1*^{-/-} cells were exposed to 2 μ M or 5 μ M MeHg for 0, 6, or 24 h and harvested for FACS analysis. (A) Representative histograms for each time point in wild-type cells, with the DNA content histogram (PI stain) shown on the left, and the corresponding BrdU-PI bivariate plot on the right. Bivariate plots are labeled with numbers corresponding to the percentage of cells in G1 (left gate), S (top gate), and G2/M (right gate) phases of the cell cycle. (B-C) Quantification of the percentage of cells (wild-type or *Ogg1*^{-/-}) in a given cell cycle phase exposed to 2 μ M (B) or 5 μ M (C) MeHg compared to untreated cells. Data shown are representative of three independent experiments. * Denotes a significant difference ($p < 0.05$) between wild-type and *Ogg1*^{-/-} cells.

The compromised survival of *Ogg1*^{-/-} cells following MeHg exposure might be attributed to an increased susceptibility to apoptosis that may be partially ROS-mediated. We have observed that a 30 min pretreatment with 500 U/ml PEG-catalase is sufficient to restore viability of wild-type and *Ogg1*^{-/-} cells incubated with 500 μ M hydrogen peroxide (positive control) for 6 h (**data not shown**). Accordingly, we quantified the percentage of apoptotic wild-type and *Ogg1*^{-/-} cells following a 30 min pretreatment with 500 U/ml PEG-catalase and a 6 h incubation with 2 μ M MeHg (**Fig. 3A-B**). Untreated wild-type and *Ogg1*^{-/-} cells were not significantly different in their viability (% viability = $86.5 \pm 3.4\%$ vs. $91.9 \pm 3.7\%$). After a 6 h exposure to 2 μ M MeHg, *Ogg1*^{-/-} cells exhibited decreased viability (% viability/% untreated viability = $87.6 \pm 4.6\%$) ($p < 0.05$) versus wild-type cells ($99.9 \pm 5.6\%$). Preincubation with the antioxidative enzyme PEG-catalase did not reduce MeHg-initiated apoptosis at micromolar concentrations, despite blocking hydrogen peroxide-initiated apoptosis ($p < 0.01$), with viability restored to untreated levels in both wild-type and *Ogg1*^{-/-} cells. The percentage of apoptotic wild-type and *Ogg1*^{-/-} cells was also quantified following an extended 24 h exposure to a submicromolar concentration (0.2 μ M) of MeHg (**data not shown**). This extended exposure regimen similarly caused no significant differences in viability between untreated wild-type and *Ogg1*^{-/-} cells ($91.1 \pm 2.5\%$ vs. $94.1 \pm 1.4\%$), nor did the viability significantly differ between wild-type and *Ogg1*^{-/-} cells exposed for 24 h to 0.2 μ M MeHg ($91.3 \pm 1.3\%$ vs. $94.2 \pm 2.8\%$).

Figure 3.

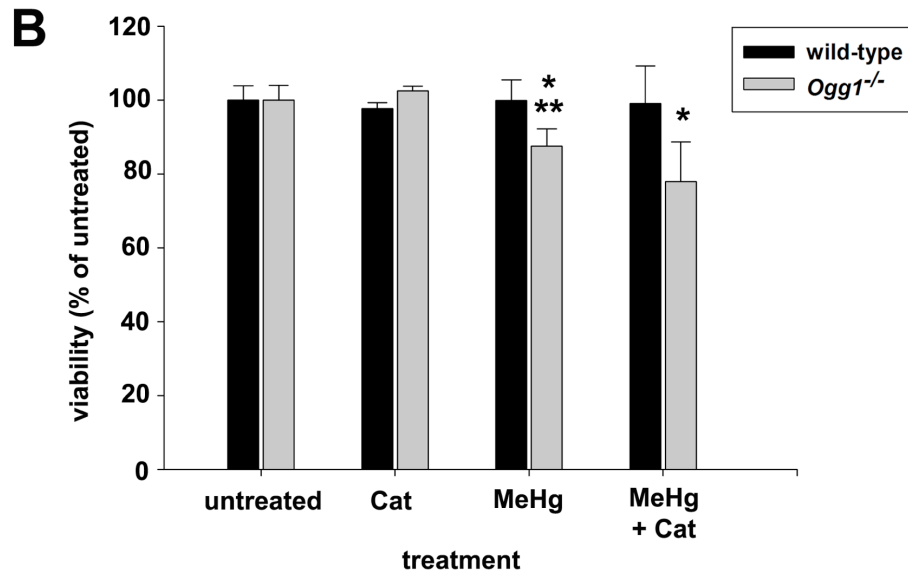
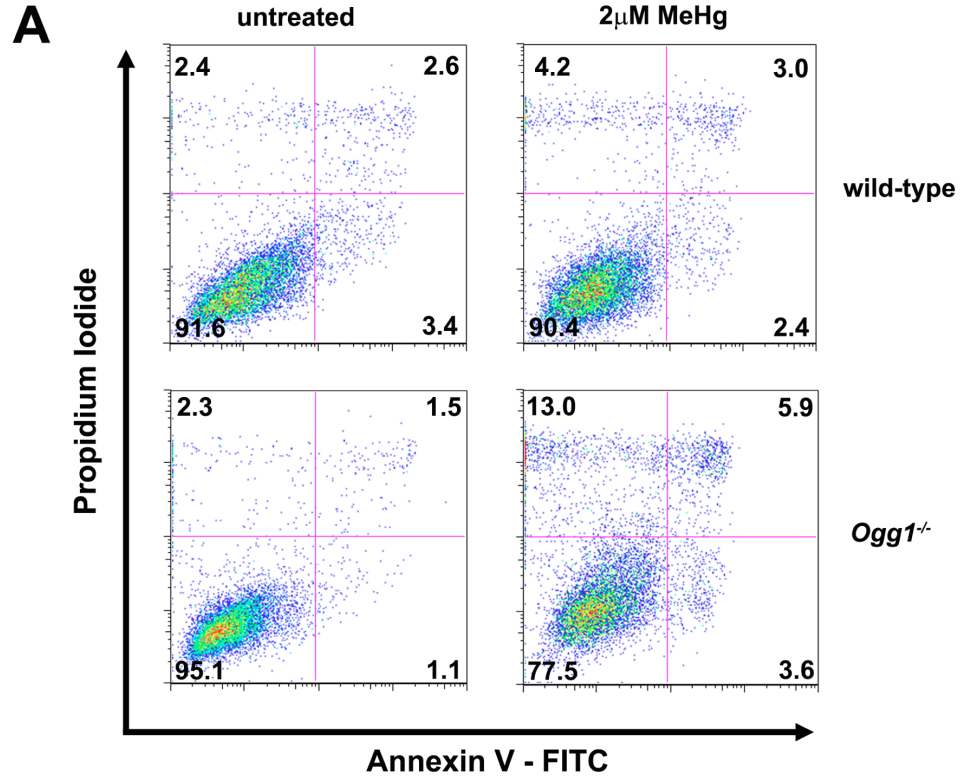


Figure 3. Susceptibility of *Ogg1*^{-/-} cells to undergo MeHg-initiated apoptosis and the inability of polyethylene glycol (PEG)-conjugated catalase to ameliorate MeHg-initiated apoptosis.

Wild-type and *Ogg1*^{-/-} cells were either untreated or exposed to 2 μ M MeHg for 6 h with and without a 30 min pretreatment with the antioxidative enzyme PEG-catalase, harvested and stained with Annexin V – FITC/PI for FACS analysis. **(A)** Representative scatter plots with Annexin V – FITC and PI on the x- and y-axes respectively. **(B)** Quantification of viable wild-type and *Ogg1*^{-/-} cells (Annexin V-FITC-low and PI-low) as the mean percent of untreated + S.D. of three independent experiments. * Statistically significant difference ($p < 0.05$) compared to untreated; ** Denotes a significant difference ($p < 0.05$) between wild-type and *Ogg1*^{-/-} cells.

As G2/M arrest is a response observed in fibroblasts exposed to agents causing chromosomal breakage (clastogenic), we investigated whether MeHg exposure resulted in DNA double-strand break (**DSB**) formation, and whether OGG1 status and antioxidant therapy (PEG-catalase) impacted the initiation of these lesions. The kinetics of DSB induction was monitored in wild-type and *Ogg1*^{-/-} cells by measuring the kinetics of H2AX phosphorylation at serine 139 (**γH2AX**). Wild-type and *Ogg1*^{-/-} cells exposed to either 2 or 5 μM MeHg for 0, 3, 6, or 12 h were analyzed for γH2AX content/cell as a function of cell cycle position by two-parameter FACS analysis. Exposure to 2 μM MeHg over a 12 h period did not generate γH2AX in wild-type cells, but resulted in a dramatic, approximately 6-fold induction of γH2AX in *Ogg1*^{-/-} cells at 6 and 12 h that was not evident at earlier time points (**Fig. 4A-B**). At the higher 5 μM concentration of MeHg, wild-type cells with elevated γH2AX were observed following exposure for 6 or 12 h, whereas *Ogg1*^{-/-} cells exposed to the same concentration accumulated more cells with elevated γH2AX at 3, 6 and 12 h than wild-type, with the extent of accumulation peaking at 6 h and then declining by the 12 h time point, the latter of which was likely due to enhanced cell death rather than a biochemical change in viable cells (**Fig. 4C-D**). When pretreated with 500 U/ml PEG-catalase for 30 min and subsequently exposed to 2 μM MeHg for 6 h, a two-fold reduction in γH2AX levels was observed in both the wild-type and *Ogg1*^{-/-} cells (p<0.05), sufficient to return wild-type γH2AX levels to those of the untreated cells (**Fig. 4E**).

Figure 4.

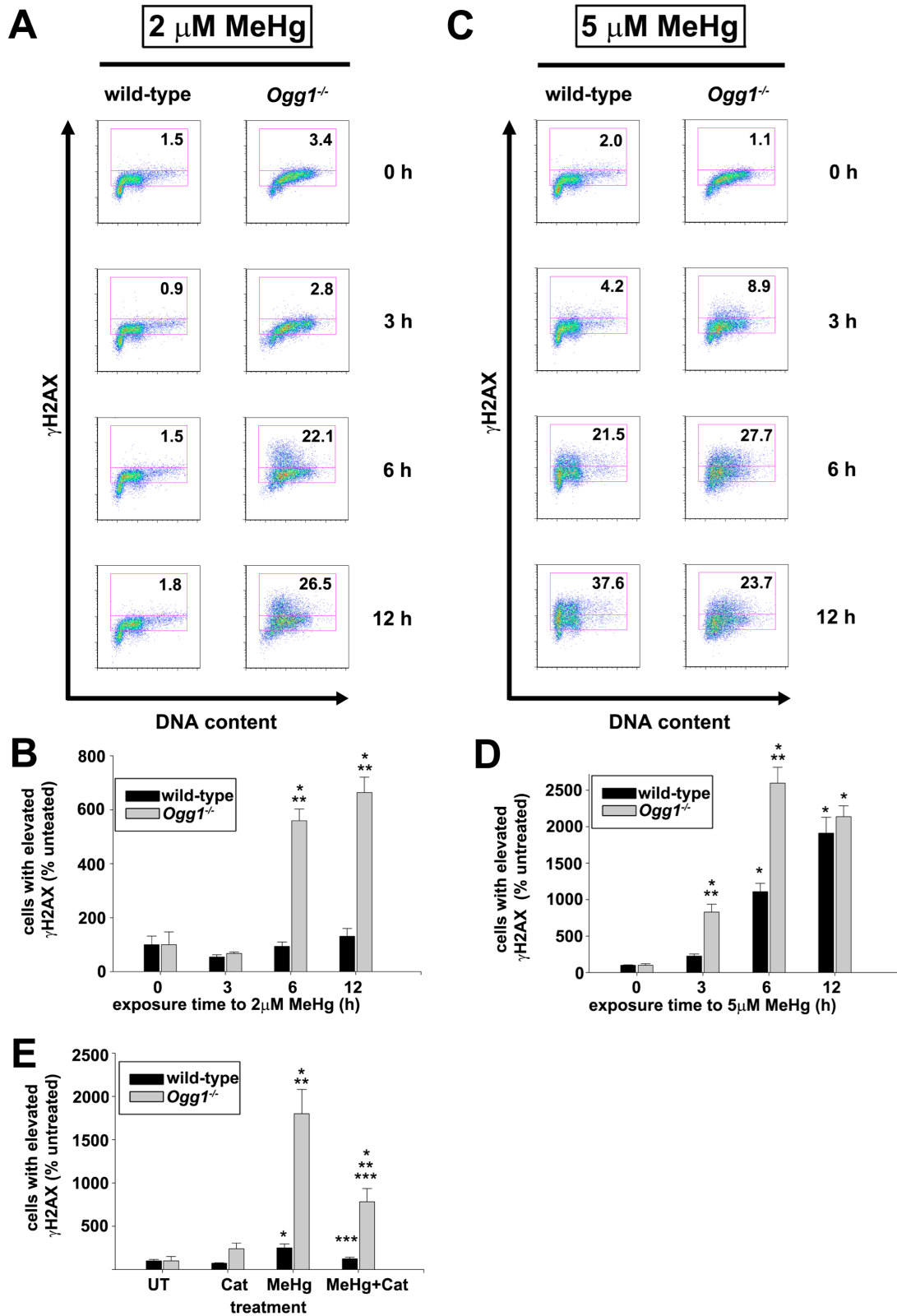


Figure 4. Increased number of *Ogg1*^{-/-} cells with elevated MeHg-initiated γ H2AX and reduction of DNA damage by PEG-catalase pretreatment.

Wild-type and *Ogg1*^{-/-} cells were exposed to 2 μ M (A-B) or 5 μ M (C-D) MeHg for 0, 3, 6, or 12 h and harvested. Representative histograms (A, C) plot the γ H2AX (y-axis) vs. DNA content (x-axis). Numbers indicate the absolute percentage of cells with elevated γ H2AX levels. The percentage of cells with elevated γ H2AX levels, and reduction of these levels by preincubation with the antioxidative enzyme PEG-catalase are plotted (B, D, E) as the mean percent of untreated + S.D. of three independent experiments. * Statistically significant difference ($p < 0.01$) compared to untreated; ** Statistically significant difference ($p < 0.001$) between wild-type and *Ogg1*^{-/-} cells at the indicated time points; *** Statistically significant difference ($p < 0.05$) from MeHg treatment alone.

We subsequently assessed levels of phospho-ATM(Ser1981) in wild-type and *Ogg1*^{-/-} fibroblasts as a function of time following exposure to MeHg. Cells were exposed to 2 μ M MeHg for 0, 3, 6, or 12 h and phospho-ATM(Ser1981) levels/cell were measured by FACS analysis. Compared to cells at 0 h, wild-type cells at 3 and 6 h showed a significant increase in the percentage of cells positive for phospho-ATM(Ser1981) ($p < 0.05$), with a subsequent decrease at 12 h to levels equivalent to untreated cells (**Fig. 5**). Interestingly, phospho-ATM(Ser1981) levels also increased at 3 and 6 h in *Ogg1*^{-/-} fibroblasts compared to cells at 0 h, but phospho-ATM(Ser1981) levels in *Ogg1*^{-/-} fibroblasts were consistently over 2-fold higher than levels observed in wild-type cells at each time point.

Figure 5.

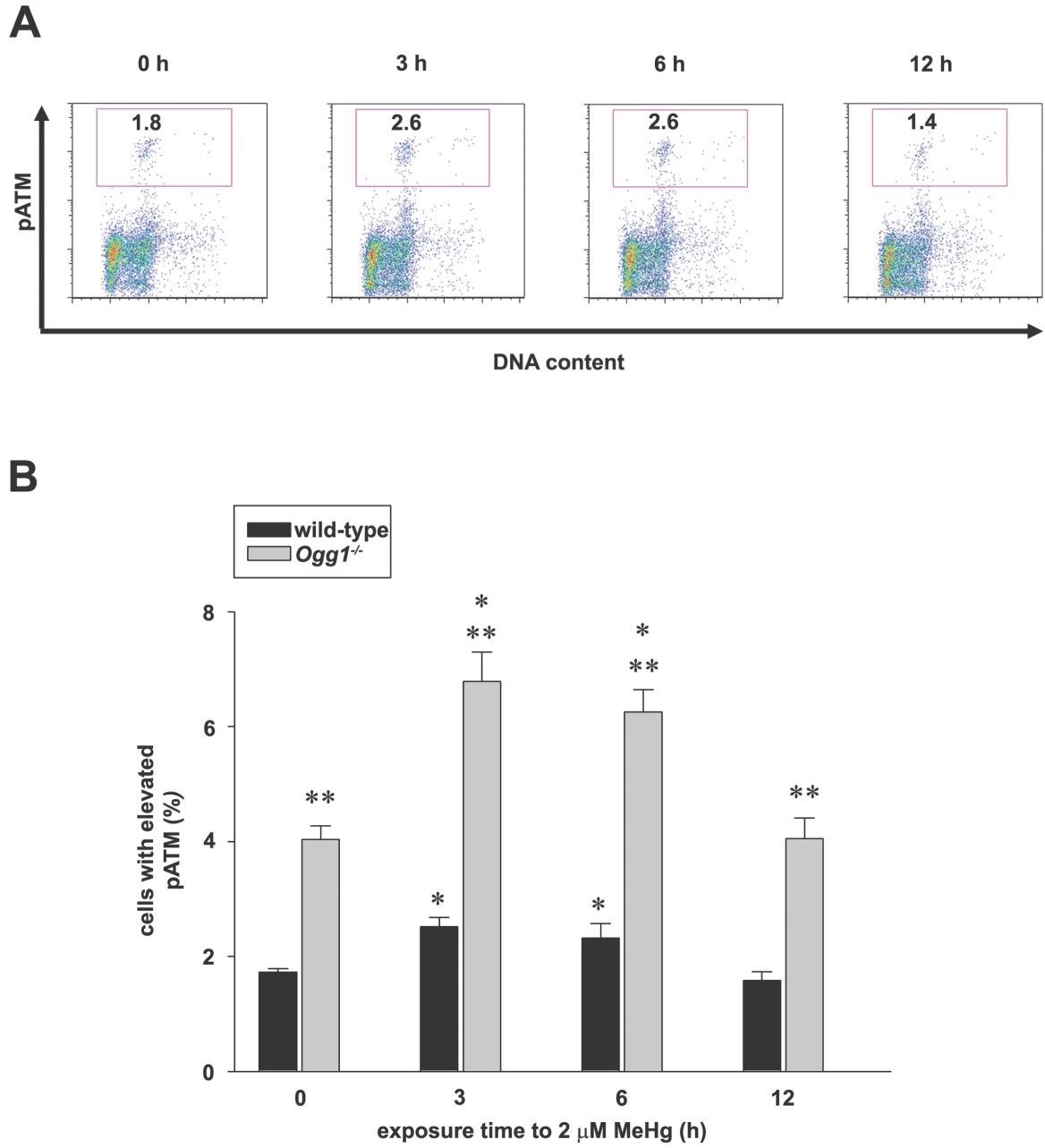


Figure 5. Increased number of *Ogg1*^{-/-} cells with elevated MeHg-initiated ATM phosphorylation at serine 1981.

Wild-type and *Ogg1*^{-/-} cells exposed to 2 μM MeHg for 0, 3, 6, or 12 h were evaluated for ATM phosphorylation at serine 1981 by FACS. (A) Representative FACS histograms generated from wild-type cells exposed to MeHg with numbers corresponding to the percentage of cells with elevated phospho-ATM(Ser1981) levels. (B) Quantification of the percentage of wild-type or *Ogg1*^{-/-} cells with elevated phospho-ATM(Ser1981) following MeHg exposure (mean + S.D.) from three independent experiments. * Statistically significant difference (p<0.01) compared to untreated cells; ** Statistically significant difference (p<0.05) between wild-type and *Ogg1*^{-/-} cells.

2.1.5 Discussion

Although it is well established that MeHg is a potent neurotoxin and teratogen, the underlying molecular mechanisms remain largely unclear. Herein, we have provided evidence of an increased sensitivity of DNA repair-deficient cells to MeHg, implying a possible role for DNA damage in the mechanism of MeHg toxicity. This is of particular significance with respect to the central nervous system (CNS) as the brain is a highly pro-oxidant environment with a high rate of oxidative activity but, like the developing embryo and fetus, has significantly lower levels of key antioxidants such as glutathione (GSH), GSH peroxidase and catalase when compared to the liver (DiMauro and Schon, 2008; Oliver *et al.*, 2011; Wells *et al.*, 2009). Thus, many cellular targets in the brain, as well as in the embryo and fetus, are particularly sensitive to oxidative insult and the consequential DNA damage. With compromised DNA repair status, DNA damage can not only lead to mutations, but may also have other non-mutational effects resulting in gene expression changes, some of which may be critical for the development, organization, function and defense of the adult CNS and/or the embryo and fetus (Wells *et al.*, 2010). Moreover, due to the possibility of varying levels of DNA repair capacity in different brain regions and cell types, there may also be regional, cellular and even gene-specific damage leading to pathway-specific effects, the latter supported by *in vivo* evidence of 8-oxoG accumulation in susceptible genomic sites rather than being randomly distributed throughout the genome (Toyokuni, 2008). Although an increasing body of evidence indicates that MeHg acts as a genotoxin, various lesions have been described in the DNA of cells exposed to MeHg, suggesting that the genotoxicity of this agent is complex. MeHg and other mercury compounds have been shown to act as clastogens given that cells exposed to these agents exhibit chromosomal aberrations (Cebulska-Wasilewska *et al.*, 2005; Yamada *et al.*, 1993), increased frequency of sister-chromatid exchange (Lee *et al.*, 1997; Morimoto *et al.*, 1982; Rao *et al.*, 2001) and increased frequency of micronuclei (Bonacker *et al.*, 2004; Franchi *et al.*, 1994; Thier *et al.*, 2003). Other studies however did not detect chromosomal aberrations, but instead demonstrated MeHg-induced changes in ploidy (Mailhes, 1983). In addition to clastogenic properties, exposure to MeHg and other mercury compounds has been shown to result in increased mutation frequency via the formation of covalent MeHg-DNA adducts (Li *et al.*, 2006; Schurz *et al.*, 2000) or ROS-initiated oxidative lesions such as 7,8-dihydro-8-oxoguanine (**8-oxoG**) (Li *et al.*, 2006; Schurz *et al.*, 2000).

Various studies have demonstrated that the ability of MeHg and related compounds to trigger oxidative stress may contribute to their genotoxicity (Di Pietro *et al.*, 2008; Ercal *et al.*, 2001; Lee *et al.*, 1997; Rao *et al.*, 2001; Schurz *et al.*, 2000). Here we have investigated whether the DNA repair protein OGG1, and the antioxidative enzyme PEG-catalase, protect cells from MeHg toxicity, and demonstrated for the first time that OGG1 guards against MeHg-initiated DNA damage, resulting in the accumulation of DSBs, and that the formation of these DSBs is attenuated in the presence of PEG-catalase.

Base excision repair (**BER**) serves to restore or limit oxidatively damaged DNA (Klungland and Lindahl, 1997; Kubota *et al.*, 1996). In this repair pathway, OGG1 operates as the predominant DNA glycosylase responsible for recognizing and removing the mutagenic lesion 8-oxoG when base-paired with cytosine (Aburatani *et al.*, 1997; Radicella *et al.*, 1997; Roldan-Arjona *et al.*, 1997). OGG1-null (**Ogg1**^{-/-}) mice spontaneously accumulate 8-oxoG over time *in vivo*, and *Ogg1*^{-/-} cells show elevated 8-oxoG levels compared to control cells (Klungland *et al.*, 1999). Interestingly, *Ogg1*^{-/-} mice exhibit no overt pathology and show a rather modest increase in spontaneous mutation rate, indicative of overlapping pathways that repair oxidatively damaged DNA (Klungland *et al.*, 1999; Minowa *et al.*, 2000). Furthermore, the role of OGG1 in preventing cytotoxicity induced by oxidative stress is somewhat unclear, as *Ogg1*^{-/-} fibroblasts appear to exhibit increased sensitivity to hydrogen peroxide only when cells are also deficient in MutY homolog (**MYH**) (Xie *et al.*, 2008), a complementary DNA glycosylase involved in the repair of 8-oxoG. In contrast, siRNA-mediated depletion of OGG1 in human fibroblasts, H1299 cells and HeLa cells results in increased sensitivity to hydrogen peroxide or menadione (de Souza-Pinto *et al.*, 2009; Youn *et al.*, 2007). *Ogg1*^{-/-} progeny exposed *in utero* to the ROS-initiating teratogen methamphetamine exhibited increased 8-oxoG levels in fetal brain and postnatal neurodevelopmental deficits compared to wild-type littermates (Wong *et al.*, 2008), indicating that the 8-oxoG lesion *in vivo* exerts pathogenic effects via mechanisms in addition to mutagenesis, possibly involving alterations in gene expression (Khobta *et al.*, 2010; Kitsera *et al.*, 2011; Pastoriza-Gallego *et al.*, 2007).

We observed that a 24 h exposure to sub-micromolar concentrations of MeHg was sufficient to reduce the clonogenic efficiency of wild-type fibroblasts, and that this sensitivity was significantly increased in the absence of OGG1. Our findings demonstrate that OGG1 protects cells from the cytotoxic effects of MeHg, and implicates MeHg-initiated DNA damage

as a contributing factor in the toxicity of this compound. Previous studies have demonstrated dose-dependent decreases in the rate of DNA synthesis and cell cycle arrest following MeHg exposure (Burke *et al.*, 2006; Falluel-Morel *et al.*, 2007; Hu *et al.*, 2005; Xu *et al.*, 2010; Zucker *et al.*, 1990). Fibroblasts deficient in OGG1 and MYH have also been shown to exhibit a greater tendency to accumulate in the G2/M phase of the cell cycle following exposure to oxidants compared to wild-type cells (Xie *et al.*, 2008). Given that the compromised survival of *Ogg1*^{-/-} cells following MeHg exposure might be explained by changes in the capacity for proliferation, we examined whether MeHg exposure altered the ability of *Ogg1*^{-/-} cells to undergo cell cycle arrest compared to wild-type cells. Both cell types exhibited a greater tendency to arrest in G2/M phases with 5 μ M MeHg compared to 2 μ M MeHg. However, *Ogg1*^{-/-} cells exposed to the lower 2 μ M concentration of MeHg for 6 h showed a greater accumulation in S phase and a decreased accumulation in G1 phase compared to wild-type cells, although this difference appeared to be transient, as the cell cycle distribution of both cell types was equivalent following exposure to MeHg for 24 h. As both wild-type and *Ogg1*^{-/-} cells were largely equivalent in their ability to undergo cell cycle arrest following exposure to MeHg, we examined whether the increased clonogenic sensitivity of *Ogg1*^{-/-} cells to MeHg could be attributed to an increased susceptibility to MeHg-induced apoptosis. Interestingly, we noted a significant reduction in the viability of *Ogg1*^{-/-} cells following a 6 h exposure to 2 μ M MeHg that was not apparent in the wild-type cells, but not following 24 hr exposure to a submicromolar concentration (0.2 μ M) of MeHg. Moreover, MeHg-initiated apoptosis at micromolar concentrations could not be reversed by pretreatment with the antioxidative enzyme PEG-catalase, suggesting that MeHg-initiated ROS may not be entirely responsible for the increased apoptosis at micromolar concentrations. Thus, the compromised clonogenic survival of *Ogg1*^{-/-} cells exposed to submicromolar concentrations of MeHg is likely not mediated via MeHg-initiated apoptosis. However, apoptosis may be responsible for cell death at micromolar concentrations of MeHg where OGG1 helps to prevent the accumulation of MeHg-initiated DNA lesions that can trigger cell death.

As the clastogenic properties of MeHg might be due to its induction of DNA double-strand breaks (DSBs), we measured DSB formation by evaluating the kinetics of γ H2AX formation in wild-type and *Ogg1*^{-/-} cells. A DSB, if unrepaired, is one of the most lethal forms of DNA damage (Karagiannis and El-Osta, 2004; Khanna and Jackson, 2001; Sedelnikova *et al.*, 2003). DSBs induce the phosphorylation of the variant H2A histone H2AX at serine 139

(γ H2AX) in the chromatin flanking the break site. Following DNA damage, H2AX becomes rapidly phosphorylated by members of the phosphatidylinositol-3 kinase family (Bonner *et al.*, 2008; Rogakou *et al.*, 1998) that includes ataxia telangiectasia mutated (ATM), ataxia telangiectasia and Rad3-related protein (ATR), and DNA-dependent protein kinase (DNA-PK) (Fernandez-Capetillo *et al.*, 2004; Stiff *et al.*, 2004; Stiff *et al.*, 2006). Of these three kinases, ATM is considered to play a prominent role in γ H2AX induction following DSB damage (Falck *et al.*, 2005; Redon *et al.*, 2002; Stiff *et al.*, 2004; Stiff *et al.*, 2006), and ATM-deficient progeny are more susceptible to *in utero* death and birth defects caused by *in utero* exposure to low-dose ionizing radiation (Laposa *et al.*, 2004).

Exposure to ionizing radiation such as X-rays, γ -radiation, α -particles, and heavy ions causes the direct formation of DNA DSBs (Cebulska-Wasilewska *et al.*, 2005; Desai *et al.*, 2005; Hanasoge and Ljungman, 2007; Usami *et al.*, 2006), which leads to a rapid rise in γ H2AX levels that are maximal 30-60 minutes after irradiation (Keogh *et al.*, 2006; Markova *et al.*, 2007; Sedelnikova and Bonner, 2006; Sedelnikova *et al.*, 2003). In contrast, DSBs in MeHg-treated wild-type cells were not apparent until cells had been exposed for at least several hours, suggesting that DSBs following MeHg exposure occur as the result of secondary processes. Importantly, we observed an earlier onset and greater extent of DSB induction in *Ogg1*^{-/-} cells compared to wild-type cells exposed to 5 μ M MeHg. Furthermore, we observed DSB induction in *Ogg1*^{-/-} cells at lower concentrations of MeHg that did not produce a significant increase in DSBs in wild-type cells, and these DSBs were attenuated in the presence of antioxidative PEG-catalase. Taken together, these findings strongly suggest that MeHg exposure leads to ROS-mediated DSB formation and that production of this form of DNA damage is exacerbated in the absence of OGG1.

To provide additional confirmation that DSB damage occurred as a result of MeHg exposure, we investigated the phosphorylation status of ATM at serine 1981. Autophosphorylation of ATM at this residue results in ATM dimer dissociation and initiates cellular ATM kinase activity (Bakkenist and Kastan, 2003). Following induction of DNA damage, the extent of ATM activation correlates strongly with the number of DSBs formed compared to other lesions generated (Ismail *et al.*, 2005). Similarly, we observed that MeHg exposure led to a significant increase in the percentage of cells showing elevated ATM phosphorylation at serine 1981 in both wild-type and *Ogg1*^{-/-} cells, with the latter showing an

even greater elevation at all time-points compared to wild-type cells. Taken together, findings of increased ATM phosphorylation at serine 1981 support our conclusion that OGG1 protects cells from accumulation of DSBs that lead to ATM activation following MeHg exposure.

Although OGG1 appears to prevent MeHg-induced DSBs, this glycosylase and associated processes that comprise the BER pathway are traditionally associated with limiting oxidative base damage, in particular the accumulation of 8-oxoG. Recent studies additionally point to a role for OGG1 in processes of recombination-mediated repair that respond to DSB damage, particularly through interactions with the RAD52 repair protein following oxidative stress (de Souza-Pinto *et al.*, 2009). The presence of 8-oxoG lesions was found to inhibit RAD52 strand annealing activity, suggesting that homologous recombination-mediated repair of DSBs could be impaired under conditions of increased oxidative damage to DNA. Accordingly, the ability of OGG1 to remove 8-oxoG in the vicinity of DNA breaks may serve to facilitate RAD52-mediated repair processes that safeguard against DSB accumulation following MeHg exposure. It will be important to determine whether ROS-mediated DSB accumulation contributes similarly to the *in vivo* pathological consequences of MeHg exposure.

Our data demonstrate for the first time an increased sensitivity of OGG1-deficient cells to MeHg, serving as the most direct evidence to date that ROS-mediated DNA damage may play a critical role in the pathological consequences of MeHg exposure. Importantly, these studies have been carried out at low, environmentally relevant concentrations of MeHg. In the notorious case of Minamata Bay, more than 900 fatalities resulted from the consumption of MeHg-contaminated seafood, which contained up to 40 ppm ($\approx 184 \mu\text{M}$) MeHg (National Institute for Minamata Disease). Other documented cases of fatal human poisonings reported levels of MeHg in the blood and cerebellum of $75 \mu\text{M}$ and $15\text{-}25 \mu\text{M}$ respectively (Hilmy *et al.*, 1976). In the United States, MeHg exposure continues to be a matter of public health concern as dietary and occupational exposure levels, which can range from $0.09\text{-}1.8 \mu\text{g/kg/day}$ (Barbosa *et al.*, 2001; Harada *et al.*, 2001; Tsuchiya *et al.*, 2008; Vahter *et al.*, 2000), can overlap those ($0.2\text{-}1.8 \mu\text{g/kg/day}$) associated with postnatal neurobehavioral deficits in humans after *in utero* MeHg exposure (Grandjean *et al.*, 1998; Grandjean *et al.*, 1997). Today, the US Environmental Protection Agency (**EPA**) employs a reference dose for MeHg of $0.1 \mu\text{g/kg/day}$, which correlates with a blood Hg level of $5.8 \mu\text{g/L}$ ($\approx 0.027 \mu\text{M}$ MeHg), where 100% of the total Hg measured is assumed to be MeHg for the purpose of risk assessment. In Canada, the allowable limit set by

the Canadian Food Inspection Agency (CFIA) for Hg in fish and seafood is 0.5 ppm ($\approx 2.3 \mu\text{M}$ MeHg). Widely consumed species of fish including swordfish, shark, pike and bass contain some of the highest concentrations of MeHg, some greater than 1 ppm ($\approx 4.6 \mu\text{M}$ MeHg) (Health Canada). Additionally, a study of Canadian aboriginals whose diet is primarily comprised of fish found 25% of this population to have blood Hg levels greater than $0.09 \mu\text{M}$, and 2% with levels greater than $0.46 \mu\text{M}$, with the highest maternal blood and cord blood concentrations reported to be $0.4 \mu\text{M}$ and $1 \mu\text{M}$ respectively (Wheatley and Paradis, 1995). Thus, our working concentrations are well below the range associated with fatalities, and within the more relevant concentration range found in various fish and seafood species, as well as in at-risk populations, and we are seeing an effect on clonogenic survival at a concentration only $0.003 \mu\text{M}$ higher than the current blood Hg equivalent of the US EPA reference dose. Furthermore, our findings reveal an essential role for OGG1 in the maintenance of genomic integrity following MeHg-initiated DNA damage, and implicate an individual's response to DNA damage and antioxidative capacity as a significant determinant of susceptibility to MeHg toxicity. Further investigation is required to more definitively elucidate the precise mechanisms by which MeHg-initiated DNA damage contributes to the mechanism of toxicity, and whether these mechanisms can be extrapolated to the *in vivo* pathogenesis following MeHg exposure. A better understanding of the mechanisms underlying MeHg toxicity will enable the identification of novel risk factors, and provide more a definitive basis for public health recommendations regarding environmental exposure to MeHg.

2.1.6 Acknowledgements

We thank Dr. Bernd Epe (University of Mainz, Germany) for the generous gift of wild-type and *Ogg1*^{-/-} fibroblasts and Meghan Larin (Dept. of Pharmacology and Toxicology, University of Toronto) for her help in harvesting cells for the Annexin V apoptosis assay.

2.2 STUDY 2: SENSITIVITY TO METHYLMERCURY TOXICITY IS ENHANCED IN OXOGUANINE GLYCOSYLASE 1 KNOCKOUT MURINE EMBRYONIC FIBROBLASTS AND IS DEPENDENT ON CELLULAR PROLIFERATION CAPACITY^a

Running title: Determinants of methylmercury toxicity

Stephanie L. Ondovcik^{*}, Laura Tamblyn[†], John Peter McPherson[†] and Peter G. Wells^{*,†,1}

Departments of ^{*}Pharmaceutical Sciences and [†]Pharmacology & Toxicology
University of Toronto
Toronto, Ontario, Canada

¹ Corresponding author:
Peter G. Wells, Pharm.D.
Faculty of Pharmacy, University of Toronto
144 College St., Toronto, Ontario, Canada M5S 3M2
Email: pg.wells@utoronto.ca
Phone 416-978-3221

a. This work was supported by operating grants from the Canadian Institutes of Health Research (CIHR) [PGW], and the Cancer Research Society Inc. [JPM]. JPM is the recipient of a Province of Ontario Early Researcher Award, and SLO is the recipient of a CIHR Frederick Banting and Charles Best Canada Graduate Scholarship.

Tamblyn, L.- Assisted in the generation of the SV40 large T antigen-immortalized wild-type and *Ogg1*^{-/-} MEFs.

McPherson, J.P.- Acted in a co-supervisory capacity.

2.2.1 Abstract

Methylmercury (**MeHg**) is a persistent environmental contaminant with potent neurotoxic action for which the underlying molecular mechanisms remain largely speculative. Our objectives herein were twofold: first, to corroborate our previous findings of an increased sensitivity of spontaneously-immortalized oxoguanine glycosylase 1-*null* (**Ogg1**^{-/-}) murine embryonic fibroblasts (**MEFs**) to MeHg through generation of Simian virus 40 (**SV40**) large T antigen-immortalized wild-type and *Ogg1*^{-/-} MEFs; and second, to determine whether MeHg toxicity is proliferation-dependent. As with the spontaneously-immortalized cells used previously, the SV40 large T antigen-immortalized cells exhibited similar tendencies to undergo MeHg-initiated cell cycle arrest, with increased sensitivity in the *Ogg1*^{-/-} MEFs as measured by clonogenic survival and DNA damage. Compared to exponentially growing cells, those seeded at a higher density exhibited compromised proliferation, which proved protective against MeHg-mediated cell cycle arrest and induction of DNA double-strand breaks (**DSBs**), measured by H2AX phosphorylation on serine 139 (**γH2AX**), and by its functional confirmation by micronucleus assessment. This enhanced sensitivity of *Ogg1*^{-/-} MEFs to MeHg toxicity using discrete SV40 immortalization corroborates our previous studies, and suggests a novel role for OGG1 in minimizing MeHg-initiated DNA lesions that trigger replication-associated DSBs. Furthermore, proliferative capacity may determine MeHg toxicity *in vivo* and *in utero*. Accordingly, variations in cellular proliferative capacity and interindividual variability in repair activity may modulate the risk of toxicological consequences following MeHg exposure.

2.2.2 Introduction

Methylmercury (**MeHg**) is an organomercurial compound highly toxic to both the adult and fetal central nervous system. Although MeHg is most notorious for two historical large-scale cases of human poisoning-via contaminated seafood in Minamata, Japan (Harada, 1995) and through tainted seed grain in Iraq (Amin-Zaki *et al.*, 1974)-there is still cause for concern today. The primary mode of human exposure to MeHg remains the consumption of larger predatory fish and mammals which have bioaccumulated MeHg that persists in their aquatic environments (Bhavsar *et al.*, 2010; Kinghorn *et al.*, 2007). Today, there is added concern for MeHg exposure with the resurgence of activities such as coal burning and gold mining which further serve as a source of environmental MeHg (Guedron *et al.*, 2011).

Despite a well-characterized toxicological profile, the mechanisms underlying the potent neurotoxic actions of MeHg remain to be definitively elucidated. A primary mechanistic focus of many groups has involved the role played by reactive oxygen species (**ROS**) and their resulting macromolecular damage and alteration of signal transduction pathways in various *in vitro* and *in vivo* models of MeHg toxicity. Accumulating evidence is consistent with a potential role for oxidatively damaged DNA and subsequent pathologic consequences as a contributing factor in the toxicological mechanism of MeHg, including its ability to generate ROS, its genotoxic potential and the attenuating effects of antioxidant pretreatment on toxicity (Ali *et al.*, 1992; Belletti *et al.*, 2002; Burke *et al.*, 2006; Chen *et al.*, 2005; Choi, 1989; Crespo-Lopez *et al.*, 2007; Ehrenstein *et al.*, 2002; Ganther, 1978; Garg and Chang, 2006; Gatti *et al.*, 2004; Jie *et al.*, 2007; Liu *et al.*, 2002; Ondovcik *et al.*, 2012; Shanker *et al.*, 2005; Silva-Pereira *et al.*, 2005).

We previously demonstrated an increased sensitivity of DNA repair-deficient cells to environmentally relevant, low micromolar concentrations of MeHg, which was blocked by the antioxidative enzyme catalase, constituting the most direct evidence to date that clastogenic DNA damage may contribute to the pathological consequences of MeHg exposure via a non-mutagenic mechanism, and that this DNA damage is ROS-mediated (Ondovcik *et al.*, 2012). We employed spontaneously-immortalized murine embryonic fibroblasts (**MEFs**) which lacked the bifunctional DNA glycosylase/apurinic/apyrimidinic lyase oxoguanine glycosylase 1 (**OGG1**), primarily responsible for initiating the repair of oxidative base damage (Klungland and Bjelland,

2007). To more confidently conclude that the increased sensitivity of the OGG1-*null* (*Ogg1*^{-/-}) cells to MeHg was due to the absence of OGG1, and not the result of other unappreciated cellular differences arising from the spontaneous nature of the immortalization process, we derived Simian virus 40 (SV40) large T antigen-immortalized wild-type and *Ogg1*^{-/-} MEFs.

Immortalization by spontaneous means relies on the accumulation of random mutations that confer a growth advantage allowing the cells to evade replicative senescence, a capacity possessed by most murine cells, but an extremely rarely occurring phenomenon in human fibroblasts and epithelial cells (Shay *et al.*, 1991). As such, different lines of spontaneously-immortalized cells may have acquired different mutations which led to their immortal state, potentially confounding the interpretation of results comparing spontaneously-immortalized cells of different genotypes. In contrast, transformation by the proto-oncogene SV40 large T antigen leads to the specific inactivation of tumor suppressors [retinoblastoma protein (**Rb**), p53 and p105], the binding to transcriptional co-activators [p300 and CREB1-binding protein (**CBP**)] and/or the induction of telomerase activity to impart a growth advantage to cells leading to their immortality (Ahuja *et al.*, 2005; Ali and DeCaprio, 2001; Shay *et al.*, 1991). As such, SV40 large T antigen-immortalized cells have taken a more controlled and potentially similar path to immortality than spontaneously-immortalized cells, providing a more definitive model to better understand and elucidate the contribution of altered DNA repair status in the mechanism of MeHg toxicity.

We further probed the mechanism of MeHg toxicity in our DNA repair-deficient model by examining the proliferation dependence of MeHg-initiated DNA damage by varying the density at which cells were seeded. A previous study found sparse cultures of human brain microvascular pericytes to be more susceptible to MeHg toxicity compared to dense cultures, a phenomenon that the authors attributed to increased expression of the L-type large neutral amino acid transporter 1 (**LAT1**) in sparse cultures, which resulted in increased transport and intracellular accumulation of MeHg (Hirooka *et al.*, 2010). Among the other biochemical and physical differences that have been noted between cells seeded at low and high densities, the hallmark lies in the limited capacity of dense cultures to divide and proliferate. Given that MeHg has also been shown decrease the rate of DNA synthesis and induce cell cycle arrest (Burke *et al.*, 2006; Falluel-Morel *et al.*, 2007; Hu *et al.*, 2005; Xu *et al.*, 2010; Zucker *et al.*, 1990), it is plausible that MeHg exerts its toxic actions in part through interference with cellular

proliferation, in which case actively proliferating cells, such as in the developing embryo and fetus, would constitute a prime target for MeHg.

Herein we provide the first corroborating evidence that, regardless of the method of cellular immortalization, OGG1 status is a critical modulator of risk for MeHg toxicity, with enhanced susceptibility in *Ogg1*^{-/-} MEFs. Further, we demonstrate for the first time that the increased susceptibility of *Ogg1*^{-/-} MEFs to MeHg-initiated DNA damage is additionally dependent on cellular proliferation capacity. These observations support a novel role for OGG1 in safeguarding against the accumulation of DNA lesions initiated by MeHg that result in the formation of replication-associated DNA double-strand breaks (**DSBs**). Together, our findings establish a critical role for OGG1 in the maintenance of genomic integrity following MeHg-initiated DNA damage, and suggest that variations in cellular proliferative capacity and interindividual variability in repair activity may modulate the risk of toxicological consequences.

2.2.3 Materials and Methods

Cell derivation and culture. Wild-type and oxoguanine glycosylase 1-null (*Ogg1*^{-/-}) murine embryonic fibroblasts (MEFs) were derived from gestational day (GD) 14.5 embryos from the mating of heterozygous *Ogg1*-null (*Ogg1*^{+/-}) mice first generated by Klungland and coworkers (Klungland *et al.*, 1999). Animals were used in accordance with protocols approved by the local institutional animal care and use committee, as per the guidelines established by the Canadian Council on Animal Care. Primary *Ogg1*^{-/-} cells displayed no significant differences in proliferation compared to wild-type cells over the first three passages. To permit their use in subsequent studies, passage-one primary wild-type and *Ogg1*^{-/-} MEFs from littermates were immortalized following transfection with a Simian virus 40 (SV40) large T antigen in pSG5 (Addgene plasmid 9053) (Agilent Technologies Canada Inc., Mississauga, Ontario) together with a puromycin resistance plasmid and selected in media containing puromycin. Cells were then maintained in Dulbecco's Modified Eagle Medium containing 4.5 g/L D-glucose, and supplemented with 1% L-glutamine, 1% penicillin/streptomycin solution, 10% heat-inactivated fetal bovine serum (all Life Technologies Inc., Burlington, Ontario) and 0.1% 2-mercaptoethanol (Sigma-Aldrich Canada Ltd., Oakville, Ontario).

Clonogenic assay. Five hundred cells were seeded into 60 mm dishes and left either untreated or exposed to 0-0.2 μ M of methylmercury (II) chloride (MeHg, Sigma-Aldrich Canada Ltd.) for 24 h. Surviving cells were allowed to grow into visible colonies for six days post-treatment, and were then fixed and stained with methylene blue in methanol. Survival curves were produced from the mean number of colonies plus or minus the standard deviation of three to six independent determinations and are presented as a percentage of untreated cells.

Cell cycle analysis by bromodeoxyuridine (BrdU) and propidium iodide (PI) double staining via flow cytometry. Wild-type and *Ogg1*^{-/-} MEFs were seeded at densities of 4×10^5 or $2 \times 10^6/100$ mm dish and left untreated or exposed to 2 μ M MeHg for 6 h. Cells were pulsed with 10 μ g/ml BrdU (Sigma-Aldrich Canada Ltd.) for 1 h prior to harvesting. Staining and analysis of BrdU and PI (BD Biosciences, Mississauga, Ontario) were performed as previously described (Ondovcik *et al.*, 2012; Tamblyn *et al.*, 2009).

Measurement of H2AX phosphorylated on serine 139 (γ H2AX) and PI double staining by flow cytometry. Cells were seeded at densities of 4×10^5 or 2×10^6 /100 mm dish, left untreated or exposed to 2 μ M MeHg for 6 h and collected by trypsinization. Cells were fixed with ice-cold 70% ethanol overnight at -20°C , washed with PBS and permeabilized with PBS containing 0.4% Triton X-100. Cells were stained for γ H2AX by incubating with an anti- γ H2AX antibody (Millipore Canada Ltd., Etobicoke, Ontario) in PBS containing 0.2% Triton X-100 and 1% donkey serum for 3 h, followed by a 30 min incubation with a fluorescein isothiocyanate (FITC)-conjugated anti-mouse secondary antibody (Jackson, Cedarlane Laboratories, Hornby, Ontario). Cells were then washed with PBS, stained with 50 μ g/ml PI for 30 min, and acquired and analyzed using a FACSCalibur flow cytometer (BD Biosciences) and FLOJO software (Tree Star Inc., Ashland, Oregon) respectively.

Assessment of micronucleus incidence via immunofluorescent (IF) staining as a functional confirmation of γ H2AX. Wild-type and *Ogg1*^{-/-} MEFs were seeded onto 20 mm x 20 mm glass cover slips in 6 well plates at densities of 6.5×10^4 or 3.25×10^5 cells, densities adjusted for surface area to maintain equivalence to the cell densities used for flow cytometric analysis of BrdU and γ H2AX. Cells were left untreated or exposed to 2 μ M MeHg for 6 h, after which they were fixed at -20°C for 15 min with ice-cold 100% methanol followed by ice-cold 100% acetone for 1 min. Cells were washed with PBS and cover slips were mounted using Vectashield mounting media containing 4'-6-Diamidino-2-phenylindole (DAPI, Vector Laboratories Canada Inc., Burlington, Ontario). Micronucleus incidence was quantified manually in triplicate in at least 200 intact nuclei in randomly selected fields of view using an Imager.Z1 Epifluorescence microscope with Axiovision software (Carl Zeiss Canada Ltd., Toronto, Ontario).

Statistical Analysis. An unpaired t-test was used to analyze data comparing two groups, while multiple comparisons were analyzed by a one-way ANOVA followed by Bonferroni's multiple comparison post-test, with the level of significance set to $p < 0.05$ (GraphPad Prism 5.0d, GraphPad Software Inc., La Jolla, CA).

2.2.4 Results

To first determine the cytotoxicity profile of methylmercury (**MeHg**) in the newly derived Simian virus 40 (**SV40**) large T antigen-immortalized wild-type and oxoguanine glycosylase 1-*null* (**Ogg1^{-/-}**) murine embryonic fibroblasts (**MEFs**), their clonogenic survival was compared following exposure to low, environmentally relevant concentrations of MeHg. As observed previously in the spontaneously-immortalized MEFs (Ondovcik *et al.*, 2012), the SV40 large T antigen-immortalized *Ogg1^{-/-}* cells similarly showed enhanced sensitivity to MeHg, exhibited as a greater concentration-dependent decrease in clonogenic survival compared to isogenic wild-type controls ($p < 0.05$ - $p < 0.0001$) following MeHg (0.03-0.2 μ M) exposure (**Fig. 1**).

Figure 1.

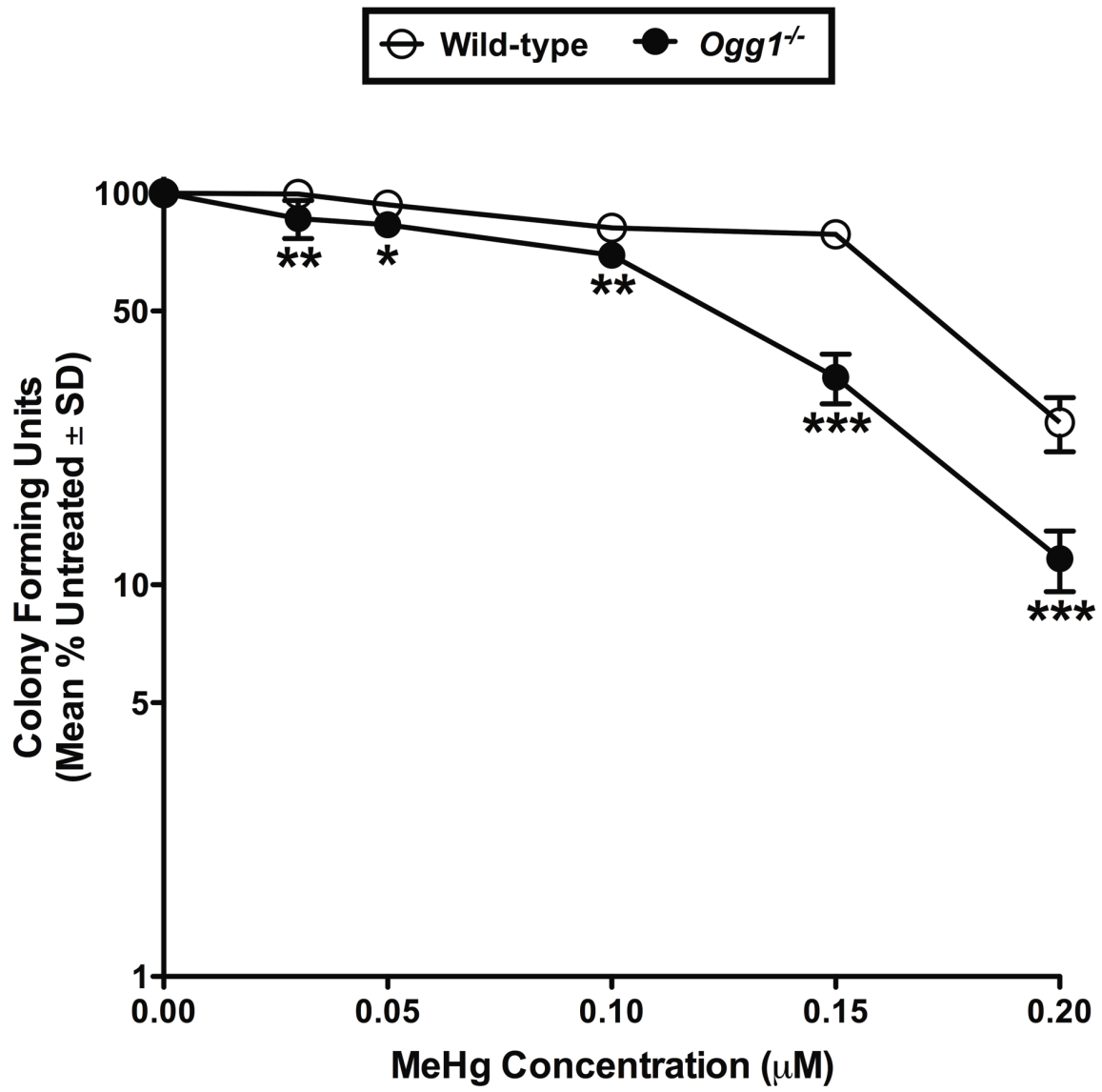


Figure 1. Simian virus 40 (SV40) large T antigen-immortalized oxoguanine glycosylase 1-null (*Ogg1*^{-/-}) cells demonstrate reduced clonogenic survival following exposure to methylmercury (MeHg).

The sensitivity of SV40 large T antigen-immortalized wild-type and *Ogg1*^{-/-} murine embryonic fibroblasts (MEFs) was measured by clonogenic assay following 24 h exposure to submicromolar concentrations of MeHg. Each datum point represents the mean plus or minus the standard deviation of three to six independent experiments. Asterisks indicate a difference in sensitivity from wild-type cells at the same concentration (* p<0.05, ** p<0.01, *** p<0.0001).

Cell cycle status of the newly derived SV40 large T antigen-immortalized wild-type and *Ogg1*^{-/-} MEFs was then assessed for two purposes: first, to demonstrate that a higher seeding density (2×10^6 cells versus 4×10^5 cells) (**Fig. 2**) resulted in a hindered proliferative capacity; and second, to confirm a similar ability of the cells to undergo MeHg-initiated cell cycle arrest as seen previously in spontaneously-immortalized MEFs (Ondovcik *et al.*, 2012). In the absence of MeHg, an increased seeding density increased the percentage of wild-type and *Ogg1*^{-/-} MEFs in G1 ($p < 0.0001$) (**Fig. 3A and Fig. 3B**), and conversely reduced the percentage ($p < 0.0001$) (**Fig. 3A and Fig. 3B**) and fluorescence intensity ($p < 0.01$) (**Fig. 3C**) of cells in S phase, confirming impaired proliferation of cells seeded at a higher density. A six-hour exposure to 2 μ M MeHg was sufficient to initiate cell cycle arrest as seen previously in spontaneously immortalized cells (Ondovcik *et al.*, 2012), exhibited by a decreased percentage of wild-type and *Ogg1*^{-/-} MEFs in G1 ($p < 0.0001$), and conversely increased percentages in S phase and G2/M ($p < 0.0001$); effects that were attenuated ($p < 0.0001$) with increased seeding density, implicating a proliferation-dependent component in MeHg toxicity (**Fig. 3A and Fig. 3B**). MeHg treatment also reduced the fluorescence intensity of S phase wild-type and *Ogg1*^{-/-} MEFs ($p < 0.05$) indicating cell cycle arrest, while increased cell seeding density reduced the magnitude ($p < 0.01$) of this effect in *Ogg1*^{-/-} MEFs, and completely attenuated ($p < 0.01$) it in wild-type cells, providing further support for the hypothesis of a proliferation-dependent component to MeHg toxicity (**Fig. 3C**).

Figure 2.

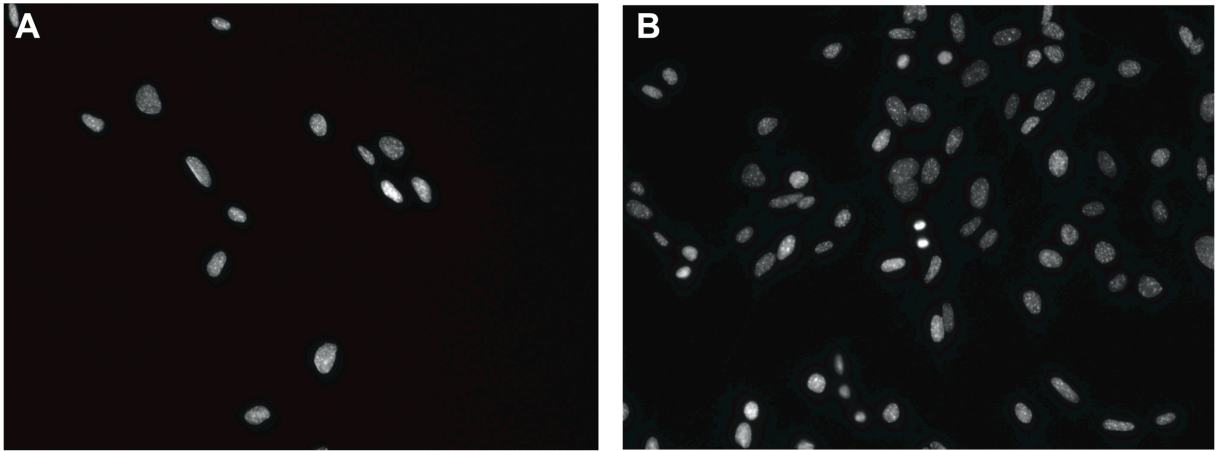


Figure 2. SV40 large T antigen-immortalized wild-type cells seeded at exponentially growing and confluent densities.

Representative fields of 4'-6-Diamidino-2-phenylindole (**DAPI**)-stained wild-type nuclei at 20X magnification illustrating the variation between (**A**) a seeding density (6.5×10^4 or 4×10^5 cells) permitting exponential growth and (**B**) a confluent seeding density (3.25×10^5 or 2×10^6 cells).

Figure 3.

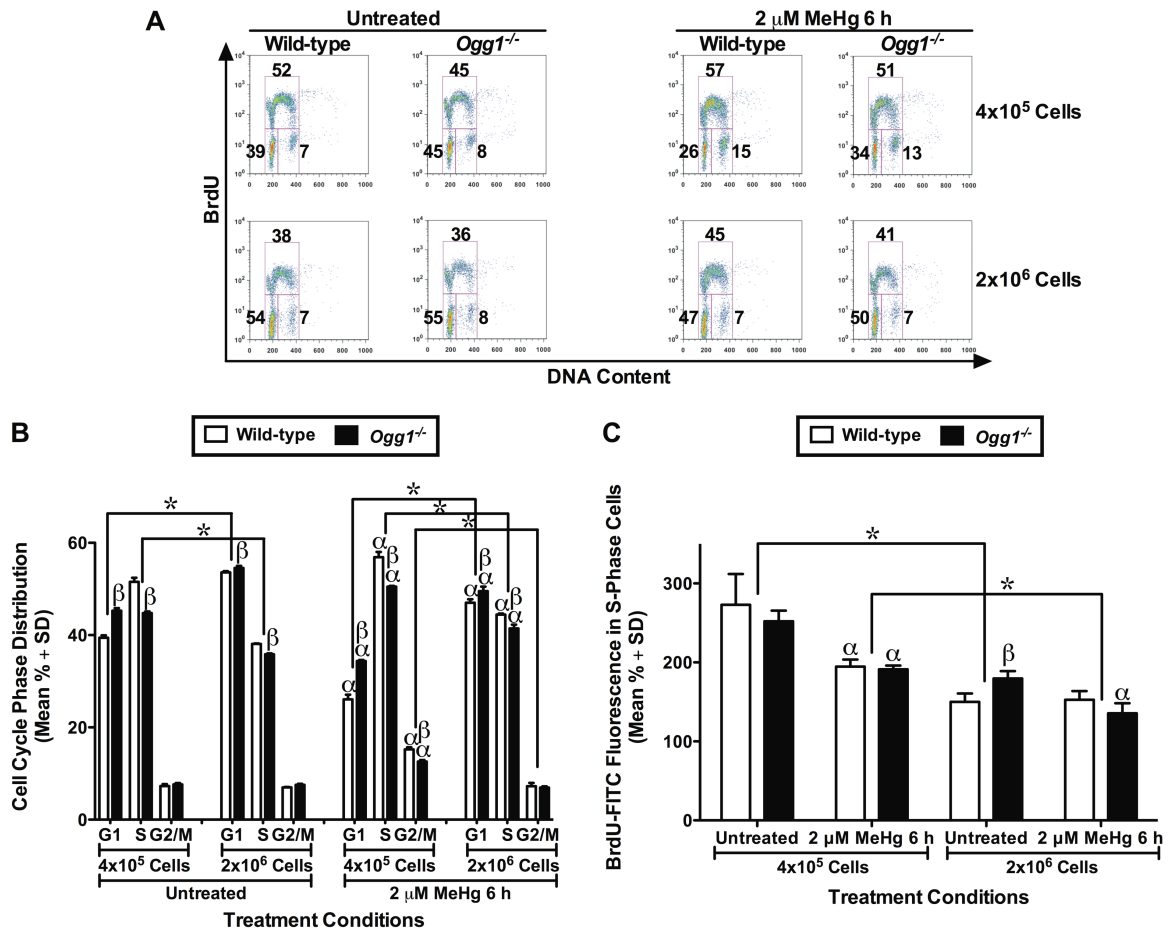


Figure 3. Increased cell seeding density leads to impaired proliferation and attenuates the susceptibility of wild-type and *Ogg1*^{-/-} cells to MeHg-initiated cell cycle arrest.

SV40 large T antigen-immortalized wild-type and *Ogg1*^{-/-} cells were seeded at densities of 4×10^5 or 2×10^6 , left untreated or exposed to 2 μ M MeHg for 6 h, and subsequently harvested for fluorescence-activated cell sorting (FACS) analysis. (A) Representative bromodeoxyuridine (BrdU)-propidium iodide (PI) bivariate plots for wild-type and *Ogg1*^{-/-} cells under each treatment condition labeled with numbers corresponding to the percentage of cells in G1 (left gate), S (top gate), and G2/M (right gate) phases of the cell cycle. (B) Quantification of the percentage of cells within each phase of the cell cycle and the effect of seeding density on cell cycle distribution, with the data presented as the mean plus standard deviation of three independent experiments. Alpha denotes a difference from untreated at the same cell number (α $p < 0.0001$). Beta indicates a difference between wild-type and *Ogg1*^{-/-} cells under the same treatment conditions (β $p < 0.01$). Asterisks signify a difference from 4×10^5 cells under same conditions (* $p < 0.0001$). (C) Quantification of the mean BrdU-fluorescein isothiocyanate (FITC) fluorescence in S phase cells and the effect of cell seeding density, with the results plotted as the mean plus standard deviation of three independent experiments. Alpha denotes a difference from untreated cells at the same cell number (α $p < 0.05$). Beta indicates a difference between wild-type and *Ogg1*^{-/-} cells under the same treatment conditions (β $p < 0.05$). Asterisks signify a difference from 4×10^5 cells under same conditions (* $p < 0.01$).

Given the above results, the proliferation dependence of MeHg-initiated DNA damage was then evaluated in the SV40 large T antigen-immortalized wild-type and *Ogg1*^{-/-} MEFs seeded at densities of 4×10^5 (exponentially growing) or 2×10^6 (confluent) cells (**Fig. 2**). Altered seeding density was pursued as a means of hindering cellular proliferative capacity, given that two independent attempts to stall proliferation via serum-starvation yielded intensified basal DNA damage in the absence of MeHg (**data not shown**), precluding the use of the latter approach. DNA damage in the form of DNA double-strand breaks (**DSBs**) was measured as the induction of H2AX phosphorylation at serine 139 (**γ H2AX**) following a 6 h exposure to 2 μ M MeHg. As hypothesized and similarly observed in spontaneously-immortalized MEFs (Ondovcik *et al.*, 2012), MeHg increased γ H2AX induction ($p < 0.01$ - $p = 0.001$) with two-fold higher levels accumulating in the *Ogg1*^{-/-} versus wild-type MEFs ($p < 0.05$) (**Fig. 4**). When the cells were seeded at a density (2×10^6 cells) confirmed to compromise proliferation, MeHg-initiated γ H2AX was decreased five- to seven-fold, down to basal levels, in both wild-type ($p < 0.001$) and *Ogg1*^{-/-} ($p < 0.0001$) MEFs, supporting the hypothesis that MeHg-initiated DNA damage is in part associated with cell proliferation (**Fig. 4**).

Figure 4.

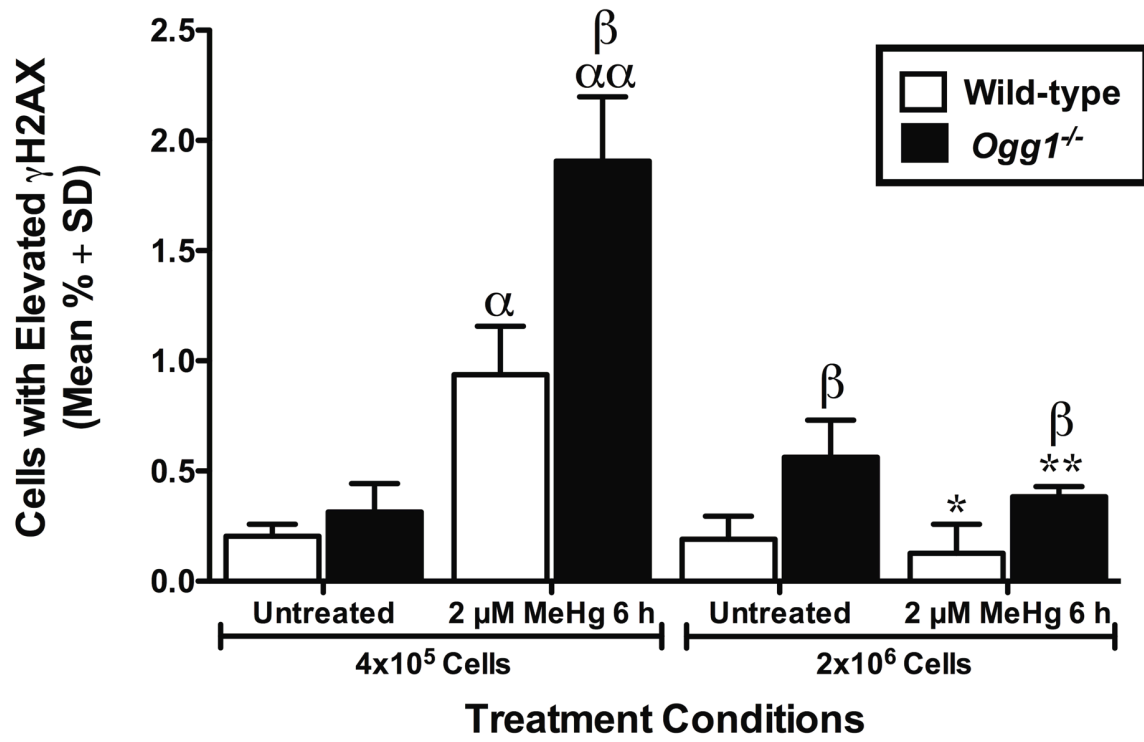


Figure 4. MeHg-initiated H2AX phosphorylation at serine 139 (γ H2AX) accumulation in SV40 large T antigen-immortalized wild-type and *Ogg1*^{-/-} cells persists and is dependent on cellular proliferation capacity.

SV40 large T antigen-immortalized wild-type and *Ogg1*^{-/-} cells were seeded at densities of 4×10^5 (exponentially growing) or 2×10^6 (confluent). Cells were either left untreated or exposed to 2 μ M MeHg for 6 h and subsequently harvested for FACS analysis. Quantification of the percentage of cells with elevated γ H2AX levels, and the effect of cell seeding density, are plotted as the mean percent plus standard deviation of three independent experiments. Alpha indicates a difference from untreated cells at the same cell number (α $p < 0.01$, $\alpha\alpha$ $p = 0.001$). Beta denotes a difference between wild-type and *Ogg1*^{-/-} cells under the same treatment conditions (β $p < 0.05$). Asterisks signify a difference from 4×10^5 cells under the same treatment conditions (* $p < 0.001$, ** $p < 0.0001$).

Subsequently, as a functional confirmation to γ H2AX formation, DNA damage was assessed as micronucleus incidence in the SV40 large T antigen-immortalized wild-type and *Ogg1*^{-/-} MEFs seeded at densities of 6.5×10^4 or 3.25×10^5 (**Fig. 2**) to further evaluate the effect of hindered cellular proliferation capacity on MeHg-initiated DNA damage. Cells were seeded at densities adjusted for plate surface area to maintain equivalence to the densities used for flow cytometric analysis of bromodeoxyuridine (**BrdU**) and γ H2AX. Six-hour exposure to 2 μ M MeHg increased micronucleus incidence ($p < 0.01$ - $p < 0.0001$) with a two-fold higher occurrence in the *Ogg1*^{-/-} versus wild-type MEFs ($p < 0.001$) (**Fig. 5A and 5B**). When the cells were seeded at a higher density (3.25×10^5 cells), the incidence of MeHg-initiated micronuclei was decreased two- to four-fold, down to basal levels, in both wild-type and *Ogg1*^{-/-} MEFs ($p \leq 0.0001$), further supporting the hypothesis that MeHg-mediated DNA damage is in part proliferation-dependent (**Fig. 5B**).

Figure 5.

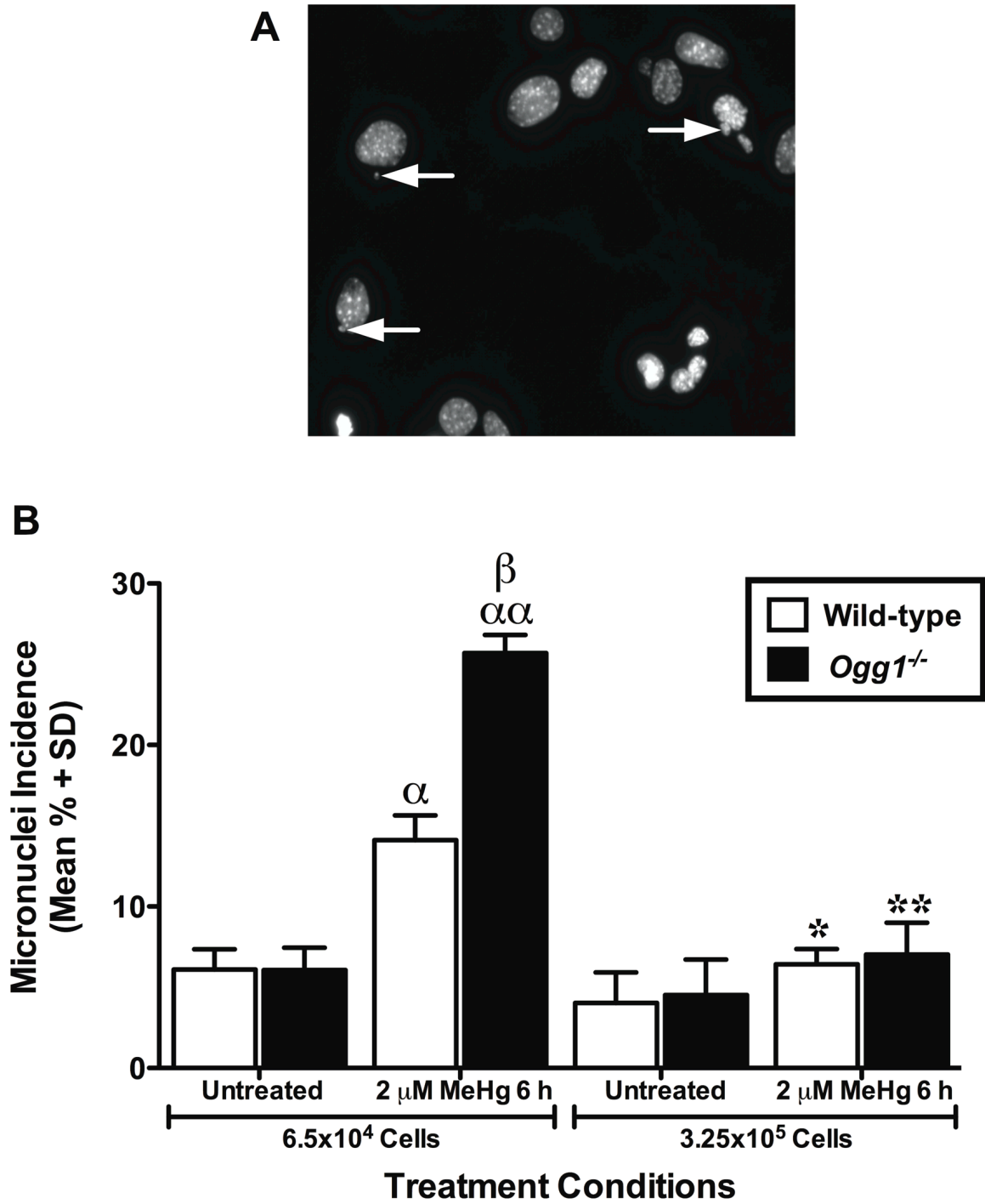


Figure 5. MeHg-initiated micronucleus formation in wild-type and *Ogg1*^{-/-} cells is also dependent on cellular proliferation capacity and functionally confirms γ H2AX results.

SV40 large T antigen-immortalized wild-type and *Ogg1*^{-/-} cells were seeded on glass cover slips at densities of 6.5×10^4 (exponentially growing) or 3.25×10^5 (confluent). Cells were left untreated or exposed to 2 μ M MeHg for 6 h fixed and stained with DAPI. **(A)** Representative field of DAPI-stained nuclei at 40X magnification where arrowheads indicate the location of micronuclei. **(B)** The incidence of micronuclei was quantified in at least 200 intact nuclei with the results plotted as the mean percent incidence plus standard deviation of three independent experiments. Alpha indicates a difference from untreated cells at the same cell number (α $p < 0.01$, $\alpha\alpha$ $p < 0.0001$). Beta denotes a difference between wild-type and *Ogg1*^{-/-} cells under the same treatment conditions (β $p < 0.001$). Asterisks signify a difference from 6.5×10^4 cells under the same treatment conditions (* $p = 0.0001$, ** $p < 0.0001$).

2.2.5 Discussion

Methylmercury (**MeHg**) toxicity persists as a significant public health concern as dietary and occupational exposure levels can range from 0.09-1.8 $\mu\text{g}/\text{kg}/\text{day}$ (Barbosa *et al.*, 2001; Harada *et al.*, 2001; Tsuchiya *et al.*, 2008; Vahter *et al.*, 2000), and overlap with those (0.2-1.8 $\mu\text{g}/\text{kg}/\text{day}$) that have been linked to adverse postnatal neurobehavioral outcomes in humans following *in utero* MeHg exposure (Grandjean *et al.*, 1998; Grandjean *et al.*, 1997). Yet, despite considerable research, the underlying molecular mechanisms leading to the potent neurotoxic action of MeHg remain largely ambiguous. Herein we have presented the first corroborating evidence that, regardless of the method of immortalization, oxoguanine glycosylase 1 (**OGG1**) status is an important determinant of risk for MeHg toxicity, with enhanced susceptibility in Simian virus 40 (**SV40**) large T antigen-immortalized OGG1-*null* (**Ogg1**^{-/-}) murine embryonic fibroblasts (**MEFs**), and demonstrated for the first time that the increased susceptibility of these *Ogg1*^{-/-} MEFs to MeHg-initiated DNA damage is additionally dependent on cellular proliferation capacity. Taken together, our findings establish OGG1 as a critical factor in the maintenance of genomic integrity following MeHg-initiated DNA damage, and in turn support the hypothesis that the mechanism of MeHg toxicity involves both DNA damage as well as a proliferation-dependent component.

Given that our previous findings were carried out in spontaneously-immortalized wild-type and *Ogg1*^{-/-} MEFs which attained immortality through accumulation of random mutations allowing them to escape senescence, we first sought to confirm that the increased sensitivity to MeHg toxicity we observed in spontaneously-immortalized *Ogg1*^{-/-} MEFs was in fact due to the absence of OGG1 and not other unappreciated genetic differences arising from the non-specific mode of immortalization. Hence, we generated SV40 large T antigen-immortalized wild-type and *Ogg1*^{-/-} MEFs and confirmed a similarly increased sensitivity of the *Ogg1*^{-/-} MEFs to low, environmentally relevant concentrations of MeHg, as evidenced by their reduced clonogenic survival, similar to the spontaneously-immortalized cells (Ondovcik *et al.*, 2012). MeHg has also been shown to reduce clonogenic survival in human neuroblastoma cells (Das *et al.*, 2011) and decrease viability in various *in vitro* models as measured by a range of endpoints (Abdalla *et al.*, 2010; Gatti *et al.*, 2004; Gribble *et al.*, 2005; Hirooka *et al.*, 2010; Tamm *et al.*, 2006). However, there has yet to be a report of differentially immortalized DNA repair-deficient cells

maintaining an increased sensitivity to MeHg. These findings confirm our previous results that OGG1 is in fact protective against MeHg-initiated cytotoxicity independent of the method of immortalization, which also implicates oxidatively damaged DNA in the pathogenic mechanism.

Examination of the cell cycle distribution in the newly derived SV40 large T antigen-immortalized wild-type and *Ogg1*^{-/-} MEFs in response to MeHg was also consistent with the induction of cell cycle arrest. As seen previously in the spontaneously immortalized cells (Ondovcik *et al.*, 2012), the percentage of SV40 large T antigen-immortalized cells in G1 was decreased, while the percentage in both S phase and G2/M was conversely increased, further confirming the independence of MeHg toxicity from the method of cellular immortalization. MeHg-initiated induction of cell cycle arrest was further supported by the observed reduction in the fluorescence intensity of S phase cells. Various groups have investigated the effects of MeHg on cell cycle and proliferation showing cell cycle arrest, inhibition/reduction of DNA and RNA synthesis, and down-regulation of cyclins D1, D3 and E which are associated with cell cycle transition and progression (Burke *et al.*, 2006; Das *et al.*, 2008; Falluel-Morel *et al.*, 2007; Gribble *et al.*, 2005; Xu *et al.*, 2010). However, little has been done to investigate the impact of altering the proliferative capacity of the cell on MeHg toxicity. One study in human brain microvascular pericytes found sparse cultures to be more susceptible to MeHg toxicity than dense cultures, observations reconciled with an increased expression of the L-type large neutral amino acid transporter 1 (LAT1) in sparse cultures, facilitating increased influx and intracellular accumulation of MeHg (Hirooka *et al.*, 2010). Although Hirooka and colleagues did not examine the cell cycle status between their sparse and dense cultures as another potential contributing factor to their differential susceptibility to MeHg toxicity, a hallmark of confluent cells lies in their limited ability to proliferate. Thus, we seeded our newly derived SV40 large T antigen-immortalized wild-type and *Ogg1*^{-/-} MEFs at a density permitting exponential growth (4×10^5 cells) and at a confluent density (2×10^6 cells) and confirmed, in the absence of MeHg, cell cycle arrest and halted replication in cells seeded at a higher density, as evidenced by an increased percentage of cells in G1 and a reduced percentage and fluorescence intensity of cells in S phase. Moreover, we showed for the first time that MeHg-initiated cell cycle arrest was attenuated with increased seeding density, implicating a proliferation-dependent component in MeHg toxicity.

Building on the above observations, we turned our focus to the proliferation-dependence of MeHg-initiated DNA damage in SV40 large T antigen-immortalized wild-type and *Ogg1*^{-/-} MEFs, and the modulatory effect of OGG1 status. We previously provided the first report of MeHg-initiated H2AX phosphorylation at serine 139 (γ H2AX), to which spontaneously-immortalized *Ogg1*^{-/-} MEFs were more susceptible, and which was attenuated in the presence of the antioxidative enzyme catalase (Ondovcik *et al.*, 2012). γ H2AX is used as a measure of one of the most lethal forms of DNA damage, DNA double-strand breaks (**DSBs**) (Karagiannis and El-Osta, 2004; Khanna and Jackson, 2001; Sedelnikova *et al.*, 2003). Following DSB formation, the variant H2A histone H2AX becomes phosphorylated at serine 139 in the chromatin flanking the break site by members of the phosphatidylinositol-3 kinase family (Bonner *et al.*, 2008; Rogakou *et al.*, 1998) including ataxia telangiectasia mutated (**ATM**), ataxia telangiectasia and Rad3-related protein (**ATR**), and DNA-dependent protein kinase (**DNA-PK**) (Fernandez-Capetillo *et al.*, 2004; Stiff *et al.*, 2004; Stiff *et al.*, 2006), to form the marker known as γ H2AX. Given that OGG1 is classically associated with the base excision repair (**BER**) pathway and the repair of oxidative base damage, these observations suggest that OGG1 is removing MeHg-induced oxidative damage that impairs or blocks replication forks, leading to the formation of replication-associated DSBs. A range of evidence exists to support the genotoxic potential of MeHg, including its ability to cause chromosomal aberrations, oxidative lesions such as 8-oxo-2'-deoxyguanosine (**8-oxodG**), form MeHg-DNA adducts, alter ploidy, as well as increase the frequency of sister-chromatid exchange and mutations (Cebulska-Wasilewska *et al.*, 2005; Lee *et al.*, 1997; Li *et al.*, 2006; Mailhes, 1983; Morimoto *et al.*, 1982; Rao *et al.*, 2001; Schurz *et al.*, 2000; Yamada *et al.*, 1993). Herein we provide the first evidence that SV40 large T antigen-immortalized *Ogg1*^{-/-} MEFs similarly accumulate γ H2AX, as observed in spontaneously-immortalized MEFs (Ondovcik *et al.*, 2012), confirming an important role for OGG1 in the protection against MeHg-initiated DSB formation. Furthermore, we provide novel evidence that the induction of DSBs following MeHg exposure is in part proliferation-dependent, given that MeHg-initiated γ H2AX formation was reduced to basal levels in both wild-type and *Ogg1*^{-/-} MEFs when cells were seeded at a confluent density (2×10^6 cells).

To provide functional confirmation of the DNA damage measured by γ H2AX formation, we examined the incidence of micronuclei in the SV40 large T antigen-immortalized wild-type and *Ogg1*^{-/-} MEFs. Micronucleus analysis is useful in detecting both clastogenic (chromosomal

breakage) and aneugenic (loss of whole chromosomes) effects of genotoxins, and is a widely used *in vitro* genotoxicity test and biomarker for assessing human exposures (Norppa and Falck, 2003). Micronuclei are formed as a result of chromosome breakage or mitotic apparatus defects, but may also arise from a fragment stemming from a broken anaphase bridge (Norppa and Falck, 2003). MeHg has previously been shown to increase the frequency of micronuclei in various models (Bonacker *et al.*, 2004; Crespo-Lopez *et al.*, 2007; Das *et al.*, 2011; Franchi *et al.*, 1994; Rocha *et al.*, 2011; Thier *et al.*, 2003); however, the two-fold increased sensitivity of *Ogg1*^{-/-} MEFs to MeHg-initiated micronuclei formation as a functional confirmation to γ H2AX reported herein has not previously been shown. Moreover, we provide additional supporting evidence that MeHg-initiated DNA damage is in part dependent on the ability of the cell to proliferate, as seeding cells at a high density that limited proliferative capacity also completely blocked MeHg-initiated formation of micronuclei, which remained at basal levels.

Our data provide the first corroborating, and most definitive, evidence that OGG1 status is a critical determinant of risk for MeHg toxicity, with increased susceptibility in *Ogg1*^{-/-} MEFs independent of cellular immortalization method, suggesting that the increased sensitivity of the *Ogg1*^{-/-} MEFs to MeHg is a reflection of genotype and not other unappreciated genetic differences resulting from the mode of immortalization. Furthermore, we demonstrate for the first time that the increased susceptibility of *Ogg1*^{-/-} MEFs to MeHg-initiated DNA damage is additionally dependent on the ability of the cell to proliferate. This observation is of critical importance in gaining a better understanding of the underlying mechanisms of MeHg toxicity, and sheds light on why, compared to the adult, the rapidly dividing and differentiating cells of the embryo and fetus are particularly sensitive to the neurotoxic effects of MeHg. Together, our findings solidify a critical role for OGG1 in the maintenance of genomic integrity following MeHg-initiated DNA damage, and suggest that variations in cellular proliferative capacity and interindividual variability in repair activity may modulate the risk of toxicological consequences. More extensive investigation is required to better understand the roles that MeHg-initiated DNA damage and altered cellular proliferation capacity play in the mechanism of MeHg toxicity, and importantly, how these players interact *in vivo*. Given that MeHg toxicity remains a significant public health concern, it is important to improve our understanding of, and gain better insights into, the molecular mechanisms underlying the toxicity of this potent neurotoxin. Doing so will

allow for the identification of novel risk factors and the creation of effective therapeutic interventions to minimize the deleterious effects of MeHg toxicity.

2.2.6 Acknowledgements

Oxoguanine glycosylase 1-*null* (**Ogg1**^{-/-}) mice were generously donated by Dr. Tomas Lindahl (Imperial Cancer Research Fund, United Kingdom) via Dr. Christi A. Walter at the University of Texas Health Science Center at San Antonio.

2.3 STUDY 3: EXPRESSION OF HUMAN OXOGUANINE GLYCOSYLASE 1 (hOgg1) OR FORMAMIDOPYRIMIDINE GLYCOSYLASE (Fpg) IN HUMAN EMBRYONIC KIDNEY (HEK) 293 CELLS EXACERBATES METHYLMERCURY (MeHg) TOXICITY *IN VITRO*^a

Running title: Enhanced DNA repair & methylmercury toxicity

Stephanie L. Ondovcik^{*}, Thomas J. Preston^{*}, Gordon P. McCallum^{*} and Peter G. Wells^{*,†,1}

Departments of ^{*}Pharmaceutical Sciences and [†]Pharmacology & Toxicology
University of Toronto
Toronto, Ontario, Canada

¹ Corresponding author:
Peter G. Wells, Pharm.D.
Faculty of Pharmacy, University of Toronto
144 College St., Toronto, Ontario, Canada M5S 3M2
Email: pg.wells@utoronto.ca
Phone 416-978-3221

a. A preliminary report of this research was presented at the 2007 annual meeting of the Teratology Society (USA) [*Birth Defects Res. Part A: Clinical and Molecular Teratology*, 79(5): 416 (P21), 2007]. This work was supported by operating grants from the Canadian Institutes of Health Research (CIHR) and the National Institute of Environmental Health Sciences (NIEHS) [grant # 1-R21-ES013848-O1A1] [PGW]; SLO was the recipient of a CIHR Frederick Banting and Charles Best Canada Graduate Scholarship; TJP and GPM were supported in part by postdoctoral fellowships from the CIHR and the Rx&D Health Research Foundation.

Preston, T.J.- Assisted with the western blotting, isolation of DNA and ELISA for quantification of 8-oxodG, and performed all aspects of the AP site assay, less the analysis of the data.

McCallum, G.P.- Carried out the HPLC quantification of dG for the 8-oxodG assay.

2.3.1 Abstract

Chronic low-level dietary exposure to methylmercury (**MeHg**) at higher concentrations due to daily fish consumption can damage both the adult and fetal central nervous system. To determine the role of reactive oxygen species (**ROS**) and oxidatively damaged DNA in the mechanism of toxicity, transgenic human embryonic kidney (**HEK**) 293 cells that express either human oxoguanine glycosylase 1 (**hOgg1**) or its bacterial homolog, formamidopyrimidine glycosylase (**Fpg**), which primarily repair the oxidative lesion 8-oxo-2'-deoxyguanosine (**8-oxodG**), were used to assess the *in vitro* effects of MeHg. Western blotting confirmed the expression of hOgg1 or Fpg in both the nuclear and mitochondrial compartments of their respective cell lines. Following acute (1-2 h) incubations with 0-10 μ M MeHg, concentration-dependent decreases in clonogenic survival and cell growth accompanied concentration-dependent increases in lactate dehydrogenase (**LDH**) release, ROS formation, 8-oxodG levels and apurinic/aprimidinic (**AP**) sites consistent with the onset of MeHg cytotoxicity. Paradoxically, hOgg1- and Fpg-expressing HEK 293 cells were more sensitive than wild-type cells to MeHg across all cellular and biochemical parameters, exhibiting reduced clonogenic survival and cell growth, and increased LDH release and DNA damage. Accordingly, upregulation of specific components of the base excision repair (**BER**) pathway may prove deleterious potentially due to the absence of compensatory enhancement of downstream processes to repair toxic intermediary abasic sites. Thus, interindividual variability in DNA repair activity may constitute an important risk factor for environmentally-initiated oxidatively damaged DNA and its pathological consequences.

2.3.2 Introduction

Methylmercury (**MeHg**) is a potent neurotoxin that persists in the environment. It is most notorious for the more than 900 human fatalities that resulted in Minamata Bay, Japan, from the consumption of MeHg-contaminated seafood that contained up to 40 ppm ($\approx 184 \mu\text{M}$) MeHg (National Institute for Minamata Disease) (Harada, 1995). Today however, society's attempt to foster a healthier lifestyle by increasing their dietary intake of fish and other seafood is posing a less catastrophic but more prevalent health threat with some widely consumed species of fish, including swordfish, shark, pike and bass, harboring high concentrations of MeHg, in some greater than 1 ppm ($\approx 4.6 \mu\text{M}$ MeHg) (Health Canada). Our studies herein have been carried out at working concentrations of MeHg well below the range associated with fatalities, and within the more commonly relevant concentration range found in various fish and seafood species.

The developing nervous system appears to be particularly susceptible to MeHg, with *in utero* MeHg exposure associated with a range of structural and functional postnatal neurodevelopmental deficits (Castoldi *et al.*, 2003; Choi, 1989; Davis *et al.*, 1994). A number of mechanisms have been postulated to explain the potent neurotoxic action of MeHg. Among them, the role of oxidative stress and its resulting pathological consequences has garnered much of the attention, yet the precise molecular mechanisms remain to be elucidated. Various groups have demonstrated the ROS-initiating ability of MeHg, its capacity to damage DNA and attenuation of toxicity with antioxidant pretreatment (Ali *et al.*, 1992; Belletti *et al.*, 2002; Burke *et al.*, 2006; Chen *et al.*, 2005; Choi, 1989; Crespo-Lopez *et al.*, 2007; Ehrenstein *et al.*, 2002; Ganther, 1978; Garg and Chang, 2006; Gatti *et al.*, 2004; Jie *et al.*, 2007; Liu *et al.*, 2002; Ni *et al.*, 2011; Ondovcik *et al.*, 2012; Rush *et al.*, 2012; Shanker *et al.*, 2005; Silva-Pereira *et al.*, 2005). Thus, considerable evidence supports a potential role for ROS-mediated oxidatively damaged DNA in the mechanism of MeHg toxicity.

The base excision repair (**BER**) pathway is one highly conserved form of DNA repair responsible for maintaining both genomic stability and integrity. It does so by removing aberrant bases from the genome, and is the pathway primarily responsible for removal of oxidatively damaged bases such as 8-oxo-2'-deoxyguanosine (**8-oxodG**), which if not repaired can lead to

potentially carcinogenic G:C to T:A transversion mutations, as well as interfere with transcriptional machinery altering gene expression (Khubta *et al.*, 2010; Kitsera *et al.*, 2011; Klungland and Bjelland, 2007; Klungland *et al.*, 1999; Pastoriza-Gallego *et al.*, 2007), the latter of which may be particularly important for normal brain development (Wells *et al.*, 2010). BER-mediated repair of 8-oxodG is initiated by the bifunctional DNA glycosylase/apurinic/aprimidinic (AP) lyase oxoguanine glycosylase 1 (**Ogg1**) in mammalian cells, and its functional homolog in bacteria, formamidopyrimidine glycosylase (**Fpg**), which is reportedly 80-times more active than Ogg1 (Asagoshi *et al.*, 2000; Klungland *et al.*, 1999). These glycosylases act to recognize and excise the damaged base creating an AP site, which can be cytotoxic without the action of the downstream short-patch BER machinery consisting of AP endonuclease 1 (**APE1**), DNA polymerase β (**POL β**), DNA ligase 3 α (**LIG3 α**) and X-ray cross-complementing 1 (**XRCC1**), all of which work in concert to complete the repair process (David *et al.*, 2007; Wilson and Bohr, 2007).

The importance of DNA repair in disease has been underscored by observations in both animals and humans where deficiencies have proved deleterious. *Ogg1*-null (**Ogg1^{-/-}**) mice accumulate hepatic 8-oxodG corresponding to a 2-3-fold increased spontaneous mutation frequency (Klungland *et al.*, 1999; Minowa *et al.*, 2000); display increased postnatal neurodevelopmental deficits following *in utero* exposure to the ROS-initiating drug methamphetamine (Wong *et al.*, 2008); and, with the combined absence of MutY homolog (**MYH**) responsible for excising adenine misincorporated opposite 8-oxodG during replication, have an increased incidence of lung and small intestine cancer (Russo *et al.*, 2004). In humans, the serine to cysteine polymorphism at amino acid residue 326 of the Ogg1 protein compromises repair activity and has been associated with an increased cancer incidence (Goode *et al.*, 2002; Hung *et al.*, 2005a). However, whether enhancement of BER capacity through overexpression of Ogg1 or Fpg is protective remains unclear, with conflicting reports in the literature. Overexpression of human Ogg1 (**hOgg1**) in the mitochondria of human hepatoma cells exacerbated cisplatin-mediated cytotoxicity (Zhang *et al.*, 2007), while the overexpression of *N*-methylpurine DNA glycosylase in human breast cancer cells similarly sensitized them to the alkylating agent methyl methanesulfonate (Rinne *et al.*, 2004). In contrast, expression of hOgg1 or Fpg in human lung epithelial cells protected against 1,3-N,N'-bis(2-chloroethyl)-N-nitrosourea (**BCNU**)-mediated DNA damage and cytotoxicity (He *et al.*, 2002), as did their expression in

human embryonic kidney (**HEK**) 293 cells against 8-oxodG accumulation and cytotoxicity initiated by menadione, cisplatin and oxaliplatin (Preston *et al.*, 2009).

The ROS-initiating and DNA-damaging abilities of MeHg likely are key players in its mechanism of toxicity. However, no studies had examined the effects of variable BER capacity on MeHg toxicity prior to our first report of an increased sensitivity of *Ogg1*^{-/-} cells to MeHg (Ondovcik *et al.*, 2012). Thus, we sought to further evaluate the contribution of ROS and oxidatively damaged DNA in the mechanism of MeHg toxicity in a reciprocal model of enhanced BER employing HEK 293 cells engineered in our lab to stably express hOgg1 or Fpg. Herein we provide the first report of an altered sensitivity of hOgg1- and Fpg-expressing cells to MeHg-initiated cytotoxicity, with a paradoxical increase in sensitivity likely resulting from their increased incision activity and subsequent accumulation of toxic repair intermediates. Our results support a role for ROS-mediated oxidatively damaged DNA in the mechanism of MeHg toxicity, and implicate interindividual variability in DNA repair activity as a potential determinant of risk.

2.3.3 Materials and Methods

Cell culture. Wild-type human embryonic kidney (**HEK**) 293 cells and HEK cells expressing human oxoguanine glycosylase 1 (**hOgg1**) or formamidopyrimidine glycosylase (**Fpg**) were obtained and derived in our laboratory as previously described (Preston *et al.*, 2009). Cells were grown at 37°C in 5% CO₂ (The Linde Group, Etobicoke, Ontario) in a humidified incubator, and maintained in Minimum Essential Medium Alpha containing 2 mM L-glutamine (Life Technologies Inc., Burlington, Ontario), and supplemented with 1200 µg/ml G418 (Geneticin) disulfate salt solution, 1% penicillin/streptomycin solution (both Sigma-Aldrich Canada Ltd., Oakville, Ontario) and 10% heat-inactivated fetal bovine serum (HyClone, Thermo Fisher Scientific, Ottawa, Ontario).

Anti-FLAG-mediated western blotting for hOgg1-FLAG and Fpg-FLAG protein expression.

Nuclear and mitochondrial protein extracts were prepared from wild-type, hOgg1- and Fpg-expressing HEK 293 cells as described previously (Dobson *et al.*, 2000). Ten micrograms of each nuclear and mitochondrial protein lysate were loaded onto a 10% polyacrylamide gel, run for 2 h at 50 V, and transferred onto a nitrocellulose membrane at 60 V for 1.5 h. The membrane was blocked in 0.1% Tween-20 in 1X Tris-buffered saline (**TBST**) containing 3% skim milk and incubated overnight at 4°C with an anti-FLAG M2 mouse monoclonal antibody (1:5000 in TBST containing 1% skim milk) (Sigma-Aldrich Canada Ltd.), followed by incubation for 1 h at room temperature with a horseradish peroxidase-conjugated goat anti-mouse IgG secondary antibody (1:2000 in TBST) (Santa Cruz Biotechnology Inc., Santa Cruz, California). Detection was accomplished using enhanced chemiluminescent detection reagents (Amersham, GE Healthcare, Baie d'Urfe, Quebec) and exposure onto Bioflex MSI film (Clonex, Markham, Ontario).

Clonogenic assay. Five hundred cells were seeded into six-well plates and treated the following day for 1 h with 0-10 µM of methylmercury (II) chloride (**MeHg**, Sigma-Aldrich Canada Ltd.). Surviving cells were allowed to grow into visible colonies for 8-10 days post-treatment, and were then fixed and stained with 0.5 % methylene blue in 100% methanol for 15 min. Clonogenic survival was determined from the mean number of colonies plus the standard deviation of three independent determinations and is presented as a percentage of untreated cells.

Assessment of cell growth via Hoechst bisbenzimidazole 33258. One thousand cells were seeded into 96-well plates, allowed to adhere overnight and left untreated or treated for 1 h with 10 μ M MeHg. In an additional 96-well plate per line, known cell numbers (0-50,000) were seeded to generate a standard curve from which cell numbers would be determined via linear regression analysis at the various days post-treatment. Cells were washed with Milli-Q water and frozen at -80°C at 0, 2, 4, 6 and 8 days post-treatment, after which they were stained with 20 $\mu\text{g}/\text{ml}$ Hoechst bisbenzimidazole 33258 (Sigma-Aldrich Canada Ltd.). Fluorescence data were measured and analyzed using a SpectraMax Gemini XS microplate spectrofluorometer (excitation, 350 nm; emission, 460 nm) and SoftMax Pro 5.4 software respectively (both MDS Analytical Technologies, Sunnyvale, California).

Lactate dehydrogenase (LDH) release as a measure of cytotoxicity. Thirty thousand cells were seeded into 96-well plates and treated the following day for 2 h with 9% v/w Triton X-100 to yield maximal membrane rupture and LDH release, or exposed to 0, 2, 4 or 8 μ M MeHg for 2 h. Two hours post-treatment, LDH release was measured as resorufin fluorescence using the CytoTox-ONE Homogeneous Membrane Integrity Assay (Promega Corporation, Madison, Wisconsin). LDH-catalyzed fluorescence was measured by a SpectraMax Gemini XS microplate spectrofluorometer (excitation, 560 nm; emission, 590 nm) with data analysis carried out via SoftMax Pro 5.4 software (both MDS Analytical Technologies), and results presented as the mean percent LDH release of maximum.

Reactive oxygen species (ROS) formation. Twenty-five thousand cells were seeded into 96-well plates and treated the following day for 1 h with 0 or 5 μ M MeHg. Following treatment, cells were loaded with 25 $\mu\text{g}/\text{ml}$ 5-(and-6)-chloromethyl-2',7'-dichlorodihydrofluorescein diacetate acetyl ester (**CM-H₂DCFDA**) (Life Technologies Inc.) and incubated in the dark at 37°C and 5% CO_2 for 2 or 24 h. ROS-mediated oxidation of CM-H₂DCFDA to fluorescent dichlorodihydrofluorescein (**DCF**) was then measured and analyzed using a SpectraMax Gemini XS microplate spectrofluorometer (excitation, 485 nm; emission, 530 nm) and SoftMax Pro 5.4 software respectively (both MDS Analytical Technologies), with results presented as the mean percent of untreated cell DCF fluorescence.

8-oxo-2'-deoxyguanosine (8-oxodG) as an indicator of oxidatively damaged DNA. DNA oxidation was determined in total DNA isolated from cells 30 min following 1 h exposure to 0, 2

or 4 μM MeHg as previously described (Preston *et al.*, 2009). One hundred and thirty micrograms of total DNA extract were analyzed using a Highly Sensitive 8-oxodG Check ELISA kit (Genox Corporation, Baltimore, Maryland) to quantify 8-oxodG. Results were normalized for total deoxyguanosine (**dG**) content as determined by high-performance liquid chromatography with detection by ultraviolet absorbance (**HPLC-UV**), and expressed as the mean ng 8-oxodG/ μg dG.

Apurinic/aprimidinic (AP) site formation as a measure of DNA damage. Genomic DNA was isolated from cells 30 min following 1 h exposure to 0 or 10 μM MeHg using the GenElute Mammalian Genomic DNA Miniprep Kit (Sigma-Aldrich Canada Ltd.) and subsequently quantified spectrophotometrically. AP site formation was then quantified using the aldehyde reactive probe (**ARP**) reagent, followed by colorimetric detection via avidin-biotin assay using a DNA Damage Quantification Kit (Biovision Inc., Milpitas, California), and results presented as the mean number of AP sites per 10^5 base pairs.

Statistical Analysis. An unpaired t-test was used to analyze data comparing two groups, while multiple comparisons were analyzed by a one-way ANOVA followed by Dunnett's or Bonferroni's multiple comparison post-test as appropriate, with the level of significance set to $p < 0.05$ in all cases (GraphPad Prism 5.0d, GraphPad Software Inc., La Jolla, California).

2.3.4 Results

To first confirm the continued stable expression of human oxoguanine glycosylase 1 (**hOgg1**)-FLAG and formamidopyrimidine glycosylase (**Fpg**)-FLAG proteins in our human embryonic kidney (**HEK**) 293 cells, anti-FLAG-mediated western blotting was performed and revealed sustained nuclear and mitochondrial expression of both hOgg1 and Fpg in the respective cell lines (**Fig. 1**). This remained consistent with the initial characterization profile of the cells where, in addition to stable protein expression, significantly enhanced 8-oxo-2'-deoxyguanosine (**8-oxodG**) incision activity was also observed (Preston *et al.*, 2009).

Figure 1.

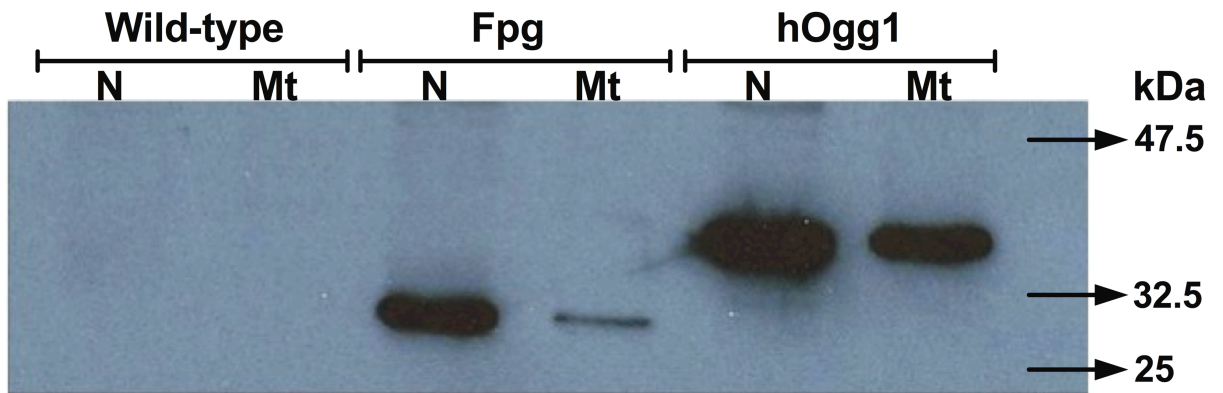


Figure 1. Anti-FLAG-mediated Western blotting confirms stable nuclear (N) and mitochondrial (Mt) expression of human oxoguanine glycosylase 1 (hOgg1)-FLAG and formamidopyrimidine glycosylase (Fpg)-FLAG proteins.

Anti-FLAG (1:5000)-mediated western analysis was performed on 10 µg of nuclear (N) or mitochondrial (Mt) protein fractions isolated from wild-type, hOgg1- and Fpg-expressing human embryonic kidney (HEK) 293 cells. Wild-type cells are void of any reactive species, while hOgg1- and Fpg-expressing cells exhibit the presence of a single reactive band at the predicated molecular weights of 39 kDa and 30.2 kDa respectively.

To assess the cytotoxicity profile of methylmercury (**MeHg**) in the wild-type, hOgg1- and Fpg-expressing HEK 293 cells, their clonogenic survival was compared following acute 1 h exposure to low micromolar concentrations of MeHg. A concentration-dependent decrease in clonogenic survival was observed in all cell lines following MeHg (2-10 μ M) treatment (**Fig. 2**). The hOgg1- and Fpg-expressing cells exhibited similarly altered sensitivities to MeHg; however, compared to wild-type controls, both showed a paradoxically greater rather than the expected reduced sensitivity to MeHg, with a 1.5-2-fold reduction in clonogenic survival ($p < 0.05$ - $p < 0.001$) following MeHg treatment (**Fig. 2**). This same paradoxical increase in sensitivity of hOgg1- and Fpg-expressing cells to MeHg was observed for all other outcomes reported below.

Figure 2.

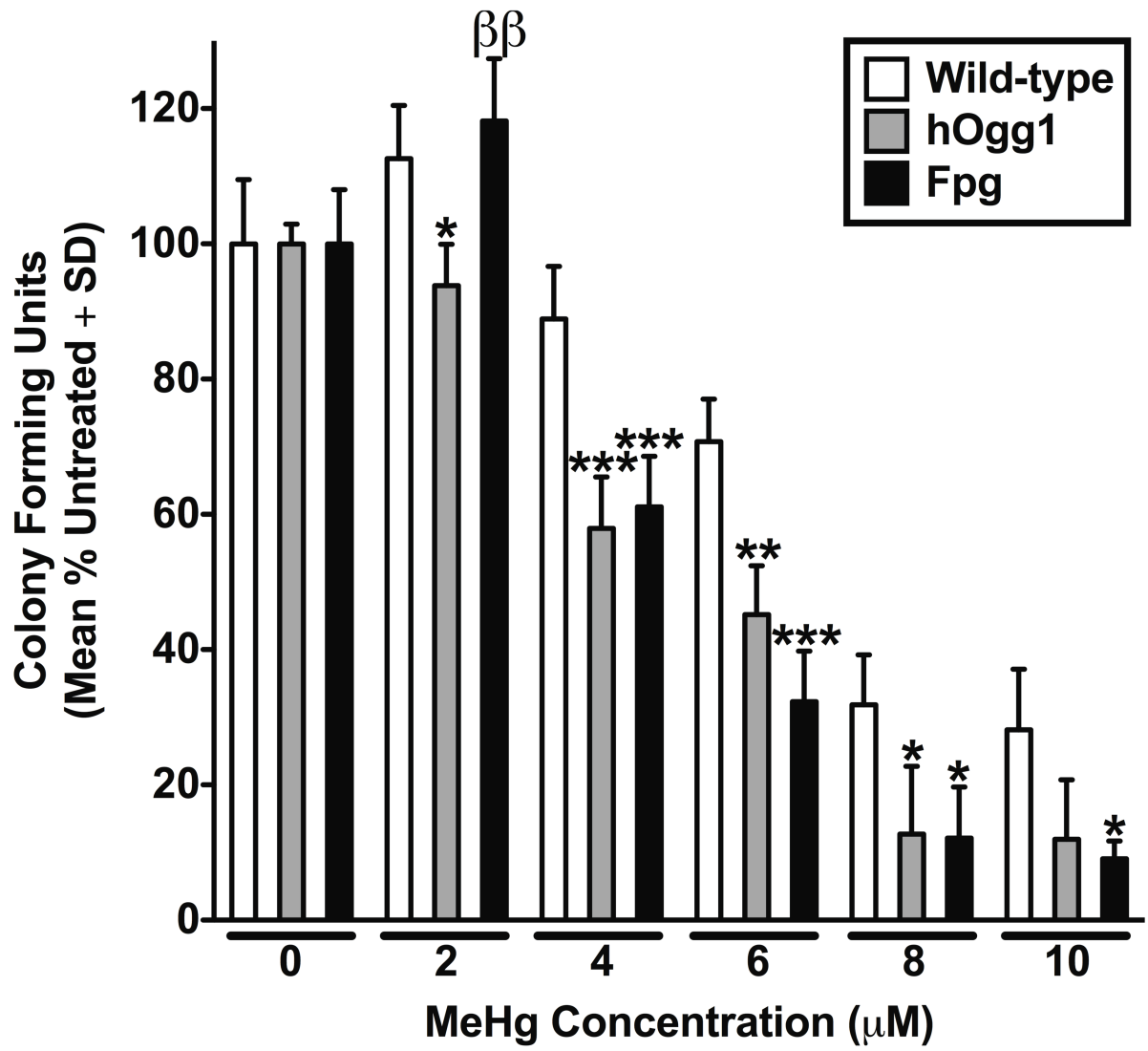


Figure 2. hOgg1- and Fpg-expressing HEK 293 cells demonstrate reduced clonogenic survival following acute exposure to methylmercury (MeHg).

Sensitivity of hOgg1- and Fpg-expressing HEK 293 cells was measured by clonogenic assay following 1 h exposure to 0-10 μ M MeHg. Results are expressed as the mean percent of untreated colony forming units plus the standard deviation of three independent experiments. Beta denotes a difference in sensitivity between hOgg1- and Fpg-expressing cells at the same concentration (β $p < 0.01$). Asterisks indicate a difference in sensitivity from wild-type cells at the same concentration (* $p < 0.05$, ** $p < 0.01$, *** $p < 0.001$).

The effects of MeHg on cell growth were further assessed in wild-type, hOgg1- and Fpg-expressing HEK 293 cells using the fluorescent dye Hoechst bisbenzimidazole 33258. Compared to wild-type controls, both hOgg1- and Fpg-expressing cells demonstrated reduced cell growth both basally, and following acute 1 h MeHg exposure (**Fig. 3**). Untreated hOgg1-expressing cells showed hindered growth at days 4-8 compared to wild-type cells ($p < 0.05-0.0001$), while growth of Fpg-expressing cells was compromised at days 4-6 ($p < 0.01-0.001$) (**Fig. 3A and Fig. 3B**). At the endpoint on day 8, hOgg1-expressing cell numbers were approximately 2-fold less than wild-type cells, while Fpg-expressing cell numbers appeared similar to wild-type controls (**Fig. 3B**). Acute exposure to 10 μ M MeHg impaired wild-type cell growth compared to untreated cells at days 2-6 ($p < 0.05-0.001$), with growth retarded in hOgg1- and Fpg-expressing cells at days 4-8 ($p < 0.05-0.0001$) versus untreated cells (**Fig. 3C and Fig. 3D**). hOgg1- and Fpg-expressing cells were also more sensitive to the effects of MeHg on cell growth, with reduced growth compared to wild-type cells at days 6-8 following acute MeHg treatment ($p < 0.05-0.0001$) (**Fig. 3C and Fig. 3D**). These differences were most pronounced at day 8 following MeHg treatment, with 2.5- and 8-fold reductions in cell numbers between hOgg1- and Fpg-expressing cells respectively, compared to wild-type controls (**Fig. 3D**).

Figure 3.

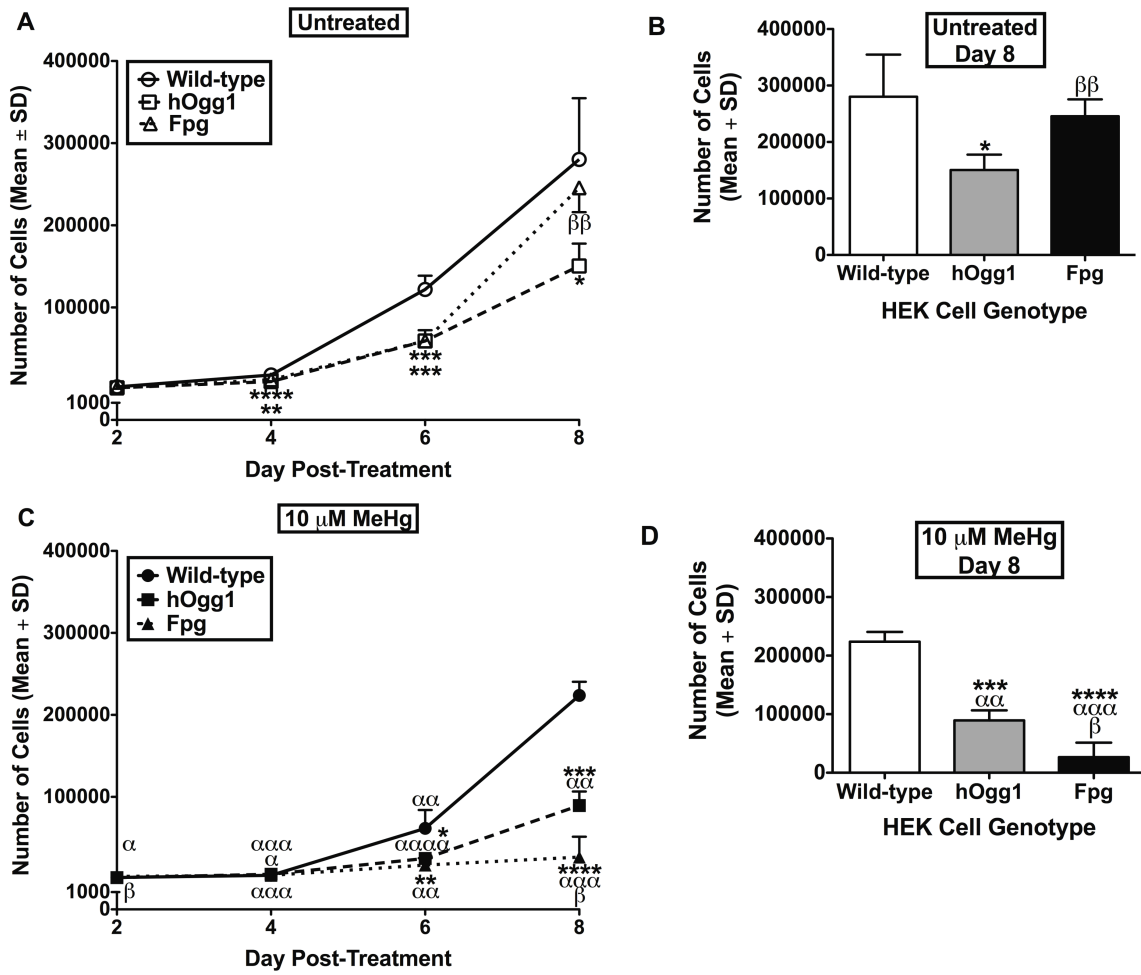


Figure 3. hOgg1- and Fpg-expressing HEK 293 cells demonstrate reduced cell growth both basally, and following acute MeHg exposure.

Cell growth was evaluated for 8 days in (A-B) untreated cells and (C-D) cells treated for 1 h with 10 μ M MeHg using the fluorescent dye Hoechst bisbenzimidazole 33258. Results are expressed as the mean number of cells as determined from a standard curve of known cell numbers for each line, plus or minus the standard deviation of three to four independent experiments. Alpha signifies a difference from untreated cells of the same genotype (α $p < 0.05$, $\alpha\alpha$ $p < 0.01$, $\alpha\alpha\alpha$ $p < 0.001$, $\alpha\alpha\alpha\alpha$ $p < 0.0001$). Beta denotes a difference between hOgg1- and Fpg-expressing cells at the same day post-treatment (β $p < 0.05$, $\beta\beta$ $p < 0.01$). Asterisks indicate a difference from wild-type cells at the specified day post-treatment (* $p < 0.05$, ** $p < 0.01$, *** $p < 0.001$, **** $p < 0.0001$).

To confirm the increased sensitivity of the hOgg1- and Fpg-expressing cells to MeHg, a biochemical indicator of cytotoxicity, lactate dehydrogenase (**LDH**) release, was quantified following acute 2-h exposure to MeHg (2-8 μ M). A concentration-dependent increase in LDH release was observed, with increased release in all cells compared to untreated controls upon exposure to the highest concentration of 8 μ M MeHg ($p < 0.05-0.001$) (**Fig. 4**). In accordance with our other cellular outcomes, hOgg1- and Fpg-expressing cells were more sensitive to MeHg-initiated cytotoxicity ($p < 0.05-0.0001$), releasing 3-5-fold more LDH compared to wild-type cells at all concentrations of MeHg (**Fig. 4**).

Figure 4.

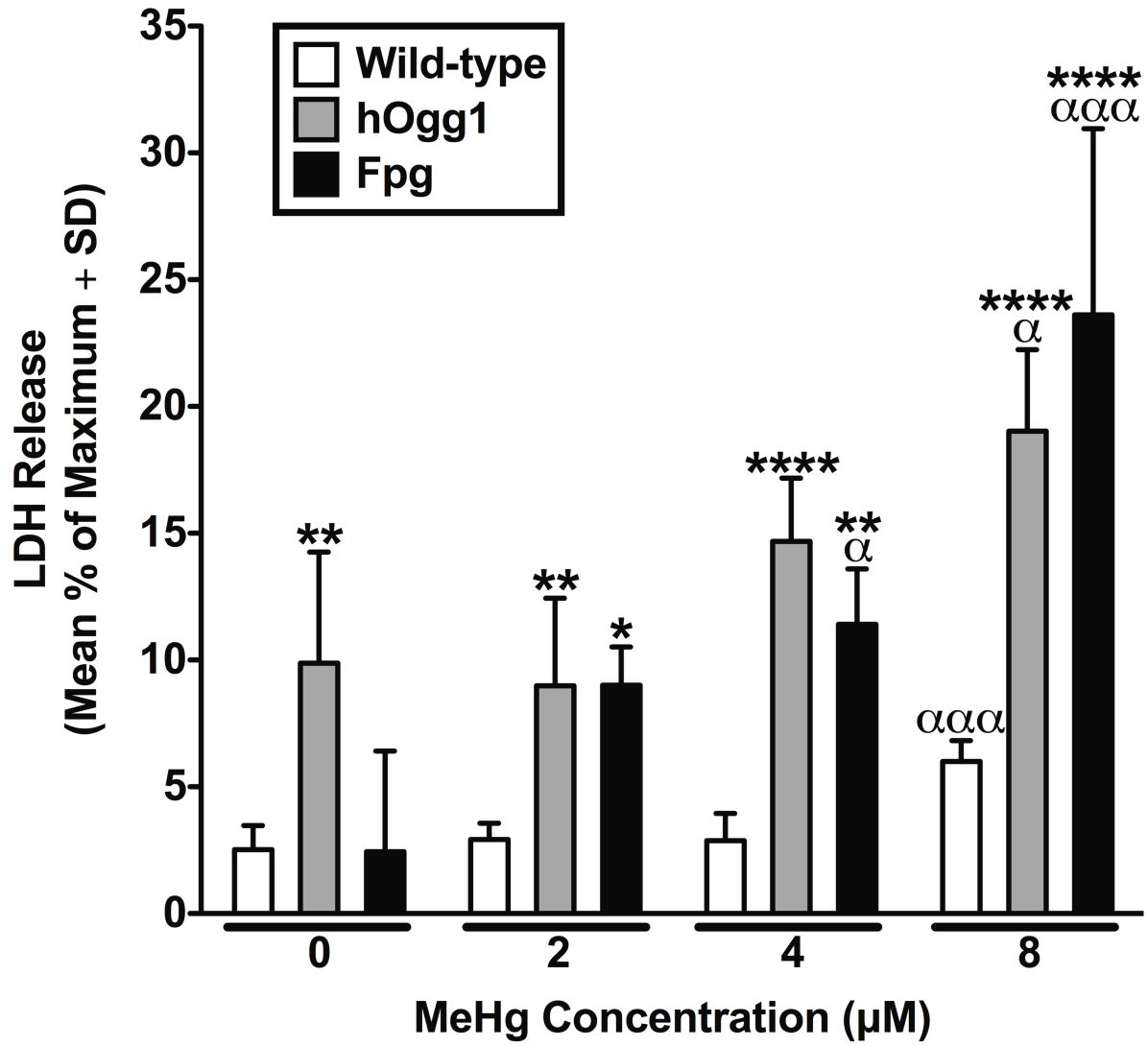


Figure 4. MeHg-initiated cytotoxicity measured as lactate dehydrogenase (LDH) release is exacerbated in hOgg1- and Fpg-expressing HEK 293 cells.

Cytotoxicity was measured as LDH release using a CytoTox-ONE Homogeneous Membrane Integrity Assay following 2 h treatment with 0, 2, 4 or 8 μ M MeHg. Results are expressed as the mean percent LDH release of maximum (9% w/v Triton X-100) plus the standard deviation of three to four independent experiments. Alpha signifies a difference from untreated cells of the same genotype (α $p < 0.05$, $\alpha\alpha\alpha$ $p < 0.001$). Asterisks indicate a difference from wild-type cells at the specified concentrations (* $p < 0.05$, ** $p < 0.01$, **** $p < 0.0001$).

To investigate whether the cytotoxic effects of MeHg may be due in part to reactive oxygen species (**ROS**)-mediated oxidatively damaged DNA, we first examined the ability of MeHg to generate ROS in wild-type cells. One-hour treatment with 5 μ M MeHg was sufficient to increase ROS production 25% above levels in untreated cells ($p < 0.01$) (**Fig. 5A**). This elevation was sustained at 24 h post-treatment, with higher levels of ROS persisting in MeHg-treated wild-type cells compared to untreated cells ($p < 0.05$) (**Fig. 5B**).

Figure 5.

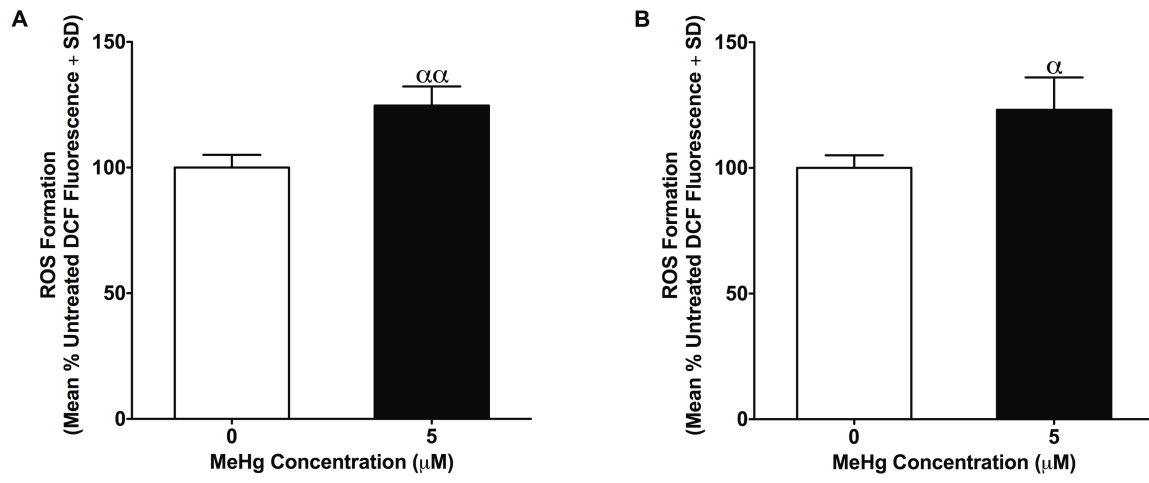


Figure 5. MeHg enhances reactive oxygen species (ROS) formation in wild-type cells with a sustained elevation persisting at 24 h.

ROS formation was measured in wild-type cells at (A) 2 and (B) 24 h post-1 h treatment with 0 or 5 μ M MeHg using the fluorescent probe 5-(and-6)-chloromethyl-2',7'-dichlorodihydrofluorescein diacetate acetyl ester (**CM-H₂DCFDA**). Results are expressed as the mean percent of untreated cell dichlorodihydrofluorescein (**DCF**) fluorescence plus the standard deviation of three to four independent experiments. Alpha signifies a difference from untreated cells (α $p < 0.05$, $\alpha\alpha$ $p < 0.01$).

Given the ability of MeHg to generate ROS in our model, we examined its capacity to oxidize DNA as measured by the oxidative lesion 8-oxodG, which is primarily repaired by Ogg1 and its functional homolog in bacteria, Fpg. Untreated cells expressing hOgg1, but not those expressing Fpg, had constitutively lower levels of DNA oxidation, with only 50% of the 8-oxodG levels observed in wild-type controls ($p < 0.05$) (**Fig. 6**). In contrast, acute 1-h exposure to MeHg resulted in a small, concentration-dependent increase in DNA oxidation in both hOgg1- and Fpg-expressing cells compared to their respective basal levels, but there was no increase in wild-type controls compared to their basal level (**Fig. 6**). A 2-fold accumulation of 8-oxodG was apparent in hOgg1-expressing cells at both 2 and 4 μM MeHg ($p < 0.05$) compared to untreated hOgg1 cells, while levels in Fpg-expressing cells were elevated 2-fold compared to untreated Fpg cells following exposure to 4 μM MeHg ($p < 0.01$) (**Fig. 6**). Cells expressing Fpg, albeit not hOgg1, appeared to accumulate MeHg-initiated 8-oxodG to a greater degree compared to wild-type cells, with a significant 1.5-fold accumulation of DNA damage observed in Fpg-expressing cells at the highest concentration of MeHg ($p < 0.05$) (**Fig. 6**).

Figure 6.

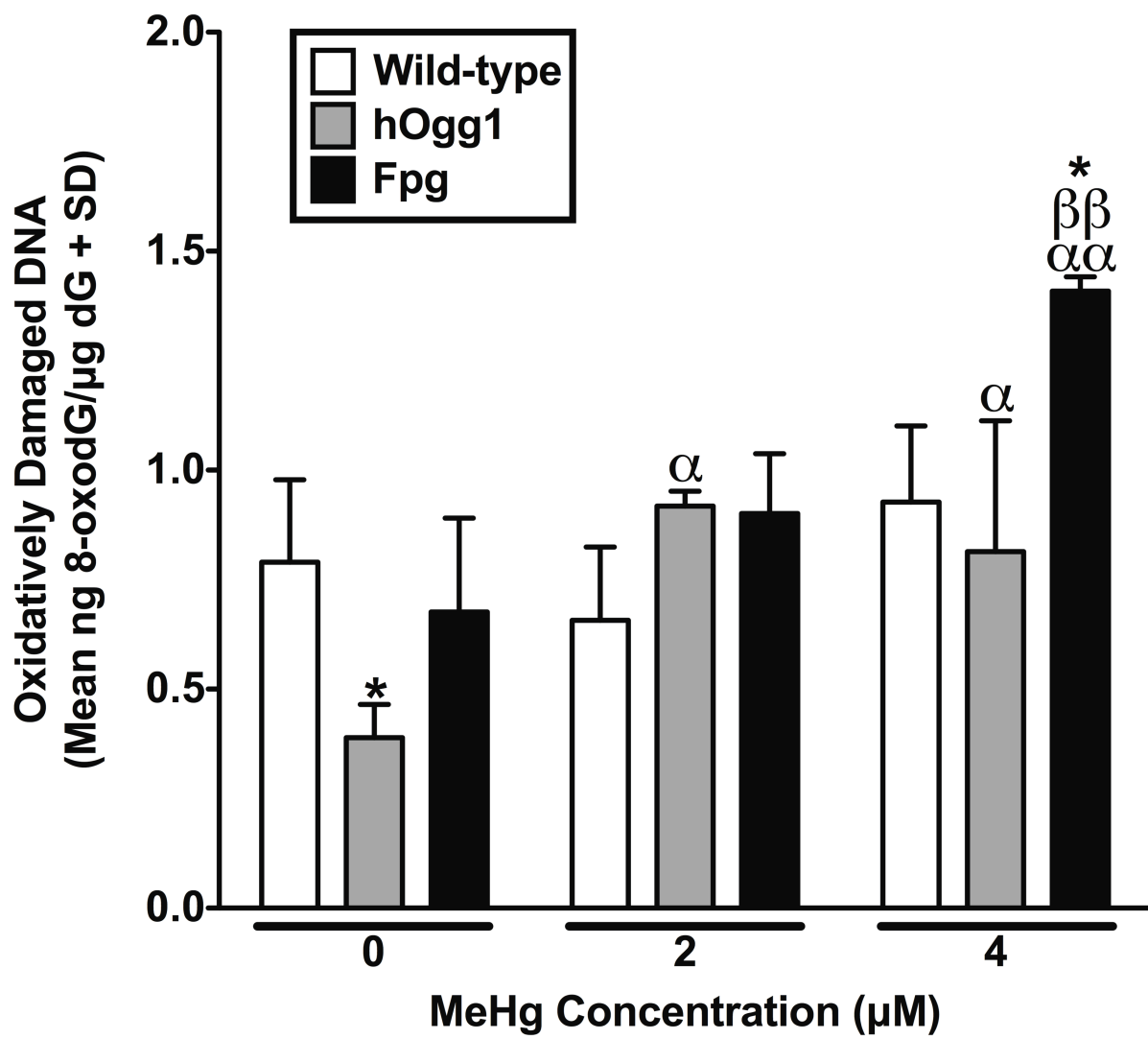


Figure 6. hOgg1- and Fpg-expressing HEK 293 cells have constitutively lower levels of 8-oxo-2'-deoxyguanosine (8-oxodG), but appear to accumulate 8-oxodG to a greater degree upon acute MeHg exposure compared to wild-type cells.

MeHg-initiated DNA oxidation was measured in isolated DNA from cells treated with 0, 2 or 4 μM MeHg for 1 h using a Highly Sensitive 8-oxodG Check ELISA kit to quantify 8-oxodG with results normalized for total deoxyguanosine (**dG**) content as determined by high-performance liquid chromatography with detection by ultraviolet absorbance (**HPLC-UV**). Results are expressed as the mean ng 8-oxodG/ μg dG plus the standard deviation of three independent experiments. Alpha signifies a significant difference from untreated cells of the same genotype (α $p < 0.05$, $\alpha\alpha$ $p < 0.01$). Beta denotes a difference between hOgg1- and Fpg-expressing cells at the same concentration ($\beta\beta$ $p < 0.01$). Asterisks indicate a difference from wild-type cells at the same MeHg concentration (* $p < 0.05$).

Finally, to investigate whether the paradoxically increased sensitivity of the hOgg1- and Fpg-expressing cells may be due in part to an accumulation of toxic repair intermediates resulting from their increased activity for incising oxidatively damaged DNA initiated by MeHg, apurinic/aprimidinic (AP) sites were measured. In comparison to wild-type controls, basal numbers of AP sites were lower in hOgg1-expressing cells ($p < 0.001$), but elevated in Fpg-expressing cells ($p < 0.01$) (**Fig. 7**); and consistent with previous observations in these cells (Preston *et al.*, 2009). With acute 1-h exposure to 10 μM MeHg, both hOgg1- and Fpg-expressing cells had more AP sites compared to both respective untreated cells of the same genotype, and to MeHg-exposed wild-type controls ($p < 0.001-0.0001$), while the incidence of AP sites was reduced in wild-type cells following MeHg exposure ($p < 0.05$) (**Fig. 7**).

Figure 7.

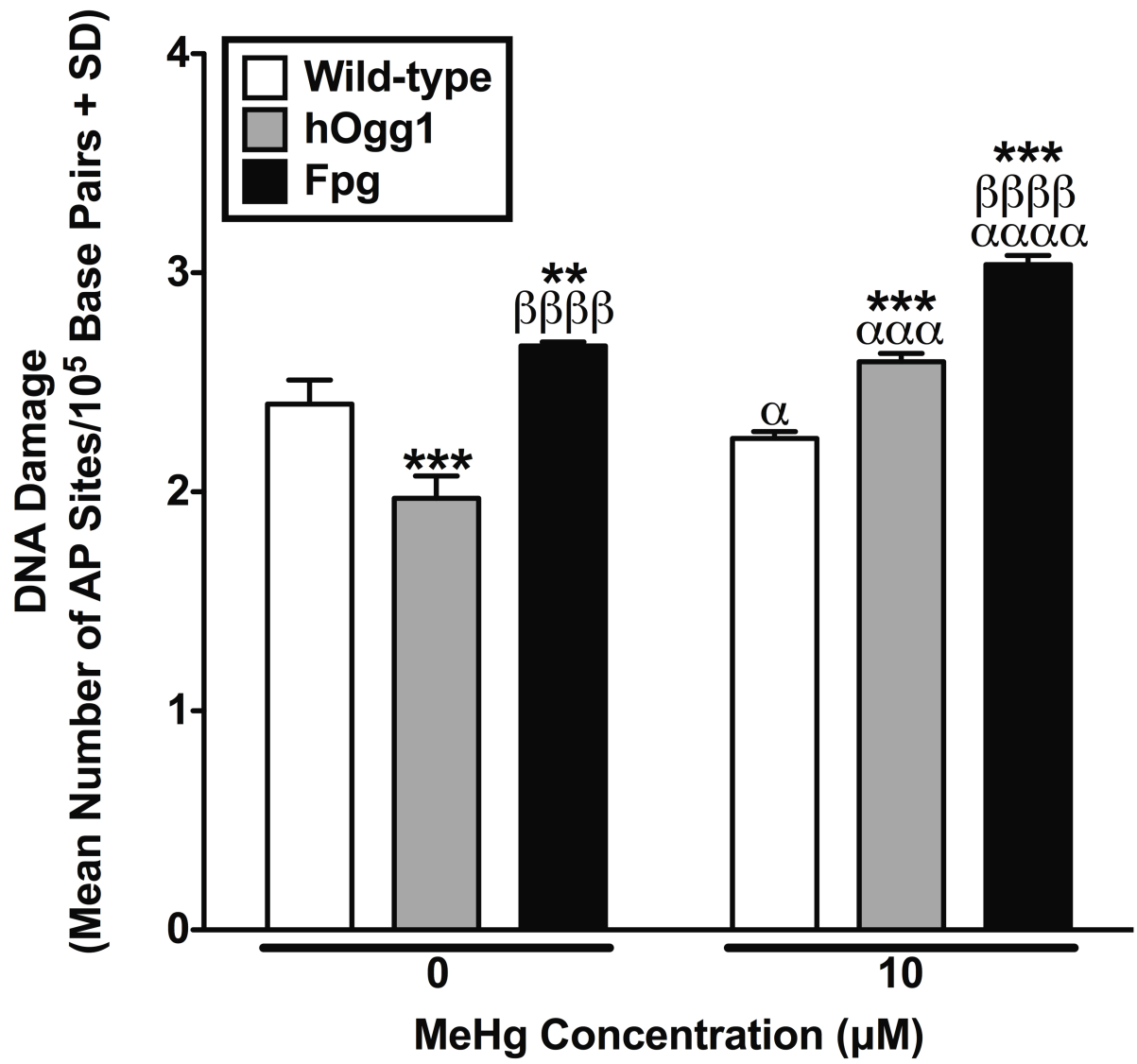


Figure 7. Apurinic/aprimidinic (AP) site formation is exacerbated in hOgg1- and Fpg-expressing HEK 293 cells upon acute exposure to MeHg compared to wild-type cells.

MeHg-initiated AP site formation was measured in isolated genomic DNA from cells treated with 0 or 10 μ M MeHg for 1 h using a DNA Damage Quantification Kit. Results are expressed as the mean number of AP sites/ 10^5 base pairs plus the standard deviation of three to four technical determinants. Alpha signifies a difference from untreated cells of the same genotype (α $p < 0.05$, $\alpha\alpha$ $p < 0.001$, $\alpha\alpha\alpha$ $p < 0.0001$). Beta denotes a difference between hOgg1- and Fpg-expressing cells at the same MeHg concentration ($\beta\beta\beta$ $p < 0.0001$). Asterisks indicate a difference from wild-type cells at the same MeHg concentration (** $p < 0.01$, *** $p < 0.001$).

2.3.5 Discussion

Today, methylmercury (**MeHg**) toxicity persists as a significant public health concern with exposure primarily a result of dietary intake of fish and seafood, and activities such as coal burning and gold mining which contribute to the environmental mercury burden (Bhavsar *et al.*, 2010; Guedron *et al.*, 2011; Kinghorn *et al.*, 2007). Despite this, our understanding of the underlying molecular mechanisms and risk factors for MeHg neurotoxicity remain to be conclusively elucidated. Herein we have presented supporting evidence that base excision repair (**BER**) status is an important determinant of risk for MeHg toxicity, providing the first report of an increased sensitivity of human oxoguanine glycosylase 1 (**hOgg1**)- and formamidopyrimidine glycosylase (**Fpg**)-expressing cells to MeHg-initiated cytotoxicity. Together, these data support a pathogenic role for enhanced BER capacity and reactive oxygen species (**ROS**)-mediated oxidatively damaged DNA in the mechanism of MeHg toxicity.

Upon confirmation of continued stable expression of hOgg1 and Fpg in our human embryonic kidney (**HEK**) 293 cell model of enhanced DNA repair, we sought to characterize the cytotoxicity profile of MeHg in these cells. As had been previously reported in human neuroblastoma cells (Das *et al.*, 2011), MeHg exposure resulted in a concentration-dependent decrease in clonogenic survival in all cells. However, the effects of MeHg in a BER-enhanced model have not been documented, and we provided the first evidence of hOgg1- and Fpg-expressing cells being paradoxically more sensitive to MeHg compared to wild-type cells.

The reduced clonogenic survival observed in response to MeHg is likely at least in part a consequence of its inhibitory effects on DNA and RNA synthesis and cell cycle progression (Burke *et al.*, 2006; Das *et al.*, 2008; Falluel-Morel *et al.*, 2007; Gribble *et al.*, 2005; Xu *et al.*, 2010). To lend support to our observed effects on clonogenic survival, we examined the growth profiles of wild-type, hOgg1- and Fpg-expressing cells basally and in the presence of MeHg. In contrast to what had been previously reported in these cells (Preston *et al.*, 2009), hOgg1- and Fpg-expressing cells exhibited hindered growth basally in the absence of MeHg, most notably throughout the middle of the growth period examined, compared to wild-type cells. This discrepancy may in part reflect variability in technique between investigators. Although measured at extended time points, unlike the remaining results presented herein, the reduced

basal cell growth is consistent with the acute observations of increased lactate dehydrogenase (**LDH**) release and apurinic/aprimidinic (**AP**) site accumulation in hOgg1- and Fpg-expressing cells respectively. In line with the effects on clonogenic survival, all cells showed a reduction in cell growth upon MeHg exposure compared to untreated cells, yet in contrast to what was previously reported in these cells for other ROS-initiating agents (Preston *et al.*, 2009), the BER-enhanced cells were paradoxically more susceptible to MeHg-mediated growth arrest at days 6-8 post-treatment.

In addition to its effects on cell survival and growth, MeHg-initiated decreases in viability have been previously implicated through a variety of biochemical measures of cytotoxicity including 3-[4,5-dimethylthiazol-2-yl]-2,5-diphenyl tetrazolium bromide (**MTT**), Alamar Blue, LDH release and trypan blue exclusion (Abdalla *et al.*, 2010; Gatti *et al.*, 2004; Gribble *et al.*, 2005; Hirooka *et al.*, 2010; Tamm *et al.*, 2006). In addition to confirming that MeHg increased LDH release in a concentration-dependent manner, we discovered that hOgg1- and Fpg-expressing cells with enhanced DNA repair released a greater amount of LDH compared to wild-type controls upon exposure to MeHg. Results of this biochemical readout of viability corroborate the cellular outcomes of survival and growth measured herein, and together, suggest a role for altered BER in the mechanism MeHg toxicity.

Given that oxidative stress and its pathological consequences have been implicated in the mechanism of MeHg toxicity, we evaluated the contribution of ROS and particularly their ensuing oxidative damage to DNA in our BER-enhanced model. As has been reported by a variety of groups (Ali *et al.*, 1992; Garg and Chang, 2006; Gatti *et al.*, 2004; Ni *et al.*, 2011; Rush *et al.*, 2012), we similarly showed the ability of MeHg to generate ROS in our model, and further demonstrated a sustained elevation in ROS formation up to 24 h post-treatment, which may in part explain the delayed consequences of MeHg exposure observed both clinically and herein on cell survival and growth.

The ROS-initiating ability of MeHg thus renders it a potent oxidant of cellular macromolecules, including DNA. The oxidative DNA lesion 8-oxo-2'-deoxyguanosine (**8-oxodG**) is one of the most prevalent, and is primarily repaired via the BER pathway initiated in mammals by Ogg1, and in bacteria by Fpg (Klungland and Bjelland, 2007; Klungland *et al.*, 1999; Lindahl, 1993). MeHg-initiated increases in 8-oxodG have been observed in glioma cell

cultures (Belletti *et al.*, 2002), as well as in human urine (Chen *et al.*, 2005). We too demonstrated the ability of MeHg to increase 8-oxodG, but found an overall trend toward MeHg-exposed BER-enhanced cells paradoxically accumulating lesion levels to a greater degree than wild-type cells; a trend that would likely prove significant in both hOgg1- and Fpg-expressing cells with an increased sample size to mitigate inherent assay variability. In untreated cells, in contrast, basal levels of oxidatively damaged DNA were lower in hOgg1-expressing cells, albeit not significantly in Fpg-expressing cells, suggesting that at least hOgg1 protects human cells against constitutive levels of oxidative stress. Although in contrast to our findings of reduced basal cell growth in BER-enhanced cells, the lower constitutive levels of 8-oxodG in hOgg1-expressing cells may be a reflection of the acute nature of this measurement compared to cell growth, or that 8-oxodG does not directly mediate the growth hindrance in the absence of exogenous stressors. Nonetheless, the observed trend toward an accumulation of 8-oxodG in hOgg1- and Fpg-expressing cells upon MeHg exposure suggests that MeHg-initiated ROS and consequent formation of 8-oxodG may be partly responsible for the cytotoxicity observed herein in response to MeHg.

Overall, the most interesting observation is the novel, paradoxically increased sensitivity of hOgg1- and Fpg-expressing cells to MeHg-initiated cytotoxicity. Our initial studies suggested that under the experimental conditions employed, MeHg did not significantly inhibit Ogg1 or Fpg protein expression and/or incision activity (unpublished data), so those possibilities did not likely contribute to the increased sensitivity of the hOgg1- and Fpg-expressing cells, despite previous reports of the ability of mercury (II) to inhibit the activity of isolated zinc finger DNA repair proteins such as Fpg (Asmuss *et al.*, 2000a; Asmuss *et al.*, 2000b). A more likely explanation for the increased susceptibility of the BER-enhanced cells to MeHg is an accumulation of toxic DNA repair intermediates, such as AP sites, resulting from the enhanced glycosylase/AP lyase activity of Ogg1 and Fpg in response to 8-oxodG. These DNA repair intermediates could prove toxic if their formation in hOgg1- or Fpg-enhanced cells exceeds the capacity for processing by basal levels of downstream components of the BER pathway, or if such downstream components cannot be upregulated sufficiently quickly. It is not clear whether similar paradoxical effects can occur *in vivo*. Although not in response to MeHg, some, albeit not all, other groups have similarly found that overexpression of DNA glycosylases can be deleterious as opposed to protective. Cisplatin-initiated cytotoxicity was exacerbated by

overexpression of hOgg1 in the mitochondria of human hepatoma cells (Zhang *et al.*, 2007), and human breast cancer cells were sensitized to the alkylating agent methyl methanesulfonate by overexpressing *N*-methylpurine DNA glycosylase (Rinne *et al.*, 2004). These effects were similarly attributed to the buildup of toxic repair intermediates, which is substantiated further by observations of increased spontaneous mutation frequency in AP endonuclease-deficient yeast cells that concomitantly overexpress MAG 3-methyladenine DNA glycosylase (Xiao and Samson, 1993). Our results support this hypothesis, at least for *in vitro* cell culture, as demonstrated by a greater accumulation of 8-oxodG in MeHg-exposed hOgg1- and Fpg-expressing cells, and the corroborating evidence of enhanced AP site formation in these BER-enhanced cells upon MeHg exposure without a similar increase in wild-type cells. The apparent increased basal AP site accrual in cells expressing Fpg, but not hOgg1, is also consistent with previous reports of elevated AP site levels in Fpg-expressing cells (Preston *et al.*, 2009), and of Fpg being 80-times more active than Ogg1 (Asagoshi *et al.*, 2000). Accordingly, the accumulation of AP sites in the BER-enhanced cells are likely responsible in part for mediating the overall increased cytotoxicity observed herein in hOgg1- and Fpg-expressing cells exposed to MeHg.

Our results support a pathogenic role for both ROS-mediated oxidatively damaged DNA, and a role for BER in the mechanism of MeHg toxicity. We have provided the first evidence of an increased susceptibility of hOgg1- and Fpg-expressing cells to MeHg-initiated cytotoxicity, implicating BER status as a critical determinant of risk. The variability in Ogg1 activity may constitute an important determinant of risk for pathologies mediated by DNA lesions repaired via BER given the range of human variability in DNA repair activity, where *Ogg1* mRNA levels were estimated to vary 5-10-fold (Vogel *et al.*, 2002), with interindividual variation in Ogg1 activity in healthy subjects estimated to be 2.8-fold (Paz-Elizur *et al.*, 2007). However, more information correlating the full range of DNA repair activities from low to substantially above average with *in vivo* consequences is required to fully understand the role of altered BER capacity as a risk factor for environmentally-initiated pathologies, as the *in vivo* consequences of altered DNA repair activity may differ significantly from those *in vitro*, and may also differ by the nature of the environmental toxin. This paradoxical effect might also prove useful in cancer therapy wherein, combined with glycosylase overexpression, the judicious selection of a DNA-damaging drug with effects similar to MeHg could be employed as a therapeutic agent for

selectively destroying proliferating cancer cells. Given that MeHg toxicity remains a significant public health concern today, and that other environmental contaminants may share similar mechanisms of action, additional research is warranted to better understand the underlying molecular mechanisms and risk factors for MeHg toxicity, especially *in vivo*. Doing so will allow for the development of novel biomarkers of exposure for environmental toxicants, and therapeutic interventions, which to date are limited in cases of MeHg poisoning.

CHAPTER 3: SUMMARY, CONCLUSIONS AND FUTURE STUDIES

3.1 SUMMARY AND CONCLUSIONS

Methylmercury (**MeHg**) is a persistent environmental contaminant with potent neurotoxic, teratogenic and likely carcinogenic properties. Historically, MeHg is most notorious for two large-scale cases of human poisoning: via contaminated seafood in Minamata, Japan (Harada, 1995) and through tainted seed grain in Iraq (Amin-Zaki *et al.*, 1974). Today, society's attempt to foster a healthier lifestyle by reaping the benefits of increased fish and seafood consumption serves as the primary source of human exposure to MeHg. MeHg remains a significant public health concern given that dietary and occupational exposure levels, which can range from 0.09-1.8 $\mu\text{g}/\text{kg}/\text{day}$ (Barbosa *et al.*, 2001; Harada *et al.*, 2001; Tsuchiya *et al.*, 2008; Vahter *et al.*, 2000), can overlap those (0.2-1.8 $\mu\text{g}/\text{kg}/\text{day}$) associated with postnatal neurobehavioral deficits in humans after *in utero* MeHg exposure (Grandjean *et al.*, 1998; Grandjean *et al.*, 1997). Moreover, the absence of an established lowest observable effect level for more subtle outcomes following low-dose MeHg exposure paradigms akin to those in fish-eating populations, together with conflicting risk assessment results from population-based studies, make definitive public health recommendations a challenge (Castoldi *et al.*, 2001; Clarkson *et al.*, 2003; Costa *et al.*, 2004).

Despite considerable research, the complex nature of MeHg toxicity and its documented interference with numerous cellular constituents and processes have made elucidation of the precise underlying molecular mechanisms of its potent neurotoxic action a challenge. The interrelated contributions of calcium (Ca^{2+}) dyshomeostasis, glutamate excitotoxicity and oxidative stress are, however, largely regarded as three likely critical events contributing to MeHg neurotoxicity (Farina *et al.*, 2011).

Oxidative stress ensues when the production of reactive oxygen species (**ROS**) exceeds the antioxidative capacity of the cell, leading to oxidative macromolecular damage, aberrant cell signaling and potentially cell death (Buonocore *et al.*, 2010; Droge, 2002; Valko *et al.*, 2007). Oxidative damage to DNA, particularly the 8-oxo-2'-deoxyguanosine (**8-oxodG**) lesion, constitutes one of the most common forms of DNA damage (Akbari and Krokan, 2008). In addition to the well-appreciated mutagenic consequences of the 8-oxodG lesion, recent interest has arisen in its non-mutational pathogenesis involving altered transcription and gene expression,

which have significant implications for structural and functional teratogenesis during development, as well as neurodegeneration in adults and old age.

The 8-oxodG lesion is primarily repaired via the highly conserved base excision repair (**BER**) pathway, initiated in mammals primarily by oxoguanine glycosylase 1 (**OGG1**), and in bacteria by its functional homolog formamidopyrimidine glycosylase (**Fpg**) (Klungland *et al.*, 1999). Deficiencies in the BER pathway, and specifically OGG1, have been implicated in aging and age-related diseases such as cancer and neurodegeneration, as well as in embryonic and fetal toxicity from endogenous and xenobiotic-enhanced oxidative stress (Wells *et al.*, 2010; Wilson and Bohr, 2007). However, whether the reciprocal enhancement of BER capacity is protective remains unclear, as the literature contains conflicting reports (Zhang *et al.*, 2007; Rinne *et al.*, 2004; Xiao and Samson, 1993; He *et al.*, 2002; Preston *et al.*, 2009).

Despite previous reports of the ability of MeHg to enhance ROS formation, damage DNA and interfere with cell cycle progression, no one has examined the impact of variable BER capacity on MeHg toxicity. Given that with compromised DNA repair, ROS-mediated DNA damage not only can lead to mutations, but also may have other non-mutational effects resulting in gene expression changes, some of which may be critical for the development, organization, function and defense of the adult central nervous system and/or the embryo and fetus, it is plausible that this may constitute a major determinant of risk for MeHg toxicity (Wells *et al.*, 2010).

Therefore, we employed (1) spontaneously- and Simian virus 40 (**SV40**) large T antigen-immortalized *Ogg1-null* (**Ogg1^{-/-}**) murine embryonic fibroblasts (**MEFs**); and, (2) human *Ogg1* (**hOgg1**)- or *Fpg*-expressing human embryonic kidney (**HEK**) cells. These two reciprocal *in vitro* cellular models, with respectively deficient and enhanced ability to repair oxidatively damaged DNA, were employed together with exogenous antioxidative catalase and varied cell seeding densities to investigate the contributions of ROS-mediated oxidatively damaged DNA, variable DNA repair and cellular proliferative capacity to the mechanism of MeHg toxicity.

The studies presented in this thesis are the first to investigate the impact of variable BER capacity on MeHg toxicity. I hypothesized that ROS-mediated oxidatively damaged DNA contributed in part to the mechanism of MeHg toxicity *in vitro*, with toxicity additionally dependent upon cellular proliferative capacity and DNA repair status, whereby actively

proliferating cells such as in the developing embryo and fetus, and cells with compromised DNA repair capacity, would be more sensitive to MeHg toxicity than cells with low proliferative capacity and enhanced DNA repair. The results are summarized as follows:

1. OGG1 protects against MeHg toxicity *in vitro* with DNA damage, but not apoptosis, attenuated by antioxidative catalase. When spontaneously-immortalized wild-type and *Ogg1*^{-/-} MEFs were exposed to environmentally relevant, low micromolar concentrations of MeHg, both underwent cell cycle arrest, but *Ogg1*^{-/-} cells exhibited a greater sensitivity to MeHg than wild-type controls with reduced clonogenic survival and increased apoptosis, DNA double-strand breaks measured by H2AX phosphorylated on serine 139 (γ H2AX), and DNA damage response activation measured by ataxia telangiectasia mutated phosphorylated on serine 1981 (pATM). Pretreatment with exogenous antioxidative catalase reduced levels of γ H2AX in both wild-type and *Ogg1*^{-/-} cells, but failed to block MeHg-initiated apoptosis at micromolar concentrations. These results support a role for ROS-mediated DNA damage in the mechanism of MeHg toxicity. Unlike apoptosis which is a more severe cellular outcome, similar to the death of an animal *in vivo* and hence may only occur at higher MeHg concentrations, ROS-mediated DNA damage may predominate in the mechanism of MeHg toxicity at the lower end of the concentration-response curve, leading to more subtle cellular outcomes such as the loss of nerve terminals or failed cellular migration, which nonetheless contribute to neurodevelopmental deficits and/or neurodegeneration (**Study 1**).

2. *Ogg1*^{-/-} MEFs are more sensitive to MeHg independent of cellular immortalization method, and their susceptibility to MeHg toxicity is additionally dependent on cellular proliferation capacity. In relation to the spontaneously-immortalized MEFs, SV40 large T antigen-immortalized cells exhibited similar tendencies to undergo MeHg-initiated cell cycle arrest, with increased sensitivity to MeHg persisting in the *Ogg1*^{-/-} MEFs measured by clonogenic survival and DNA damage; a significant observation given that distinct cellular phenotypes may result following different methods of cellular transformation (Kelekar and Cole, 1987; Boukamp *et al.*, 1988; Pecoraro *et al.*, 1989). Importantly, cells seeded at a higher density exhibited compromised proliferation, which protected against MeHg-mediated cell cycle arrest and DNA damage as measured by γ H2AX and its functional confirmation in micronuclei. These results provide novel mechanistic insight into MeHg toxicity, suggesting that toxicity may be exerted in part through interference with cellular proliferation, and shed light on why, compared

to the adult, the rapidly dividing, differentiating and proliferating embryo and fetus are particularly sensitive to the neurotoxic effects of MeHg. Moreover, these results highlight the complexity of extrapolating findings from *in vitro* studies to assess potential risk *in vivo*, as the incorrect choice of cell number could confound the interpretation of results and misguide future studies (**Study 2**).

3. Acute MeHg exposure exacerbates toxicity in HEK 293 cells expressing hOgg1 or Fpg. In the reciprocal model of enhanced DNA repair, hOgg1- and Fpg-expressing HEK cells appeared paradoxically more sensitive to acute MeHg exposure across all cellular and biochemical outcomes, exhibiting a greater reduction in clonogenic survival and cell growth, and a greater increase in cytotoxicity measured by lactate dehydrogenase (**LDH**) release and oxidatively damaged DNA measured as 8-oxodG compared to wild-type controls, potentially due to the accumulation of toxic intermediary apurinic/apyrimidinic (**AP**) sites that cannot be adequately managed due to the lack of compensatory upregulation of downstream components of the BER pathway. These results reinforce the key principle that biological systems thrive when in balance, and underscore the importance of supplementary *in vivo* studies to aid in interpreting *in vitro* data given that complementary repair systems *in vivo*, not active in an isolated cell, may handle the intermediary AP sites generated and mitigate toxicity. Nonetheless, exploiting BER pathway imbalances via glycosylase overexpression may prove useful in cancer treatment, wherein the prudent selection of a DNA-damaging agent with effects similar to MeHg could be used as a therapeutic agent for selectively destroying proliferating cancer cells (**Study 3**).

These results provide the first evidence that OGG1 status is a critical protector of genomic integrity and modulator of risk for MeHg toxicity, independent of the method of cellular immortalization. The attenuation of toxicity by both antioxidative catalase and hindered proliferative capacity constitutes the most direct evidence to date that clastogenic DNA damage may contribute to the pathological consequences of MeHg exposure via a non-mutagenic mechanism, and that this DNA damage is both ROS-mediated and proliferation-dependent. Accordingly, variations in cellular proliferation capacity as found in the highly proliferative developing conceptus and cancer cells, and interindividual variability in antioxidative and DNA repair activity, may constitute important determinants of risk for environmentally-initiated oxidatively damaged DNA and its pathological consequences.

3.2 FUTURE STUDIES

The results described herein provide a solid foundation for further exploration of the contribution of ROS-mediated oxidatively damaged DNA, as well as variable DNA repair and cellular proliferative capacity to the mechanism of MeHg toxicity.

In pursuing *in vitro* cellular studies, it would be informative to derive cells of a neuronal or astrocytic lineage from our *Ogg1*^{-/-} mice to better understand the contribution of altered DNA repair status in the mechanism of MeHg toxicity in the brain using known cellular targets for MeHg. A previous report found mouse neuroblastoma cells to be more sensitive to MeHg compared to nontransformed human foreskin fibroblasts, accumulating higher levels of MeHg resulting in greater microtubule disruption (Sager and Syversen, 1984). These observations may be due to an increased expression in the mouse neuroblastoma cells of the L-type large neutral amino acid transporter 1 (LAT1), which is responsible for facilitating MeHg transport. The high proliferative capacity of the neuroblastoma cells in comparison to nontransformed human foreskin fibroblasts might also contribute to their observed increased sensitivity to MeHg. However, examination of this differential sensitivity profile has yet to be carried out in a model with variable BER capacity, and would be worth pursuing.

MeHg pharmacokinetics were not evaluated within our cellular models, but it would be advantageous to determine the intracellular concentration of MeHg achieved under our experimental conditions. This would allow for more direct correlation between the intracellular MeHg concentration required to illicit a given response, and may reveal that a significantly lower level of MeHg is required than currently implicated as clinically-relevant. These data would also be informative given that MeHg exposure results in cell type-dependent mercury accumulation, whereby mouse neuroblastoma cells achieved on average 4-fold higher mercury levels compared to human fibroblasts (Sager and Syversen, 1984). Determining whether MeHg levels vary with altered DNA repair capacity would also reveal the novel possibility of a relationship between DNA repair and MeHg transport, the latter of which is facilitated by the LAT system (Kerper *et al.*, 1992).

Studies examining alterations in gene expression, which to date are limited, would provide invaluable insight into the mechanism of MeHg toxicity, particularly at the lower range

of the concentration-response relationship. This would facilitate a more definitive elucidation of the precise mechanisms by which MeHg-initiated DNA damage contributes to the mechanism of toxicity, and the identification of novel risk factors. Such studies would also permit an evaluation of the contribution of ROS-mediated alterations in signal transduction to the mechanism of toxicity. Similarly, the emerging field of oxygenomics suggests the exciting possibility of regional, cellular and even gene-specific damage leading to pathway-specific effects, the latter supported by *in vivo* evidence of 8-oxodG accumulation in susceptible genomic sites rather than being randomly distributed throughout the genome (Toyokuni, 2008). Identification of MeHg-initiated gene-specific 8-oxodG damage would help to explain the effects observed both herein and clinically, and advance therapeutic interventions at the molecular level, such as the potential for gene therapy, in cases of MeHg poisoning.

Of greatest importance arising from this work would be subsequent evaluations of similar outcomes in a more complex system such as the developing embryo in culture. Using a whole embryo culture (WEC) model would enable testing of our hypothesis in an integrated, developing, multicellular system in the absence of maternal influence, yet would still allow for the use of controlled pharmacologic intervention in delineating the involvement of pathways of interest. Unlike cultured cells which are limited in the information they can provide, the embryo offers a full spectrum of outcomes, from subtle changes in cellular differentiation, migration, function and interaction, which are likely to predominate in the toxicological mechanism of MeHg at lower exposure levels, to the most severe outcomes of cell and embryonic death. Moreover, the WEC model will allow for assessment of the effects of MeHg exposure at specific gestational stages, and for the correlation of periods of rapid proliferation with increased susceptibility to MeHg, thereby corroborating our *in vitro* findings of a proliferation-dependent component to MeHg toxicity.

Lastly, in addition to determining whether the mechanisms implicated herein can be extrapolated to the *in vivo* pathogenesis following MeHg exposure, it will particularly interesting to see whether the hOgg1-expressing transgenic mice are, like the cells, more sensitive to MeHg compared to wild-type controls, or conversely protected. Should the two models provide contradictory results, a comparison of gene expression changes between the two would prove enlightening with regard to their differential susceptibility, and may highlight the additional *in*

vivo capability to deal with toxic intermediary abasic sites, underscoring the importance of *in vivo* toxicological testing to complement *in vitro* studies.

A better understanding of the mechanisms underlying MeHg toxicity will enable the identification of novel risk factors and therapeutic interventions, and provide a more definitive basis for public health recommendations regarding environmental exposure to MeHg.

CHAPTER 4: REFERENCES

- Abdalla, F. H., Belle, L. P., De Bona, K. S., Bitencourt, P. E., Pigatto, A. S. and Moretto, M. B. (2010). Allium sativum L. extract prevents methyl mercury-induced cytotoxicity in peripheral blood leukocytes (LS). *Food Chem Toxicol* **48**, 417-21.
- Abe, T., Haga, T. and Kurokawa, M. (1975). Blockage of axoplasmic transport and depolymerisation of reassembled microtubules by methyl mercury. *Brain Res* **86**, 504-8.
- Aburatani, H., Hippo, Y., Ishida, T., Takashima, R., Matsuba, C., Kodama, T., Takao, M., Yasui, A., Yamamoto, K. and Asano, M. (1997). Cloning and characterization of mammalian 8-hydroxyguanine-specific DNA glycosylase/apurinic, apyrimidinic lyase, a functional mutM homologue. *Cancer Res* **57**, 2151-6.
- Ahuja, D., Saenz-Robles, M. T. and Pipas, J. M. (2005). SV40 large T antigen targets multiple cellular pathways to elicit cellular transformation. *Oncogene* **24**, 7729-45.
- Akbari, M. and Krokan, H. E. (2008). Cytotoxicity and mutagenicity of endogenous DNA base lesions as potential cause of human aging. *Mech Ageing Dev* **129**, 353-65.
- Al-Gubory, K. H., Fowler, P. A. and Garrel, C. (2010). The roles of cellular reactive oxygen species, oxidative stress and antioxidants in pregnancy outcomes. *Int J Biochem Cell Biol* **42**, 1634-50.
- Ali, S. F., LeBel, C. P. and Bondy, S. C. (1992). Reactive oxygen species formation as a biomarker of methylmercury and trimethyltin neurotoxicity. *Neurotoxicology* **13**, 637-48.
- Ali, S. H. and DeCaprio, J. A. (2001). Cellular transformation by SV40 large T antigen: interaction with host proteins. *Semin Cancer Biol* **11**, 15-23.
- Allen, J. W., Mutkus, L. A. and Aschner, M. (2001). Methylmercury-mediated inhibition of 3H-D-aspartate transport in cultured astrocytes is reversed by the antioxidant catalase. *Brain Res* **902**, 92-100.
- Amin-Zaki, L., Elhassani, S., Majeed, M., Clarkson, T., Doherty, R. and Greenwood, M. (1974). Intra-uterine Methylmercury Poisoning in Iraq. *Pediatrics* **54**, 587-595.
- Asagoshi, K., Yamada, T., Terato, H., Ohyama, Y. and Ide, H. (2000). Enzymatic properties of Escherichia coli and human 7,8-dihydro-8-oxoguanine DNA glycosylases. *Nucleic Acids Symp Ser*, 11-2.
- Aschner, M., Du, Y. L., Gannon, M. and Kimelberg, H. K. (1993). Methylmercury-induced alterations in excitatory amino acid transport in rat primary astrocyte cultures. *Brain Res* **602**, 181-6.
- Asmuss, M., Mullenders, L. H., Eker, A. and Hartwig, A. (2000a). Differential effects of toxic metal compounds on the activities of Fpg and XPA, two zinc finger proteins involved in DNA repair. *Carcinogenesis* **21**, 2097-104.
- Asmuss, M., Mullenders, L. H. and Hartwig, A. (2000b). Interference by toxic metal compounds with isolated zinc finger DNA repair proteins. *Toxicol Lett* **112-113**, 227-31.
- Auten, R. L. and Davis, J. M. (2009). Oxygen toxicity and reactive oxygen species: the devil is in the details. *Pediatr Res* **66**, 121-7.
- Bakkenist, C. J. and Kastan, M. B. (2003). DNA damage activates ATM through intermolecular autophosphorylation and dimer dissociation. *Nature* **421**, 499-506.

- Ballatori, N. and Clarkson, T. W. (1982). Developmental changes in the biliary excretion of methylmercury and glutathione. *Science* **216**, 61-3.
- Barbosa, A. C., Jardim, W., Dorea, J. G., Fosberg, B. and Souza, J. (2001). Hair mercury speciation as a function of gender, age, and body mass index in inhabitants of the Negro River basin, Amazon, Brazil. *Arch Environ Contam Toxicol* **40**, 439-44.
- Belletti, S., Orlandini, G., Vettori, M. V., Mutti, A., Uggeri, J., Scandroglio, R., Alinovi, R. and Gatti, R. (2002). Time course assessment of methylmercury effects on C6 glioma cells: Submicromolar concentrations induce oxidative DNA damage and apoptosis. *Journal of Neuroscience Research* **70**, 703-711.
- Bhavsar, S. P., Gewurtz, S. B., McGoldrick, D. J., Keir, M. J. and Backus, S. M. (2010). Changes in Mercury Levels in Great Lakes Fish Between 1970s and 2007. *Environmental Science & Technology* **44**, 3273-3279.
- Boiteux, S. and Radicella, J. P. (2000). The human OGG1 gene: structure, functions, and its implication in the process of carcinogenesis. *Arch Biochem Biophys* **377**, 1-8.
- Bonacker, D., Stoiber, T., Wang, M., Bohm, K. J., Prots, I., Unger, E., Thier, R., Bolt, H. M. and Degen, G. H. (2004). Genotoxicity of inorganic mercury salts based on disturbed microtubule function. *Arch Toxicol* **78**, 575-83.
- Bonner, W. M., Redon, C. E., Dickey, J. S., Nakamura, A. J., Sedelnikova, O. A., Solier, S. and Pommier, Y. (2008). GammaH2AX and cancer. *Nat Rev Cancer* **8**, 957-67.
- Boukamp, P., Petrussevska, R.T., Breitkreutz, D., Hornung, J., Markham, A. and Fusenig, N.E. (1988). Normal keratinization in a spontaneously immortalized aneuploid human keratinocyte cell line. *J Cell Biol* **106**, 761-771.
- Buonocore, G., Perrone, S. and Tataranno, M. L. (2010). Oxygen toxicity: chemistry and biology of reactive oxygen species. *Semin Fetal Neonatal Med* **15**, 186-90.
- Burke, K., Cheng, Y., Li, B., Petrov, A., Joshi, P., Berman, R. F., Reuhl, K. R. and DiCiccio-Bloom, E. (2006). Methylmercury elicits rapid inhibition of cell proliferation in the developing brain and decreases cell cycle regulator, cyclin E. *Neurotoxicology* **27**, 970-81.
- Castoldi, A. F., Barni, S., Turin, I., Gandini, C. and Manzo, L. (2000). Early acute necrosis, delayed apoptosis and cytoskeletal breakdown in cultured cerebellar granule neurons exposed to methylmercury. *J Neurosci Res* **59**, 775-87.
- Castoldi, A. F., Coccini, T., Ceccatelli, S. and Manzo, L. (2001). Neurotoxicity and molecular effects of methylmercury. *Brain Res Bull* **55**, 197-203.
- Castoldi, A. F., Coccini, T. and Manzo, L. (2003). Neurotoxic and molecular effects of methylmercury in humans. *Rev Environ Health* **18**, 19-31.
- Cebulska-Wasilewska, A., Panek, A., Zabinski, Z., Moszczynski, P. and Au, W. W. (2005). Occupational exposure to mercury vapour on genotoxicity and DNA repair. *Mutat Res* **586**, 102-14.
- Chance, B., Sies, H. and Boveris, A. (1979). Hydroperoxide metabolism in mammalian organs. *Physiol Rev* **59**, 527-605.

- Chen, C. Y., Qu, L. Y., Li, B., Xing, L., Jia, G., Wang, T. C., Gao, Y. X., Zhang, P. Q., Li, M., Chen, W. and Chai, Z. F. (2005). Increased oxidative DNA damage, as assessed by urinary 8-hydroxy-2'-deoxyguanosine concentrations, and serum redox status in persons exposed to mercury. *Clin Chem* **51**, 759-767.
- Choi, B. H. (1989). The effects of methylmercury on the developing brain. *Progress in Neurobiology* **32**, 447-470.
- Clarkson, T. W., Magos, L. and Myers, G. J. (2003). The toxicology of mercury--current exposures and clinical manifestations. *N Engl J Med* **349**, 1731-7.
- Costa, L. G., Aschner, M., Vitalone, A., Syversen, T. and Soldin, O. P. (2004). Developmental neuropathology of environmental agents. *Annu Rev Pharmacol Toxicol* **44**, 87-110.
- Crespo-Lopez, M. E., Lima de Sa, A., Herculano, A. M., Rodriguez Burbano, R. and Martins do Nascimento, J. L. (2007). Methylmercury genotoxicity: a novel effect in human cell lines of the central nervous system. *Environ Int* **33**, 141-6.
- Dare, E., Gotz, M. E., Zhivotovsky, B., Manzo, L. and Ceccatelli, S. (2000). Antioxidants J811 and 17beta-estradiol protect cerebellar granule cells from methylmercury-induced apoptotic cell death. *J Neurosci Res* **62**, 557-65.
- Das, K., Siebert, U., Gillet, A., Dupont, A., Di-Poi, C., Fonfara, S., Mazzucchelli, G., De Pauw, E. and De Pauw-Gillet, M. C. (2008). Mercury immune toxicity in harbour seals: links to in vitro toxicity. *Environ Health* **7**, 52.
- Das, S., Nageshwar Rao, B. and Satish Rao, B. S. (2011). Mangiferin attenuates methylmercury induced cytotoxicity against IMR-32, human neuroblastoma cells by the inhibition of oxidative stress and free radical scavenging potential. *Chem Biol Interact* **193**, 129-40.
- David, S. S., O'Shea, V. L. and Kundu, S. (2007). Base-excision repair of oxidative DNA damage. *Nature* **447**, 941-50.
- Davis, L. E., Kornfeld, M., Mooney, H. S., Fiedler, K. J., Haaland, K. Y., Orrison, W. W., Cernichiari, E. and Clarkson, T. W. (1994). Methylmercury poisoning: long-term clinical, radiological, toxicological, and pathological studies of an affected family. *Ann Neurol* **35**, 680-8.
- de Souza-Pinto, N. C., Maynard, S., Hashiguchi, K., Hu, J., Muftuoglu, M. and Bohr, V. A. (2009). The recombination protein RAD52 cooperates with the excision repair protein OGG1 for the repair of oxidative lesions in mammalian cells. *Mol Cell Biol* **29**, 4441-54.
- Desai, N., Davis, E., O'Neill, P., Durante, M., Cucinotta, F. A. and Wu, H. (2005). Immunofluorescence detection of clustered gamma-H2AX foci induced by HZE-particle radiation. *Radiat Res* **164**, 518-22.
- Di Pietro, A., Visalli, G., La Maestra, S., Micale, R., Baluce, B., Matarese, G., Cingano, L. and Scoglio, M. E. (2008). Biomonitoring of DNA damage in peripheral blood lymphocytes of subjects with dental restorative fillings. *Mutat Res* **650**, 115-22.
- Dickey, J. S., Redon, C. E., Nakamura, A. J., Baird, B. J., Sedelnikova, O. A. and Bonner, W. M. (2009). H2AX: functional roles and potential applications. *Chromosoma* **118**, 683-92.
- DiMauro, S. and Schon, E. A. (2008). Mitochondrial disorders in the nervous system. *Annu Rev Neurosci* **31**, 91-123.

- Dizdaroglu, M. (2003). Substrate specificities and excision kinetics of DNA glycosylases involved in base-excision repair of oxidative DNA damage. *Mutat Res* **531**, 109-26.
- Dobson, A. W., Xu, Y., Kelley, M. R., LeDoux, S. P. and Wilson, G. L. (2000). Enhanced mitochondrial DNA repair and cellular survival after oxidative stress by targeting the human 8-oxoguanine glycosylase repair enzyme to mitochondria. *J Biol Chem* **275**, 37518-23.
- Dringen, R. (2000). Metabolism and functions of glutathione in brain. *Prog Neurobiol* **62**, 649-71.
- Droge, W. (2002). Free radicals in the physiological control of cell function. *Physiol Rev* **82**, 47-95.
- Ehrenstein, C., Shu, P., Wickenheiser, E. B., Hirner, A. V., Dolfen, M., Emons, H. and Obe, G. (2002). Methyl mercury uptake and associations with the induction of chromosomal aberrations in Chinese hamster ovary (CHO) cells. *Chem Biol Interact* **141**, 259-74.
- Ercal, N., Gurer-Orhan, H. and Aykin-Burns, N. (2001). Toxic metals and oxidative stress part I: mechanisms involved in metal-induced oxidative damage. *Curr Top Med Chem* **1**, 529-39.
- Falck, J., Coates, J. and Jackson, S. P. (2005). Conserved modes of recruitment of ATM, ATR and DNA-PKcs to sites of DNA damage. *Nature* **434**, 605-11.
- Falluel-Morel, A., Sokolowski, K., Sisti, H. M., Zhou, X., Shors, T. J. and Diccico-Bloom, E. (2007). Developmental mercury exposure elicits acute hippocampal cell death, reductions in neurogenesis, and severe learning deficits during puberty. *J Neurochem* **103**, 1968-81.
- Farina, M., Dahm, K. C., Schwalm, F. D., Brusque, A. M., Frizzo, M. E., Zeni, G., Souza, D. O. and Rocha, J. B. (2003). Methylmercury increases glutamate release from brain synaptosomes and glutamate uptake by cortical slices from suckling rat pups: modulatory effect of ebselen. *Toxicol Sci* **73**, 135-40.
- Farina, M., Rocha, J. B. and Aschner, M. (2011). Mechanisms of methylmercury-induced neurotoxicity: evidence from experimental studies. *Life Sci* **89**, 555-63.
- Featherstone, D. E. (2010). Intercellular glutamate signaling in the nervous system and beyond. *ACS Chem Neurosci* **1**, 4-12.
- Fernandez-Capetillo, O., Lee, A., Nussenzweig, M. and Nussenzweig, A. (2004). H2AX: the histone guardian of the genome. *DNA Repair (Amst)* **3**, 959-67.
- Franchi, E., Loprieno, G., Ballardini, M., Petrozzi, L. and Migliore, L. (1994). Cytogenetic monitoring of fishermen with environmental mercury exposure. *Mutat Res* **320**, 23-9.
- Franco, J. L., Braga, H. C., Stringari, J., Missau, F. C., Posser, T., Mendes, B. G., Leal, R. B., Santos, A. R., Dafre, A. L., Pizzolatti, M. G. and Farina, M. (2007). Mercurial-induced hydrogen peroxide generation in mouse brain mitochondria: protective effects of quercetin. *Chem Res Toxicol* **20**, 1919-26.
- Franco, J. L., Posser, T., Dunkley, P. R., Dickson, P. W., Mattos, J. J., Martins, R., Bairy, A. C., Marques, M. R., Dafre, A. L. and Farina, M. (2009). Methylmercury neurotoxicity is associated with inhibition of the antioxidant enzyme glutathione peroxidase. *Free Radic Biol Med* **47**, 449-57.

- Frosina, G. (2006). Prophylaxis of oxidative DNA damage by formamidopyrimidine-DNA glycosylase. *Int J Cancer* **119**, 1-7.
- Fruhwrth, G. O. and Hermetter, A. (2008). Mediation of apoptosis by oxidized phospholipids. *Subcell Biochem* **49**, 351-67.
- Ganther, H. E. (1978). Modification of methylmercury toxicity and metabolism by selenium and vitamin E: possible mechanisms. *Environ Health Perspect* **25**, 71-6.
- Garg, T. K. and Chang, J. Y. (2006). Methylmercury causes oxidative stress and cytotoxicity in microglia: attenuation by 15-deoxy-delta 12, 14-prostaglandin J2. *J Neuroimmunol* **171**, 17-28.
- Gatti, R., Belletti, S., Uggeri, J., Vettori, M. V., Mutti, A., Scandroglio, R. and Orlandini, G. (2004). Methylmercury cytotoxicity in PC12 cells is mediated by primary glutathione depletion independent of excess reactive oxygen species generation. *Toxicology* **204**, 175-185.
- Gilboa, R., Zharkov, D. O., Golan, G., Fernandes, A. S., Gerchman, S. E., Matz, E., Kycia, J. H., Grollman, A. P. and Shoham, G. (2002). Structure of formamidopyrimidine-DNA glycosylase covalently complexed to DNA. *J Biol Chem* **277**, 19811-6.
- Giorgio, M., Trinei, M., Migliaccio, E. and Pelicci, P. G. (2007). Hydrogen peroxide: a metabolic by-product or a common mediator of ageing signals? *Nat Rev Mol Cell Biol* **8**, 722-8.
- Goode, E. L., Ulrich, C. M. and Potter, J. D. (2002). Polymorphisms in DNA repair genes and associations with cancer risk. *Cancer Epidemiol Biomarkers Prev* **11**, 1513-30.
- Graf, E. and Eaton, J. W. (1990). Antioxidant functions of phytic acid. *Free Radic Biol Med* **8**, 61-9.
- Grandjean, P., Weihe, P., White, R. F. and Debes, F. (1998). Cognitive performance of children prenatally exposed to "safe" levels of methylmercury. *Environ Res.* **77**, 165-72.
- Grandjean, P., Weihe, P., White, R. F., Debes, F., Araki, S., Yokoyama, K., Murata, K., Sorensen, N., Dahl, R. and Jorgensen, P. J. (1997). Cognitive deficit in 7-year-old children with prenatal exposure to methylmercury. *Neurotoxicol Teratol.* **19**, 417-28.
- Gribble, E. J., Hong, S. W. and Faustman, E. M. (2005). The magnitude of methylmercury-induced cytotoxicity and cell cycle arrest is p53-dependent. *Birth Defects Res A Clin Mol Teratol* **73**, 29-38.
- Guedron, S., Grimaldi, M., Grimaldi, C., Cossa, D., Tisserand, D. and Charlet, L. (2011). Amazonian former gold mined soils as a source of methylmercury: evidence from a small scale watershed in French Guiana. *Water Res* **45**, 2659-69.
- Hailer-Morrison, M. K., Kotler, J. M., Martin, B. D. and Sugden, K. D. (2003). Oxidized guanine lesions as modulators of gene transcription. Altered p50 binding affinity and repair shielding by 7,8-dihydro-8-oxo-2'-deoxyguanosine lesions in the NF-kappaB promoter element. *Biochemistry* **42**, 9761-70.
- Hanasoge, S. and Ljungman, M. (2007). H2AX phosphorylation after UV irradiation is triggered by DNA repair intermediates and is mediated by the ATR kinase. *Carcinogenesis* **28**, 2298-304.

- Hansen, J. M. (2006). Oxidative stress as a mechanism of teratogenesis. *Birth Defects Res C Embryo Today* **78**, 293-307.
- Hansen, J. M., Gong, S. G., Philbert, M. and Harris, C. (2002a). Misregulation of gene expression in the redox-sensitive NF-kappaB-dependent limb outgrowth pathway by thalidomide. *Dev Dyn* **225**, 186-94.
- Hansen, J. M., Harris, K. K., Philbert, M. A. and Harris, C. (2002b). Thalidomide modulates nuclear redox status and preferentially depletes glutathione in rabbit limb versus rat limb. *J Pharmacol Exp Ther* **300**, 768-76.
- Harada, M. (1995). Minamata Disease: Methylmercury poisoning in Japan caused by environmental-pollution. *Critical Reviews in Toxicology* **25**, 1-24.
- Harada, M., Fujino, T., Oorui, T., Nakachi, S., Nou, T., Kizaki, T., Hitomi, Y., Nakano, N. and Ohno, H. (2005). Followup study of mercury pollution in indigenous tribe reservations in the Province of Ontario, Canada, 1975-2002. *Bull Environ Contam Toxicol* **74**, 689-97.
- Harada, M., Nakanishi, J., Yasoda, E., Pinheiro, M. C., Oikawa, T., de Assis Guimaraes, G., da Silva Cardoso, B., Kizaki, T. and Ohno, H. (2001). Mercury pollution in the Tapajos River basin, Amazon: mercury level of head hair and health effects. *Environ Int* **27**, 285-90.
- Hashiguchi, K., Stuart, J. A., de Souza-Pinto, N. C. and Bohr, V. A. (2004). The C-terminal alphaO helix of human Ogg1 is essential for 8-oxoguanine DNA glycosylase activity: the mitochondrial beta-Ogg1 lacks this domain and does not have glycosylase activity. *Nucleic Acids Res* **32**, 5596-608.
- Hazra, T. K., Das, A., Das, S., Choudhury, S., Kow, Y. W. and Roy, R. (2007). Oxidative DNA damage repair in mammalian cells: a new perspective. *DNA Repair (Amst)* **6**, 470-80.
- He, Y. H., Xu, Y., Kobune, M., Wu, M., Kelley, M. R. and Martin, W. J., 2nd (2002). Escherichia coli FPG and human OGG1 reduce DNA damage and cytotoxicity by BCNU in human lung cells. *Am J Physiol Lung Cell Mol Physiol* **282**, L50-5.
- Hidalgo, C. and Donoso, P. (2008). Crosstalk between calcium and redox signaling: from molecular mechanisms to health implications. *Antioxid Redox Signal* **10**, 1275-312.
- Hilmy, M. I., Rahim, S. A. and Abbas, A. H. (1976). Normal and lethal mercury levels in human beings. *Toxicology* **6**, 155-9.
- Hirooka, T., Fujiwara, Y., Minami, Y., Ishii, A., Ishigooka, M., Shinkai, Y., Yamamoto, C., Satoh, M., Yasutake, A., Eto, K. and Kaji, T. (2010). Cell-density-dependent methylmercury susceptibility of cultured human brain microvascular pericytes. *Toxicol In Vitro* **24**, 835-41.
- Hu, B., Han, W., Wu, L., Feng, H., Liu, X., Zhang, L., Xu, A., Hei, T. K. and Yu, Z. (2005). In situ visualization of DSBs to assess the extranuclear/extracellular effects induced by low-dose alpha-particle irradiation. *Radiat Res* **164**, 286-91.
- Hung, R. J., Brennan, P., Canzian, F., Szeszenia-Dabrowska, N., Zaridze, D., Lissowska, J., Rudnai, P., Fabianova, E., Mates, D., Foretova, L., Janout, V., Bencko, V., Chabrier, A., Borel, S., Hall, J. and Boffetta, P. (2005a). Large-scale investigation of base excision repair genetic polymorphisms and lung cancer risk in a multicenter study. *J Natl Cancer Inst* **97**, 567-76.

- Hung, R. J., Hall, J., Brennan, P. and Boffetta, P. (2005b). Genetic polymorphisms in the base excision repair pathway and cancer risk: a HuGE review. *Am J Epidemiol* **162**, 925-42.
- Ismail, I. H., Nystrom, S., Nygren, J. and Hammarsten, O. (2005). Activation of ataxia telangiectasia mutated by DNA strand break-inducing agents correlates closely with the number of DNA double strand breaks. *J Biol Chem* **280**, 4649-55.
- Jie, X. L., Jin, G. W., Cheng, J. P., Wang, W. H., Lu, J. and Qu, L. Y. (2007). Consumption of mercury-contaminated rice induces oxidative stress and free radical aggravation in rats. *Biomed Environ Sci* **20**, 84-9.
- Kahles, T. and Brandes, R. P. (2012). Which NADPH Oxidase Isoform Is Relevant for Ischemic Stroke? The Case for Nox 2. *Antioxid Redox Signal*.
- Karagiannis, T. C. and El-Osta, A. (2004). Double-strand breaks: signaling pathways and repair mechanisms. *Cell Mol Life Sci* **61**, 2137-47.
- Kaur, P., Aschner, M. and Syversen, T. (2006). Glutathione modulation influences methyl mercury induced neurotoxicity in primary cell cultures of neurons and astrocytes. *Neurotoxicology* **27**, 492-500.
- Kelekar, A. and Cole, M.D. (1987). Immortalization by c-myc, H-ras, and Ela oncogenes induces differential cellular gene expression and growth factor responses. *Mol Cell Biol* **7**, 3899-3907.
- Kennedy, J. C., Memet, S. and Wells, P. G. (2004). Antisense evidence for nuclear factor-kappaB-dependent embryopathies initiated by phenytoin-enhanced oxidative stress. *Mol Pharmacol* **66**, 404-12.
- Keogh, M. C., Kim, J. A., Downey, M., Fillingham, J., Chowdhury, D., Harrison, J. C., Onishi, M., Datta, N., Galicia, S., Emili, A., Lieberman, J., Shen, X., Buratowski, S., Haber, J. E., Durocher, D., Greenblatt, J. F. and Krogan, N. J. (2006). A phosphatase complex that dephosphorylates gammaH2AX regulates DNA damage checkpoint recovery. *Nature* **439**, 497-501.
- Kerper, L. E., Ballatori, N. and Clarkson, T. W. (1992). Methylmercury transport across the blood-brain barrier by an amino acid carrier. *Am J Physiol* **262**, R761-5.
- Khanna, K. K. and Jackson, S. P. (2001). DNA double-strand breaks: signaling, repair and the cancer connection. *Nat Genet* **27**, 247-54.
- Khobta, A., Anderhub, S., Kitsera, N. and Epe, B. (2010). Gene silencing induced by oxidative DNA base damage: association with local decrease of histone H4 acetylation in the promoter region. *Nucleic Acids Res* **38**, 4285-4295.
- Kinghorn, A., Solomon, P. and Chan, H. M. (2007). Temporal and spatial trends of mercury in fish collected in the English-Wabigoon river system in Ontario, Canada. *Sci Total Environ* **372**, 615-23.
- Kitsera, N., Stathis, D., Luhnendorf, B., Muller, H., Carell, T., Epe, B. and Khobta, A. (2011). 8-Oxo-7,8-dihydroguanine in DNA does not constitute a barrier to transcription, but is converted into transcription-blocking damage by OGG1. *Nucleic Acids Res* **39**, 5926-34.
- Klaunig, J. E. and Kamendulis, L. M. (2004). The role of oxidative stress in carcinogenesis. *Annu Rev Pharmacol Toxicol* **44**, 239-67.

- Klungland, A. and Bjelland, S. (2007). Oxidative damage to purines in DNA: role of mammalian Ogg1. *DNA Repair (Amst)* **6**, 481-8.
- Klungland, A. and Lindahl, T. (1997). Second pathway for completion of human DNA base excision-repair: reconstitution with purified proteins and requirement for DNase IV (FEN1). *EMBO J* **16**, 3341-8.
- Klungland, A., Rosewell, I., Hollenbach, S., Larsen, E., Daly, G., Epe, B., Seeberg, E., Lindahl, T. and Barnes, D. E. (1999). Accumulation of premutagenic DNA lesions in mice defective in removal of oxidative base damage. *Proc Natl Acad Sci U S A* **96**, 13300-5.
- Kubota, Y., Nash, R. A., Klungland, A., Schar, P., Barnes, D. E. and Lindahl, T. (1996). Reconstitution of DNA base excision-repair with purified human proteins: interaction between DNA polymerase beta and the XRCC1 protein. *EMBO J* **15**, 6662-70.
- Kung, M. P., Kostyniak, P., Olson, J., Malone, M. and Roth, J. A. (1987). Studies of the in vitro effect of methylmercury chloride on rat brain neurotransmitter enzymes. *J Appl Toxicol* **7**, 119-21.
- Laposa, R. R., Henderson, J. T., Xu, E. and Wells, P. G. (2004). Atm-null mice exhibit enhanced radiation-induced birth defects and a hybrid form of embryonic programmed cell death indicating a teratological suppressor function for ATM. *FASEB J* **18**, 896-8.
- Lee, C. H., Lin, R. H., Liu, S. H. and Lin-Shiau, S. Y. (1997). Distinct genotoxicity of phenylmercury acetate in human lymphocytes as compared with other mercury compounds. *Mutat Res* **392**, 269-76.
- Li, Y., Jiang, Y. and Yan, X. P. (2006). Probing mercury species-DNA interactions by capillary electrophoresis with on-line electrothermal atomic absorption spectrometric detection. *Anal Chem* **78**, 6115-20.
- Lindahl, T. (1993). Instability and decay of the primary structure of DNA. *Nature* **362**, 709-15.
- Lindqvist, O. and Rodhe, H. (1985). Atmospheric mercury-a review. *Tellus* **37B**, 136-159.
- Liu, X., Sun, Z. and Shi, L. (2002). [A study on DNA damage of mouse livers induced by methylmercury]. *Zhonghua Yu Fang Yi Xue Za Zhi* **36**, 5-7.
- Lodish, H., Berk, A., Zipursky, S. L. and al., e. (2000). *Molecular Cell Biology*, Ed. ^ Eds.), 4th Edition ed. W. H. Freeman, New York.
- Machlin, L. J. and Bendich, A. (1987). Free radical tissue damage: protective role of antioxidant nutrients. *FASEB J* **1**, 441-5.
- Mailhes, J. B. (1983). Methylmercury effects on Syrian hamster metaphase II oocyte chromosomes. *Environ Mutagen* **5**, 679-86.
- Markova, E., Schultz, N. and Belyaev, I. Y. (2007). Kinetics and dose-response of residual 53BP1/gamma-H2AX foci: co-localization, relationship with DSB repair and clonogenic survival. *Int J Radiat Biol* **83**, 319-29.
- Marnett, L. J. (2000). Oxyradicals and DNA damage. *Carcinogenesis* **21**, 361-70.
- Marty, M. S. and Atchison, W. D. (1998). Elevations of intracellular Ca²⁺ as a probable contributor to decreased viability in cerebellar granule cells following acute exposure to methylmercury. *Toxicol Appl Pharmacol* **150**, 98-105.

- Matyja, E. and Albrecht, J. (1993). Ultrastructural evidence that mercuric chloride lowers the threshold for glutamate neurotoxicity in an organotypic culture of rat cerebellum. *Neurosci Lett* **158**, 155-8.
- Methylmercury, C. o. t. T. E. o., Studies, B. o. E., Toxicology and Council, N. R. (2000). Toxicological Effects of Methylmercury. The National Academies Press.
- Michaels, M. L. and Miller, J. H. (1992). The GO system protects organisms from the mutagenic effect of the spontaneous lesion 8-hydroxyguanine (7,8-dihydro-8-oxoguanine). *J Bacteriol* **174**, 6321-5.
- Miller, D. M., Buettner, G. R. and Aust, S. D. (1990). Transition metals as catalysts of "autoxidation" reactions. *Free Radic Biol Med* **8**, 95-108.
- Minowa, O., Arai, T., Hirano, M., Monden, Y., Nakai, S., Fukuda, M., Itoh, M., Takano, H., Hippou, Y., Aburatani, H., Masumura, K., Nohmi, T., Nishimura, S. and Noda, T. (2000). Mmh/Ogg1 gene inactivation results in accumulation of 8-hydroxyguanine in mice. *Proc Natl Acad Sci U S A* **97**, 4156-61.
- Miura, K., Inokawa, M. and Imura, N. (1984). Effects of methylmercury and some metal ions on microtubule networks in mouse glioma cells and in vitro tubulin polymerization. *Toxicol Appl Pharmacol* **73**, 218-31.
- Mori, N., Yasutake, A. and Hirayama, K. (2007). Comparative study of activities in reactive oxygen species production/defense system in mitochondria of rat brain and liver, and their susceptibility to methylmercury toxicity. *Arch Toxicol* **81**, 769-76.
- Morimoto, K., Iijima, S. and Koizumi, A. (1982). Selenite prevents the induction of sister-chromatid exchanges by methyl mercury and mercuric chloride in human whole-blood cultures. *Mutat Res* **102**, 183-92.
- Naganuma, A., Miura, K., Tanaka-Kagawa, T., Kitahara, J., Seko, Y., Toyoda, H. and Imura, N. (1998). Overexpression of manganese-superoxide dismutase prevents methylmercury toxicity in HeLa cells. *Life Sci* **62**, PL157-61.
- Nauseef, W. M. (2008). Nox enzymes in immune cells. *Semin Immunopathol* **30**, 195-208.
- Ni, M., Li, X., Yin, Z., Sidoryk-Wegrzynowicz, M., Jiang, H., Farina, M., Rocha, J. B., Syversen, T. and Aschner, M. (2011). Comparative study on the response of rat primary astrocytes and microglia to methylmercury toxicity. *Glia* **59**, 810-20.
- Nierenberg, D. W., Nordgren, R. E., Chang, M. B., Siegler, R. W., Blayney, M. B., Hochberg, F., Toribara, T. Y., Cernichiari, E. and Clarkson, T. (1998). Delayed cerebellar disease and death after accidental exposure to dimethylmercury. *N Engl J Med* **338**, 1672-6.
- Nordstrand, L. M., Ringvoll, J., Larsen, E. and Klungland, A. (2007). Genome instability and DNA damage accumulation in gene-targeted mice. *Neuroscience* **145**, 1309-17.
- Norppa, H. and Falck, G. C. (2003). What do human micronuclei contain? *Mutagenesis* **18**, 221-33.
- Oliver, P. L., Finelli, M. J., Edwards, B., Bitoun, E., Butts, D. L., Becker, E. B., Cheeseman, M. T., Davies, B. and Davies, K. E. (2011). Oxr1 is essential for protection against oxidative stress-induced neurodegeneration. *PLoS Genet* **7**, e1002338.

- Ondovcik, S. L., Tamblyn, L., McPherson, J. P. and Wells, P. G. (2012). Oxoguanine Glycosylase 1 (OGG1) Protects Cells from DNA Double-Strand Break Damage Following Methylmercury (MeHg) Exposure. *Toxicol Sci* **128**, 272-83.
- Park, J. S., Lee, S. H., Na, H. J., Pyo, J. H., Kim, Y. S. and Yoo, M. A. (2012). Age- and oxidative stress-induced DNA damage in Drosophila intestinal stem cells as marked by Gamma-H2AX. *Exp Gerontol* **47**, 401-5.
- Park, S. T., Lim, K. T., Chung, Y. T. and Kim, S. U. (1996). Methylmercury-induced neurotoxicity in cerebral neuron culture is blocked by antioxidants and NMDA receptor antagonists. *Neurotoxicology* **17**, 37-45.
- Pastoriza-Gallego, M., Armier, J. and Sarasin, A. (2007). Transcription through 8-oxoguanine in DNA repair-proficient and Csb(-)/Ogg1(-) DNA repair-deficient mouse embryonic fibroblasts is dependent upon promoter strength and sequence context. *Mutagenesis* **22**, 343-51.
- Paz-Elizur, T., Elinger, D., Leitner-Dagan, Y., Blumenstein, S., Krupsky, M., Berrebi, A., Schechtman, E. and Livneh, Z. (2007). Development of an enzymatic DNA repair assay for molecular epidemiology studies: distribution of OGG activity in healthy individuals. *DNA Repair (Amst)* **6**, 45-60.
- Pecoraro, G., Morgan, D. and Defendi, V. (1989). Differential effects of human papillomavirus type 6, 16, and 18 DNAs on immortalization and transformation of human cervical epithelial cells. *Proc Natl Acad Sci U S A* **86**, 563-567.
- Pompella, A., Visvikis, A., Paolicchi, A., De Tata, V. and Casini, A. F. (2003). The changing faces of glutathione, a cellular protagonist. *Biochem Pharmacol* **66**, 1499-503.
- Preston, T. J., Henderson, J. T., McCallum, G. P. and Wells, P. G. (2009). Base excision repair of reactive oxygen species-initiated 7,8-dihydro-8-oxo-2'-deoxyguanosine inhibits the cytotoxicity of platinum anticancer drugs. *Mol Cancer Ther* **8**, 2015-26.
- Radicella, J. P., Dherin, C., Desmaze, C., Fox, M. S. and Boiteux, S. (1997). Cloning and characterization of hOGG1, a human homolog of the OGG1 gene of *Saccharomyces cerevisiae*. *Proc Natl Acad Sci U S A* **94**, 8010-5.
- Rajanna, B., Rajanna, S., Hall, E. and Yallapragada, P. R. (1997). In vitro metal inhibition of N-methyl-D-aspartate specific glutamate receptor binding in neonatal and adult rat brain. *Drug Chem Toxicol* **20**, 21-9.
- Rao, M. V., Chinoy, N. J., Suthar, M. B. and Rajvanshi, M. I. (2001). Role of ascorbic acid on mercuric chloride-induced genotoxicity in human blood cultures. *Toxicol In Vitro* **15**, 649-54.
- Redon, C., Pilch, D., Rogakou, E., Sedelnikova, O., Newrock, K. and Bonner, W. (2002). Histone H2A variants H2AX and H2AZ. *Curr Opin Genet Dev* **12**, 162-9.
- Reynolds, I. J. and Hastings, T. G. (1995). Glutamate induces the production of reactive oxygen species in cultured forebrain neurons following NMDA receptor activation. *J Neurosci* **15**, 3318-27.
- Riley, P. A. (1994). Free radicals in biology: oxidative stress and the effects of ionizing radiation. *Int J Radiat Biol* **65**, 27-33.

- Rinne, M., Caldwell, D. and Kelley, M. R. (2004). Transient adenoviral N-methylpurine DNA glycosylase overexpression imparts chemotherapeutic sensitivity to human breast cancer cells. *Mol Cancer Ther* **3**, 955-67.
- Rocha, C., Cavalcanti, B., Pessoa, C. O., Cunha, L., Pinheiro, R. H., Bahia, M., Ribeiro, H., Cestari, M. and Burbano, R. (2011). Comet assay and micronucleus test in circulating erythrocytes of *Aequidens tetramerus* exposed to methylmercury. *In Vivo* **25**, 929-33.
- Rocha, J. B., Freitas, A. J., Marques, M. B., Pereira, M. E., Emanuelli, T. and Souza, D. O. (1993). Effects of methylmercury exposure during the second stage of rapid postnatal brain growth on negative geotaxis and on delta-aminolevulinate dehydratase of suckling rats. *Braz J Med Biol Res* **26**, 1077-83.
- Rogakou, E. P., Pilch, D. R., Orr, A. H., Ivanova, V. S. and Bonner, W. M. (1998). DNA double-stranded breaks induce histone H2AX phosphorylation on serine 139. *J Biol Chem* **273**, 5858-68.
- Roldan-Arjona, T., Wei, Y. F., Carter, K. C., Klungland, A., Anselmino, C., Wang, R. P., Augustus, M. and Lindahl, T. (1997). Molecular cloning and functional expression of a human cDNA encoding the antimutator enzyme 8-hydroxyguanine-DNA glycosylase. *Proc Natl Acad Sci U S A* **94**, 8016-20.
- Rush, T., Liu, X., Nowakowski, A. B., Petering, D. H. and Lobner, D. (2012). Glutathione-mediated neuroprotection against methylmercury neurotoxicity in cortical culture is dependent on MRP1. *Neurotoxicology* **33**, 476-81.
- Russo, M. T., De Luca, G., Degan, P., Parlanti, E., Dogliotti, E., Barnes, D. E., Lindahl, T., Yang, H., Miller, J. H. and Bignami, M. (2004). Accumulation of the oxidative base lesion 8-hydroxyguanine in DNA of tumor-prone mice defective in both the Myh and Ogg1 DNA glycosylases. *Cancer Res* **64**, 4411-4.
- Sager, P. R. and Syversen, T. L. (1984). Differential responses to methylmercury exposure and recovery in neuroblastoma and glioma cells and fibroblasts. *Exp Neurol* **85**, 371-82.
- Sakamoto, M., Ikegami, N. and Nakano, A. (1996). Protective effects of Ca²⁺ channel blockers against methyl mercury toxicity. *Pharmacol Toxicol* **78**, 193-9.
- Sarafian, T. A., Vartavarian, L., Kane, D. J., Bredesen, D. E. and Verity, M. A. (1994). bcl-2 expression decreases methyl mercury-induced free-radical generation and cell killing in a neural cell line. *Toxicol Lett* **74**, 149-55.
- Schurz, F., Sabater-Vilar, M. and Fink-Gremmels, J. (2000). Mutagenicity of mercury chloride and mechanisms of cellular defence: the role of metal-binding proteins. *Mutagenesis* **15**, 525-30.
- Scientists of the Bureau of Chemical Safety, F. D., Health Products and Food Branch, Health Canada (2007). Human health risk assessment of mercury in fish and health benefits of fish consumption, Ed.^ Eds.).
- Sedelnikova, O. A., Pilch, D. R., Redon, C. and Bonner, W. M. (2003). Histone H2AX in DNA damage and repair. *Cancer Biol Ther* **2**, 233-5.
- Sedelnikova, O. A. and Bonner, W. M. (2006). GammaH2AX in cancer cells: a potential biomarker for cancer diagnostics, prediction and recurrence. *Cell Cycle* **5**, 2909-13.

- Sedelnikova, O. A., Redon, C. E., Dickey, J. S., Nakamura, A. J., Georgakilas, A. G. and Bonner, W. M. (2010). Role of oxidatively induced DNA lesions in human pathogenesis. *Mutat Res* **704**, 152-9.
- Shanker, G., Syversen, T., Aschner, J. L. and Aschner, M. (2005). Modulatory effect of glutathione status and antioxidants on methylmercury-induced free radical formation in primary cultures of cerebral astrocytes. *Brain Res Mol Brain Res* **137**, 11-22.
- Shay, J. W., Wright, W. E. and Werbin, H. (1991). Defining the molecular mechanisms of human cell immortalization. *Biochim Biophys Acta* **1072**, 1-7.
- Silva-Pereira, L. C., Cardoso, P. C., Leite, D. S., Bahia, M. O., Bastos, W. R., Smith, M. A. and Burbano, R. R. (2005). Cytotoxicity and genotoxicity of low doses of mercury chloride and methylmercury chloride on human lymphocytes in vitro. *Braz J Med Biol Res* **38**, 901-7.
- Stadtman, E. R. and Levine, R. L. (2000). Protein oxidation. *Ann N Y Acad Sci* **899**, 191-208.
- Stiff, T., O'Driscoll, M., Rief, N., Iwabuchi, K., Lobrich, M. and Jeggo, P. A. (2004). ATM and DNA-PK function redundantly to phosphorylate H2AX after exposure to ionizing radiation. *Cancer Res* **64**, 2390-6.
- Stiff, T., Walker, S. A., Cerosaletti, K., Goodarzi, A. A., Petermann, E., Concannon, P., O'Driscoll, M. and Jeggo, P. A. (2006). ATR-dependent phosphorylation and activation of ATM in response to UV treatment or replication fork stalling. *EMBO J* **25**, 5775-82.
- Stringari, J., Nunes, A. K., Franco, J. L., Bohrer, D., Garcia, S. C., Dafre, A. L., Milatovic, D., Souza, D. O., Rocha, J. B., Aschner, M. and Farina, M. (2008). Prenatal methylmercury exposure hampers glutathione antioxidant system ontogenesis and causes long-lasting oxidative stress in the mouse brain. *Toxicol Appl Pharmacol* **227**, 147-54.
- Tamblyn, L., Li, E., Sarras, H., Srikanth, P., Hande, M. P. and McPherson, J. P. (2009). A role for Mus81 in the repair of chromium-induced DNA damage. *Mutat Res* **660**, 57-65.
- Tamm, C., Duckworth, J., Hermanson, O. and Ceccatelli, S. (2006). High susceptibility of neural stem cells to methylmercury toxicity: effects on cell survival and neuronal differentiation. *J Neurochem* **97**, 69-78.
- Thier, R., Bonacker, D., Stoiber, T., Bohm, K. J., Wang, M., Unger, E., Bolt, H. M. and Degen, G. (2003). Interaction of metal salts with cytoskeletal motor protein systems. *Toxicol Lett* **140-141**, 75-81.
- Toyokuni, S. (2008). Molecular mechanisms of oxidative stress-induced carcinogenesis: from epidemiology to oxygenomics. *IUBMB Life* **60**, 441-7.
- Tsuchiya, A., Hinnert, T. A., Burbacher, T. M., Faustman, E. M. and Marien, K. (2008). Mercury exposure from fish consumption within the Japanese and Korean communities. *J Toxicol Environ Health A* **71**, 1019-31.
- Usami, N., Maeda, M., Eguchi-Kasai, K., Maezawa, H. and Kobayashi, K. (2006). Radiation-induced gamma-H2AX in mammalian cells irradiated with a synchrotron X-ray microbeam. *Radiat Prot Dosimetry* **122**, 307-9.
- Vahter, M., Aakesson, A., Lind, B., Bjoers, U., Schuetz, A. and Berglund, M. (2000). Longitudinal Study of Methylmercury and Inorganic Mercury in Blood and Urine of

- Pregnant and Lactating Women, as Well as in Umbilical Cord Blood. *Environ Res.* **84**, 186-94.
- Valko, M., Leibfritz, D., Moncol, J., Cronin, M. T., Mazur, M. and Telser, J. (2007). Free radicals and antioxidants in normal physiological functions and human disease. *Int J Biochem Cell Biol* **39**, 44-84.
- Viswanathan, A. and Doetsch, P. W. (1998). Effects of nonbulky DNA base damages on Escherichia coli RNA polymerase-mediated elongation and promoter clearance. *J Biol Chem* **273**, 21276-81.
- Vogel, U., Moller, P., Dragsted, L., Loft, S., Pedersen, A. and Sandstrom, B. (2002). Inter-individual variation, seasonal variation and close correlation of OGG1 and ERCC1 mRNA levels in full blood from healthy volunteers. *Carcinogenesis* **23**, 1505-9.
- Wasteneys, G. O., Cadrin, M., Reuhl, K. R. and Brown, D. L. (1988). The effects of methylmercury on the cytoskeleton of murine embryonal carcinoma cells. *Cell Biol Toxicol* **4**, 41-60.
- Wells, P. G., Bhuller, Y., Chen, C. S., Jeng, W., Kasapinovic, S., Kennedy, J. C., Kim, P. M., Laposa, R. R., McCallum, G. P., Nicol, C. J., Parman, T., Wiley, M. J. and Wong, A. W. (2005). Molecular and biochemical mechanisms in teratogenesis involving reactive oxygen species. *Toxicol Appl Pharmacol* **207**, 354-66.
- Wells, P. G., McCallum, G. P., Chen, C. S., Henderson, J. T., Lee, C. J., Perstin, J., Preston, T. J., Wiley, M. J. and Wong, A. W. (2009). Oxidative stress in developmental origins of disease: teratogenesis, neurodevelopmental deficits, and cancer. *Toxicol Sci* **108**, 4-18.
- Wells, P. G., McCallum, G. P., Lam, K. C., Henderson, J. T. and Ondovcik, S. L. (2010). Oxidative DNA damage and repair in teratogenesis and neurodevelopmental deficits. *Birth Defects Res C Embryo Today* **90**, 103-9.
- Wheatley, B. and Paradis, S. (1995). Exposure of Canadian aboriginal peoples to methylmercury. *Water, Air, Soil Pollut.* **80**, 3-11.
- Wilson, D. M., 3rd and Bohr, V. A. (2007). The mechanics of base excision repair, and its relationship to aging and disease. *DNA Repair (Amst)* **6**, 544-59.
- Wong, A. W., McCallum, G. P., Jeng, W. and Wells, P. G. (2008). Oxoguanine glycosylase 1 protects against methamphetamine-enhanced fetal brain oxidative DNA damage and neurodevelopmental deficits. *J Neurosci* **28**, 9047-54.
- Xiao, W. and Samson, L. (1993). In vivo evidence for endogenous DNA alkylation damage as a source of spontaneous mutation in eukaryotic cells. *Proc Natl Acad Sci U S A* **90**, 2117-21.
- Xie, Y., Yang, H., Miller, J. H., Shih, D. M., Hicks, G. G., Xie, J. and Shiu, R. P. (2008). Cells deficient in oxidative DNA damage repair genes Myh and Ogg1 are sensitive to oxidants with increased G2/M arrest and multinucleation. *Carcinogenesis* **29**, 722-8.
- Xu, M., Yan, C., Tian, Y., Yuan, X. and Shen, X. (2010). Effects of low level of methylmercury on proliferation of cortical progenitor cells. *Brain Res* **1359**, 272-80.

- Yamada, H., Miyahara, T., Kozuka, H., Matsubishi, T. and Sasaki, Y. F. (1993). Potentiating effects of organomercuries on clastogen-induced chromosome aberrations in cultured Chinese hamster cells. *Mutat Res* **290**, 281-91.
- Yamamori, T., Yasui, H., Yamazumi, M., Wada, Y., Nakamura, Y., Nakamura, H. and Inanami, O. (2012). Ionizing radiation induces mitochondrial reactive oxygen species production accompanied by upregulation of mitochondrial electron transport chain function and mitochondrial content under control of the cell cycle checkpoint. *Free Radic Biol Med* **53**, 260-70.
- Youn, C. K., Song, P. I., Kim, M. H., Kim, J. S., Hyun, J. W., Choi, S. J., Yoon, S. P., Chung, M. H., Chang, I. Y. and You, H. J. (2007). Human 8-oxoguanine DNA glycosylase suppresses the oxidative stress induced apoptosis through a p53-mediated signaling pathway in human fibroblasts. *Mol Cancer Res* **5**, 1083-98.
- Zhang, H., Mizumachi, T., Carcel-Trullols, J., Li, L., Naito, A., Spencer, H. J., Spring, P. M., Smoller, B. R., Watson, A. J., Margison, G. P., Higuchi, M. and Fan, C. Y. (2007). Targeting human 8-oxoguanine DNA glycosylase (hOGG1) to mitochondria enhances cisplatin cytotoxicity in hepatoma cells. *Carcinogenesis* **28**, 1629-37.
- Zucker, R. M., Elstein, K. H., Easterling, R. E. and Massaro, E. J. (1990). Flow cytometric analysis of the mechanism of methylmercury cytotoxicity. *Am J Pathol* **137**, 1187-98.

CHAPTER 5: APPENDICES

I. SUPPLEMENTAL FIGURES FOR STUDY 1:**OXOGUANINE GLYCOSYLASE 1 (OGG1) PROTECTS CELLS FROM DNA DOUBLE-STRAND BREAK DAMAGE FOLLOWING METHYLMERCURY (MeHg) EXPOSURE**

Running title: OGG1 and DNA damage following MeHg exposure

Stephanie L. Ondovcik^{*}, Laura Tamblyn[†], John Peter McPherson[†] and Peter G. Wells^{*,†,1}

Departments of ^{*}Pharmaceutical Sciences and [†]Pharmacology and Toxicology

University of Toronto

Toronto, Ontario, Canada

Figure S-1.

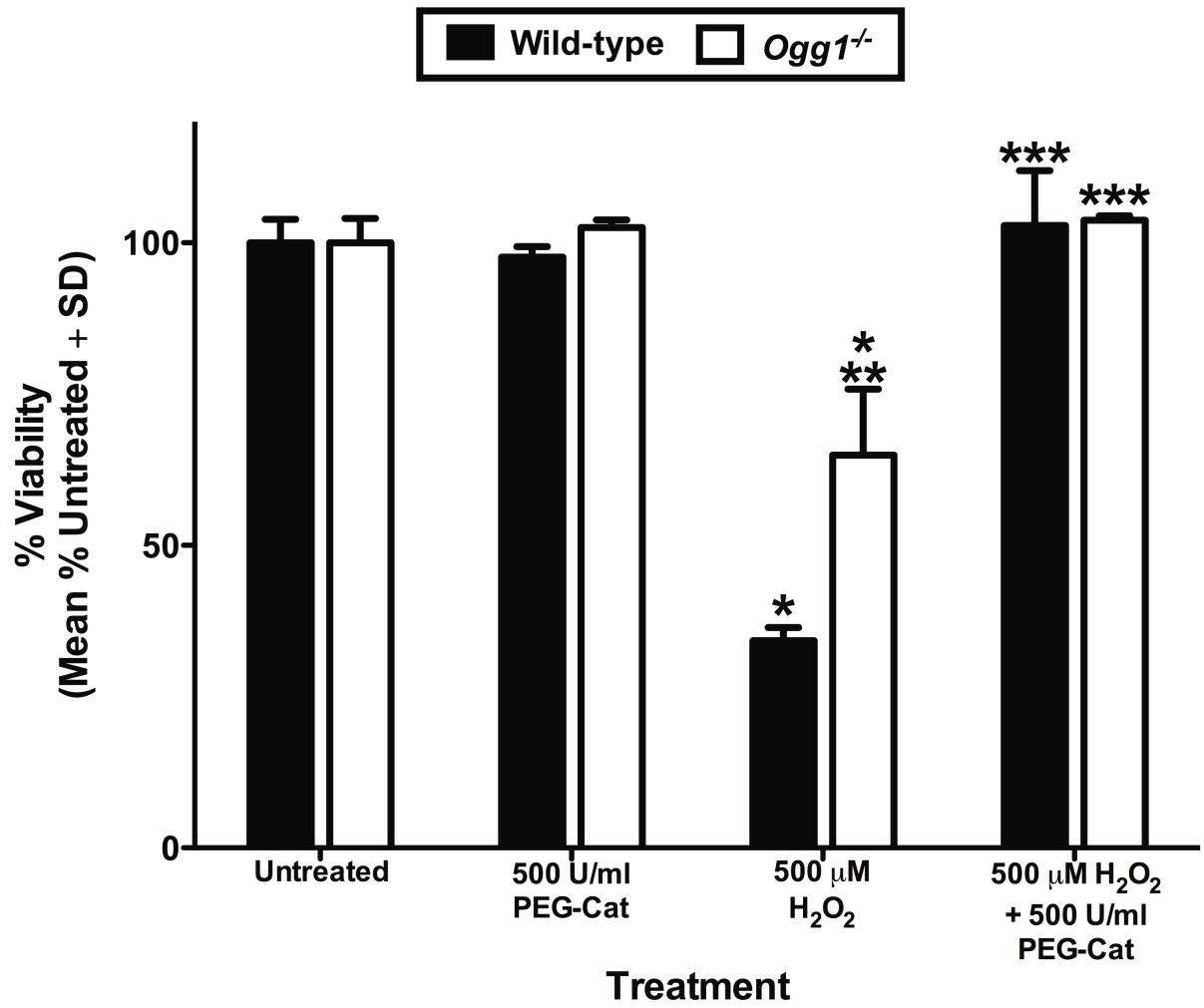


Figure S-1. Polyethylene glycol (PEG)-conjugated catalase attenuates hydrogen peroxide (H₂O₂)-initiated apoptosis in spontaneously-immortalized wild-type and OGG1-null (*Ogg1*^{-/-}) cells, despite its inability to similarly mitigate MeHg-initiated apoptosis.

Wild-type and *Ogg1*^{-/-} cells were either untreated or exposed to 500 μM H₂O₂ for 6 h with and without a 30 min pretreatment with the antioxidative enzyme PEG-catalase (500 U/ml), stained with Annexin V-fluorescein isothiocyanate (FITC)/propidium iodide (PI) and harvested for fluorescence activated cell sorting (FACS) analysis. Viable wild-type and *Ogg1*^{-/-} cells (Annexin V-FITC-low and PI-low) were quantified as the mean percent of untreated plus the standard deviation of three to six independent experiments. Despite its inability to attenuate MeHg-initiated apoptosis, PEG-catalase completely abolished H₂O₂-mediated apoptosis confirming its efficacy under the assay conditions employed. * Different from untreated cells of the same genotype (p<0.001); ** Different from wild-type cells with the same treatment (p<0.0001); *** Different from cells of the same genotype treated with H₂O₂ alone (p<0.01).

Figure S-2.

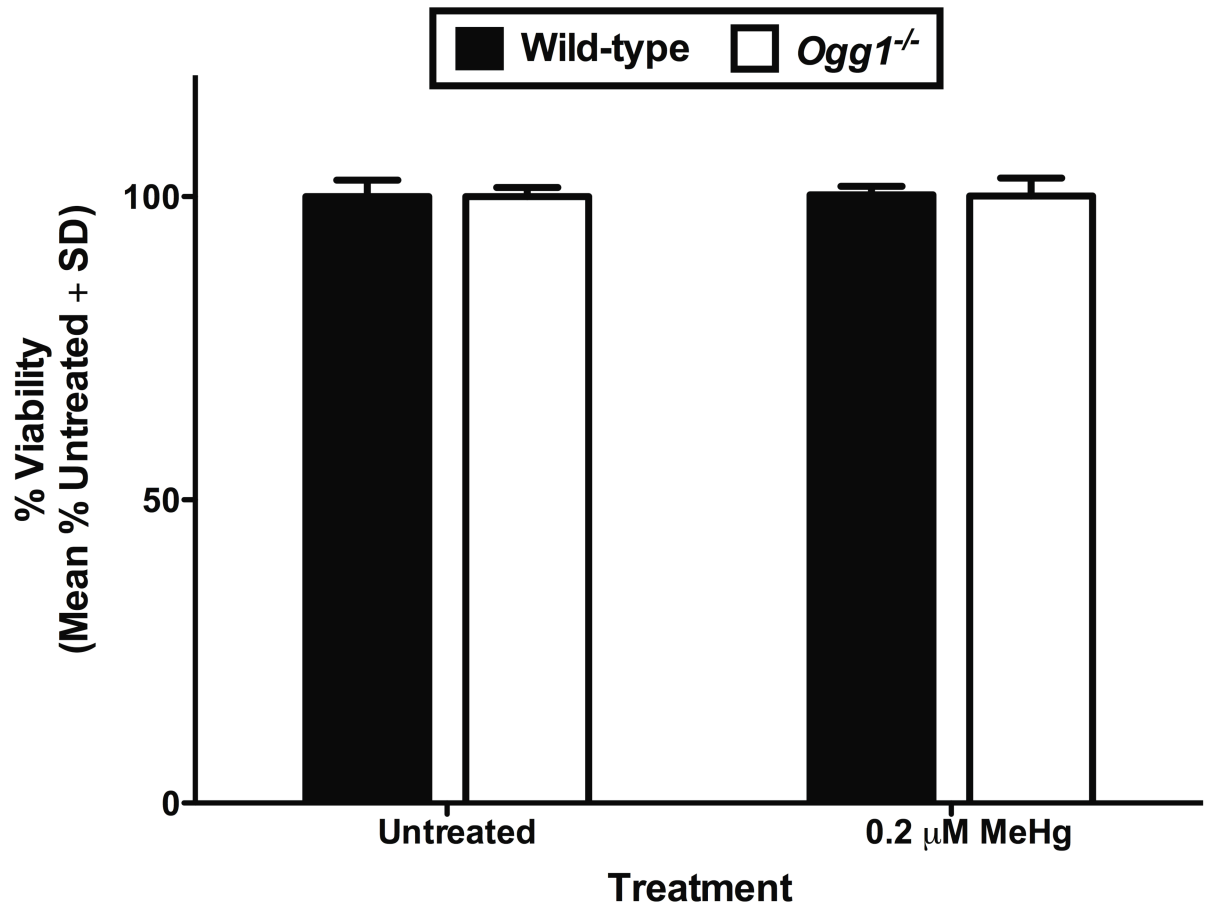


Figure S-2. Extended exposure to a submicromolar concentration of MeHg does not illicit increased apoptosis in spontaneously-immortalized wild-type and *Ogg1*^{-/-} cells.

Wild-type and *Ogg1*^{-/-} cells were either untreated or exposed to 0.2 μM MeHg for 24 h, stained with Annexin V-FITC/PI and harvested for FACS analysis. Viable wild-type and *Ogg1*^{-/-} cells (Annexin V-FITC-low and PI-low) were quantified as the mean percent of untreated cells plus the standard deviation of three independent experiments. The absence of increased apoptosis measured as reduced viability following extended exposure to a submicromolar concentration of MeHg indicates that the compromised clonogenic survival of the *Ogg1*^{-/-} cells previously observed is likely not mediated via MeHg-initiated apoptosis. Nonetheless, apoptotic cell death may contribute to the mechanism of toxicity at higher, micromolar concentrations of MeHg.

II. SUPPLEMENTAL FIGURE FOR STUDY 2:

SENSITIVITY TO METHYLMERCURY TOXICITY IS ENHANCED IN OXOGUANINE GLYCOSYLASE 1 KNOCKOUT MURINE EMBRYONIC FIBROBLASTS AND IS DEPENDENT ON CELLULAR PROLIFERATION CAPACITY

Running title: Determinants of methylmercury toxicity

Stephanie L. Ondovcik^{*}, Laura Tamblyn[†], John Peter McPherson[†] and Peter G. Wells^{*,†,1}

Departments of ^{*}Pharmaceutical Sciences and [†]Pharmacology and Toxicology

University of Toronto

Toronto, Ontario, Canada

Figure S-1.

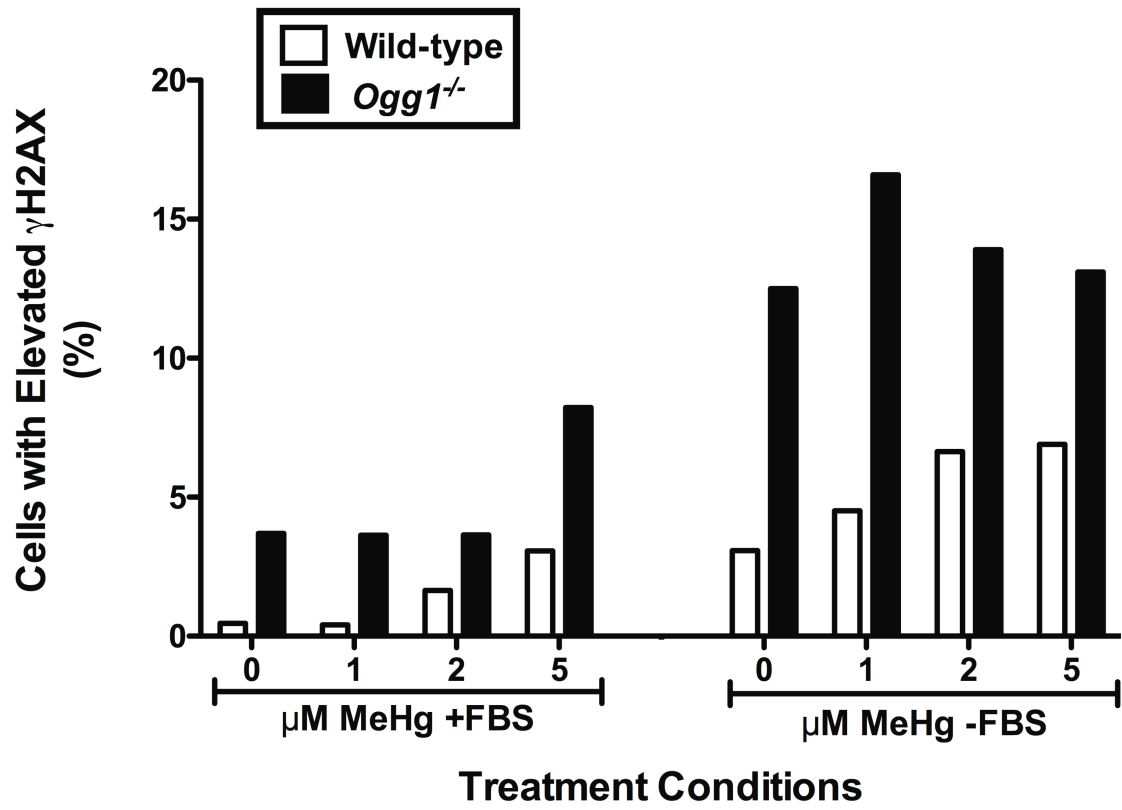


Figure S-1. MeHg-initiated H2AX phosphorylation at serine 139 (γ H2AX) is exacerbated in Simian virus 40 (SV40) large T antigen-immortalized wild-type and *Ogg1*^{-/-} cells when serum starvation is used as a means of stalling cellular proliferation.

Twenty-four hours after seeding 2×10^5 SV40 large T antigen-immortalized wild-type and *Ogg1*^{-/-} cells in 5 ml complete media containing 10% fetal bovine serum (FBS), cells were arrested in 0.5% FBS-containing media (-FBS) for 24 h. Cells were then left untreated, or exposed to 1, 2 or 5 μ M MeHg for 6 h and subsequently harvested for FACS analysis. Quantification of the percentage of cells with elevated levels of γ H2AX, and the effect of serum starvation, were plotted as the mean percent of a single determination. Serum starvation exacerbated levels of γ H2AX, including the basal value, in both wild-type and *Ogg1*^{-/-} cells. Serum starvation is commonly used as a means of synchronizing cells because of its methodological simplicity, and eliminates of the need for pharmacological inhibition of the cell cycle. However, under the conditions employed herein, this practice appeared to enhance steady-state levels of DNA damage due either to enhanced formation and/or reduced elimination of DNA double-strand breaks (DSBs), and these altered cellular changes reflected by γ H2AX may confound the interpretation of subsequent results. This confounding effect of serum starvation precluded its further use as a means of inducing cell cycle arrest.

III. MODULATORY EFFECT OF THE FREE RADICAL SPIN TRAP, α -PHENYL-N-TERT-BUTYLNITRONE (PBN), ON MeHg-INITIATED DECREASED CELLULAR VIABILITY AND REACTIVE OXYGEN SPECIES FORMATION

Figure 1.

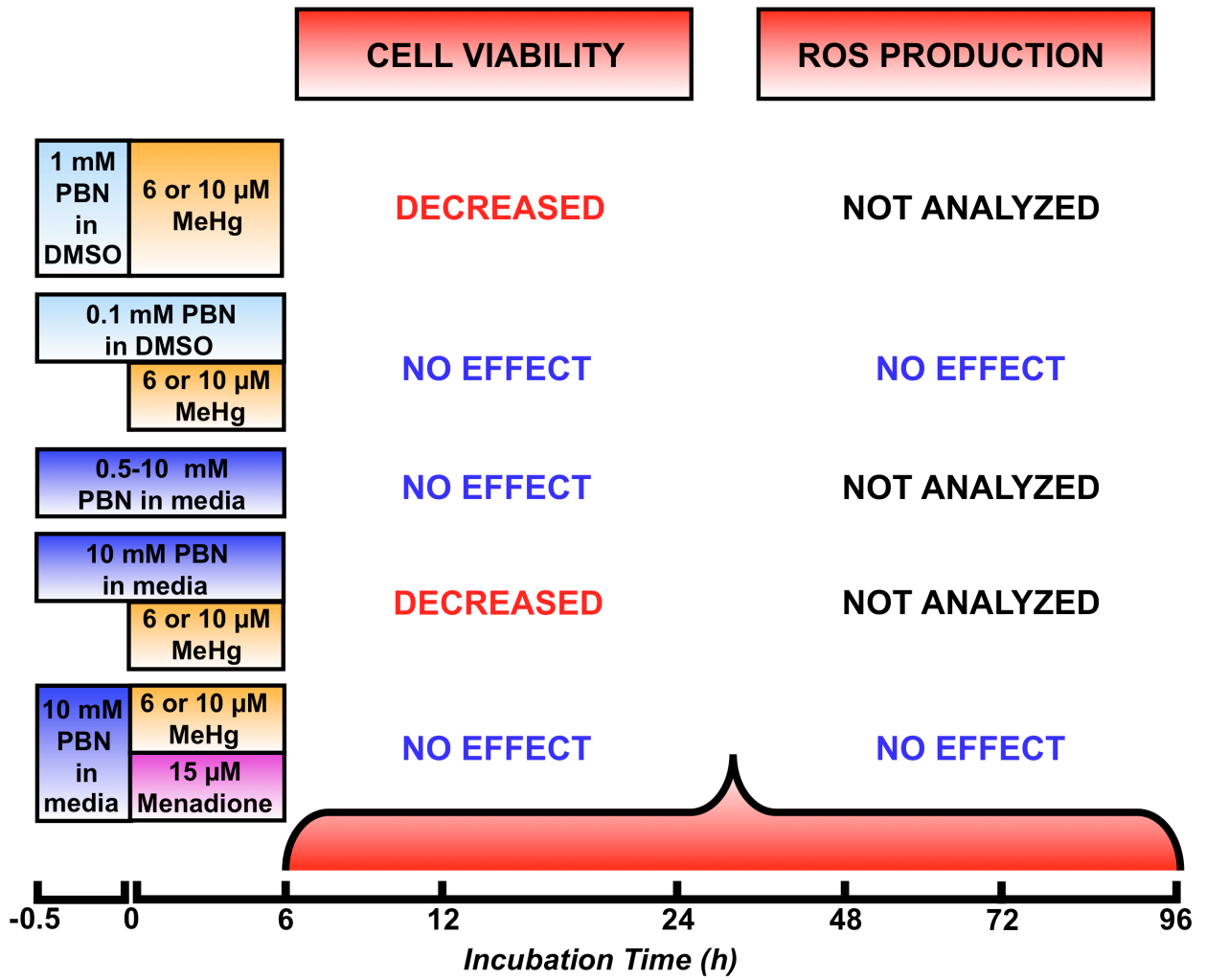


Figure 1. An experimental summary of the modulatory effect of the free radical spin trap, PBN, on cellular viability and reactive oxygen species (ROS) production in spontaneously-immortalized wild-type and *Ogg1*^{-/-} MEFs.

A number of treatment paradigms were employed to determine whether PBN could attenuate MeHg-initiated decreases in cellular viability and increases in ROS production, thereby implicating ROS in the mechanism of toxicity. The treatment paradigms used are summarized within the left-hand panel of boxes, wherein the presence of a solid vertical line between PBN and MeHg treatment signifies pretreatment washout, while a solid horizontal line indicates a coincubation between PBN and MeHg. The incubation timeline in hours is provided along the x-axis, with the effect listed under each outcome referring to the effect of PBN on MeHg-initiated decreased cell viability as measured by the alamarBlue® Cell Viability Reagent, or increased ROS production measured via the fluorescent probe 5-(and-6)-chloromethyl-2',7'-dichlorodihydrofluorescein diacetate acetyl ester (**CM-H₂DCFDA**). Overall, PBN had no biologically significant effect in attenuating MeHg-initiated decreased cellular viability or increased ROS formation, suggesting that MeHg-initiated decreased cell viability is not ROS-mediated. However, the fact that PBN also could not attenuate ROS formation initiated by the menadione positive control, which is known to enhance ROS formation (Preston *et al.*, 2009), suggests a suboptimal PBN pretreatment paradigm, possibly complicated by unappreciated confounding effects of MeHg and its interaction with PBN. Instances in which PBN pretreatment appeared to potentiate MeHg-mediated decreases in viability may involve an interaction with the solvent dimethyl sulfoxide (**DMSO**), the formation of a toxic adduct between PBN and MeHg, or an effect of PBN on some protective biochemical pathway.

IV. THE MODULATORY EFFECT OF PEG-CATALASE ON MeHg-INITIATED DECREASED CELLULAR VIABILITY AND ROS FORMATION

Figure 1.

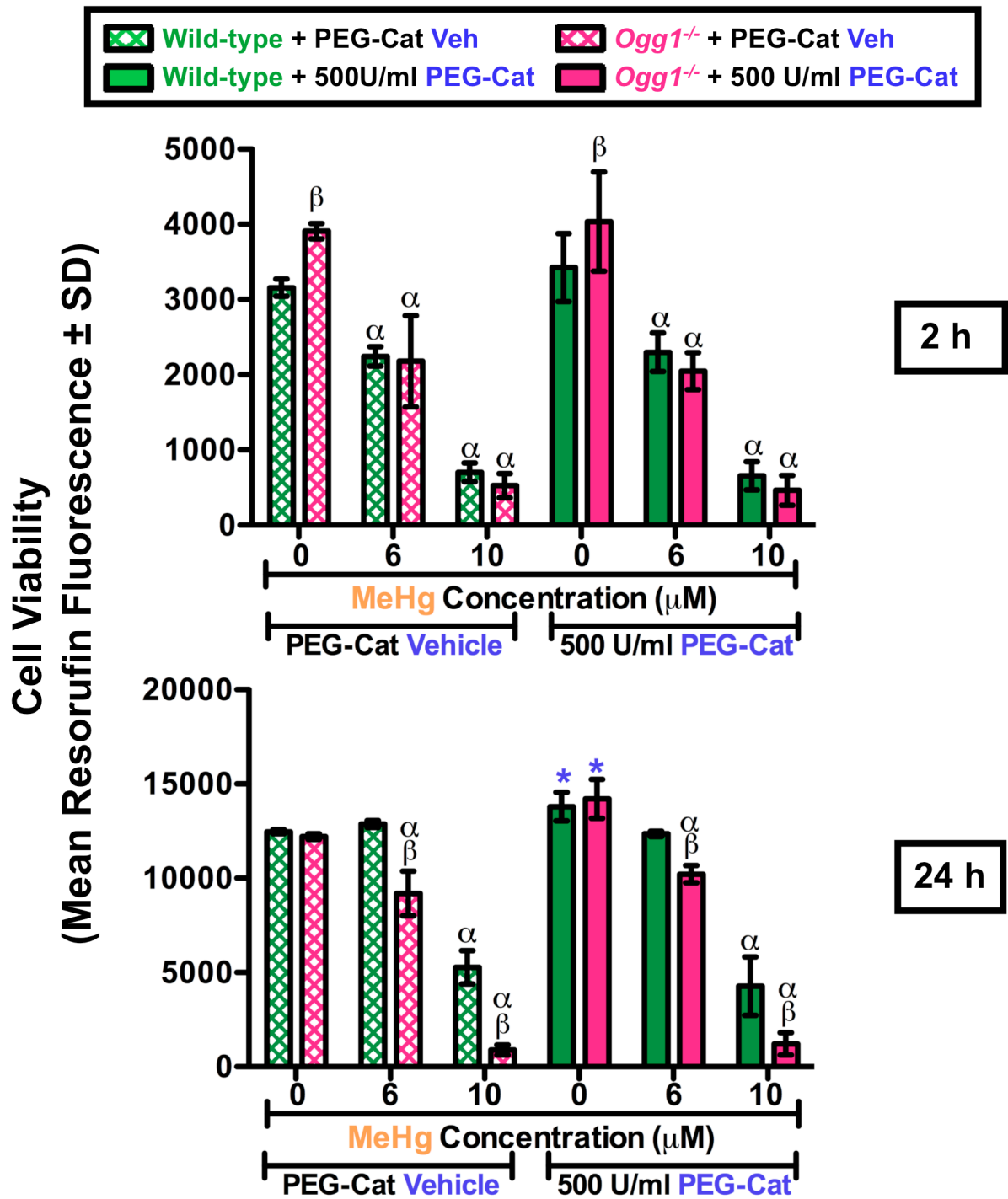


Figure 1. Antioxidative PEG-catalase does not attenuate MeHg-initiated decreased cellular viability in spontaneously-immortalized wild-type and *Ogg1*^{-/-} MEFs.

Fifteen thousand cells were seeded, preincubated for 30 min with 500 U/ml PEG-catalase, and subsequently exposed to 6 or 10 μ M MeHg for 6 hr. Cellular viability was measured 2 h (top panel) and 24 h (bottom panel) post-treatment by the alamarBlue® Cell Viability Reagent, with results expressed as the mean resorufin fluorescence plus or minus the standard deviation of five independent experiments. MeHg decreased cellular viability in a concentration-dependent manner in all cells, with the *Ogg1*^{-/-} MEFs significantly less viable at all concentrations of MeHg compared to the wild-type cells only at 24 h. Preincubation with PEG-catalase failed to attenuate the MeHg-initiated decrease in cellular viability in both wild-type and *Ogg1*^{-/-} MEFs, although it did slightly but significantly enhance basal viability in untreated cells at extended time points. These results corroborate our previous data showing PEG-catalase was unable to mitigate MeHg-initiated apoptosis, as well as the inability of PBN to alleviate MeHg-initiated decreases in viability. In summary, both a free radical spin trap and an antioxidative enzyme failed to attenuate MeHg-initiated decreases in cell viability. Together, these data suggest either that the underlying mechanism of cytotoxicity is not predominantly ROS-mediated, or that under the given conditions, the protective efficacy of such interventions is insufficient. Asterisks denote a difference from cells preincubated with PEG-catalase vehicle ($p < 0.05$). Alpha indicates a difference from untreated cells ($p < 0.05$). β signifies a difference from wild-type cells under the same treatment conditions ($p < 0.05$).

Figure 2.

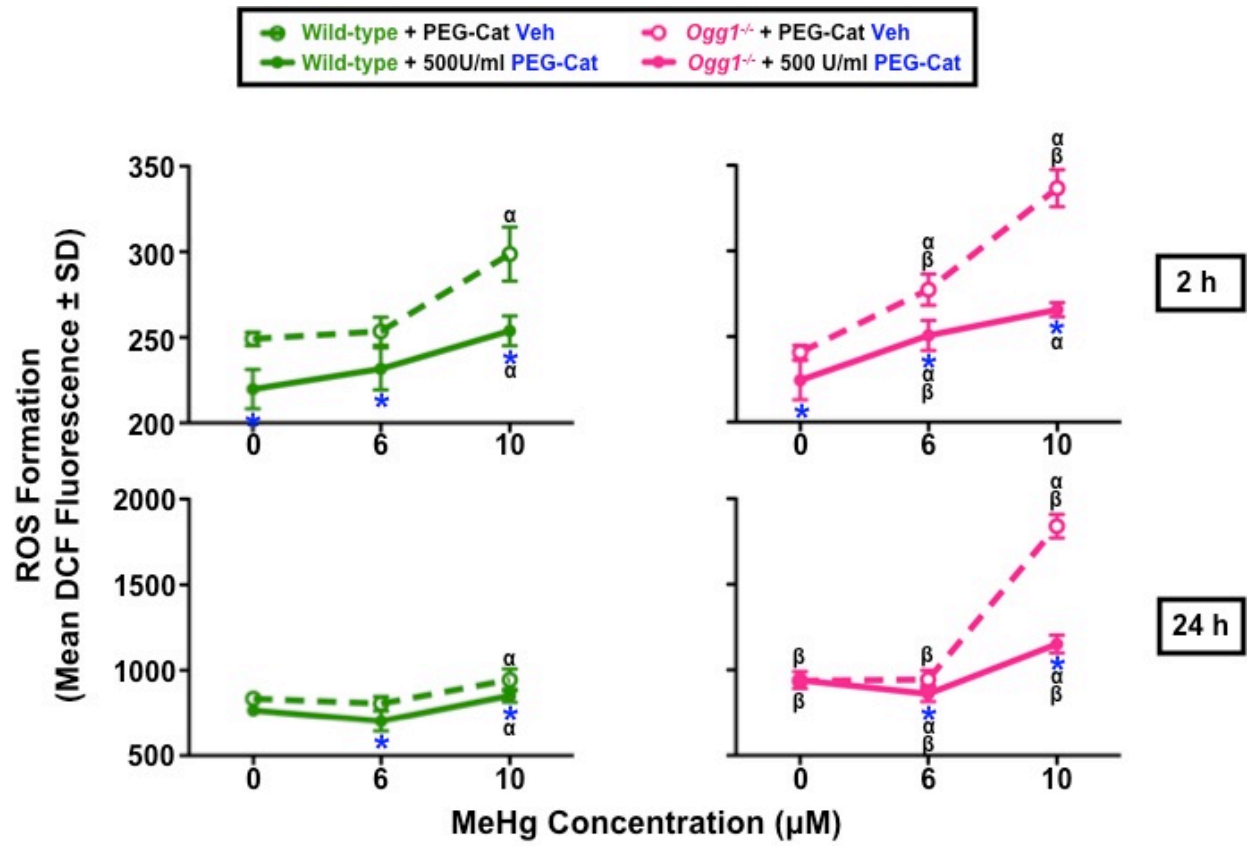


Figure 2. Antioxidative PEG-catalase attenuates both basal and MeHg-initiated ROS formation in spontaneously-immortalized wild-type and *Ogg1*^{-/-} MEFs.

Fifteen thousand cells were seeded, preincubated for 30 min with 500 U/ml PEG-catalase, and subsequently exposed to 6 or 10 μ M MeHg for 6 hr. ROS production was measured 2 h (top panel) and 24 h (bottom panel) post-treatment using 25 μ g/ml of the fluorescent probe CM-H₂DCFDA, with results expressed as the mean dichlorodihydrofluorescein (DCF) fluorescence plus or minus the standard deviation of five independent experiments. MeHg significantly enhanced ROS formation in all cells, with the *Ogg1*^{-/-} MEFs producing significantly more ROS compared to the wild-types, which may in part reflect declining cell health rather than drug-induced ROS formation. Preincubation with PEG-catalase significantly reduced both basal and MeHg-initiated ROS formation in wild-type and *Ogg1*^{-/-} MEFs. The converse failure of the free radical spin trapping agent PBN to reduce MeHg-initiated ROS formation is paradoxical in the face of PEG-catalase protection, the latter of which implies a potential role for ROS in the mechanism of MeHg toxicity. It is not clear whether the absence of protection by PBN is due to a technical problem, an unappreciated confounding interaction with MeHg or a true biological absence of a role for ROS in MeHg toxicity. Asterisks denote a difference from cells preincubated with PEG-catalase vehicle ($p < 0.05$). α indicates a difference from untreated cells ($p < 0.05$). β signifies a difference from wild-type cells under the same treatment conditions ($p < 0.05$).

V. HUMAN OXOGUANINE GLYCOSYLASE 1-EXPRESSING TRANSGENIC MICE

Table 1.

<u>hOgg1-expressing transgenic mouse line</u>	<u>PCR-mediated transgene expression</u>	<u>Anti-FLAG-mediated western analysis of protein expression</u>		<u>Anti-FLAG-mediated immunohistochemical analysis of protein expression and localization (Henderson Laboratory)</u>	
		<u>Initial analysis (8 week old mice)</u>	<u>Subsequent analysis (8 week old mice)</u>	<u>Initial analysis (8 week old mice)</u>	<u>Subsequent analysis (7 month old mice)</u>
15 Line	Positive	Liver and select brain samples	Spleen and lung	Cerebellar glial cells [Bergmann glia, glia of the facial nucleus and commissural (axon) tract] and ~50% of hepatocytes	No signal
17 Line	Positive	Liver	Spleen, lung, liver, kidney and heart	Not performed	Cerebellar Purkinje cells & Bergmann glia, Cerebral cortex (moderate glial expression; weak neuronal expression), lung cells surrounding alveoli and ~35% of hepatocytes

Table 1. Overview of the *in vivo* characterization profile completed on 15 and 17 Line human Ogg1-expressing transgenic mice.

Initial anti-FLAG (1:6000)-mediated western analyses of 20 µg of brain and liver homogenates from 8 week old Lines 15 and 17 wild-type (+/+) and human Ogg1 (**hOgg1**)-expressing heterozygous transgenic (**Tg/+**) mice revealed the presence of a single reactive species with the predicated molecular weight of approximately 39 kDa in liver and select brain samples of Tg/+ mice. Further anti-FLAG (1:10000)-mediated western blotting was performed using 10 µg of brain, liver, spleen, lung, kidney and heart homogenates from 8 week old Lines 15 and 17 +/+ and Tg/+ mice. Analyses revealed the presence of a single reactive species of the predicated molecular weight of approximately 39 kDa in the spleen and lung samples of Line 15 mice, while spleen, lung, liver, kidney and heart samples of Line 17 Tg/+ mice appeared positive for expression of the hOgg1 protein, with +/+ mice of both lines lacking transgenic protein expression in any organs analyzed.

Initial anti-FLAG (1:400)-mediated immunohistochemical (**IHC**) analysis performed in the laboratory of Dr. Jeffrey Henderson on sagittal brain sections and hepatic cross-sections from 8 week old Line 15 Tg/+ mice visualized under FITC yielded a positive signal in cerebellar glial cells including Bergmann glia, and glial cells of the facial nucleus and commissural (axon) tract, while approximately 50% of hepatocytes were positive for expression of the hOgg1 protein. Subsequent anti-FLAG (1:400)-mediated IHC analysis was conducted by the Henderson Laboratory on frozen, bisected and transversely sectioned brain, liver, spleen, lung, kidney and heart samples from 7 month old Lines 15 and 17 +/+ and Tg/+ mice. Visualization under FITC yielded a positive signal in approximately 35% of hepatocytes, in cerebellar Purkinje cells and Bergmann glia, in the cerebral cortex with some moderately stained glia and weakly stained neurons, and in lung cells surrounding the alveoli of Line 17 Tg/+, but not +/+ mice, while Line 15 Tg/+ mice failed to show any discernible signal in the organs analyzed.

The above studies demonstrate continued transgenerational expression of the *hOgg1* transgene, and expression of hOgg1 protein in various organs of both lines of hOgg1 transgenic mice. Discrepancies between preliminary western and IHC analyses of hOgg1 protein expression in the two transgenic lines generated may be due to age-related expression differences, in which transgenic protein expression decreases with age, resulting in more limited expression via IHC,

as these studies involved significantly older mice. Variations in expression patterns between lines could reflect differences in the site of transgene insertion. Determination of definitive hOgg1 protein expression and activity patterns will provide an invaluable tool for examining the effect of enhanced DNA repair capacity both in developmental and neurodegenerative models, with the unique ability to investigate the effect of organ-specific increases in DNA repair.

V.i. Rederivation of hOgg1-expressing transgenic mice to specific and opportunistic pathogen free status by embryo transfer.

This initiative was carried out with the help of the combined efforts of staff from the Department of Cellular and Systems Biology (Zoology), the Division of Comparative Medicine (DCM) and the Toronto Centre for Phenogenomics (TCP). Briefly, on Day 1, six donor female CD-1 (Charles River Laboratories) or hOgg1 mice, six weeks of age, were superovulated with an intraperitoneal (i.p.) injection of 0.1 ml pregnant mares' serum gonadotropin (PMSG). The following day, recipient CD-1 females were mated with vasectomized males at TCP. Superovulation continued on Day 3 with donor females receiving an i.p. injection of 0.1 ml human chorionic gonadotropin (HCG), following which they were mated with a proven hOgg1 male breeder of the appropriate Line and genotype to generate wild-type (+/+) x heterozygous (Tg/+) matings. Meanwhile, recipient females were checked for plugs, and the presence of a vaginal plug was designated gestational day (GD) 0.5. Superovulated donor females were checked for a plug on Day 4, and its presence designated GD 0.5. On Day 5, now GD 1.5 donor females were sacrificed and their uterine horns and fallopian tubes removed and transferred to TCP. There, under a dissecting microscope, embryos were flushed from the fallopian tubes into the uterine horns for collection using an embryo nutrient solution M2. Upon collection, embryos were rinsed in M2 and equilibrated potassium simplex optimized medium (KSOM) solutions, and subsequently 10 embryos were transferred into the uterine horns of now GD 2.5 recipient females. Three weeks later, recipient females littered out, and pups were weaned and tail clipped four weeks later. DNA was extracted from tail clips and employed in PCR-mediated genotyping for verification of hOgg1 transgene expression in both Lines 15 and 17 rederived mice, with transgene-positive mice displaying a single band of the predicted molecular weight of approximately 1100 base pairs (Fig. 1). The health of the pups was monitored for another four weeks, at which point they were deemed specific and opportunistic pathogen free (SOPF) and transferred to the Centre for Cellular and Biomolecular Research (CCBR).

Modified from SOP provided by: Tracy McCook (DCM), 2009.

Figure 1.

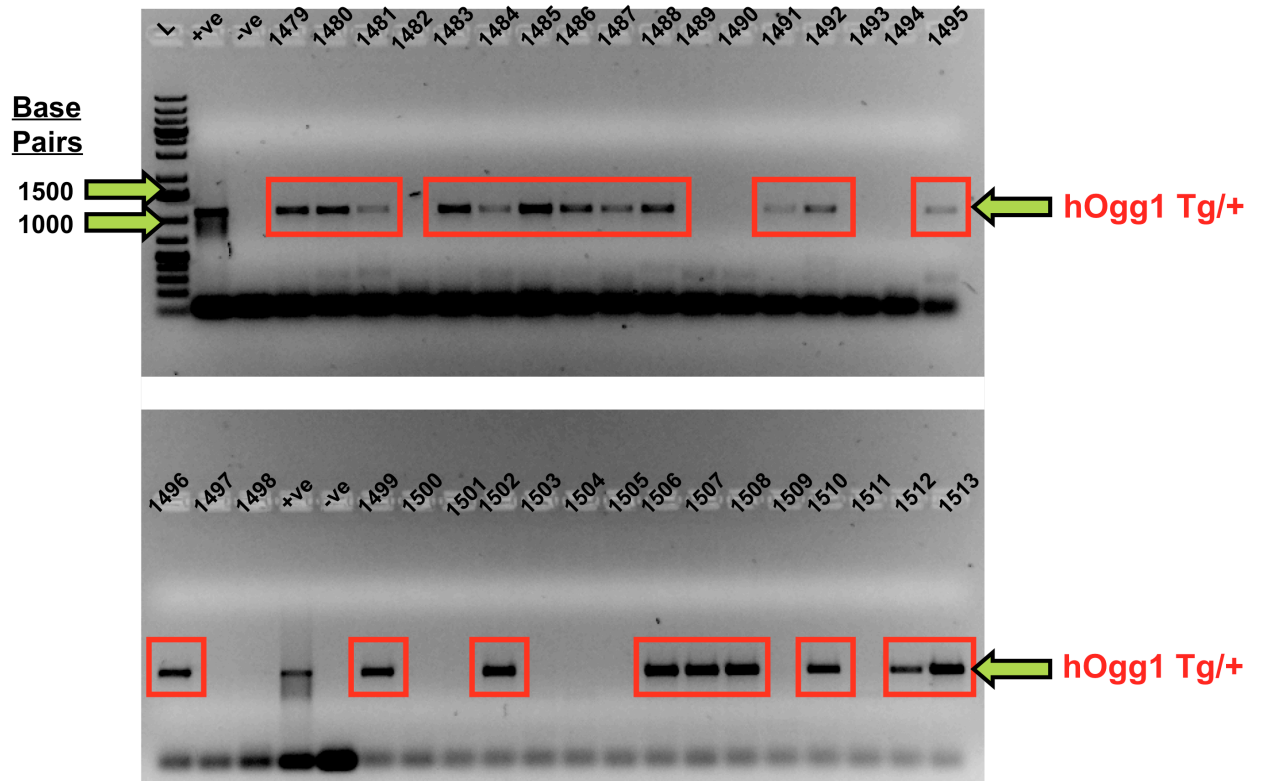


Figure 1. Representative genotyping gel confirming continued *hOgg1* transgene expression following rederivation.

DNA was crudely extracted from tail clips at 95°C for 10-15 min in 300 µl 10 mM NaOH/0.1 mM EDTA. PCR reactions consisted of 1 µl crude sample DNA extract, 1X hot-start buffer, 1.5 mM MgCl₂, 0.2 mM dNTPs, 0.3 µM of each forward (5'-AGA GAA TTC GGG CCA TGC CTG CCC GCG CGC TTC-3') and reverse (5'-AGA GAA TTC TCA CTT GTC ATC GTC GTC CTT GTA GTC-3') primers, and 0.5 U hot-start Taq DNA polymerase in a total reaction volume of 20 µl. The PCR was run using the “Neo” program as follows: 5 min 94°C, 1 min 94°C (denaturation), 1.5 min 55°C (annealing), 2 min 72°C (synthesis), 10 min 72°C (hold synthesis) and hold 4°C infinitely, with denaturation, annealing and synthesis repeated for 35 cycles. The PCR product was run on a 1% agarose gel for 1 h at 100 V, with transgene-positive mice (**Tg/+**) displaying a single band of the predicted molecular weight of approximately 1100 base pairs. Rederivation of both Lines was successful, with Line 15 yielding 35 pups born, of which 21 were Tg/+; and Line 17 yielding 19 pups born, of which 13 were Tg/+.

Abbreviations: L, ladder; +ve, positive control (DNA extract from *hOgg1*-expressing cell line); -ve, negative control (DNA extract from *Ogg1* knockout mouse tail clip); four-digit numbers identify the specific mice tested.